An evaluation of statistical synoptic models of rainfall in Spain

By

G. Spellman

Submitted as partial fulfilment of the requirements of the higher degree of Doctor of Philosophy

University of Leicester

2003

Abstract

This study investigates the control of atmospheric circulation patterns on rainfall incidence in Spain. The main objective of the research is to evaluate a range of statistical synoptic approaches with the aim of identifying the scheme that best models circulation to association.

Spatial patterns of rainfall in Spain are first investigated using Principal Components Analysis and Cluster Analysis. Distinct precipitation affinity groups emerge that display covariant rainfall behaviour and reflect differences in latitude, the influence of topography and distance from the synoptic feature responsible for rainfall. The method allows seasonal redefinition of boundaries and the investigation of the effect of climate change.

In total 24 synoptic models are investigated. The best performing models (a daily weather type model and a monthly airflow index model) use standardized data and the 500hPa contour surface. Some of the problems associated with non-stationarity are attempted by modifying models using kinematic information. Adjustments to the models (inclusion of frontal information and stochastic modelling) can improve results on a sub-regional scale.

Effective models are then used to empirically downscale from General Circulation Model (GCM) scenarios obtained from the Canadian Centre for Climate Modelling and Analysis. The downscaling procedure is of limited use due to errors in GCM output but results suggest strongly increasing anticyclonicity in the Iberian area and a decrease in rainfall in many areas. There are uncertainties associated with regional scale climate change estimation using current empirical methods, nevertheless as GCM output inevitably becomes more accurate the scope for detailed regional assessment will improve.

Contents

Chapter Three. Synoptic Climatology- daily manual classification

Chapter Four. Synoptic climatological methods
Static Approaches: Daily Models

Chapter Five. Synoptic climatological methods Static Approaches: Monthly models

Chapter Six. Evaluation of synoptic models

Chapter Seven. Downscaling from empirical models

Chapter Eight. Conclusions

List of figures

List of tables

Acknowledgements

Climatic Research Unit, University of East Anglia for supply of data.
The Instituto de Meteorologia, Spain for supply of data and charts.
Meteorological Office (UK) for supply of data and charts.
John McClatchey, Duncan McCollin and Chris Holt for constructive criticism.
Karen Spellman for support and patience.

Chapter One
Introduction to the thesis

1.1 Introduction

Synoptic climatology examines the relationship between atmospheric circulation and surface variables. By far the most common application of synoptic methods has been to the study of precipitation variability, for instance, in the British Isles (Lamb 1950, O'Hare and Sweeney 1992), in the Netherlands and Northern Germany (Beckmann and Buishand 2002), and in the South West of the United States of America (Brown and Comrie 2002). Precipitation processes are controlled by those thermodynamic and hydrodynamic features that can be readily assessed by the examination of circulation patterns. Most synoptic studies aim to identify statistically distinct rainfall behaviour associated with regional scale circulation patterns. This study describes and examines the synoptic climatology of the Iberian Peninsula and investigates its control on precipitation variability in Spain, the larger country on the peninsula.

Mechanisms and processes involving a diverse range of environmental variables are influenced by the circulation of the atmosphere. These include air quality (*e.g.* Spellman 1998a), the boundary layer of snow surfaces (Grundstein and Leathers 1999), the incidence of ischaemic heart disease (McGregor 1999), wildfire events (Skinner *et al* 2002) and viticulture (Jones and Davis 2000). Synoptic climatology examines the relationship between local or regional environmental parameters and atmospheric circulation patterns. In addition to being of use to other studies, synoptic climatology has its own intrinsic merits as a science. Yarnal (1993 p.2) comments that it represents *'...a bridge to the functional (computer model) simulations of the complex climate system...'* and an understanding of atmosphere-surface interactions.

The foundations of synoptic climatology were established once the relationship of observed winds to the spatial patterns of pressure was appreciated (Leighly 1949). The first serious synoptic climatological analysis is attributed to the German meteorologist Dove (1827), and later Köppen (1874) examined the effects of surface airflow on weather in St. Petersburg, Russia using six direction-based airflow classes. In Britain, Abercromby (1883, 1887) considered an airflow framework (four classes - N, S, E and W) to explain the variability of weather conditions and this idea was subsequently pursued by Gold (1920) who developed a classification of pressure patterns over the British Isles and adjacent areas for the period 1905-1918. Significant work was undertaken by Baur (1931, 1936a, 1936b) who examined large-scale circulation patterns

(*Grosswetter*) over Europe and the eastern North Atlantic. Bergeron (1928, 1930) proposed the concept of air masses and this became integrated into the discipline of synoptic climatology.

In the nineteen-fifties the most cited synoptic classification in the literature, that of Lamb (1950, 1972) emerged, although long period catalogues of surface airflow types for the British Isles (1898-1947) had been drawn up by Levick (1949, 1950) before this date. The Lamb Weather Type (LWT) daily airflow catalogue was more elaborate than that of Levick, and (now) extends back to 1861. It continues to be updated by the Climatic Research Unit (CRU) at the University of East Anglia (UEA) although the manual method has been replaced by an objective indexing method (Jenkinson and Collison 1977). By the end of the twentieth century more than 400 separate synoptic climatological classification schemes had been proposed for a large number of regions including recent work in Estonia (Keevalik *et al* 1999), New Zealand (Kidson 2000), Sweden (Chen 2000), Norway (Hanssen-Bauer and Førland 2000), mid-latitude Asia (Aizen *et al* 2001) and Iran (Alijani 2002).

In addition to class-based approaches circulation indices have been extensively employed. Large-scale teleconnections, as assessed by the North Atlantic Oscillation Index (NAOI) and North Pacific Oscillation (PDO), were first investigated by Walker (1923, 1924) and Walker and Bliss (1930). In the mid-sixties and early seventies small-scale indexing methods such as PSCM indices for the UK (Murray and Lewis 1966, Murray and Benwell 1970, Murray 1973) were developed. Indexing methods continue to feature highly in the synoptic literature (*e.g.* El Dessouky and Jenkinson 1975, Conway *et al* 1996, Spellman 1997a). In the course of this analysis both class-based and index-based approaches are considered.

1.2 Precipitation variability in the Western Mediterranean

Precipitation variability in space and time is one of the defining characteristics of the Western Mediterranean climate. In many parts of this region rainfall is both a deficient resource (Quereda 1983) and a potentially catastrophic agent (Gil Olcina 1989). Sixty to eighty percent of the water supply in Spain is typically used in agriculture and irrigation (Smith 1997) and recently there has been additional demand in many parts of the country from the tourist industry (Roberts 2002). Changes in global climate during the twenty-first century are likely to be dominated by the influence of the greenhouse effect (IPCC 1995, IPCC 2001a) and evidence from climate change models is emerging that indicate precipitation changes may take place on a global (Hulme *et al* 1998) and on a regional scale, including in the Mediterranean basin (Rodriguez-Puebla *et al*

1998). These changes may occur in terms of variability as well as average amounts (Mearns *et al* 1996) and the changes in the former may actually have a greater impact on water resources (Katz and Brown 1992). At present General Circulation Model (GCM) predictions and historical observations seem to agree to a generalized decrease in rainfall in the eastern (Maheras 1988, Amanatidis *et al* 1993, 1997), central (Piervitali *et al* (1998), and western (Esteban-Parra *et al* 1998, De Luis *et al* 2000) Mediterranean. The role of synoptic climatological analysis is to investigate whether these changes are related to observed (and projected) shifts in circulation mode.

Changes in precipitation variability are likely to exert the most significant impacts in areas that, under current conditions, are already under stress. These could be regions with climate-related water shortages (in semi-arid and arid areas) or those where there is excessive water demand (De Luis *et al* 2000). Mediterranean regions are transitional climate zones where it is suggested that climatic changes may have the greatest effects (Lavorel *et al* 1998). In parts of Spain both supply deficiencies and demand pressure (primarily from tourism and agriculture) combine to exaggerate the problem.

The Intergovernmental Panel on Climate Change (IPCC 2001a) has predicted an increase in aridity in Spain throughout the year in future decades. In the early 1990s the southern half of Spain experienced a drought episode that severely affected agricultural activities. This suggested that the drought was one step away from a generalized process of desertification across the peninsula (Estrela *et al* 2000).

Climate dynamics are the primary driving force for the hydrologic cycle on Earth. Due to its direct social and economic impacts, occurring mostly in response to changes in the hydrologic cycle, climate variability has been the subject of many studies at different spatial and temporal scales. GCMs are used to assess the potential impact that an increased loading of the atmosphere with greenhouse gases (and sometimes atmospheric aerosols) might have on the climate and hydrologic system. An increasing number of applied studies have used the output of GCM modelled data as an input scenario, yet there still remain drawbacks of employing such data. Current GCMs perform relatively poorly at many sub-grid scale applications because of their coarse spatial (typically on the scale of 50,000 km^2) and temporal resolution (Wigley *et al* 1990, Carter *et al* 1994, Wilby and Wigley 1997). GCMs describe fluid dynamics on a continental scale where fields are smoothly varying (Hughes and Guttorp 1994) and must parameterize regional and small scale processes (Wilby and Wigley 1997), yet it is the mismatches in scale that involve crucial parts of the climate model - water vapour and cloud feedback effects (Rind *et al* 1992). Precipitation is particularly difficult to model due to its discrete nature in time and space. Many processes governing precipitation operate at a sub-grid scale and therefore simulation quality is poor (Saunders and Byrne 1998). Consequently GCM outputs should be considered only as possible scenarios for future climate change rather than predictions (*figure 1.1*).

Downscaling approaches have emerged as the principal means for translating regional-scale circulation patterns into station or small area-scale meteorological series (Karl *et al* 1990, Hay *et al* 1991, 1992). Methods are now firmly established in climate research and involve relating historic station (or areal) data to a given weather classification system (Yarnal 1993). Although the term 'downscaling' in climatology has only recently become widespread, conceptually this method has been employed for many years as 'synoptic climatological analysis'. Reviews of earlier work have been undertaken by Barry and Perry (1973), Smithson (1986, 1987, 1988) and Yarnal (1993).

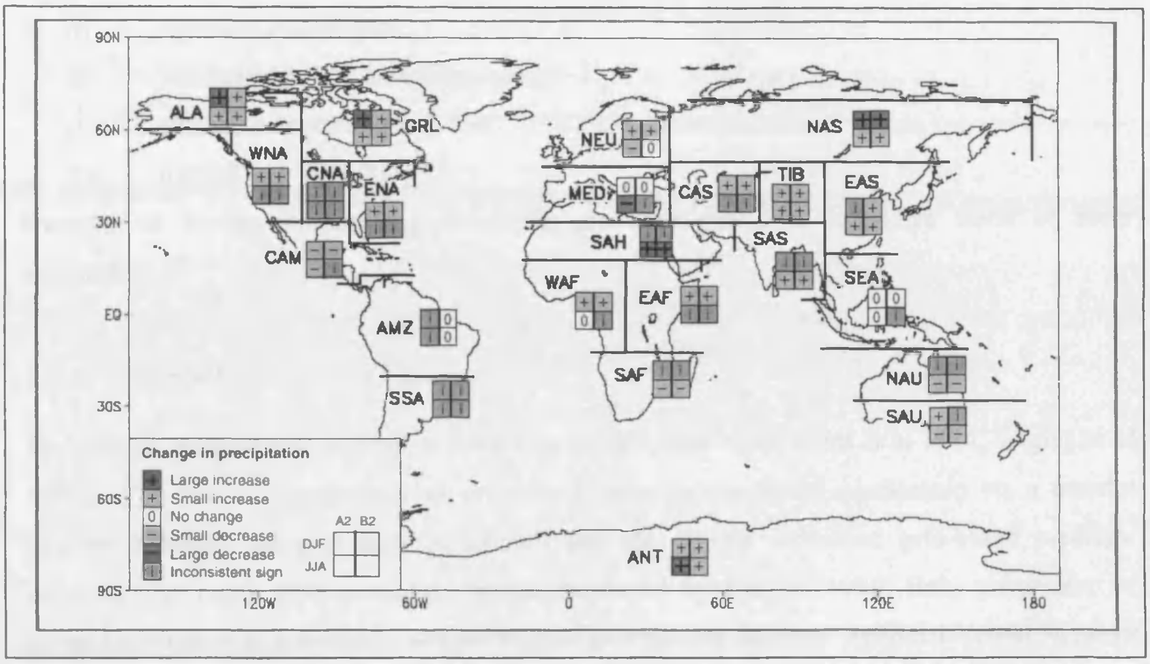

Figure 1.1 Analysis of inter-model consistency in regional precipitation change. Regions are classified as showing either agreement on increase with an average change of greater than 20% ('Large increase'), agreement on increase with an average change between 5 and 20% ('Small increase'), agreement on a change between –5 and +5% or agreement with an average change between –5 and 5% ('No change'), agreement on decrease with an average change between –5 and -20% ('Small decrease'), agreement on decrease with an average change of less than -20% ('Large decrease'), or disagreement ('Inconsistent sign'). A consistent result from at least seven of the nine models is deemed necessary for agreement (from IPCC 2001b).

1.3 Synoptic climatology and downscaling techniques

The use of downscaling grew in the 1990s (Hewitson and Crane 1996, Joubert and Hewitson 1997, Wilby and Wigley 1997, Xu 1999) and Yarnal *et al* (2001) comment on its prominent place in the Intergovernmental Panel on Climate Change (IPCC) Working Group I Third Assessment Report. The general limitations, theory and practice of downscaling are described thoroughly in the literature (*e.g.* Grotch and MacCracken 1991, Von Storch *et al* 1993; Wilby 1994, Wilby 1997, Wilby and Wigley 1997).

In essence all downscaling techniques relate observed mesoscale, free atmosphere predictor variables to observed sub-grid scale or station-scale predictands. Wilby and Wigley (1997) identify four categories of downscaling, three of these can be termed 'empirical-downscaling' and the fourth 'physical modelling', *(i)* regression techniques,

(ii) weather pattern-based techniques,

(iii) stochastic weather generators

(iv) limited area modelling.

However in reality downscaling techniques are more likely to hybridize some of these approaches.

1.3.1 Regression

The earliest downscaling techniques were largely regression-based (Kim *et al* 1984, Wigley *et al* 1990). The aim of regression is to establish a linear or non-linear relationship via a transfer function between sub-grid scale parameters and the coarser resolution grid-based predictor variables. A more sophisticated technique employed by Bürger (1996) links covariance of general circulation to covariance of local climate in a bilinear fashion. Artificial Neural Network (ANN) models can also be included in this type of technique since neuron weights are similar to regression coefficients. ANNs have recently attracted significant attention as they free the researcher from many of the confines of traditional techniques. In climatology use has been made by Olsson *et al* (2001) and Hewitson and Crane (2002).

A range of predictor variables have been used in the construction of regression models (Wilby and Wigley 2000). Huth (1999), for instance, used the predictors 500hpa height, sea level pressure, 850hpa temperature and 1000-500hpa thickness in an investigation of Central European climate variables. A number of studies have recently used airflow indices rather than actual variables as predictors. Spellman (2000a) employed a simple linear regression model to relate upper airflow index values to gridded precipitation over the Iberian peninsula. Hellström *et al* (2001) used four circulation indices (two components of geostrophic wind, total vorticity and 850hpa temperature) as predictors for precipitation in Sweden.

1.3.2 Weather Typing

Weather type downscaling techniques involve the identification of statistically significant associations between station/areal climatological data and a subjectively or objectively derived weather classification scheme. Numerous techniques exist and continue to be refined as knowledge expands, new problems arise and computer resources grow (Yarnal 1993). Automated classification schemes include those constructed by principal components analysis

(PCA) (White *et al* 1991), canonical correlation analysis (CCA) (Xoplaki *et al* 2000, Chen and Chen 2003), fuzzy rules (Bárdossy *et al* 1995, Bárdossy *et al* 2002), compositing (Moses *et al* 1987, Hartley and Keables 1998), artificial neural networks (ANN) (Bárdossy *et al* 1994), correlation-based techniques (Lund 1963, El-Kadi and Smithson 1996) and analogue procedures (Martin *et al* 1997).

Classification schemes are then related to surface variables, such as precipitation, by deriving a conditional probability distribution for observed data (*e.g.* mean rainfall amount) associated with each type. In the case of precipitation it is customary to subdivide series data by season or by the dominant precipitation mechanisms (Wilby *et al* 1995).

Wilby and Wigley (1997) comment that the weather type technique remains appealing because it is founded on sensible linkages between climate on a large-scale and weather on a local scale. Nevertheless investigation of issues related to the wide range of decisions in any classification process, the ambiguity at the boundaries of classes and the non-stationarity of weather type-rainfall association continue to dominate the research (Spellman 1997a). Some of these problems are overcome by the employment of indexing techniques which use a continuous characterization of atmospheric flow rather than discrete categories.

1.3.3 Stochastic Modelling

Stochastic models are convenient and computationally fast and are useful in a number of applications where the observed climate record is inadequate with respect to length, completeness or spatial coverage (Wilks 1999). They are commonly employed in two ways: they can be used to generate (*i*) likely precipitation amounts from a probability distribution for a certain atmospheric circulation type or (*ii*) a series of weather types where precipitation series are generated using first or multiple order Markov chains (Wilby 1995). These series are typically based on a 'chain-dependent process' (Todorovic and Woolhiser 1975, Katz 1977) in which separate component models are used to represent precipitation occurrence (the primary time series of precipitation occurrence and non-occurrence in a sequence of day) and precipitation intensities.

Nevertheless a number of studies have demonstrated the failure of data produced by stochastic weather generators to mimic the statistical properties of observed climate data (Hayhoe 2000).

Stochastic daily precipitation models have been deficient with respect to two potentially important characteristics. Firstly, the portrayal of interannual variability of precipitation as indicated by the year-to-year variation in monthly or seasonal precipitation is typically smaller than in the real climate (Katz and Parlange 1996). Secondly, the frequency with which these models reproduce extreme precipitation events, particularly extended droughts, has also been reported as less than observed (Semenov and Porter 1994). Nevertheless there are a number of examples in the literature of the use of this approach to downscaling, *e.g.* Bellone *et al* (2000) for Washington State, USA and Stehlík and Bárdossy (2002) for Central Europe and the Eastern Mediterranean.

1.3.4 Limited Area Modelling

Limited Area Model (LAM) downscaling involves the development of regional dynamic models at mesoscale or finer resolution with the large-scale information from a GCM (Jenkins and Barron 1996). Detailed information at spatial scales down to 10-20 km may be achieved at temporal scales of hours (*e.g.* Giorgi 1990). Although these deterministic process-based approaches are considered to give the greatest long term potential (Hewitson and Crane 1996), they are computationally demanding. Furthermore a problem exists at the interface between the GCM and the LAM, that is, how the coarse resolution grid cell of the GCM is related to the boundary conditions of the far finer LAM. This study chooses to investigate only empirical methods which use deductive rather than inductive approaches. Yarnal (1993 p6) comments that an inductive-deductive split in science is not new and should, in any case, be regarded as complementary. The synoptic climatologist '*...teases empirical relationship out of the observed record...upon which the dynamic climatologist bases his or her work. The dynamicist...develops theory which synopticians use to figure out those processes for which they should be looking.*'

1.3.5 Choice between downscaling methods

One of the drawbacks of synoptic climatology is that it has no recognizable theory and methodology. This research evaluates a number of methods and techniques that together create an appropriate synoptic climatological methodology for the chosen area.

Rummukainen (1997) offers the following choice of methods, *(i)* *Downscaling with surface variables.* This involves the establishment of empirical relationship between large-scale averages of surface variables and local scale surface variables using local time series (Kim *et al* 1984, Wilks 1989).

(ii) *The Perfect Prognosis (PP) method* (Zorita *et al* 1995) in which observations of large-scale free tropospheric variables and local surface variables are related.

(iii) *The Model Output Statistics (MOS) method (e.g.* Karl *et al* 1990) which is similar to the PP method but the free atmospheric variables are taken from GCM output.

Each of these methods offers advantages and disadvantages and the appropriate selection depends on a balance between the needs of the research, the skills of the investigator and the nature of the data (Frakes and Yarnal 1997). There is a pressing need for intercomparisons of methodologies (including both techniques and methods) and a clear quantification of their relative accuracy (DoE 1996, Wilby *et al* 1998). Investigators have no basis on which to judge which synoptic method is most suitable to their application (Yarnal 1993). A number of studies have made progress by applying several synoptic/downscaling techniques to a common data set and evaluating their relative performance. Examples of validation studies include Huth (1999) who compared CCA, singular value decomposition and three multiple regression models for precipitation estimation at 39 stations in central Europe, Trigo and Palutikof (1999) who compared results derived from linear and non-linear techniques in Spain, Zorita and Von Storch (1999) who evaluated the relative merits of simple and sophisticated statistical models, Benestad (2001) who has compared PCA and analysis of robustness and Schoof and Pryor (2001) who compared regression and ANN methods in mid-west USA. Xu (1999) compared statistical downscaling approaches using *table 1.1.* This table effectively summarizes the methods undertaken in the present study. In addition to a comparison of statistical techniques it is proposed that a full synoptic methodology should be evaluated and this includes investigation of alternative data formats.

	Procedures	Advantages and shortcomings
Regression Method	1. Identify large-scale predictor, *G*, that controls a local parameter, *L*. 2. Find a statistical relationship between *L* and *G*. 3. Validate the relationship with independent data. 4. If the relationship can be confirmed, *G* can be derived from GCM experiments to estimate *L*.	Simple and less computationally demanding. Application is limited to sites, variables and seasons when the local climate is related well to the conditions in the free troposphere. Very long observation series are needed.
Circulation Method	1. Classify atmospheric circulation patterns into a limited number of classes. 2. Simulate weather types through the use of stochastic models. 3. Link the likelihood of rainfall occurring to weather type, using conditional probabilities. 4. Simulate rainfall and/or other hydro-meteorological processes using weather types.	Possible to generate daily sequences of precipitation at any point for any number of days based on limited historic datasets. Weather classification schemes are somehow parochial and/or subjective. There is a need for more general classification systems (Wilby 1994).
Weather Generator Method	1. Use observed daily rainfall data to determine the probability of the state of a day. 2. Use exponential (or other) distribution to fit and estimate the amount of rainfall on a wet day. 3. Condition the other weather variables on the wet/dry states of the day.	Able to generate realistic statistical characteristics of daily rainfall series. Relies on GCM predicted changes in mean precipitation which are known to be unreliable – a problem that is of primary importance to hydrology and that has yet to be resolved (Mearns *et al* 1995).

Table 1.1 A comparison of the main forms of statistical downscaling (from Xu 1999).

1.4 Aims and objectives of this study

The overall aim of this study is to determine an appropriate synoptic methodology for the examination of rainfall in Spain. The achievement of this requires the development of a number of synoptic catalogues and the empirical evaluation of the utility of these catalogues to the explanation of rainfall amounts. Subsidiary aims include the investigation of other characteristics of the atmospheric circulation (such as persistence and trends), aspects of the rainfall distribution (the incidence of extreme events) and the assessment of the success of empirical modelling to the estimation of future rainfall amounts. These are only preliminary studies and illustrate the great utility of the method and the potential scope of further work.

The first stage of many synoptic climatological analysis is to identify spatial variation over a sample area (Yarnal 1993) and this procedure is undertaken in *Chapter 2*. In *Chapters 3-6* a variety of techniques for characterizing circulation are developed and evaluated (*i.e.* the PP method). Techniques are subdivided as follows,

(i) on the basis of temporal resolution – daily and monthly;

(ii) on the basis of determination method – manual and automated;

(iii) on the basis of data type - nominal or interval;

(iv) on the basis of atmospheric circulation – surface or mid-tropospheric.

The study takes a further step in *Chapter 7* by using synoptic catalogues to downscale future rainfall scenarios (*i.e.* the MOS method*)*. Climate Change scenarios in this project were supplied by the Canadian Centre for Climate Modelling and Analysis (CCCMA). CCCMA is a division of the Climate Research Branch of the Meteorological Service of Canada and conducts research into coupled and atmospheric climate modelling, sea-ice modelling, climate variability and predictability and the carbon cycle. CCCMA have developed a number of climate simulation models for climate prediction and the study of climate change and variability (see *appendix 1.1).* In 1999 the U.S. National Academy of Science identified CGCM1 of CCCMA as one of the leading performers in climate systems simulation and recommended that its result be used in the U.S. National Climate Change Assessment (CCCMA 2003). Results were also used by the Intergovernmental Panel on Climate Change (IPCC 2001a). The success of downscaling depends on accurate GCM output, Bengtsson (1995) comments that regional climate prediction requires) good global prediction by coupled climate models as '*...without it regional simulations are useless.*' The overall structure of this thesis is depicted in *figure 1.2.*

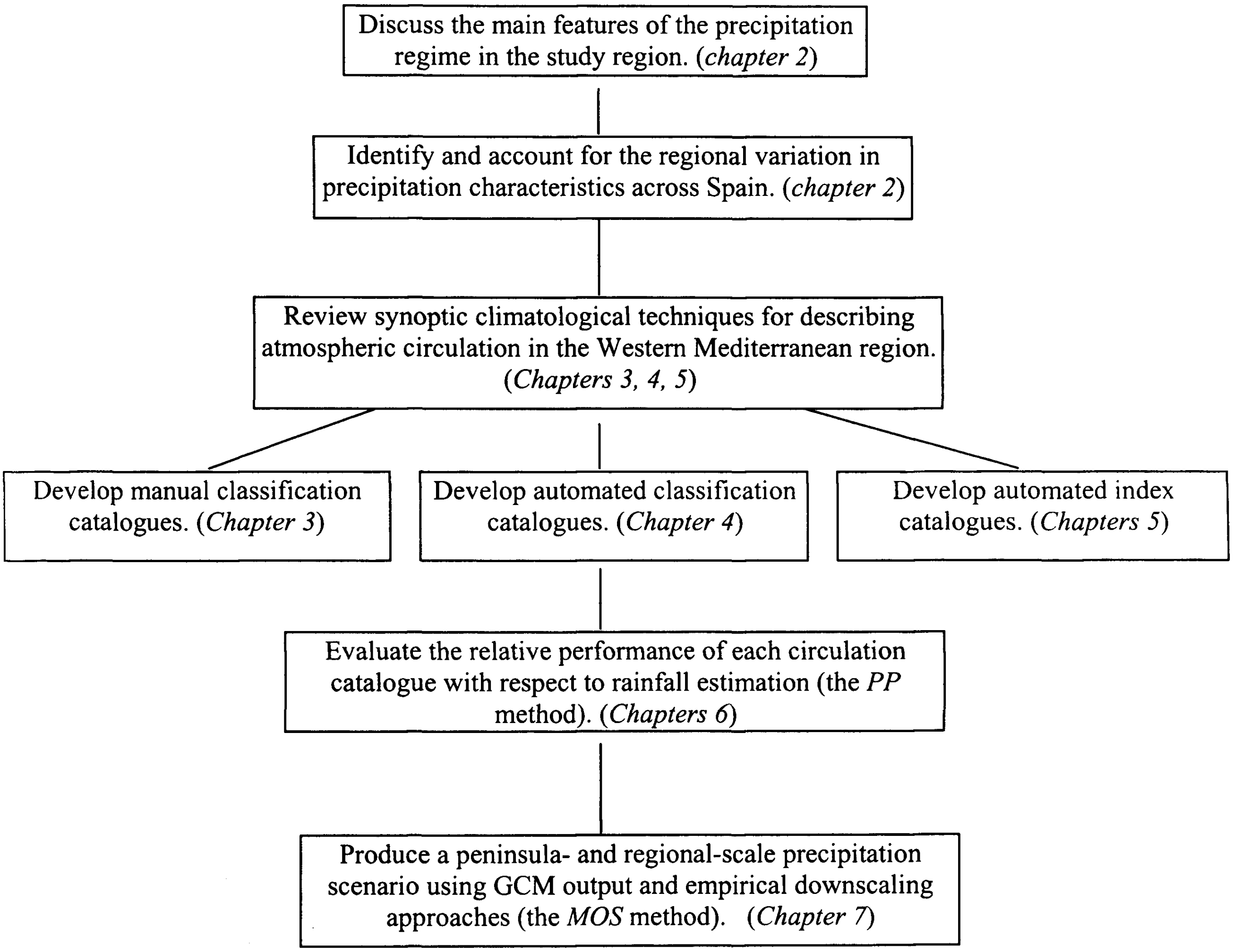

Figure 1.2 The structure of this thesis.

Chapter Two
Characteristics of precipitation in Spain

2.1 Introduction

A considerable amount of recent work has been undertaken on aspects of the precipitation variability of the Iberian Peninsula, particularly for Spain (Serra *et al* 1998, Rodrigo *et al* 1999, Rocha 1999, Romero *et al* 1999, Lana and Burgueño 2000, Rodrigo *et al* 2000, Spellman 2000a, 2000b, Sumner *et al* 2001, Ramos 2001, Garcia 2002). A number of reasons can be proposed for this surge in academic interest ranging from the significant temporal and spatial variability of Spanish rainfall to the serious consequences for the water resource that have been suggested by climate model scenarios (IPCC 2001a). This chapter outlines geographical aspects and the patterns of precipitation in the study region (*figure 2.1*).

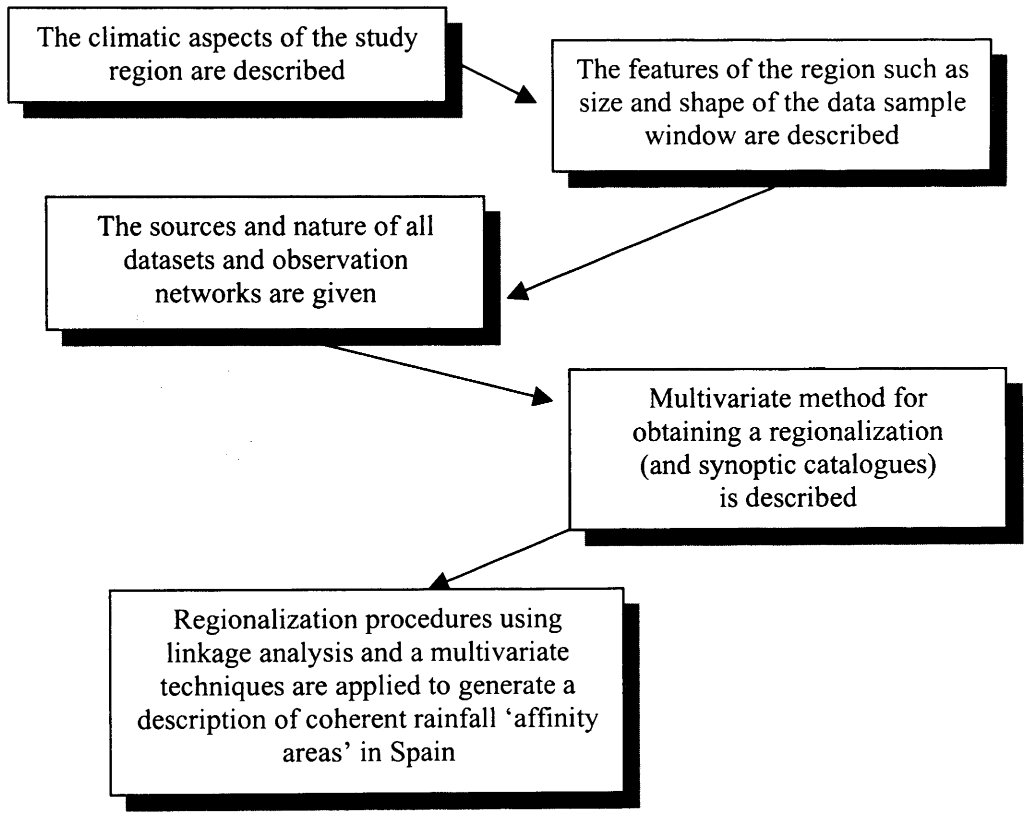

Figure 2.1. Outline of Chapter 2.

2.2 *The meteorology and climatology of Spain*

The climatology of rainfall over the Iberian peninsula (*figure 2.2*) is distinguished by two key features – seasonal and regional variability (Wheeler 1996). Precipitation variability is of primary importance due to its considerable impact on those social and economic activities that are heavily reliant on water resources, for instance agricultural production and tourism (Kent *et al* 2002).

Figure 2.2 Schematic representation of the location of Spain and the Iberian Peninsula.

2.2.1 *Seasonal variation*

The distinct seasonal variation in rainfall occurrence is broadly explained by hemispheric-scale shifts in the patterns of atmospheric circulation (Spellman 1997a). The surface barometric pressure field of the entire Mediterranean region is controlled by changes in the position and intensity of the quasi-permanent Azores Anticyclone, the winter Siberian Anticyclone, the north-west extension of South Asia summer thermal lows, as well as more transient travelling anticyclones and depressions *(figures 2.3 and 2.4).*

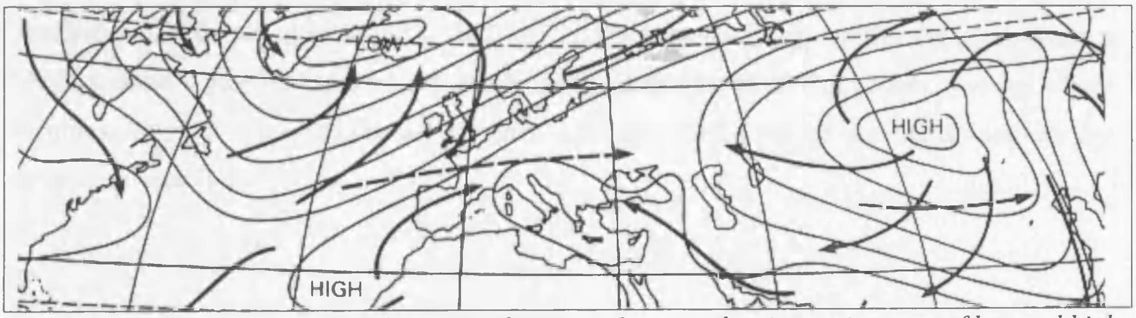

Figure 2.3 General atmospheric circulation in January showing main areas of low and high pressure (adapted from Musk 1988).

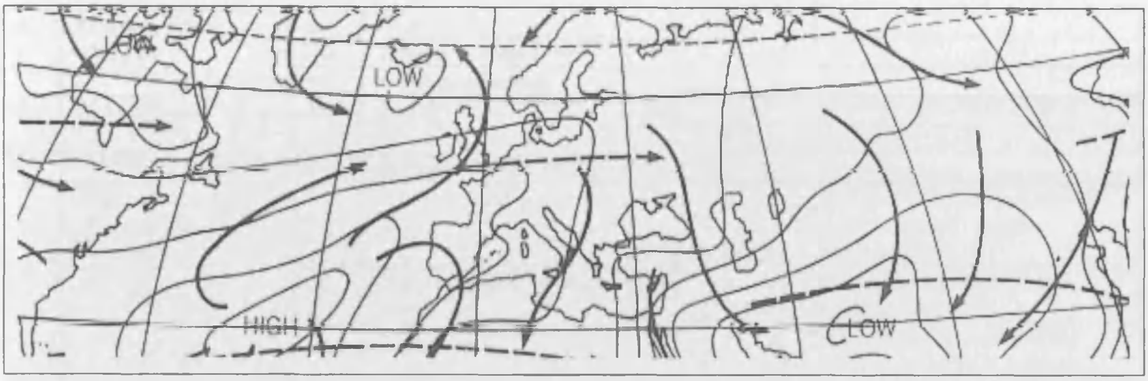

Figure 2.4 General atmospheric circulation in July showing main areas of low and high pressure (adapted from Musk 1988).

2.2.2 Regional climatic variation in Spain

Köppen's climate regionalization, still the most commonly employed system, divided the Iberian peninsula into the distinct climatic zones listed in *table 2.1* and depicted in *figure 2.5* (Barry and Chorley 1998). Although this zonation is based on all climatic elements, precipitation distribution is probably the most important differentiating factor in Spain. Broad differences are described as; (*i*) a consequence of the surrounding thermally distinct water bodies and (*ii*) the latitude of the zone. There is a clear distinction between the influence of the Atlantic Ocean in the north and west and the Mediterranean Sea in the south and east. Superimposed on these maritime effects is that of continentality, and topographic/altitudinal effects. What *figure 2.5* does not capture are the seasonal shifts in these boundaries. The regionalization technique employed in *section 2.10* does, however, show these movements.

The Mediterranean climatic region has been described as a transitional zone between the continental influences of Europe and Asia, the desert climate of North Africa and the oceanic effect of the Atlantic (Maheras *et al* 1999). A defining feature is the virtual absence of precipitation in the summer period. Tarifa (36°N 5°W) (*figure 2.6a*), typifies the south-western Mediterranean region (Köppen's *Csa*), exhibiting a monthly mean rainfall pattern in which winter months have more or less uniformly high[1] (over 120 mm) rainfall yet the summer is relatively dry (mean July total is 3 mm).

[1] With respect to the Iberian peninsula.

A	**Tropical Rainy Climates**	*AF*	*Tropical Rainy*		
		Aw	*Tropical wet-and Dry*		
		Am	*Tropical Monsoon*		
B	**Dry Climates**	*BS*	*Steppe*	Bsh	Mean annual temperature above 18° C
				Bsk	Mean annual temperature below 18° C
		Bw	*Desert*		
C	**Mid latitude rainy climates, mild winter**	*Cs*	*Mediterranean*	Csa	Three times as much rainfall in a winter month as in driest summer month. Warmest month is over 22°C.
		Cf	*Mid-latitude rainy, mild winter*	Cfa	At least 30mm rainfall in each month. Warmest month is over 22°C.
				Cfb	At least 30mm rainfall in each month. Warmest month is under 22°C but four months are over 10° C.
				Cfsb	Three times as much rainfall in a winter month as in driest summer month. At least 30mm rainfall in each month. Warmest month is under 22°C but four months are over 10° C.
		Cw	*Mid latitude wet-and-dry, mild winter*		
D	**Mid latitude rainy climates, cold winter**	*Dw*	*Mid latitude wet and dry, cold winter*		
		Df	*Mid latitude rainy, cold winter*		
E	**Polar Climates**	*ET*	*Tundra*		
		EF	*Ice cap*		
H	**Highland Climate**				

Table 2.1 Climatic zones on the Iberian peninsula (see figure 2.5). Source: El Païs 1992.

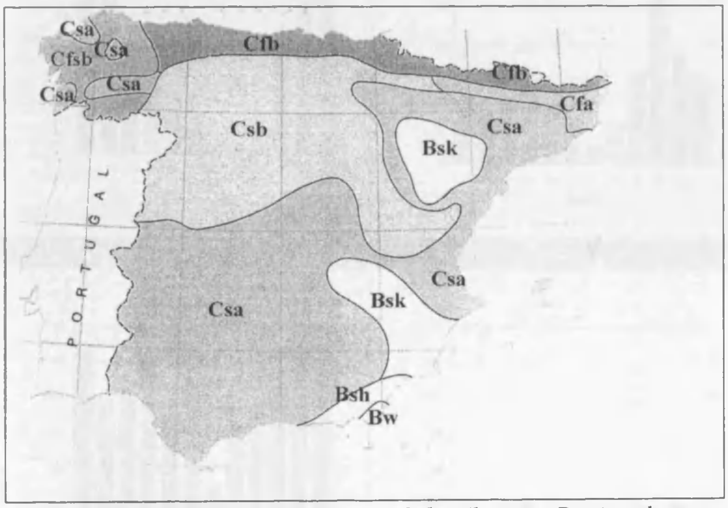

Figure 2.5 Climatic zones of the Iberian Peninsula according to Köppen (Source: El Païs 1992). See table 2.1 for key to abbreviations.

In the north-east temporal distribution of rainfall is very different, although this region is still classified as 'Mediterranean'. Maheras (1988) identifies a summer dry period but an uneven monthly distribution in the rainy period, namely, a primary maximum in autumn and a secondary one in spring. These peaks are related to meridional (north-south) atmospheric flow (Wheeler 1990), commonly regarded to be a main agent governing precipitation incidence over the whole Mediterranean (Etienne and Godard 1970). It is exemplified by the mean monthly pattern for Valencia (39°N 0°W) (*figure 2.6b*), which displays a distinct peak in October (October has 60% more rainfall than November, the next highest month). This station is also in Köppen's *Csa* but there a distinct difference in rainfall regime is noted.

Atlantic rainfall climates (*Cfb*), as exemplified by Santander (43°N 4°W) (*figures 2.6c)* exhibit higher rainfall and often a reduced, but still apparent, degree of seasonality. The least seasonality is experienced by locations towards the eastern end of the north coastal fringe. Finally inland Spain (*e.g.* Avila (41°N 5°W) (*figure 2.6d)*) exhibits a drier and less seasonal regime with peaks in spring and late autmmn (*Csb*).

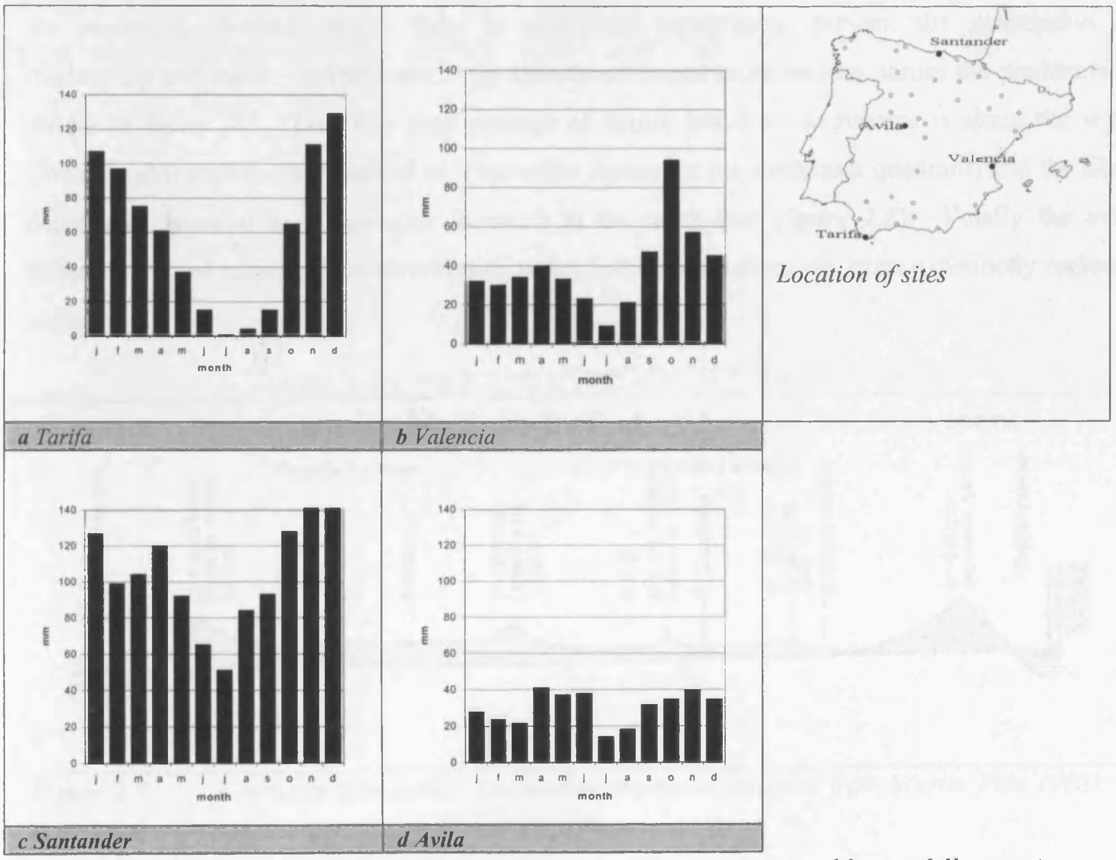

Figure 2.6 Contrasting rainfall climatologies in Spain (mean monthly rainfall in mm).

It is relatively commonplace in regional climatological studies to use the 'nation-state' as the study region rather than any physiographic unit (*e.g.* Goldreich 1994, Trigo and Dacamara 2000). Consequently this study does not examine rainfall in Portugal. Furthermore problems are raised as daily precipitation records from the locations in the latter country have a considerable number of missing values.

Three geographic characteristics explain Spain's climatic regionality (Wheeler 1996). The first relates to its size: Spain is one of Europe's largest nations with a surface area of 492,246 km^2 (excluding island groups) and so distance from the sea (at a maximum of over 500 km) and subsequent climatic continentality are important controlling factors. The second, which enhances the effects of the first, is altitude. More than half of the surface area of Spain is over 500 metres above sea level (asl) and 84,000 km^2 (17%) is above 1000 metres asl (the mean altitude is 600 metres asl). Altitude can accentuate the effects of continentality in some regions and in others influence levels of precipitation through orographic enhancement (forced lifting and promotion of convective heating) and downwind rainshadow effects. Furthermore the narrow coastal plains of the peninsula, 'behind' which there is significant topography, prevent the penetration of moderating and moist maritime air. An altitude-enhanced cross-section across the peninsula is shown in *figure 2.7*. The only easy passage of humid low-level airstreams is along the wide Gualdalquivir depression (marked as '*Depresion Betica*' in the south-east quadrant) and the Ebro depression (marked as '*Depresion Iberica'*) in the north-east (*figure 2.8*). Finally the very different thermal nature of the surrounding water bodies, will ultimately exert a distinctly regional impact.

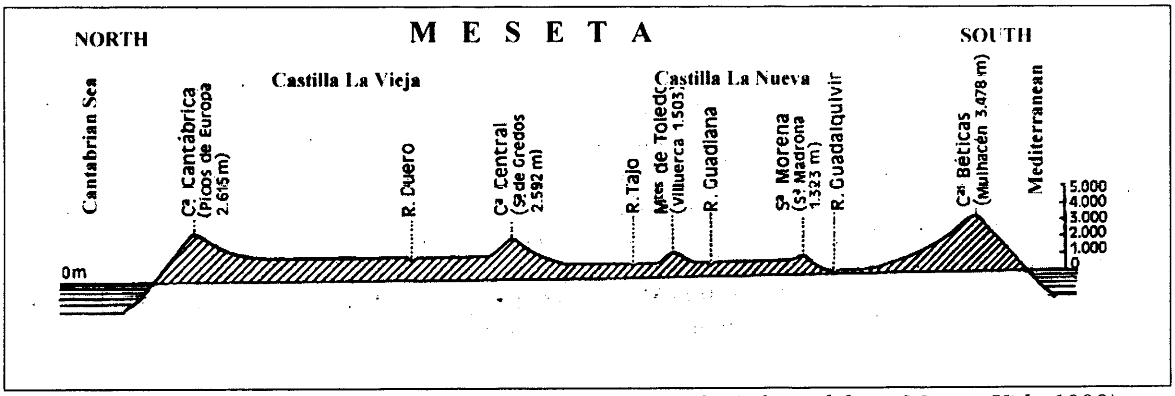

Figure 2.7 *A cross section across the Iberian peninsula (adapted from Martin Vide 1988).*

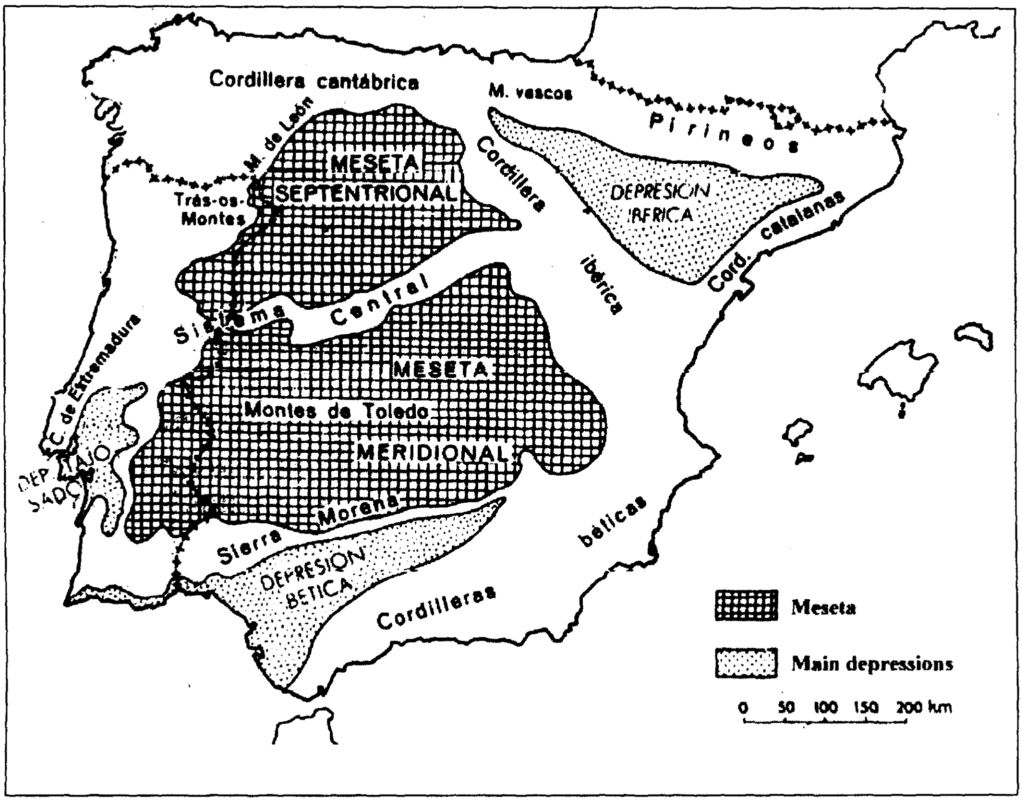

Figure 2.8 Some geographic influences of the Iberian peninsula on rainfall amounts (adapted from Martin Vide 1988).

2.3 *The sample window*

Features of the sample window (or the study area) can combine to influence the success of synoptic climatological methods with respect to: (*i*) the validity of a regional atmospheric circulation assessment; (*ii*) the relative importance of synoptic controls against other controlling geographical variables and (*iii*) the inter-relationship between circulation and these geographic features. The main features of the sample window are size, shape, elevation and the nature of topography. Description of sample window shape is given in *appendix 2.1.*

2.3.1 Size

The output of any synoptic climatological approach will depend on the nature (density and spatial extent) of data sampling. Nevertheless there has been relatively little discussion in the literature of the effect of the size of data windows. Saunders and Byrne (1998) state that the spatial extent of a sample window is important and, commenting on their analysis of the synoptic controls on snowfall in Canadian Prairie provinces, concede that a larger window could result in a stronger relationship between the surface variable and synoptic conditions. Reflecting on the methodology for the examination of circulation over the British Isles, El-Kadi and Smithson (1996 p144) note that the, '*...grid should have covered a larger area, extending further west in the direction of approach of most pressure systems...*' On the other hand, increased variability of within-type circulation will confuse the assessment of the synoptic control on the environment and this inevitably will increase with greater areal extent. Mayes (1996) has examined the application problems that can arise when regional variations occur under LWT classifications of the British Isles. *Figure 2.9* illustrates this problem with respect to the Iberian peninsula. In the north-west of the peninsula flow is westerly and in the east it is northerly. This situation is often associated with the passage of depression systems.

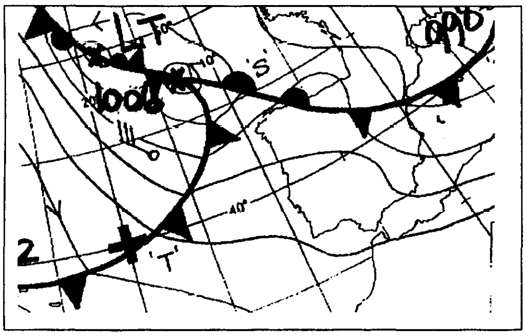

Figure 2.9 Regional variation in flow direction on 24.11.88.

Much greater pattern variation is found in sea level circulation patterns compared to higher atmospheric altitudes. At the latter level airflow patterns become smoother and coherent structures can be found covering much wider areas (examples are given in *figure 2.10*).

At the outset of this study a sample of one hundred and thirty two sea level isobaric charts and eighty 500hPa contour height charts (drawn from the period 1981-1990) were qualitatively examined for the effect of sub-window regional variability and the study area was (subjectively) adjusted to reduce this impact (see *appendix 2.2*). The sample window (*figure 2.11*) encapsulates the region bounded by 20°W-10°E and 35°N-45°N (except for predetermined synoptic indices (*i.e.* North Atlantic Oscillation Index and the Zonal Index)). It includes an upwind region to the west and a region to the east of the peninsula in order to capture both the more common westerly flow and the less frequent, but nonetheless rain-bearing, easterlies.

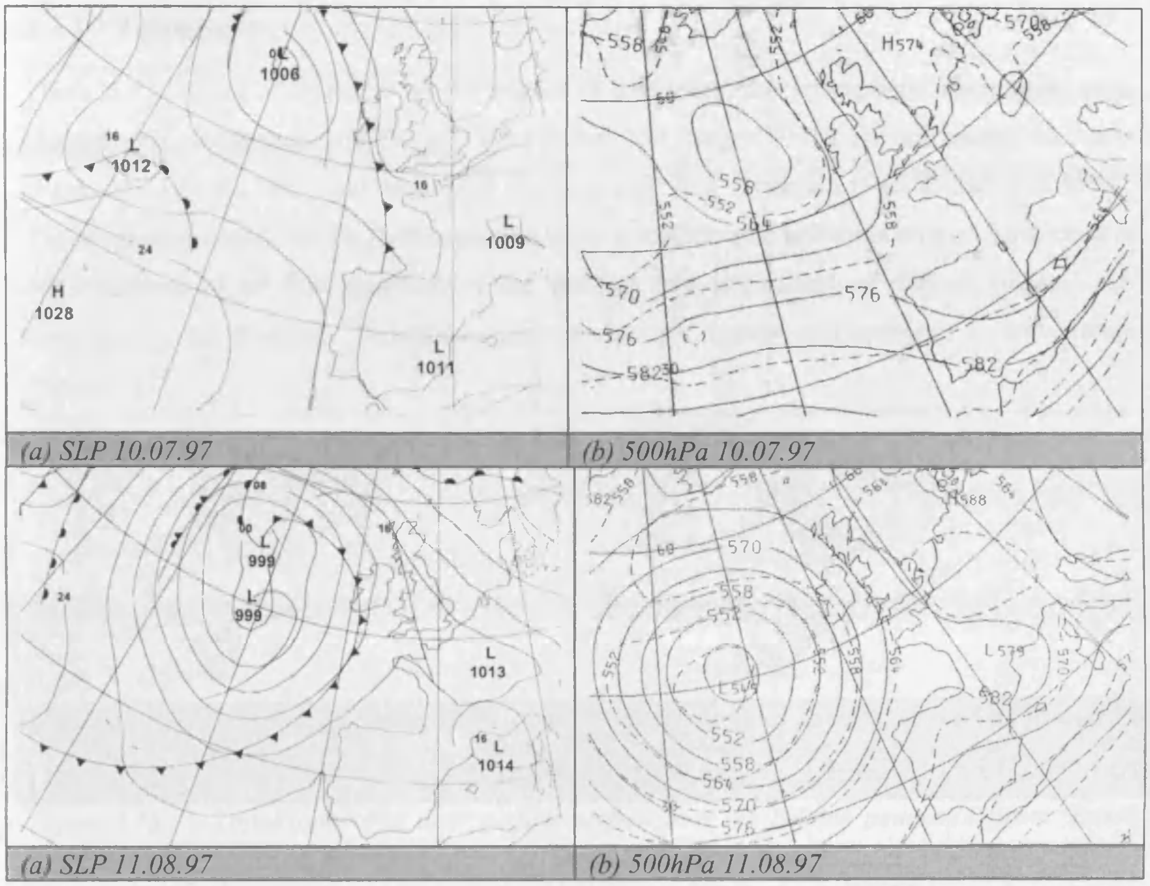

Figure 2.10 Contrast in pattern complexity between (a) SLP and (b) 500hPa.

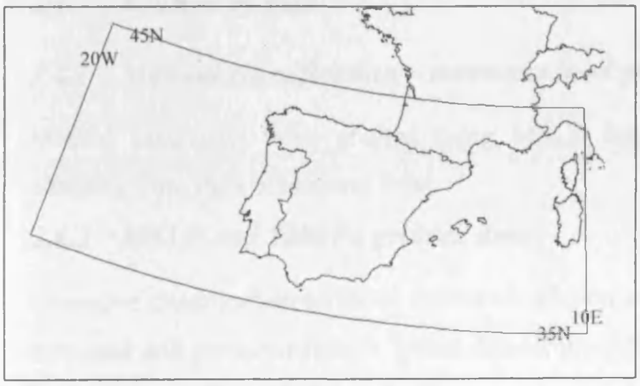

Figure 2.11 The sample window.

2.3.2 Elevation

Elevation will strengthen vertical air movement by encouraging the forced uplift of air. This is not captured by a (two-dimensional) synoptic catalogue interpretation of airflow yet surface height will influence the precipitation response to circulation pattern.

2.3.3 Topography

There is a plethora of literature on the impact of topography on atmospheric circulation (*e.g.* Danard 1976, Whiteman and Doran 1993, Weber and Furger 2001), the movement of fronts (Egger and Hoinka 1992) and on rainfall characteristics (*e.g.* Bonacina 1945, Basist *et al* 1994). The orographic context of the Iberian peninsula has a considerable influence on the characteristics and behaviour of air flow (particularly the blocking and channelling of cold air masses) and consequently the climate. Topography provides barriers against, and openings to, air currents (*figure 2.12).*

(a) Topographic barriers and gateways exist to allow the penetration of maritime air into the peninsula.

(b) Orographic corridors also exist to allow flow of air towards the sea from the interior

Figure 2.12 Topography and near surface airflow over the Iberian peninsula (from Garcia and Reija 1994).

2.4 Sources of data

2.4.1 Manual classification – mean sea level pressure (MSLP) and 500hPa charts

Manual catalogues were created using MSLP and 500hPa charts (1958-1997) which were obtained from the UKMO and INM.

2.4.2 MSLP and 500hPa gridded data

Objective classification series of surface circulation are constructed using grid-point pressure data extracted and prepared from a global dataset provided by the UKMO. The MSLP and 500hPa catalogues use a grid 2.5 degrees longitude by 2.5 degrees latitude bounded by 45°N, 20°W and 35°N, 10°E (see *figure 2.13*).

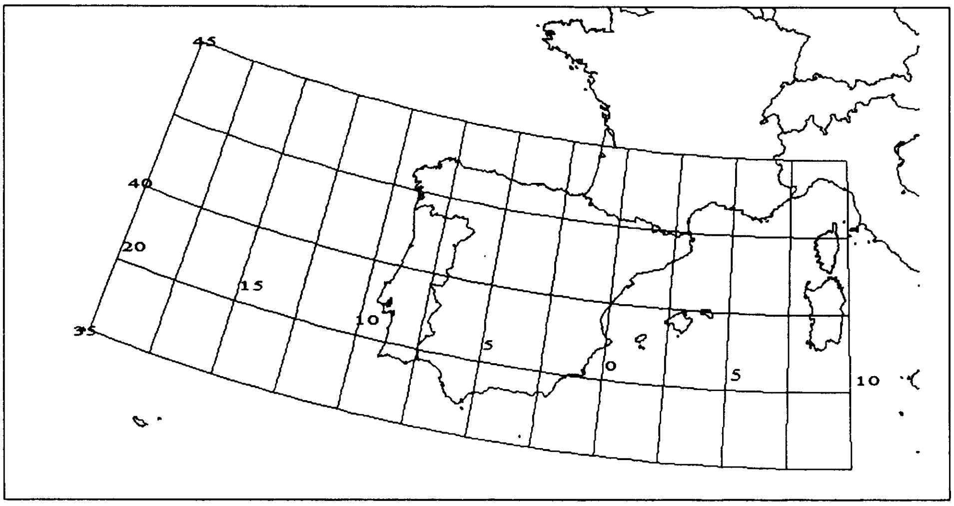

Figure 2.13 *Grid used for MSLP and 500hPa datasets.*

Craddock (1965) comments that if the network of points chosen for a study area is too widely spaced, so that observations at adjacent points are uncorrelated, then features of importance can go unrecognized. Small systems may pass through the grid and be lost altogether (Kidson 1994) or affect single points where they appear as 'noise' (Craddock 1973). On the other hand correlations between points can be too high if the network is dense and sample size is therefore unnecessarily large. Numerous synoptic studies have used MSLP data yet there is little agreed convention on the spacing distance of MSLP grid points (El-Kadi and Smithson 1996).

2.4.3 Index data

Index datasets were calculated either from the UKMO gridded data or obtained in a final format from CRU (2002).

2.4.4 Precipitation data

The study uses a variety of precipitation time series.

(a) *Station series (supplied by INM)*

- Annual precipitation series from the *INM Series K* (and derived from monthly sources).
- Monthly precipitation from 44 principal observation stations in Spain 1961-1990 (*figure 2.14*) obtained from *INM Valores Normales Y Estadisticos de Estaciones Principales (1961-1990)* and supplemented by monthly data sets derived from daily INM data.
- Daily precipitation series from principal INM observation stations in Spain (1958-1997).

(b) *Areal average series (supplied by CRU)*

- Monthly gridded precipitation extracted from a global precipitation dataset (1958-1997) (*figure 2.15*).

For the necessity of brevity daily data for stations representative of precipitation regions in Spain (as defined *section 2.10*) are used to evaluate the daily models. Grid point areal average data are employed to examine the monthly synoptic models.

Figure 2.14 Monthly precipitation locations 1961-1990 (see appendix 2.3).

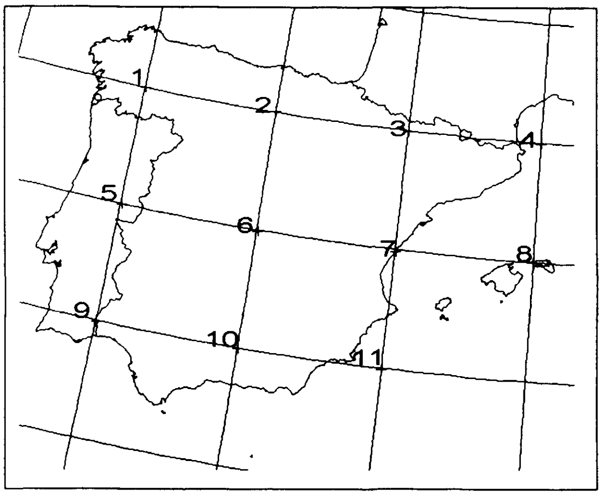

Figure 2.15 *Grid points used in areal precipitation dataset (see appendix 2.4)*

2.4.5 Description of pluviometric network

The network of principal stations reflects the spatial distribution of significant urban centres in Spain (of the 44 stations used ~75% are located in urban areas amongst the largest[2] 40 urban centres in Spain). The shape and dispersion of sample points is therefore dictated by the social, historical and economic factors that created the settlement distribution in the country rather than any pre-determined rules of required station spacing (see Linacre 1992).

The spread of the station data can be examined for dispersion using a simple Nearest-Neighbour Index (NNI) (Clark and Evans 1954). In this case the calculated NNI is 1.81 (*figure 2.16*) which indicates that the distribution of rainfall observation sites in Spain cannot be regarded as significantly dispersed at $p<0.050$. *Figure 2.17* depicts that, as a result, some extensive regions (most noticeably the eastern meseta) are not represented by principal observation stations. This is a response to the low population density in certain areas. This will affect the regionalization process as precipitation region boundaries will be impossible to locate precisely in this area. The areal average dataset also uses data derived from secondary pluviometric stations and thus is not affected by this problem.

[2] over 130,000 inhabitants

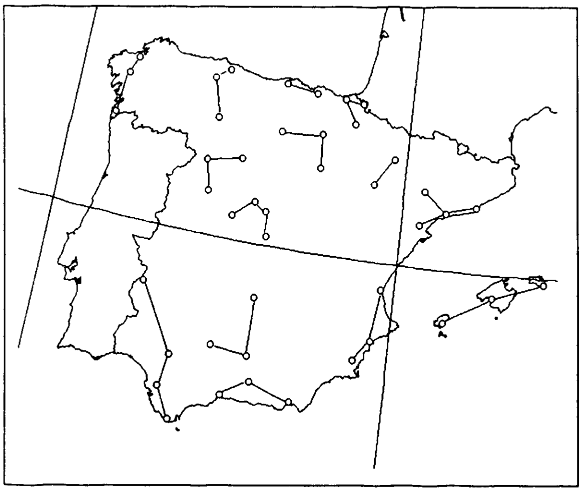

Figure 2.16 Distances used in the calculation of the NNI.

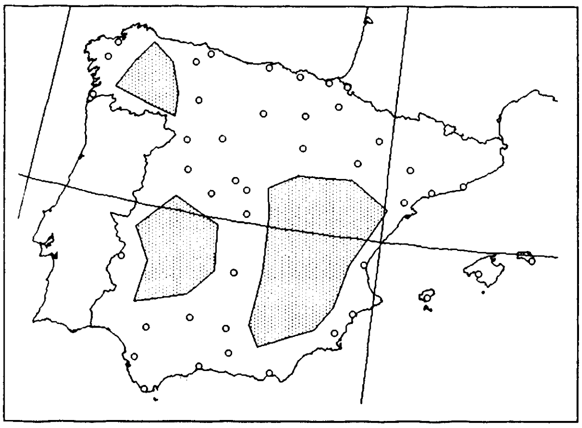

Figure 2.17 Approximate areas that are outside the maximum NNI distance of the rainfall network.

2.5 Summarizing the dataset

2.5.1 Data type

A comparison of rain day incidence permits an identification of the spatial extent of the precipitation mechanism (*e.g.* frontal/cyclone passage or isolated convective storm). Regionalization using raindays is described first (*section 2.13*) as it better reflects rainfall mechanisms – variability in rainfall incidence under a given synoptic feature is considerably less than variability in rainfall amounts due to local influences on the latter. On the other hand rainfall totals are of greater practical application, are more readily available and is the variable that is modelled by current GCMs. This study considers both rain days and amounts but concentrates on the latter.

2.5.2 *Dataset size*

The World Meteorological Organization states that the 30-year averaging period commonly used for climatological purposes is sufficient to capture any extremes expected in a climate dataset. This study circumvents some sample size problems by using the full 40-year period (1958-1997) for which extensive reliable data are available however it is likely that even this time period will not adequately capture the upper end of the rainfall distribution and this should be noted in any empirically derived future scenario.

2.5.3 *Data subdivision*

A variety of temporal scales of precipitation behaviour can be examined (annual, seasonal, monthly and daily). Considerable attention in the study is given to the seasonal scale. A motivation for downscaling in Spain is the examination of water resource deficits and the associated ecological problems of desertification and forest fires (Lavorel *et al* 1998, Puidefabregas and Mendizabal 1997). Seasonal scale changes are therefore of greatest concern. Many of the seasonal summaries in this study employ a simple high-sun season (AMJJAS[3]) and low-sun season (ONDJFM[4]) (used by Mearns *et al* 1997). The traditional four season division is not universally applicable and not entirely relevant to the Iberian region (Spellman 2003). Some 'all year' data summaries are also listed.

2.6 *Missing data*

It is rare for any instrumental record to be complete. Consequently it is often necessary to apply a technique to provide realistic estimates of missing values. Sumner (1983) states that in an area where topography has a limited influence, this can be done by taking the mean value of values from three or four 'surrounding' gauges. Although the problem of missing data is insignificant due to the completeness of the INM and areal datasets, in the few instances where this is necessary this study uses a method used by Rodriguez-Puebla *et al* (1998) to complete small gaps in the daily record. A correlation matrix was computed amongst the time series to select the four surrounding precipitation series with rainfall characteristics that most resembled those of the station with missing data then a linear spatial regression was derived in order to interpolate the missing values.

[3] April, May, June, July, August, September.
[4] October, November, December, January, February, March.

2.7 *Areal data*

For many hydrological and engineering studies a detailed point-based assessment of precipitation patterns is not required. Instead some measure of the total volume of water falling on an area is preferred and therefore areal data is often of greater use than point source figures. The simplest measure of areal precipitation is to calculate an arithmetic mean from the values of all gauges in an area. This can be undertaken when there is an even spread of gauges and when topography is relatively flat and even. In this study a historical monthly precipitation dataset (*gu23wld0098.dat (Version 1.0)*) for global land areas from 1900 to 1998, gridded at 2.5° latitude by 3.75° longitude resolution was obtained and the relevant region and time period extracted. This dataset was constructed by CRU and supplied by Hulme (2000). The gridding method used to obtain the areal data is explained by Hulme (1992, 1994) and Hulme *et al* (1998).

Table 2.2 lists the precipitation characteristics of gridpoints and *figure 2.18* depicts the statistical association (Pearson's Product Moment (PPM) correlation coefficient '$r = 0.700$'[5]) between the 11 grid point data series and station data (monthly rainfall amounts). In some cases (*i.e.* 2, 5, 6, 9, 10) the gridpoint data is highly correlated to monthly point data, even outside the region that is used to calculate the areal data. On the other hand monthly totals at eastern points (*i.e.* 4, 7 and 8) display weaker statistical relationships with station totals although if a lesser, although significant at $p<0.050$, r-value is plotted then significant associations do emerge. Eastern areal data is therefore less representative of points within their respective regions than areal data from the western side of the peninsula.

Grid point	Latitude	Longitude	Mean annual rainfall (mm)	Mean monthly winter rainfall (mm)	Mean monthly summer rainfall (mm)	SI
1	42.5°N	7.50°W	1152.5	132.2	59.9	0.35
2	42.5 °N	3.75°W	750.7	71.5	53.7	0.18
3	42.5 °N	0.00 °W	634.9	52.4	53.4	0.16
4	42.5 °N	3.75°E	615.2	58.7	43.8	0.24
5	40.0 °N	7.50°W	811.4	97.2	38.1	0.43
6	40.0°N	3.75°W	452.6	44.4	31.1	0.24
7	40.0°N	0.00°W	475.3	45.5	33.8	0.31
8	40.0°N	3.75°E	593.2	67.2	31.7	0.41
9	37.5 °N	7.50°W	578.8	75.9	60.6	0.54
10	37. 5°N	3.75°W	515.2	64.5	21.4	0.49
11	37.5°N	0.00°W	266.0	28.4	15.9	0.39

Table 2.2 Precipitation statistics for gridpoint based areal data (SI – seasonality Index see appendix 2.4).

[5] The use of r = 0.700 means that r-squared = 0.490, *i.e.* almost half of the variance is explained.

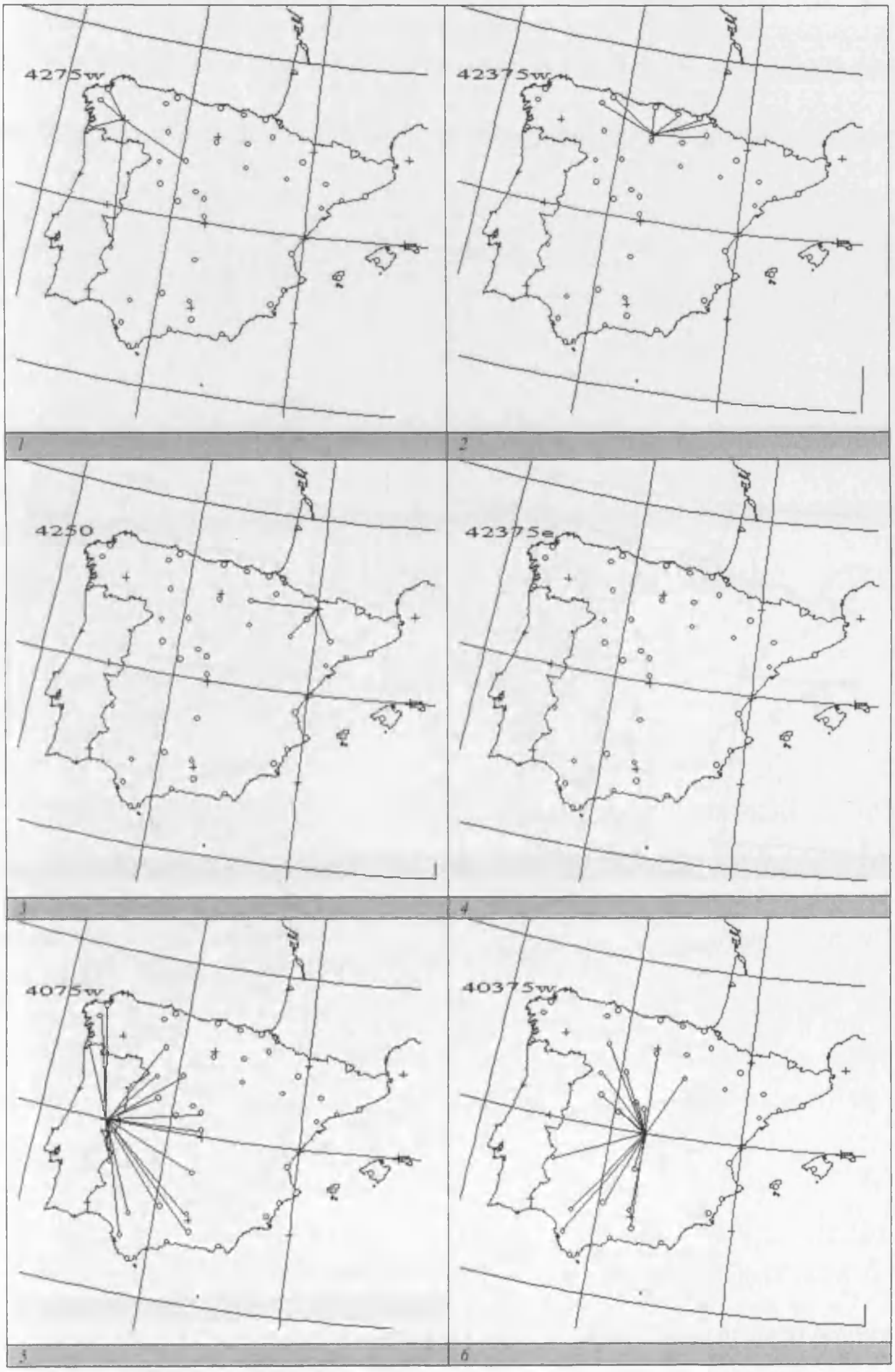
4275w
42375w
1
2
4250
42375e
3
4
4075w
40375w
5
6

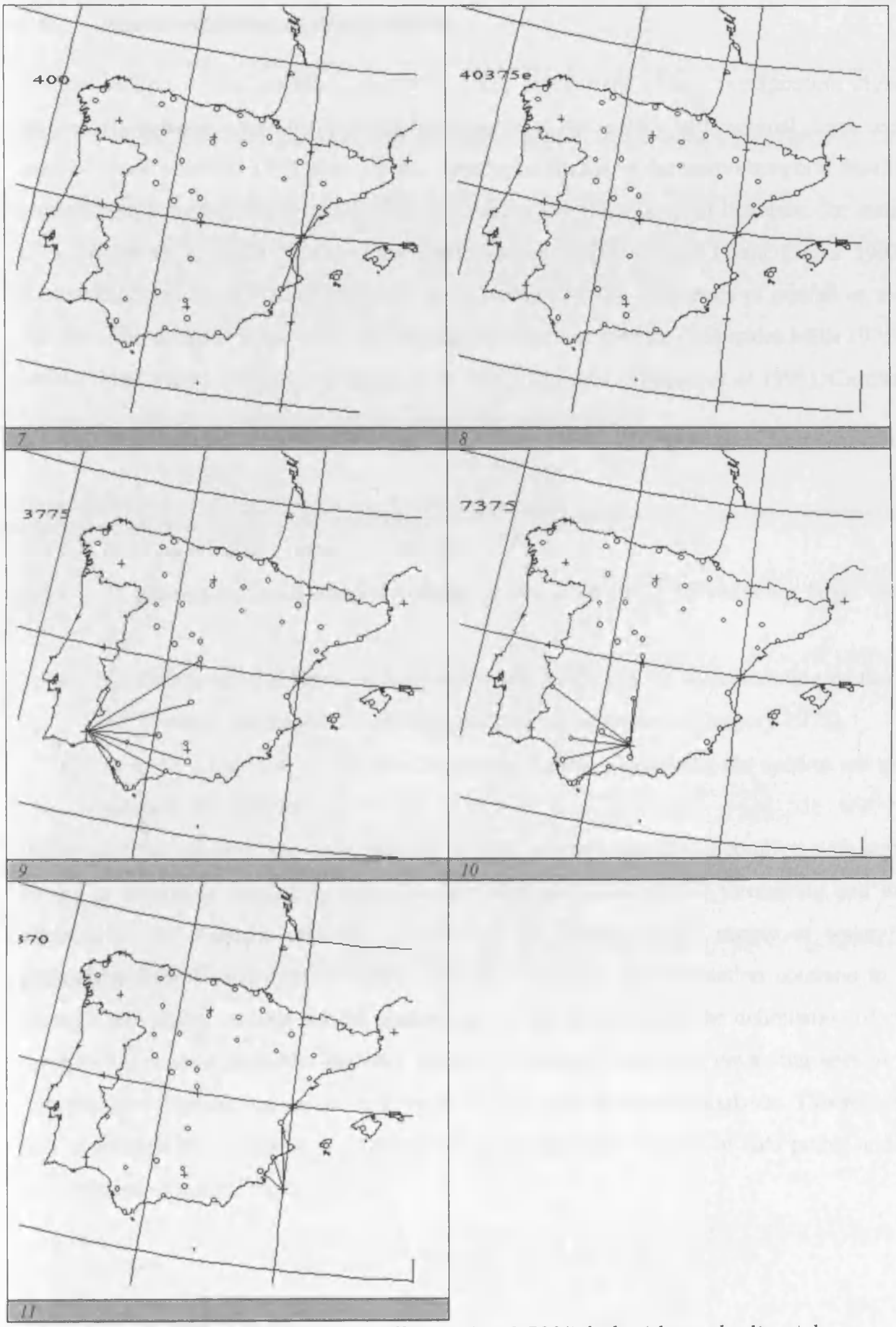

Figure 2.18 PPM correlation coefficient ('r>0.700') links (shown by lines) between monthly gridpoint data and monthly station data.

2.8 Regionalization of precipitation

The delineation of precipitation regions is a key component of any precipitation climatology, particularly in cases where the topographical nature of the surface and regional shape renders the analysis more complex (Willmott 1978). Numerous studies of the spatio-temporal distribution of precipitation in a plethora of regions can be found in the climatological literature, for instance, the USA (Walsh *et al* 1982), Wales (Bonell and Sumner 1992), Croatia (Gajic-Capka 1993), Israel (Goldreich 1994) and Iran (Domroes *et al* 1998) amongst others. The study of rainfall on the Iberian Peninsula has attracted some work, not only for the region as a whole (Fernandez Mills 1995), but for smaller areas within: Catalonia (Periago *et al* 1991), Mallorca (Sumner *et al* 1993), Castilla y Leon (Andres *et al* 2000) and the Segura River basin (Spellman 2000c).

Regionalization is undertaken for the following reasons:

- To bring structure, order and simplicity.
- To provide an intellectual shorthand (Abler *et al* 1971) by reducing large volumes of data.
- To identify spatial limits or boundaries and hence aid the understanding of the physical and dynamic processes that govern precipitation occurrence (Gregory 1975).
- To serve a practical as well as a theoretical function - avoiding the need to use all sample points in the analysis.

Regionalization improves the understanding of how geographical factors combine with atmospheric factors to determine rainfall, to improve short term and local rainfall forecasting and to aid the organisation and strategic planning of activities that depend on the supply of water. This is particularly important in regions where complex orography and circulation combine to result in sporadic and highly variable rainfall occurrence. In the present study the delimitation of co-variant precipitation regions facilitates the later synoptic analysis. Identifying covarying sites in terms of precipitation behaviour reduces the amount of sites that require detailed analysis. This procedure was also undertaken by Andres *et al* (2000) in order to reduce the amount of data points and simplify interpretation of rainfall mechanisms.

2.9 *Expressing regional rainfall affinity*

A number of methods are commonly used to identify rainfall regions. The most common, and straightforward, method is the production of contour or isoplethic maps (see *figure 2.19*). Although these clearly reveal the general nature of precipitation patterns they do not yield any information on the covariant behaviour of locations and the extent to which locations possess similar precipitation dynamics. As a result numerous correlation-based (Lund 1963, Wilmott 1987) and multivariate methods have been successfully developed. A correlation-based method for examining spatial patterns of rainfall in Spain is outlined in *appendix 2.5* but not outlined in this thesis due to space restrictions.

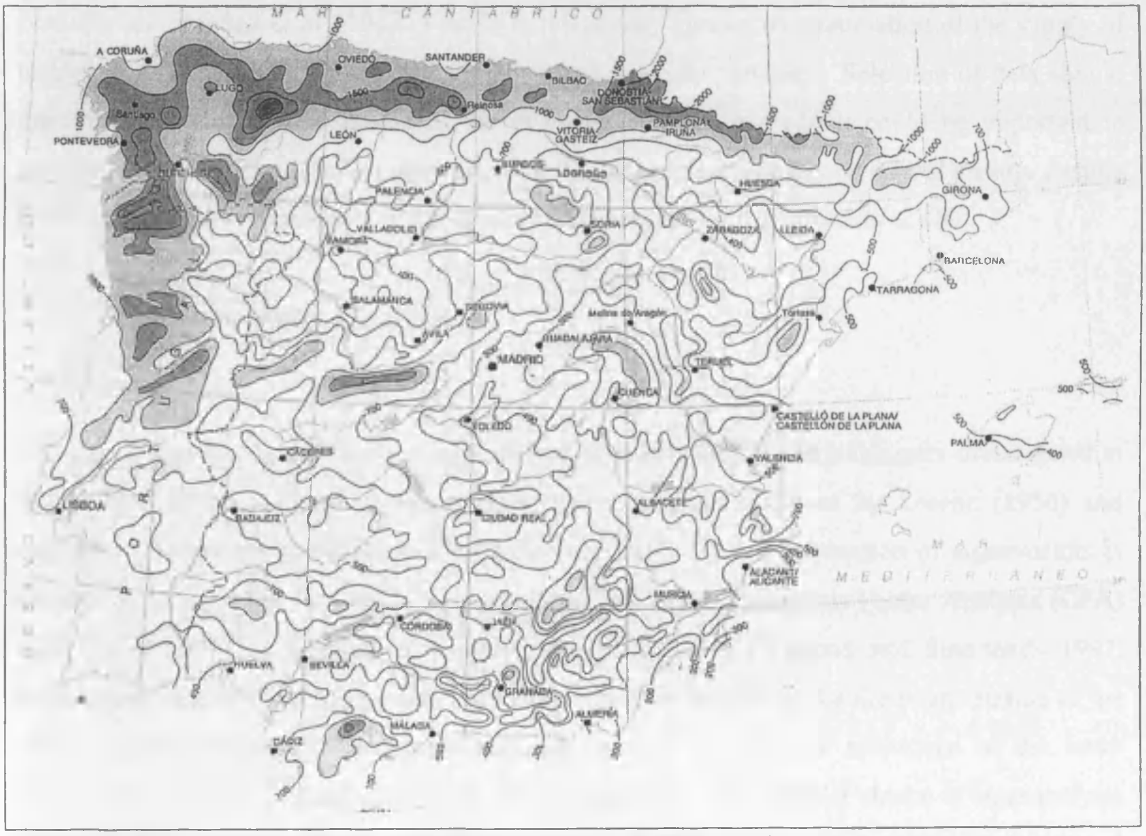

Figure 2.19 Annual rainfall (mm) Spain (source: El Païs 1992).

2.10 *Multivariate statistical methods for rainfall regionalization*

Precipitation Affinity Areas (PAA) are identified using Principal Component Analysis (PCA). PCA was applied to a 12 x 12 inter-month (and 3 x 3 inter-month in the case of seasonal analysis) covariance matrix generated from 41 monthly precipitation time series. Regionalization procedure is applied to the following six parameters,

- Raindays – All year (APAAd), summer (SPAAd), winter (WPAAd).
- Rainfall amounts – All year (APAAt), summer (SPAAt), winter (WPAAt).

Precipitation regionalization could then be constructed using a variety of measures - either the number of raindays or the total amount of rainfall on a variety of timescales daily, monthly, by season or annual. The use of monthly values could lead to unrepresentative results due to the considerable amount of irregularity which can arise when large single month values have been influenced by isolated single storm activity. On the other hand, a procedure involving the entire frequency distribution of daily rainfall amounts can produce too much data and be too cumbersome (Periago *et al* 1991). Finally raindays may give an overestimation of the supply of rainfall at a location if most of that rainfall is low intensity 'drizzle'. Selection of data should therefore be driven by the nature of the investigations, for instance it could be important to regionalize on the basis of seasonality or variability rather than monthly or annual means. Listing of procedural results (evolution of the similarity indices) is given in *appendix 2.10.*

2.11 Eigenvector-based technique

2.11.1 Procedure

The eigenvector-based technique is also used to develop many of the catalogues investigated in this study. It was originally pioneered for meteorological purposes by Lorenz (1956) and examples of early applications include Craddock (1965). The determination of eigenvectors is undertaken using either Principal Component Analysis (PCA), Common Factor Analysis (CFA) (Lolis *et al* 2002) or empirical orthogonal functions (EOF) (Walland and Simmonds 1997, Roswintiarti *et al* 1998). All are data reduction techniques and allow for the interpretation of the main structural features of a dataset although there is no obvious advantage of the latter techniques over PCA (Yarnal *et al* 2001). PCA remains the most popular choice of eigenanalysis due to its mathematical compactness and statistical robustness (Yarnal *et al* 2001), yet it is not without its disadvantages – it is a linear technique, there are many subjective decisions that need to be made in its application, components can be difficult to interpret and statistical artifacts can be generated by certain data distributions. Mathematical theory can be consulted in Griffith and Amrhein (1997) and Hair (1995).

In PCA total variance of the original dataset is redistributed amongst new uncorrelated variables or components (PCs) or eigenvectors, that are ordered by their proportion of explained variance. The number of components that result is equivalent to the number of original input variables and account for 100 percent of the total original variance. A PCA procedure involves a range of *a priori* methodological decisions including the choice of mode of PCA, whether to use a covariance or correlation matrix, what normalization to adopt, how many components to retain and whether or not to rotate (Joliffe 1990). The exact procedure for computing the eigenvectors is described extensively elsewhere (*e.g.* Daultrey 1973, Preisendorfer 1981) (see *appendix 2.6*).

The relative success of covariance or correlation matrices is extensively discussed elsewhere (Craddock and Flood 1969, Wilmott 1978). Legates (1991) advocates that covariance is a better measure of similarity as it preserves the metric, however as this problem is univariate (*i.e.* pressure), PCA can start from either similarity measure (Fernandez Mills 1995).

Usually only a few components will account for the majority of total variance and, as a result, if the data can be represented by a fewer number of components without a substantial loss of information, it may be unnecessary to retain all the PCs. (Sharma 1996). A number of methods (*appendix 2.7*) exist for the determination of the number of components (Craddock and Flood 1969, Preisendorfer and Barnett 1977, Joliffe 1990), but often the decision will not be entirely objective but depends on how much information (unaccounted variance) a researcher is willing to sacrifice.

A common method is Cattell's scree test (1966) (*figure 2.20*) in which the explained variance is plotted against the component number; an 'elbow' in the plot is then identified and the components located on the flattened part of the curve are not retained. A considerable amount of subjectivity is involved in the identification of the 'elbow' and Sharma (1996) comments that in many cases the scree plot may be so smooth that it is impossible to determine its location. Another relatively simple method is to extract only those components with an eigenvalue (ξ) greater than one (Spellman 1996). The rationale behind this is that for standardised data the amount of variance extracted by each component should be, at a minimum, equal to the variance of at least one variable (Sharma 1996). Under the $\xi > 1$ rule, however, too many or too few components can commonly result. Moreover this method does not apply when a covariance matrix is used in the analysis as in this case eigenvalues are of a different magnitude. Stone (1989) comments that the main problem is 'underfactoring' as 'overfactoring' is of little consequence and therefore, as a 'rule of thumb', suggests that satisfactory explanatory power can be achieved by retaining a number of components that together account for more than 80% of the total variance. This approximate 80% rule is used in this study.

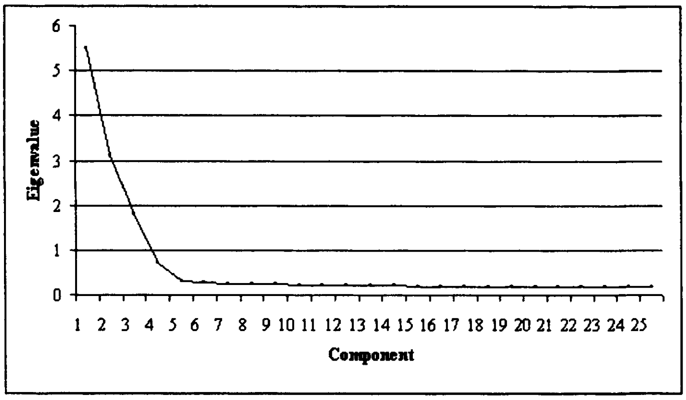

Figure 2.20 A typical scree plot for determining the number of retained components (after Cattell 1966).

2.12 Cluster analysis

The next stage of this methodology is to group or cluster objects on the basis of similar component score structure. Clustering algorithms require that object characteristics are uncorrelated hence the need for prior application of PCA (Bonell and Sumner 1992). The objectives of cluster analysis (CA) are to arrange observations into groups (clusters) such that each is as homogeneous as possible, but different from other groups with respect to the chosen parameter(s). Five stages of this procedure are identified,

1. The selection of the technique of clustering (hierarchical or non-hierarchical).
2. The selection of a measure of similarity.
3. The determination of method for the selected technique (*eg* centroid).
4. The decision regarding the number of clusters.
5. The interpretation of the cluster solution.

2.12.1 Hierarchical clustering

There exists a range of clustering techniques. These divide into hierarchical and non-hierarchical procedures (*appendix 2.9*). In the first step of hierarchical procedures the chosen similarity measure identifies the two subjects that are most similar and these are merged. The next two similar subjects are then identified and merged, and the procedure continues until all the clusters are merged into one group.

There are no hard rules about which distance measure, or consequently, which linkage method (for merging objects) to use. One approach is to try different linkage methods, using different distance measures for each (Everitt 1980). If these different combinations yield similar results then there will be greater assurance about the final groupings of clusters. This analysis uses Euclidean distance (see *appendix 2.9.2*).

2.12.2 Techniques

Hierarchical CA methods are distinguished by the rule for determining the distance or similarity between two clusters consisting of more than one object. Some methods are susceptible to a 'chaining' or 'linking' effect, where observations are sometimes assigned to existing clusters rather than being grouped in new clusters (Stooksbury and Michaels 1991), a particular problem if chaining begins early in the cluster procedure (Sharma 1996). Reports of empirical evaluation of the performance of clustering algorithms give mixed results. Mojeno (1977) and Yarnal (1993) state that Ward's algorithm outperforms other methods, yet Kalkstein *et al* (1987) and Spellman (1996) demonstrate that average linkage is better. This latter method is commonly used in the two-stage cluster analysis developed by Davis and Kalkstein (1990) and is therefore also used here.

2.12.3 Cluster numbers

The final decision on the appropriate number of clusters is still an unresolved problem (Everitt 1980), prone to subjectivity and dictated by experience. Although objective statistical rules exist to guide the termination of cluster mergers, even these tend to be somewhat subjective. Using the PCA–based method to classify circulation Corte-Real *et al* (1999) selected four circulation clusters for Portugal whereas in contrast Ekström *et al* (2002) chose fourteen classes for Sweden. A similarity index guides the operator. In each stage of the process two groups are fused if their similarity index is minimum. As the process continues the number of groups decreases and the minimum index corresponding to that of two classes will increase. When a sharp increase of the index, related to fusion, is noticed then the optimal division is the preceding group structure before this fusion (Gower and Banfield 1975).

An advantage of hierarchical clustering methods is that they do not require an *a priori* knowledge of the number of clusters or the starting partition. However once an object is assigned to a cluster it cannot be reassigned to another cluster at a later stage in the process. It has been advocated that hierarchical methods should be used in an exploratory fashion and then the resulting solution be submitted to a non-hierarchical method to optimize the cluster solution. Thus Sharma (1996) sees the cluster methods as complementary rather than competing.

2.12.4 Nonhierarchical clustering

Non-hierarchical CA differs from hierarchical CA in that the initial group numbers must be stated and reallocation of objects does take place during the process. The *k-means* algorithm used here follows Hartigan and Wong (1979). The objective is to find groups that minimize the total within cluster sum-of-squares over all the clusters. The algorithm provides a 'local' optimum in that no movement of an observation from one cluster to another will reduce the within-cluster sum-of-squares. The procedure is as follows; first, the number of cluster and their centroid values (or seeds) is established. Objects are then assigned to the closest cluster. Each observation is then reallocated to one of the *k* clusters according to a pre-determined stopping rule. A variety of methods exist for determining initial seeds including the random selection of observations, or the selection of the first *k* observations in the dataset.

A popular method is to combine hierarchical and non-hierarchical methods so that the former method calculates cluster numbers and centroids that then act as seeds in the non-hierarchical procedure (Gong and Richman 1992, Spellman 1998a). Davis and Kalkstein (1990) demonstrate that principal components coupled with average linkage and *k-means* can provide the most separable systems of clusters, resulting in the most concentrated clusters.

2.13 Regionalization results

2.13.1 All year - rainday numbers

	PC1	PC2	PC3	PC4
Eigenvalue	4373.2	947.1	535.4	387.9
Proportion	0.598	0.129	0.073	0.053
Cumulative	0.598	0.727	0.800	0.853

Table 2.3 Eigenanalysis of covariance matrix.

Table 2.3 lists the eigenvalues and cumulative proportion of explained variance related to the four retained unrotated principal components. A covariance matrix was used therefore the '*eigenvalue greater than 1*' rule is of no use and was replaced by the '*approximate 80%*' rule (Stone 1989) in determining the retention of components.

Figure 2.21 depicts the spatial distribution of component one (PC1) scores. All locations score negatively on PC1. High negative loadings are found in the north and north-western regions of the peninsula where the rainfall regime is associated with travelling Atlantic depressions. Scores grade to a minimum at points most removed from the Atlantic (*e.g.* the Balearic Islands). For PC2 higher loadings correspond to warmer season rainfall and negative loadings to winter fall. Where summer rainfall makes a significant contribution to total amounts in the north PC scores are highest. High negative scores group to the south and east of the peninsula where summer rainfall is very low. PC3 reflects the high rainfall activity of spring that is a feature of inland stations such as Avila *(see figure 2.6c)*. PC4 is difficult to interpret but appears to be associated with depressions travelling from the south-west into the Mediterranean.

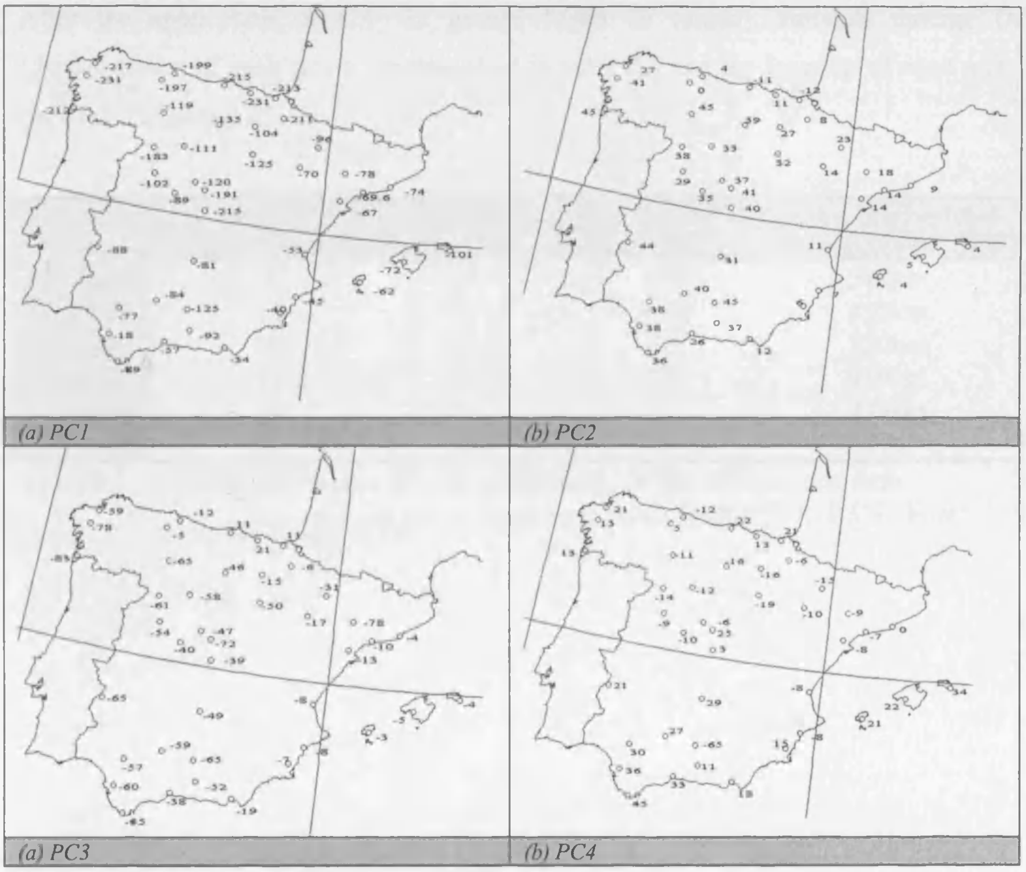

Figure 2.21 Spatial distribution of PC scores (monthly raindays).

The component scores are then grouped using a two-stage classification method (Davis and Kalkstein 1990). In the first instance the number of groups is determined using an average linkage algorithm. Changes in a similarity index can be tracked to the point where there is a sudden increase in the difference in that index step from one cluster group to the next.

Cluster Number	Number of stations	Within cluster sum of squares	Average distance from centroid	Maximum distance from centroid
APAA1d	4	1235.2	13.5	23.1
APAA2d	11	1693.4	17.4	31.2
APAA3d	8	2018.2	12.2	29.1
APAA4d	11	3535.3	16.3	28.8
APAA5d	6	2132.3	15.2	24.2
APAA6d	1	0	0	0

Table 2.4 *Results of the clustering procedure (centroid distances) using monthly rainday numbers.*

After the application of CA six groups based on rainday amounts emerge (*table 2.4*). Characteristics of each group are described in *table 2.5* and the location of each affinity area is depicted in *figure 2.22.*

	Number of stations	Mean r value	Mean raindays	Furthest geographical separation
APAA1d	4	0.837	158	510km
APAA2d	11	0.714	106	450km
APAA3d	8	0.838	82	320km
APAA4d	11	0.584	73	640km
APAA5d	6	0.801	172	335km
APAA6d	1	N/a	119	N/a

Table 2.5 *Characteristics of each group based on monthly rainday data.*

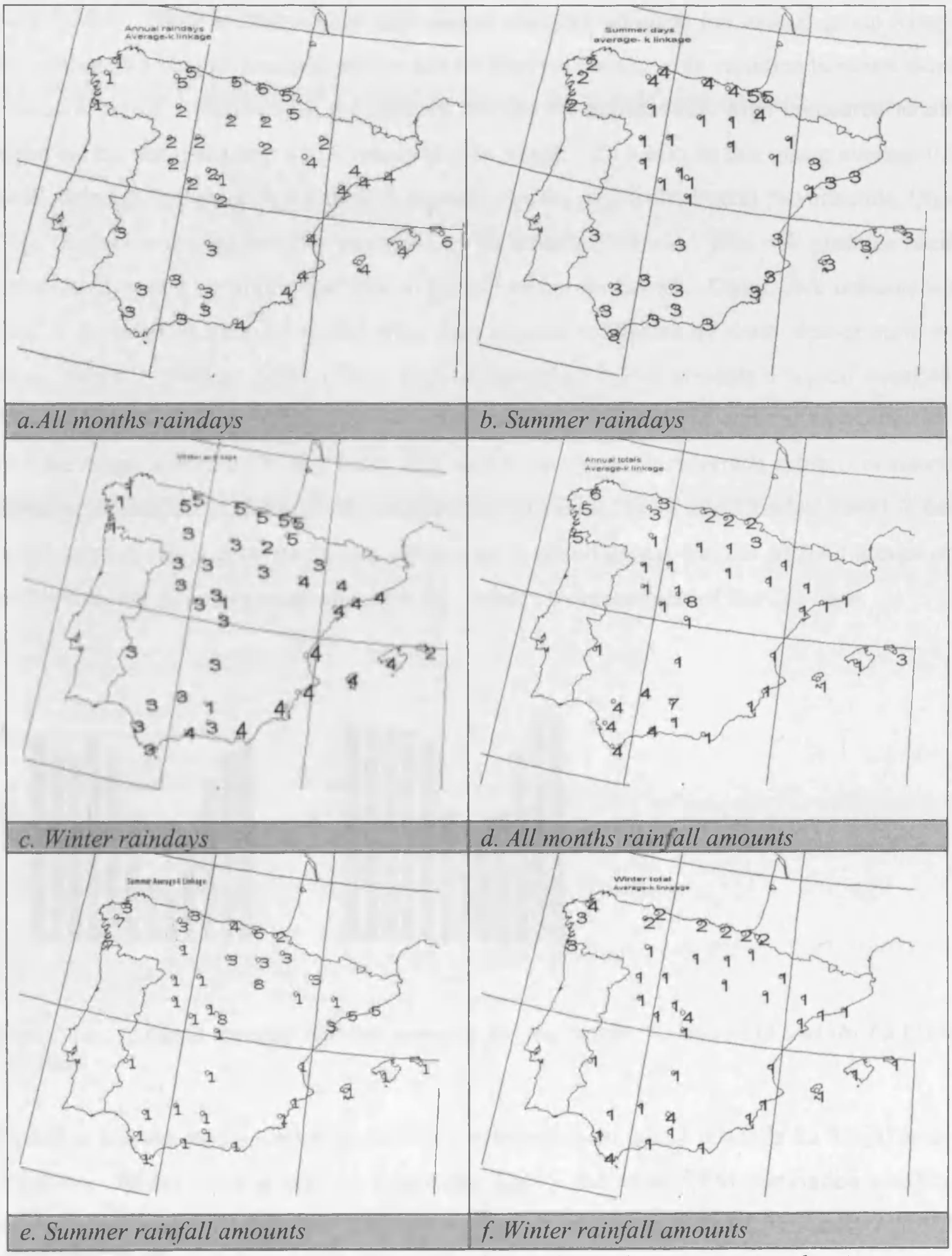

a.All months raindays *b. Summer raindays*

c. Winter raindays *d. All months rainfall amounts*

e. Summer rainfall amounts *f. Winter rainfall amounts*

Figure 2.22 Precipitation affinity areas (numbers refer to cluster group numbers).

APAA1d includes stations in the north-western corner of the peninsula in the province of Galicia (*figure 2.22a*). These locations have high annual rain day numbers (an annual group mean of 158). Although a distinct seasonal pattern can be detected there is little variation between months in the cool season. Raindays in the summer months are significantly high compared to other stations on the peninsula (*e.g* a JJA[6] mean of 6 in Vigo). SI values in this group average 0.25. Also included in this group is a station in the centre of the peninsula, Puerto Navacerrada, (*figure 2.23a*). Inclusion can be partially explained by its altitude (1890m). This will promote rainfall under those synoptic situations that lead to rainfall in the north-west. Orographic influences are critical in the intensification of rainfall when the peninsula is affected by south-west or north-west cyclonic flows (Fernandez Mills 1995). La Coruña (*figure 2.23b*) presents a typical example of APAA1d stations. Group homogeneity is strong with an average PPM correlation coefficient of 0.837 (the range is from 0.727 to 0.960). La Coruña and Puerto Navacerrada exhibit considerable geographic separation (510 km). The Köppen classification (Barry and Chorley 1998) is based on mean rainfall amounts rather than covariance but it would appear that the APAAd groups draw parallels with the Köppen system and APAAd1 reflects characteristics of the *Cfa* class.

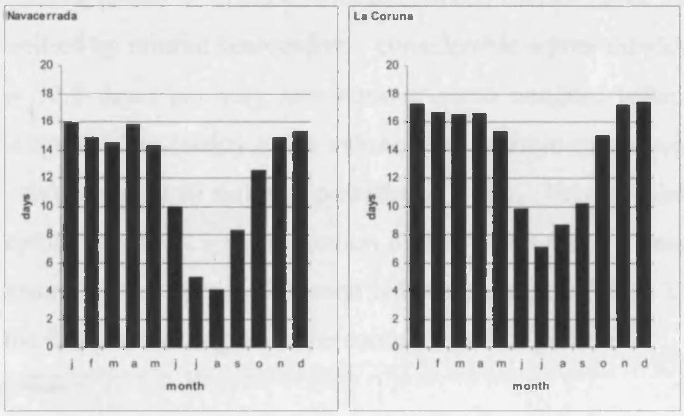

Figure 2.23 Mean monthly rainday numbers for (a) Puerto Navacerrada and (b) La Coruña in APAAd1.

APAAd2 is a broad region comprising stations in the northern inland (Castilla-La Vieja) areas of the *meseta.* Group homogeneity is reasonably high – the mean PPM correlation coefficient between member stations is 0.714. Highest monthly raindays numbers are frequently reached in May (for instance there are 11 May raindays in Valladolid (*figure 2.24*)) when Atlantic depressions are active as a consequence of the strong thermal contrast between the land and surrounding sea. Summer numbers are low, on average between about 3 and 6 days. The

[6] June July August – meteorological summer.

Mediterranean influence on stations in this group is limited as suggested by the lack of correspondence between the autumnal increase in Mediterranean cyclonicity and rainfall amounts.

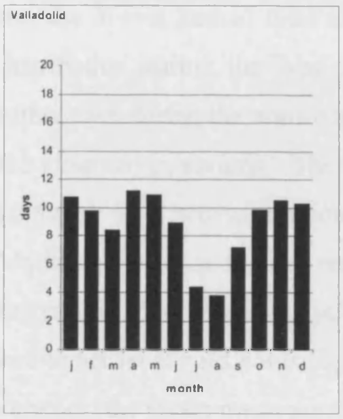

Figure 2.24 Mean monthly rainday numbers at Valladolid (APAAd2).

APAAd3 is located to the south of the peninsula (Andalucia). This is a homogenous group of 8 stations (mean '*r*' is 0.838 with a relatively narrow range between 0.784 and 0.926). Stations are unified by rainfall seasonality – considerable winter rainday numbers (the December group mean is 10.2 days) but very low summer mean numbers (often below 1 in the months of July and August). Seasonality index values increase from east to west with a value of 0.49 (the highest SI value amongst all stations) recorded at Cadiz. This is mainly a consequence of large-scale global circulation shifts - the migration of rain-bearing low pressure systems into higher latitudes. An example of an APAAd3 station is Badajoz (*figure 2.25*). This group covers a comparable area to the Köppen *Csa* region in the south part of the peninsula.

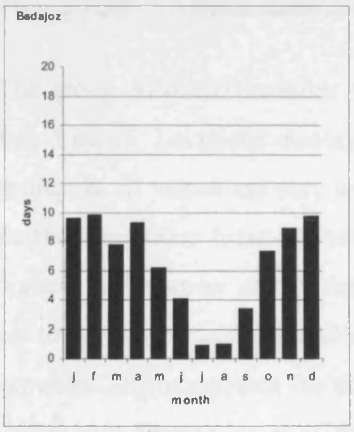

Figure 2.25 Mean monthly rainday numbers for Badajoz (APAAd3).

Stations in APAAd4 show a lesser degree of coherence (mean *'r'* = 0.584) than other groups. Stations are found along the east-facing Mediterranean coast (Communidad Valenciana, Murcia, Catalunya *e.g.* Barcelona in *figure 2.26*) and the Balearic Islands (except Menorca). This group has the lowest annual total number of raindays (the group mean is 73) and displays a unique distribution during the year. Peak monthly rainday numbers occur in the spring and autumn rather than during the winter months as in APAAd1, 2 and 3. Maximum monthly rainfall values are observed in autumn. There is the return of northerly air masses under meridional circulation patterns. This provides a considerable thermal contrast between atmosphere and surface as the Mediterranean Sea surface temperature is highest in September and October. The result is an increase in Mediterranean cyclogenesis. Particularly important at this time of the year are troughs and upper level cold pools (Spellman 1998b, 2000a). Minimum rainday numbers are recorded in summer (the group mean number is 3.5 days) although the drought is not as severe as in APAAd3 locations.

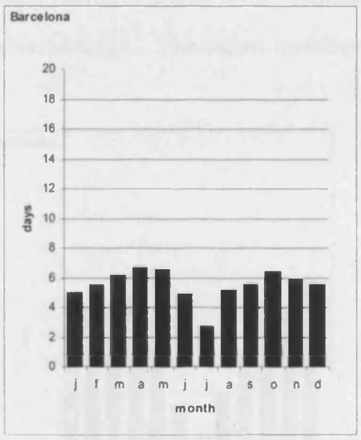

Figure 2.26 Mean monthly rainday numbers forBarcelona (APAAd4).

The group APAAd5 includes stations on the north coast of the peninsula (Cantabria, Asturias, Pais Vasco). Locations display a remarkably reduced seasonality compared to other parts of the peninsula. SI values are very low, for instance 0.08 at San Sebastian (*figure 2.27)* and Santander. Furthermore these locations have the greatest numbers of raindays per year (the annual mean is highest in Santander at 189 days). These stations are on the north-facing Cantabrian coast and are thus exposed to north and north-westerly airflow from the Atlantic. The linkage analysis in *appendix 2* demonstrates the strong isolation of this group. Analysis by Rodriguez-Puebla *et al* (1998) and Serrano *et al* (1999) have highlighted the individuality of this group compared to others on the peninsula, even suggesting that there are strong downstream correlations in winter with Croatia and Greece.

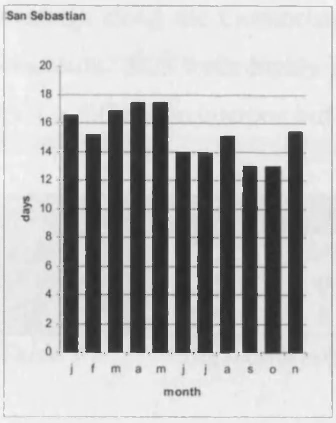

Figure 2.27 *Mean monthly rainday numbers for San Sebastian (APAAd5).*

APAAd6 is a single station group that remarkably displays statistically different precipitation behaviour to its closest neighbours. The station at Mahon on Menorca (*figure 2.28*), although only some 130km from Palma de Mallorca and 250km from Ibiza, exhibits a unique rainfall climatology. The mean number of annual raindays is 119. SI for rainday numbers is 0.28.

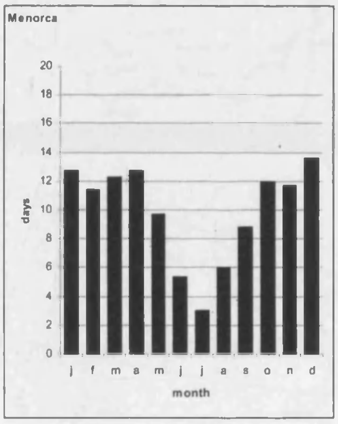

Figure 2.28 *Mean monthly rainday numbers for Menorca (APAAd6).*

2.13.2 All year - rain amounts

The regionalization procedure was also conducted with rainfall amounts (mm) as the input variable. A covariance matrix was employed to generate five principal components that explained 83.9% of the original variance (*table 2.6*). PC1 depicts maximum (negative) scores in the north and north-west (*figure 2.29)* where rainfall is governed by westerlies and an Atlantic influence. Less extreme loadings are seen in northern inland areas at stations shielded by topography. PC2 has strong positive loadings along the Cantabrian coast. Negative loadings are clustered in the southern part of the peninsula. PC3 loads highly in the south west and Mediterranean coasts (similar to raindays PC4). PC4 is difficult to interpret but very high negative loadings can be seen in the north-east region.

	PC1	PC2	PC3	PC4
Eigenvalue	772638	248866	79854	53754
Proportion	0.539	0.174	0.056	0.037
Cumulative	0.539	0.713	0.768	0.806

Table 2.6 Eigenanalysis of covariance matrix (annual rain amounts (mm)).

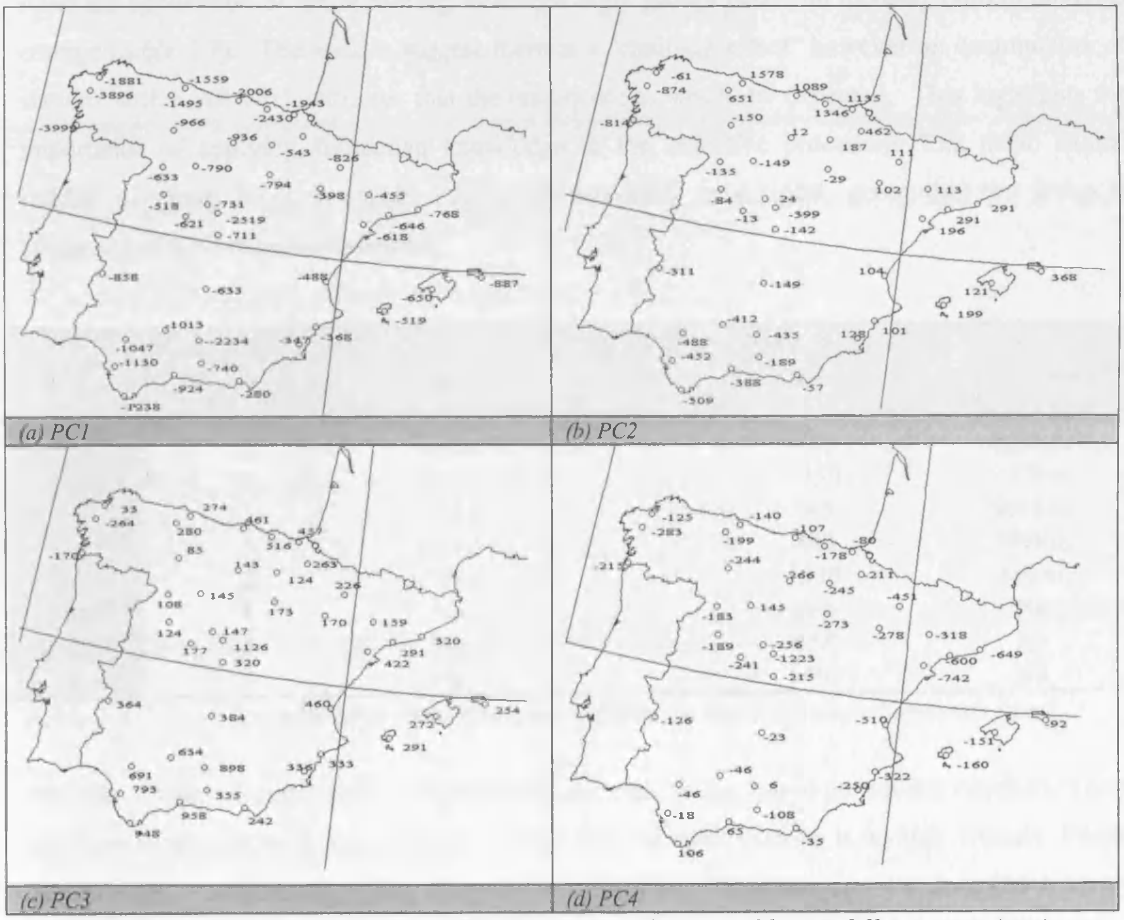

Figure 2.29 Spatial distribution of PC scores based on monthly rainfall amounts (mm).

Cluster Number	No of observations	Within cluster sum of squares	Average distance from centroid	Maximum distance from centroid
1	25	1767047.9	239.1	449.9
2	3	490826.4	267.0	482.5
3	3	332209.5	211.0	425.6
4	5	153626.0	136.1	228.8
5	2	11660.2	50.9	76.4
6	1	0	0	0
7	1	0	0	0
8	1	0	0	0

Table 2.7 Results of the clustering procedure (centroid distances) using monthly rainfall amounts (mm).

After the application of the clustering technique eight groups based on monthly rainfall amounts emerge (*table 2.7*). The results suggest there is a 'chaining effect' however an examination of stations within APAAt1 indicates that the results are as would be expected. This highlights the importance of applying subjective knowledge to the objective procedure. The mean annual rainfall of group APAA1t (*table 2.8)* is not especially meaningful, given that the group is composed of well-dispersed stations.

	Number of stations	Average r value	Mean SI index	Mean annual rainfall (mm)	Furthest geographical separation
APAA1t	25	0.324		789	820km
APAA2t	3	0.821		1359	145km
APAA3t	3	0.514		843	900km
APAA4t	5	0.810		588	190km
APAA5t	2	0.941		1930	80km
APAA6t	1	Na		996	Na
APAA7t	1	Na		558	Na
APAA8t	1	Na		1409	Na

Table 2.8 Characteristics of station groups based on monthly rainfall amounts (mm).

The rain amounts classification is significantly different to that based on rainday numbers. There are three single station groups (*figure 2.22d*). One of these stations is at high altitude, Puerto Navacerrada at 1890m (APAA8t). Scrutiny of topographic maps suggests that Jaen (APAA7t) is affected by significant topographic sheltering to the west and south (rain-bearing airflow directions in this region). Finally La Coruña (APAA6t), although related to Vigo and Santiago in the annual rainday group APAA1d, actually receives considerably less rain amounts (La Coruña has an annual mean of 996 mm compared to 1952 mm at Vigo and 1915 mm at Santiago). There is one very large group (APAA1t) representing a merger of inland and eastern Mediterranean stations, in other words, rainday groups APAA2d and APAA4d. The other two notable clusters are the three–station northeast group APAA2t and the five-station south-west group (APAA4t). Examples of representative stations are given in *figure 2.30.*

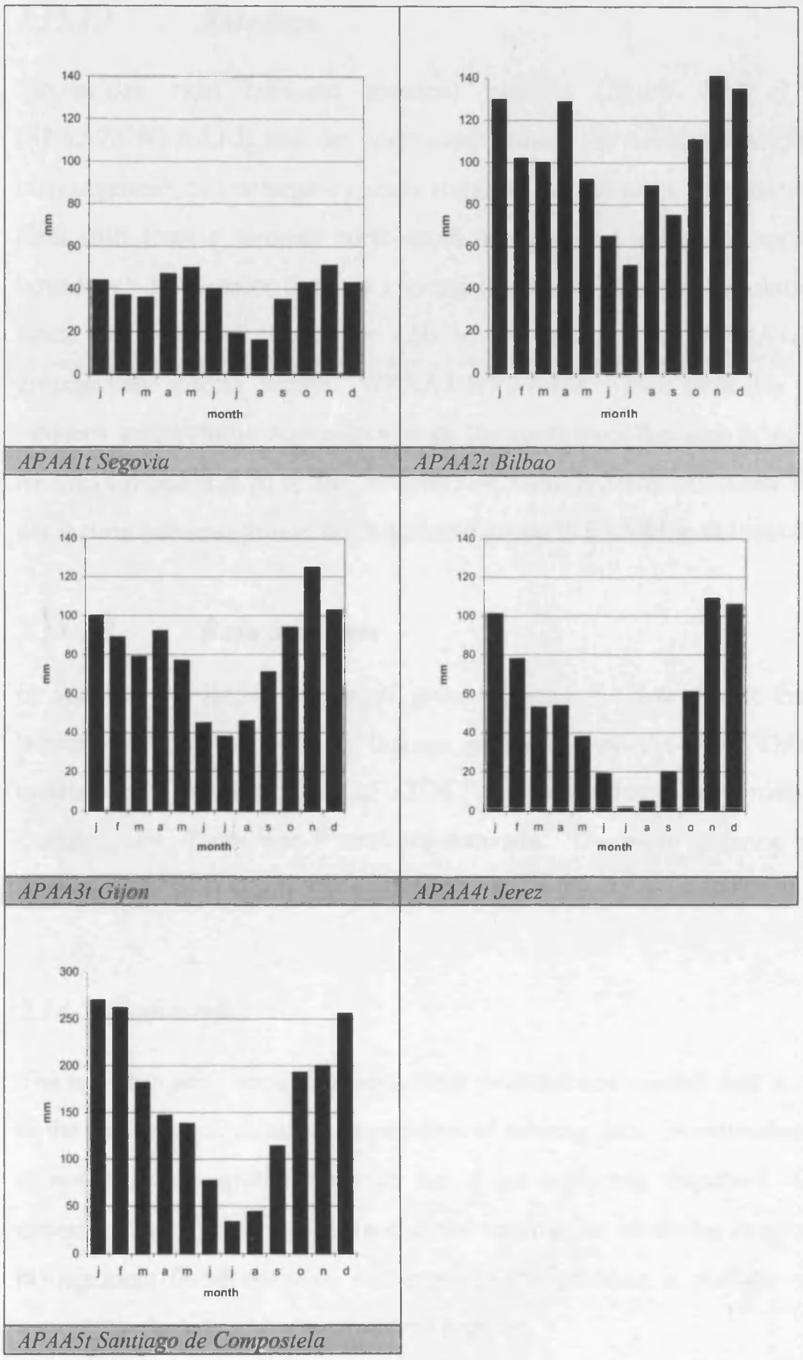

Figure 2.30 Examples of rainfall regimes under each precipitation affinity area (mean monthly rainfall amounts).

2.13.3 Seasonal patterns

Seasonal regionalization was also conducted for both metrics. Only the main differences are outlined here.

2.13.3.1 Raindays

Similarities exist between seasonal patterns *(figure 2.22b,c)* - the north-west cluster (SPAA2d/WPAA1d) and the north coast cluster (SPAA4d/WPAA5) retain their identities. The rearrangement of the largest groups suggests the influence of atmospheric circulation. There is a clear shift from a summer north-south division to a more longitudinally-orientated main group boundary. In summer there is a group (SPAA3d)) comprising stations in the south and east of Spain and a group containing sites in the inland north (SPAA1d) this shifts to a west-east arrangement during winter (WPAA3/WPAA4d). This indicates the seasonally-based swing between anticyclonic dominance from the south over the area in summer (as reflected by group SPAA3d membership) to the incursion of zonal Atlantic influence in winter (as reflected by the distinction between group WPAA3d and group WPAA4d in the rainshadow of the high *meseta*).

2.13.3.2 Rain amounts

In summer the large number of groups *(figure 2.22e,f)* reflect the lack of spatial correlation between stations indicated by linkage analysis *(appendix 2.5)*. There is a large coherent group consisting of stations south of 43°N. The most interesting group is SPAAt4 comprising La Coruña, Jaen, Tarifa and Puerto Navacerrada. The mean distance between locations is 680km. Rain in the warm season could primarily be a response to scattered convective activity.

2.14 Comment

The use of quality controlled secondary pressure and rainfall data in this study brings confidence to the analysis and reduces the problem of missing data. Nevertheless the INM network has been shown to have a spatial coverage that is not uniformly dispersed. Given that synoptic analysis generally leads towards a surface-based application involving human activity (agriculture, water management flood analysis, soil erosion) this problem is perhaps not so crucial given the low population density in the unobserved regions.

Key outcomes of this chapter are outlined in *table 2.9*. This study has shown that an initial understanding of modes of rainfall behaviour across Spain is provided by the statistical regionalization procedures. Distinct rainfall affinity areas are identified which reflect covariant behaviour and are related to synoptic process unlike annual (or seasonal) mean values. The spatial extent of these 'regions' cannot be confidently constructed due to the relatively low number of stations and therefore regions are actually no more than clusters of covariant stations without true boundaries. Emergent groupings, based on all-seasons, tend to mirror those of the more general climatic classifications (*i.e.* Köppen) and therefore suggest regional boundaries (relating to topography, continentality, proximity to synoptic features) are related. It could be concluded that the technique does not inform the researcher much more than is already known.

On the other hand, it is argued that this technique provides more information for the climatologist than any conventional regionalization. It is able to automatically redefine climate boundaries on a seasonal timescale and it can identify how given climate change scenarios will affect the patterns of rainfall behaviour in the future. Neither of these applications has been extensively undertaken in the climate literature. With respect to the former, this study demonstrates that rainfall behaviour is considerably more homogeneous in the high sun season and very different to a regionalization, such as that of Fernandez Mills (1995), developed from 'all year' data. Given the strong seasonal control on the water resource and hence on applications, it is evident in these latitudes seasonally-based regionalizations are desirable.

Secondly the purpose of downscaling is to provide an estimation of future rainfall at a regional scale. If reliable estimates are obtained this technique clearly can be used to delineate precipitation affinity areas for future time periods and this is essential for long-term water management planning.

An important finding of this study is that significant variability in region boundaries emerge between a regionalization based on rain day numbers compared to one based on rainfall amounts. For instance in the north-west of the peninsula, although La Coruña accompanies Vigo and Santiago in group APAA1d (because it rains at all sites under the same synoptic patterns), it does not belong to the same group if rainfall amounts are considered. This has important implications for applications of the method – if an understanding of rainfall occurrence is required then rainday amounts are preferred, on the other hand covariance of rainfall amounts are useful to water resource managers but less related to synoptic mechanisms as local conditions will dictate absolute rainfall amounts. This issue is not recognized by Fernandez Mills (1995) who employed a PCA/CA technique to this to regionalize rainfall using monthly amounts and inferred circulation controls from the emergent patterns.

Finally a crucial aspect of the regionalization process is to simplify patterns for later interpretation and hence it is a means to an end rather than an end in itself. PCA/CA is a data reduction technique and facilitates the selection of key stations within the resultant groups which can be employed in daily synoptic catalogues. Areal data is sufficient for monthly catalogues.

Key Outcomes
• Emergent ('all year' data) regions reflect traditional regionalizations. • Unlike traditional classifications the automated technique in this study can easily be reapplied to demonstrate seasonal rearrangement of covariance. • The automated technique can be undertaken using climate change scenario data to identify future rainfall regions. • Distinct differences emerge depending on the rainfall metric employed to develop the regionalization. This is an important consideration that has not been addressed elsewhere. • The technique identifies stations that can be sampled for model evaluation later in the study.

Table 2.9 Key outcomes of chapter 2.

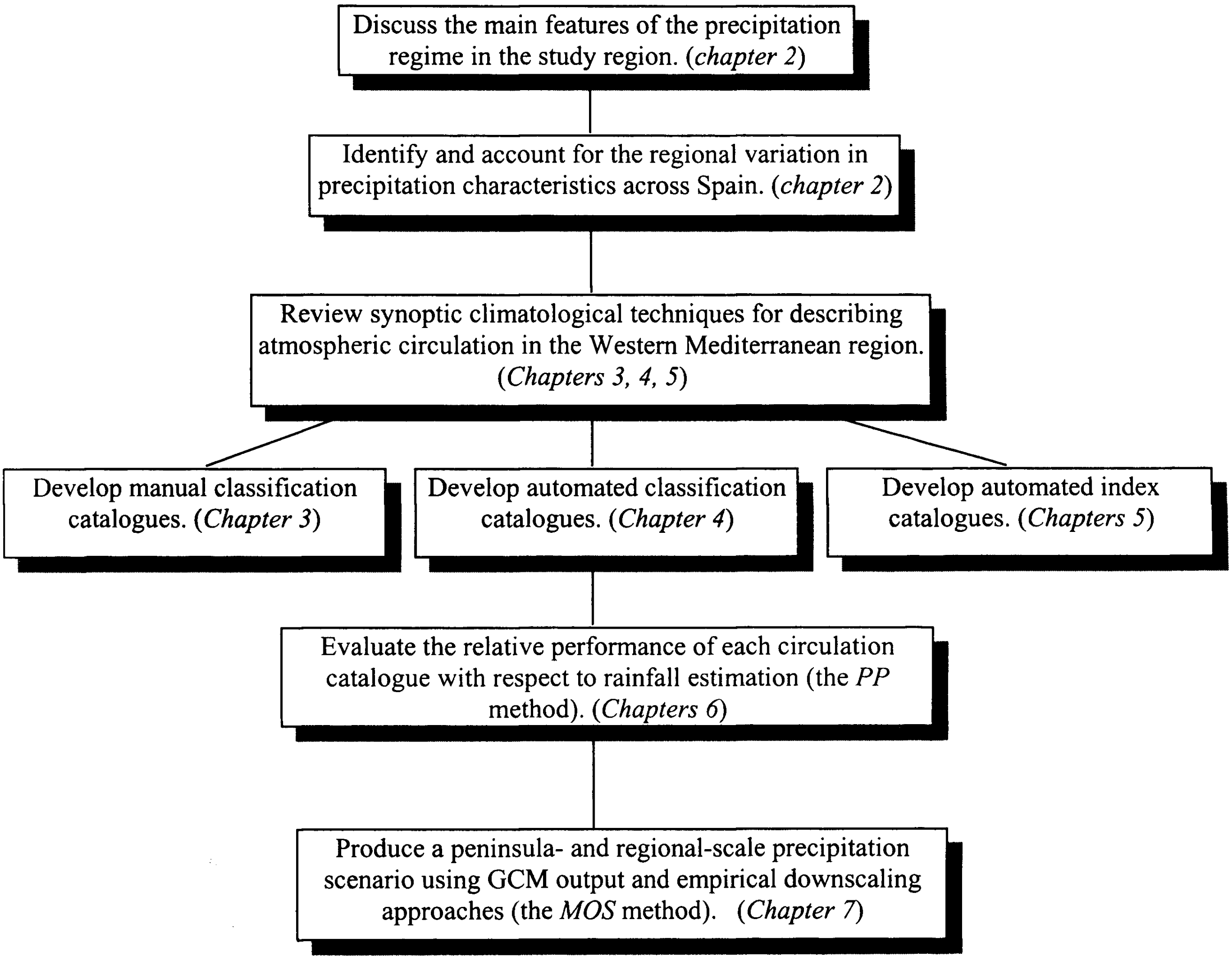

Figure 1.2 The structure of this thesis.

Chapter Three
Synoptic climatology
Daily manual classification

3.1 Introduction

Fundamental to synoptic climatological analysis is the description of mapped pressure patterns. This is traditionally achieved by either manual or automated discrete classifications which divide into,

- static approaches
- kinematic approaches.

Static approaches involve the description of the entire pressure pattern and its significant features. They are usually based on daily or monthly charts of either the surface pressure field (*e.g.* LWT[1] for the UK), upper atmospheric contour charts or, very rarely, isohyptic (thickness) patterns. It is related to air mass climatology (see *appendix 3.1).* Kinematic approaches trace anticyclone, depression and frontal tracks and investigate aspects such as the variability in frequency, latitude of track, speed and direction of system movement and system intensity. The latter method is not examined in great detail in this study but is incorporated in selected static approaches. The format of this chapter is described in *figure 3.1.*

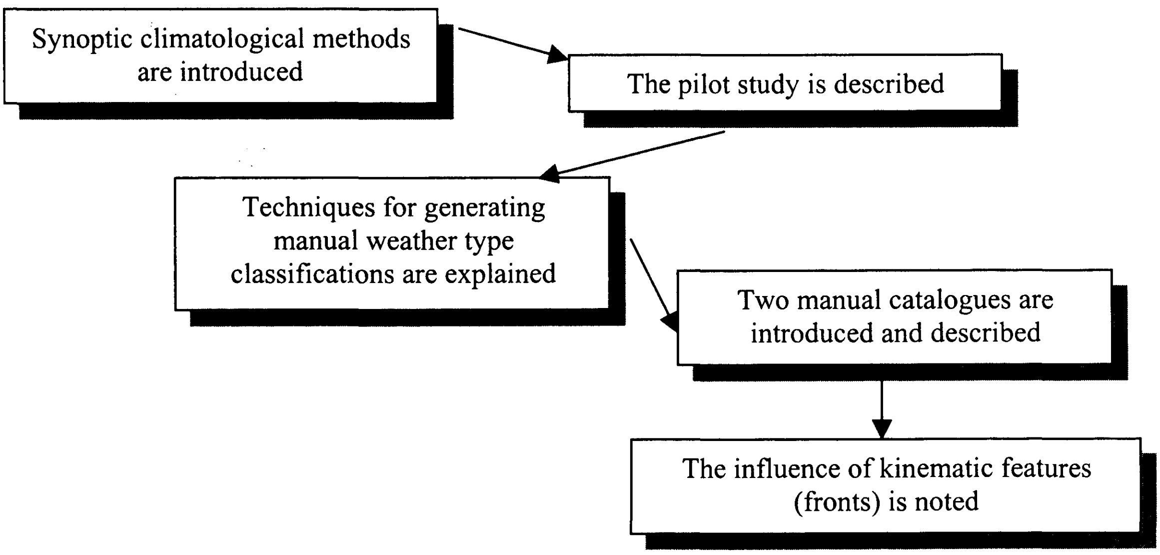

Figure 3.1 Outline of Chapter 3.

[1] Although Lamb also considered cloud patterns and the location of precipitation.

3.2 Classification level

Three circulation parameters are identified as potential inputs to synoptic analysis. Time series of these parameters can be modified (normalized or seasonal anomalies) if there is good reason to believe that any variation is seasonally dependent (*i.e.* the height of the 500hPa pressure surface or 1000-500hPa thickness). Without such transformations a classification may merely reflect the gross seasonal characteristics of the data. On the other hand, it could be argued that seasonality is a critical aspect of the circulation-environment relationship, especially over Mediterranean regions (Spellman 2000a) and raw data should be retained.

3.2.1 Sea level

Mean sea level pressure is the most frequently used synoptic parameter (Wilby 1994, Katz and Parlange 1996, Biau *et al* 1999, Busuioc *et al* 1999). MSLP is either portrayed on isobaric charts or converted to grid-point values. Surface charts provide a good representation of synoptic scale systems and are able to indicate the interaction of low-level flow with topography (Kidson 1997). This analysis is linked to air mass studies (*appendix 3.1*).

3.2.2 Upper air

Charts are also routinely prepared for constant pressure levels in the atmosphere (contour charts). The standard pressure surfaces used are 1000, 850, 700, 500, 300, 200 and 100hPa. El Kadi and Smithson (1992) comment that surface flow is more closely related to lower tropospheric circulations than mid-tropospheric flow yet concede that a consideration of the latter level is, at times, advantageous because: (*i*) flow in the mid-troposphere is strongly related to the steering of depressions and anticyclones, (*ii*) charts yield information on strength of flow and (*iii*) patterns are far less complex and therefore easier to classify. The most commonly available upper air chart is that for the 500hPa surface (about 5.5 km in middle latitudes) which approximates to the mean level of non-divergence in middle and higher latitudes (Barry and Perry 1973). The 500hPa surface is commonly used in synoptic classification, for instance, Kruizinga (1979), Cohen (1983), Hoard and Lee (1986), Bürger (1996), Wibig (1999), Spellman (2000b) and Quadrelli *et al* (2001). Other less frequently used levels include 700hPa (Inamdar and Singh 1993, Plaut and Simonnet 2001, Brinkmann 2002) and 850hPa (Weichert and Burger 1998, Sailor and Li 1999).

Furthermore the choice of atmospheric level is influenced by regional attributes. For instance, although sea-level patterns can identify the role of surface depressions, Tout and Wheeler (1990) note that surface charts give very little assistance because of the frequent absence of clues such as cyclogenesis or well-defined frontal zones in Mediterranean settings. They suggest that attention needs to be focused on the atmosphere from 700hPa upwards. It is often the case that circulation patterns and air masses cannot be identified in the summer months because sea level pressure does not vary over a substantial area of the western Mediterranean basin. In addition upper air cut-off lows (*'gotas frias'*), which are responsible for very heavy rainfall events at all times of the year, do not feature on surface maps which at times even show anticyclonic patterns (Llasat 1991).

3.2.5 Combined levels

A multi-level (500hPa/surface) manual classification for the Iberian area is that of Paricio and Nadal (1979) which was employed to examine rainfall in the Valencia region (see *appendix 3.3.3*). Thickness (relative topography) charts are generally used in weather forecasting but have been used in some climatological analysis (Cavazos 1997, Huth 1999, Huth and Kysely 2000). The thickness of an air layer (z_2-z_1) between two pressure surfaces (*e.g.* 1000 hPa and 500hPa) is proportional to its mean temperature (*equation 3.1*),

$$z_2 - z_1 = \frac{RTv}{g} \ln \frac{p_1}{p_2} \quad (Eqn\ 3.1)$$

where Tv is the mean virtual temperature of the layer in degrees Kelvin (virtual temperature is the temperature of dry air at the same pressure and density as the given moist air sample), R is the specific gas constant for dry air (2.687 x $10^2 m^2 s^{-2} K^{-1}$), g is the acceleration due to gravity (9.81 ms^{-2}) and p_1 and p_2 are the two pressure surfaces.

Thickness charts therefore have the potential to incorporate information regarding the whole depth of the lower troposphere rather than one level.

3.3 *Pilot study - daily catalogues*

This research project has investigated 24 synoptic catalogues (and sub-schemes) but, due to the limitations imposed by space, only selected schemes will be fully reported in the thesis. Detailed reviews are provided because they are useful in the depiction of circulation patterns and because they offer distinct advantages in the analysis of circulation-to-environment relationships.

All class-based catalogues (*table 3.1)* were initially examined[2] for a short sample period – 1800 randomly sampled daily charts from the period 1988-1997. This permitted early identification of catalogues that were either replicating information or were not modelling precipitation satisfactorily. Methods and techniques that were ruled out at this early stage included both subjective and objective catalogues based on thickness patterns (THICKANN, THICKAUT) and a multi-level classification (MULTIAUT) despite its expected value for Mediterranean latitudes. Catalogues and precipitation models generated by artificial neural networks (classifications produced by Kohonen self-organizing maps (SOM) and circulation-precipitation transfer functions described by the back propagation (BP) method were also evaluated and were shown not to improve on the results obtained by traditional linear statistical techniques. The development of ANNs (both SOM and BP) is largely a process of constructing network architectures through trial and error experimentation (with the number of neurons and layers). This is extremely time consuming and, furthermore, network architectures will change depending on the nature of the dataset presented to them. Extensive validation of result synoptic models and the use of ANN transfer functions in precipitation modelling did not warrant their use. Nevertheless the potential of ANN applications to synoptic studies is great (given software advances) and is discussed extensively elsewhere (Hewitson and Crane 1994, 2002). Other non-linear techniques such as multi adaptive regressive splines (MARS) could also have considerable potential. Some evaluative results of rejected models are listed in *appendix 3.2.*

[2] Using the RPI and ANOVA analysis used in *section 6.3*

Method	Technique	Data Input	Model
Manual		Surface charts	SLPMAN
		Upper Air Charts	500MAN
		Thickness Charts	THICKMAN
Automated	PCA	Surface charts	SLPAUT
		Upper Air Charts	500AUTR/500AUT
		Thickness Charts	THICKAUT
		Multi-level (MSLP/500hPa)	MULTIAUT
	Index method	Surface charts	SLPINDC
		Upper Air Charts	500INDC
	ANN	Surface charts	SLPANN
		Upper Air Charts	500ANN
		Thickness Charts	THICKANN

Table 3.1 Static class-based synoptic catalogues explored in the pilot sample. The use of mean, linear regression and ANN transfer functions was investigated for all models.

3.4 Manual classification of synoptic types

The main advantage of manual classification is that it can be modified to the research needs, for instance, the spatial and temporal window can be expanded so as to integrate knowledge of past and future weather conditions up and downwind. This then goes beyond instantaneous pattern recognition to capture the essence of the dynamic evolving atmosphere (Frakes and Yarnal 1997). However this becomes a problem as it increases the inconsistency and irreplicability of the procedure. No two workers will classify an entire time period in the same way. This often quoted assertion, which is usually unsupported in the literature, is examined in *section 3.5.1.1.* Furthermore, the work is labour-intensive and time-consuming and it is likely that a significant amount of synoptic data will be ambiguous or fall at the borders of two classes.

3.3.1 Existing manual classifications for the Iberian Peninsula

Several manual catalogues for the region have been proposed (*e.g.* Paricio and Nadal 1979, Florit and Jansa 1979, Sanchez Rodriguez 1993) but after evaluation of these it was judged that entirely different or modified methods would be more successful. Classifications are listed in *appendix 3.3.*

3.4 A manual classification of Iberian air flow

Two subjective manual catalogues of circulation over the Iberian peninsula were developed and are described here. Iberian circulation classes in this study are termed 'Weather Types' after Lamb (1950), although they are called 'Pressure Patterns' (El-Kadi and Smithson 1996, 2000) and 'Circulation Patterns' (Stéhlik and Bárdossy 2002) by other authors. SLPMAN is based on MSLP fields and 500MAN is based on the 500hPa constant pressure surface. 500MAN is essentially a modified version of a scheme originally proposed by Olcina (1994) and described by Spellman (1997b). Airflow aloft can be deduced from patterns in the 500hPa constant pressure surface (300hPa in the original) and trajectories can identify the air mass affecting the Iberian peninsula. Some basic circulation type-rainfall links are described however the schemes did not perform as well as the automated systems.

3.5.1 SLPMAN

SLPMAN was based entirely on the UK LWT scheme. There are 27 types in the classification, eight of which are directional and then subdivided according to curvature of the isobars across the Iberian peninsula (to make 16 further types). Of the three remaining categories one is anticyclonic (A), one cyclonic (C) and the third is an unclassifiable category (U). The scheme is listed in *table 3.2* and some examples are given shown in *figure 3.2*. The mean annual and seasonal frequency of SLPMAN types is listed in *table 3.3*. Overall anticyclonic patterns dominate. A far greater proportion of days are classified in the 'U' class as compared to the LWT system in the UK indicating that 'slack' atmospheric flow is much more common at this latitude. Although this scheme is straightforward to apply identification becomes difficult in summer situations when these unidentifiable patterns or shallow (and therefore misleadingly important) thermal low pressure systems dominate the daytime atmosphere above the peninsula.

System types	Pure directional types	Anticyclonic hybrid types	Cyclonic hybrid types	Unclassified types
A	NE	ANE	CNE	U
C	E	AE	CE	
	SE	ASE	CSE	
	S	AS	CS	
	SW	ASW	CSW	
	W	AW	CW	
	NW	ANW	CNW	
	N	AN	CN	

Table 3.2 Classes used in the SLPMAN classification.

Type	Percentage frequency	Type	Percentage frequency	Type	Percentage frequency
A	23.94	NE	6.71	C	14.70

ANE	1.60	E	4.29	CNE	2.92
AE	1.54	SE	0.87	CE	1.08
ASE	0.63	S	0.59	CSE	0.17
AS	0.50	SW	1.88	CS	0.15
ASW	1.44	W	4.52	CSW	0.23
AW	2.44	NW	3.81	CW	0.36
ANW	1.80	N	3.90	CNW	0.70
AN	1.20	U	16.78	CN	1.65

Table 3.3 *Annual frequencies of the SLPMAN classification.*

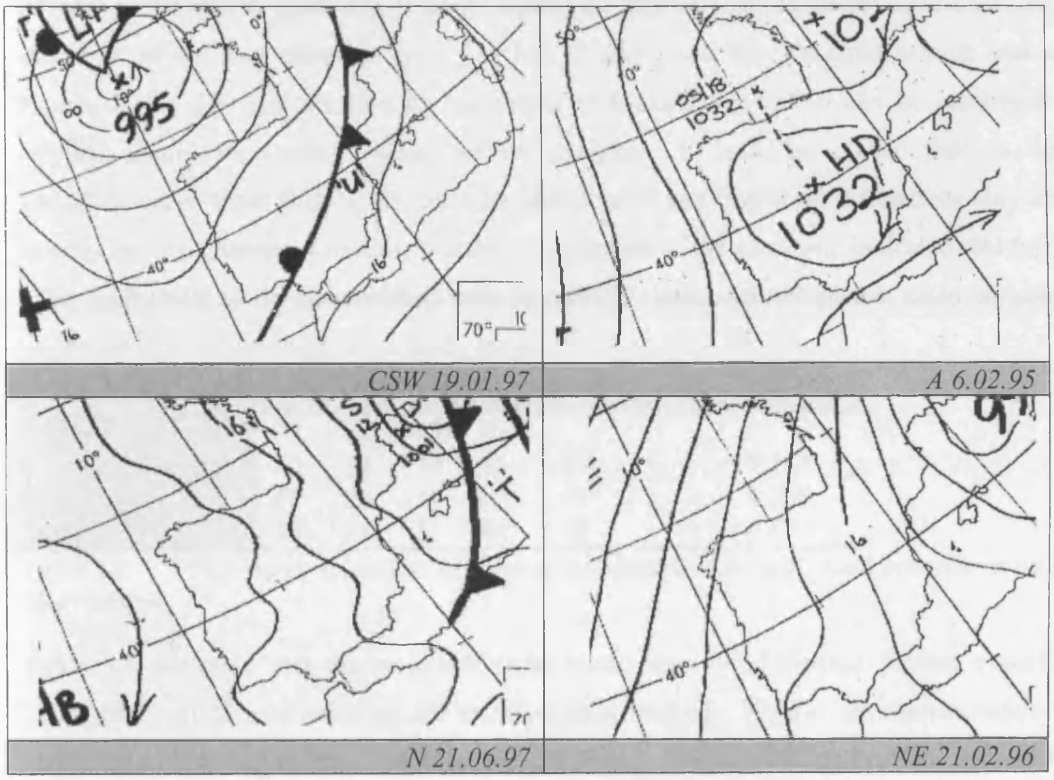

Figure 3.2 *Examples of weather types used in SLPMAN classification.*

3.5.1.1 Test of replicability

SLPMAN was tested for replicability. A random sample of 300 daily charts was selected from the original classified catalogue. Results were validated by three check procedures,

1. A classification by an independent classifier (a non-climatologist).
2. A reclassification undertaken approximately one year later by the researcher.
3. A reclassification undertaken approximately one year later by the same independent classifier as in stage 1.

	Number of Charts	Percentage agreement with classification 1
Classification 1	300	n/a

Classification 2	300	85
Reclassification 1	300	83
Reclassification 1	300	80

Table 3.4 Results of a simple test for replicability of SLPMAN.

Percentage agreement between classifications is given in *table 3.4* and a two-sample chi-square (χ^2) test was employed to determine if any significant differences (at $p<0.050$) could be found between the original classification and any of the three check procedures. Due to the infrequency of some of the hybrid types, which would violate the requirements of the chi-square test, only the incidence of the four common types (A, NE, C and U) in the 300-chart sample was tested. Results (*table 3.5)* indicate that no significant difference at $p<0.050$ can be identified. The original classification was retained for the analysis. It could be argued that an 'agreed' identification of these four types could be unequivocal and important differences may actually exist in the less common varieties. Further examination of the catalogue indicated that types that were most likely to be misclassified were hybrid 'C' types which depicted, often considerable, variations in wind direction in the study region.

	A	NE	C	U	χ^2	df	p-value
Classification 1	70	20	45	50			
Classification 2	60	23	30	60	4.49	3	0.213
Reclassification 1	68	29	50	40	3.05	3	0.385
Reclassification 2	59	24	51	49	1.68	3	0.642

Table 3.5 Chi-square analysis of the original classification and check procedures on a 300-chart sample.

Table 3.6 indicates that the objective index-based version of surface pattern classification (SLPINDC) produces similar results to the manual method. Figures are representative of the classified sample and do not represent the proportion of identical classifications achieved. For instance although SLPMAN tallies 2230 'U' charts and SLPINDC tallies 2229 there was only perfect agreement on 91% of days. Nevertheless this renders the need for manual pattern classification redundant and, although advantages still do exist, further details of this scheme are not described.

	A	C	U	E	N	ASW	CNE
SLPMAN	3181	1954	2230	570	484	192	388
SLPINDC	3126	2006	2229	574	472	201	382
					DF	χ^2	**P-value**
					6	1.58	0.954

Table 3.6 Chi square analysis of manual and index-based sea level classifications.

3.5.2 500MAN

500MAN was prepared using daily upper air charts (1200Z) obtained from the UKMO. Replicability of the procedure was investigated and the results (*table 3.7*) indicate a greater degree of replicability than for SLPMAN. The chi-square test applied to the incidence of four patterns (CR, ZN, ZS and WT) indicates no significant differences (at $p<0.050$) between the original classification and the three subsequent classifications (*table 3.8*). 500MAN types are shown in *figure 3.3* and are briefly summarized in *section 3.5.2.1*. Actual examples of 500MAN weather types are depicted in *figure 3.4*.

	Number of charts	Percentage agreement with classification 1
Classification 1	300	
Classification 2	300	95
Reclassification 1	300	96
Reclassification 1	300	94

Table 3.7 Results of a test of replicability of 500MAN.

	CR	ZS	ZN	WT	χ^2	df	p-value
Classification 1	61	30	29	27			
Classification 2	55	25	34	29	1.18	3	0.758
Reclassification 1	60	29	35	26	0.58	3	0.902
Reclassification 2	54	26	29	27	0.29	3	0.963

Table 3.8 Chi-square analysis of the original classification (500MAN) and check procedures on a 300- chart sample.

3.5.2.1 500MAN weather types

1. Anticyclonic ridge patterns related to the northerly expansion of subtropical (continental and maritime) air masses:

Centred ridge (CR) and *Mediterranean ridge (MR),* the expansion of a ridge of the subtropical subsidence anticyclone over the peninsula (and Mediterranean) supplying subtropical continental air (Tc) to the region. These are very common in summer (about a quarter of all days).

Atlantic ridge (AR) - the expansion of the Azores anticyclone north eastwards supplying tropical maritime air (Tm).

2. Upper troughs associated with polar air masses. These are troughs in the upper air long wave pattern and are defined by their longitudinal position:

Western trough (WT) (transistional Pm air), *Centred trough (CT)* (Pm), *Mediterranean trough (MT)* (Pm)

3. Cut off lows (*gotas frias*) and cold depressions. The former are only recognisable in the mid-troposphere. These are defined by their geographical position and can result from

cyclogenesis within the area. These types are more common in the 'shoulder seasons'.

Peninsula low (PL) (Pm), *South east low (SEL)* (Pm), *South west low (SWL)* (Pm), *Low to the north (LN)* (Pm).

4. Zonal circulations bringing maritime air masses (polar or tropical):

Zonal north westerly (ZN) (Pm), *Zonal south westerly (ZS)* (Tm)

5. Retrograde (north easterly) circulations with European continental air:

Retrograde centred trough (RCT) (Pc), *Retrograde Mediterranean trough (RMT)* (Pc). Virtually absent in summer.

6. Meridional circulation bringing arctic air masses.

Peninsula cold low (PCL) (A), Mediterranean cold trough (MCT) (A). Virtually absent in summer.

Table 3.9 shows the mean annual and seasonal frequency of each 500MAN type for the period 1958-1997.

Air mass	Weather Type	Annual	Spring	Summer	Autumn	Winter
A	PCL	5.32	7.22	0.42	4.22	9.51
	MCT	2.88	4.22	0.09	2.65	4.58
PC	RCT	1.48	1.00	0.20	2.11	2.68
	RMT	1.44	1.19	0.11	2.24	2.29
TC	CR	13.70	10.6	24.00	8.70	11.50
	MR	14.00	11.4	25.14	8.75	10.55
TM	AR	8.85	7.57	7.55	10.05	10.23
	ZS	12.34	10.38	10.88	13.5	14.6
PM	PL	6.08	8.18	4.22	7.54	4.38
	SEL	5.12	6.87	3.57	7.52	2.52
	LN	1.43	1.33	1.51	1.62	1.26
	ZN	7.67	8.44	4.86	9.34	8.04
	WT	4.61	4.66	3.88	5.01	4.89
	CT	5.89	8.22	5.01	8.05	2.28
	CT	6.65	7.58	5.56	7.01	6.45
	SWL	2.53	3.55	1.44	3.12	2.01

Table 3.9 *Mean annual and seasonal frequency (percentages) of each 500MAN type.*

(Next five pages)

Figures 3.3 *500MAN weather types.*

Figure 3.4 *Examples of 500MAN weather types.*

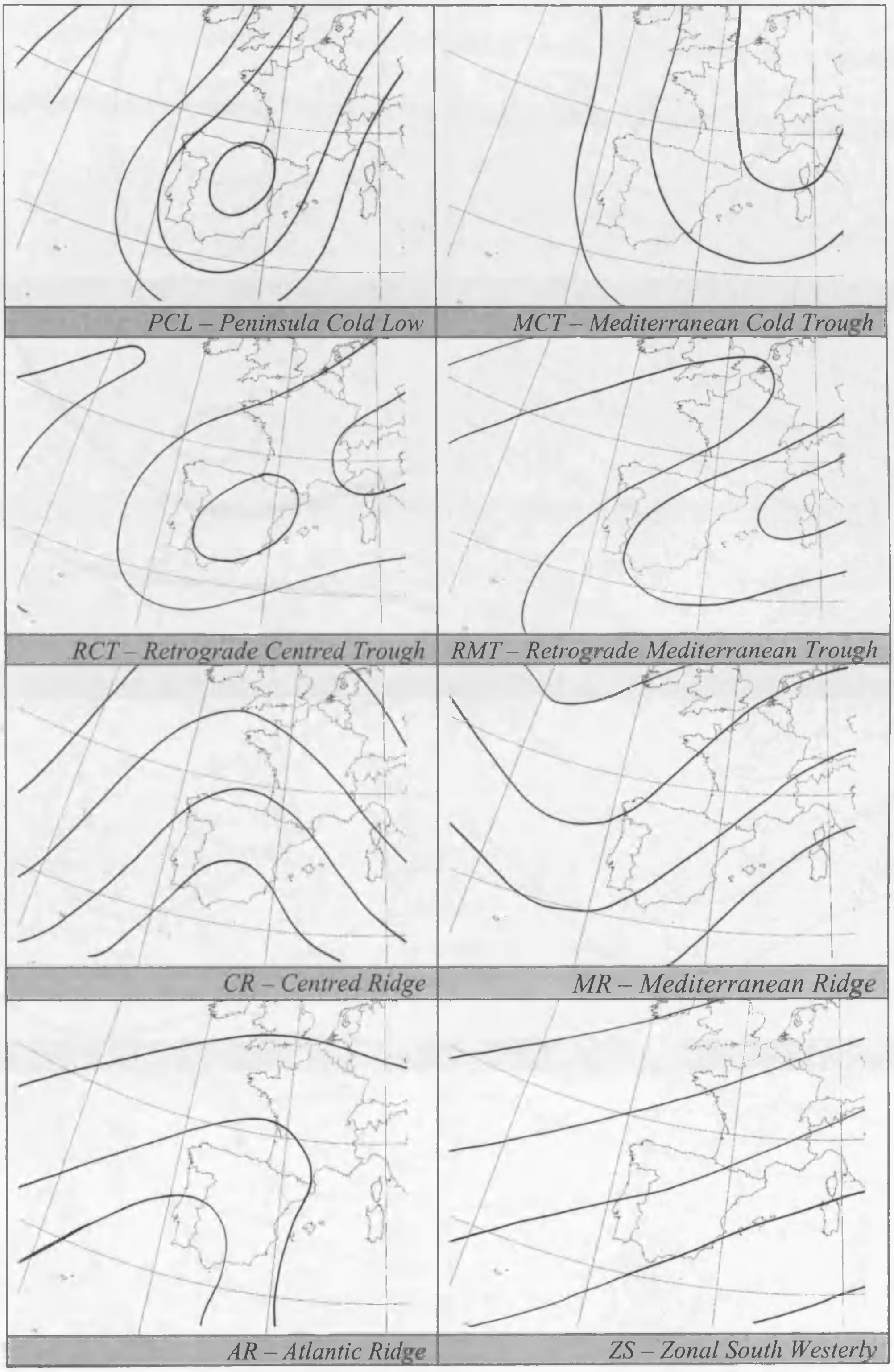
PCL – Peninsula Cold Low
MCT – Mediterranean Cold Trough
RCT – Retrograde Centred Trough
RMT – Retrograde Mediterranean Trough
CR – Centred Ridge
MR – Mediterranean Ridge
AR – Atlantic Ridge
ZS – Zonal South Westerly

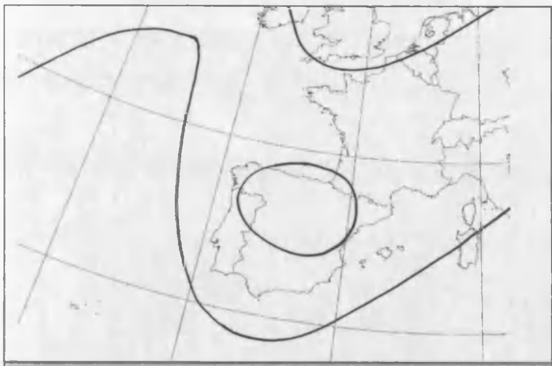

PL – Peninsula Low

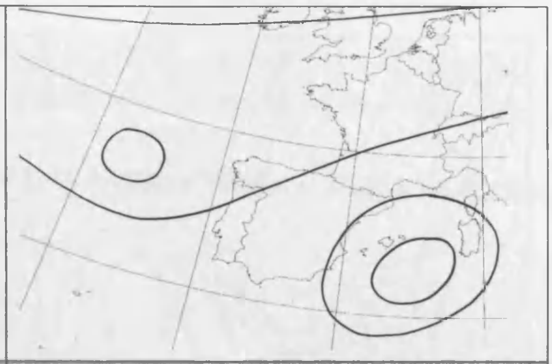

SEL –South east Low

LN - Low to the North

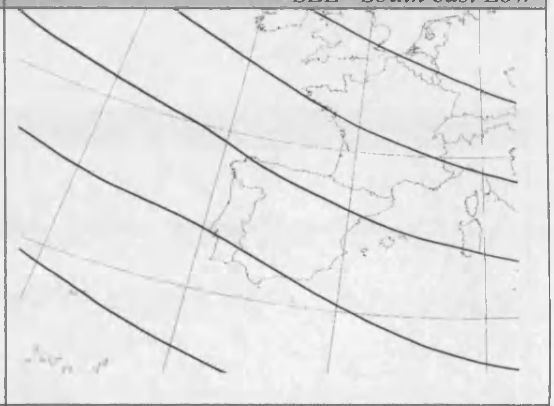

ZN – Zonal North Westerly

WT – Western trough

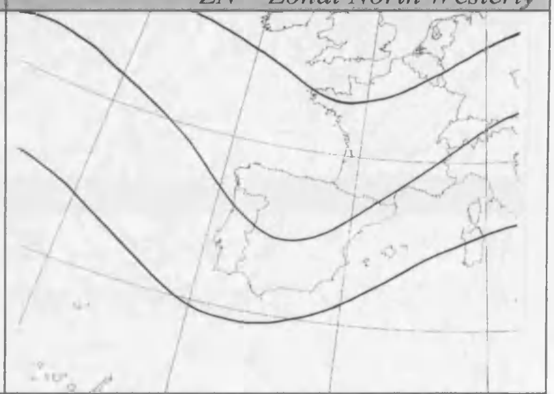

CT – Centred Trough

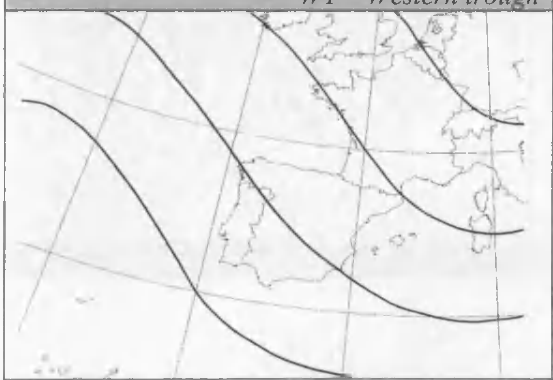

MT – Mediterranean Trough

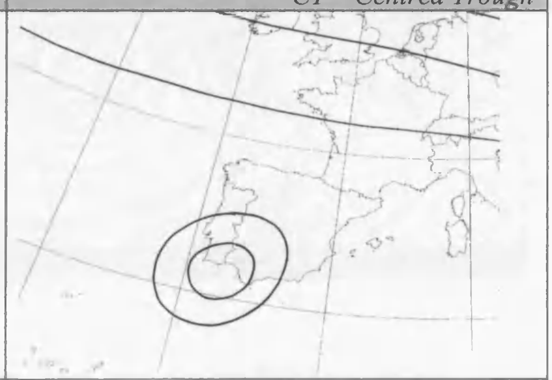

SWL – South West Low

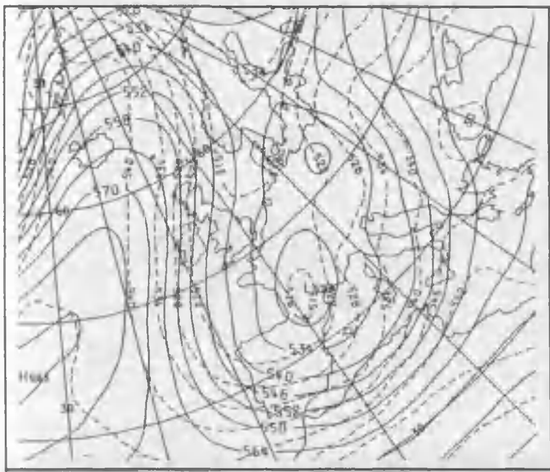

PCL 20.02.96

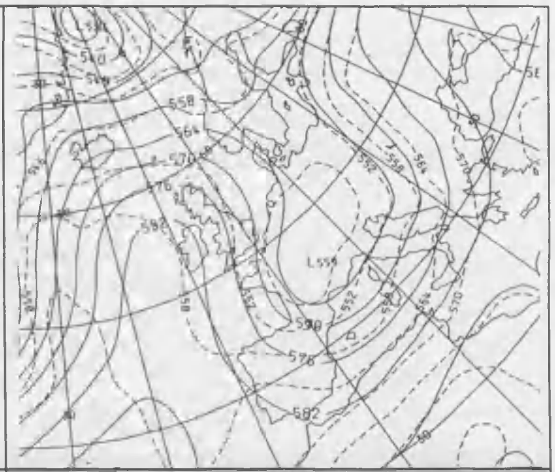

MCT – 23.06.96

RCT 25.06.95

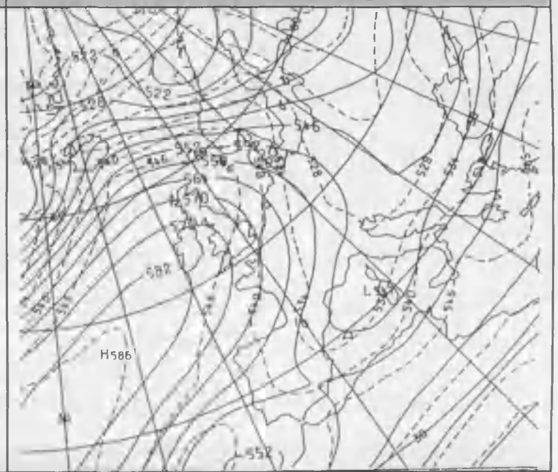

RMT 15.02.96

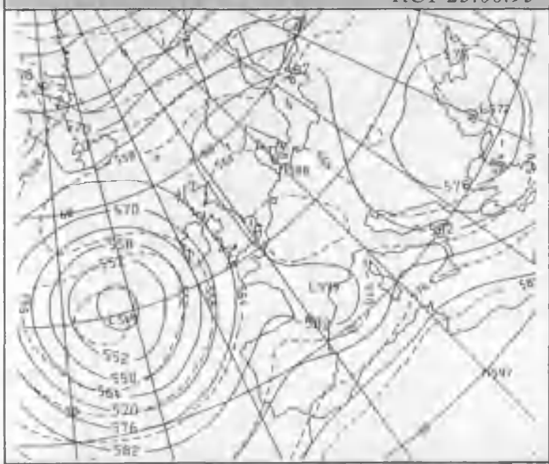

CR 11.08.97

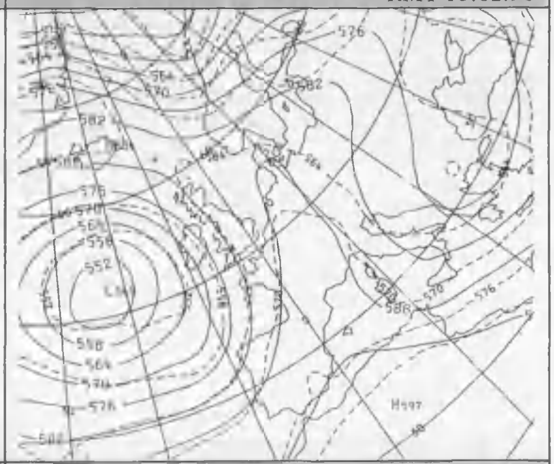

MR 12.08.97

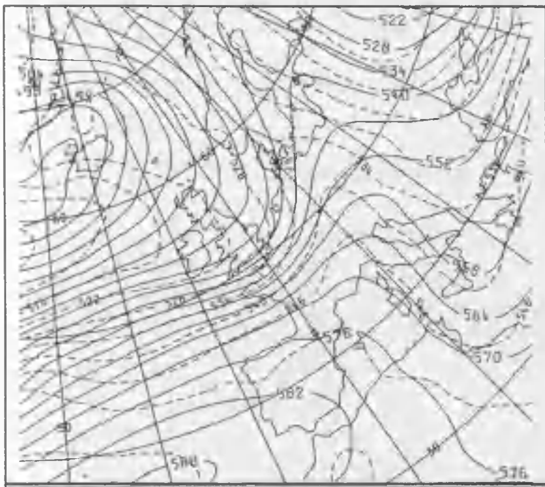

AR 18.02.97

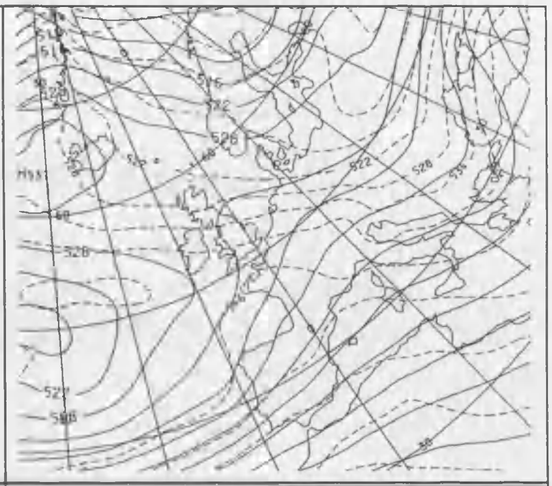

ZS 30.12.97

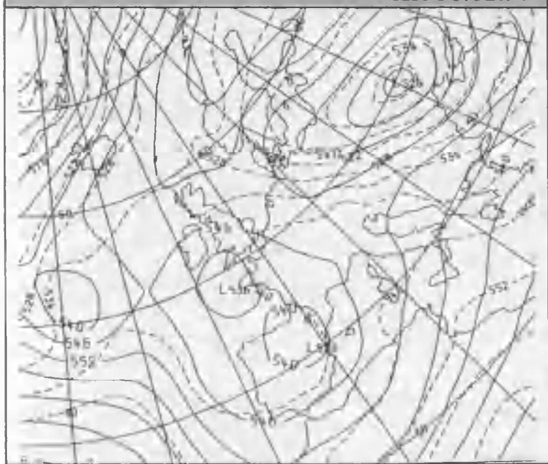

PL 24.01.96

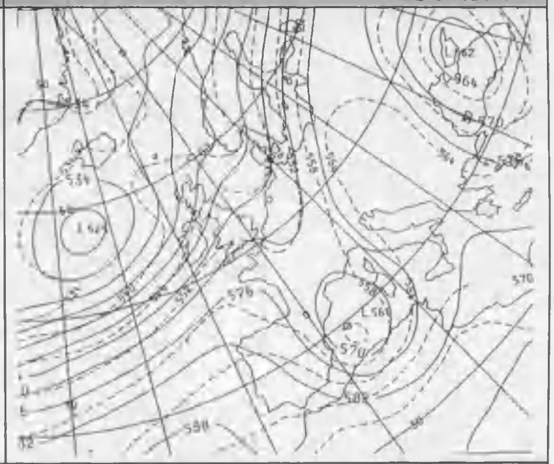

SEL 03.06.96

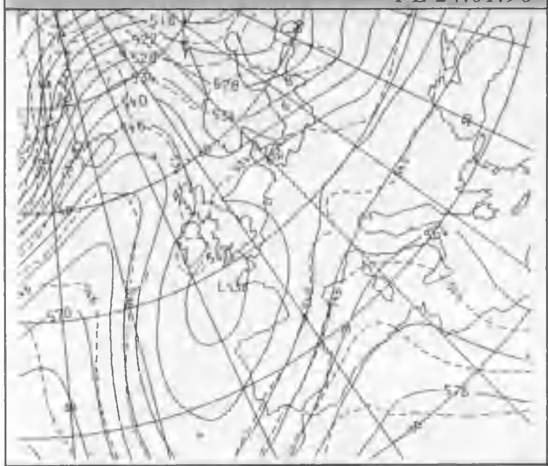

LN 19.01.97

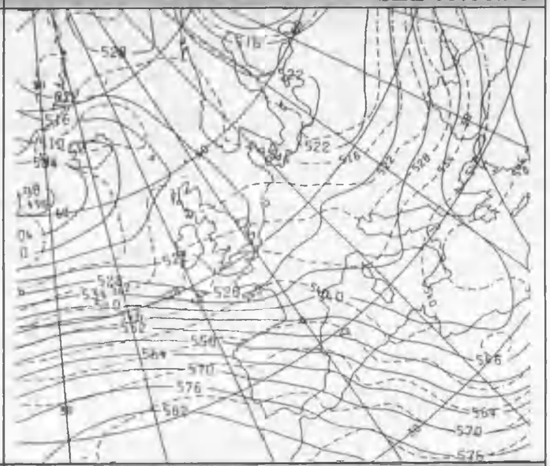

ZN 07.02.96

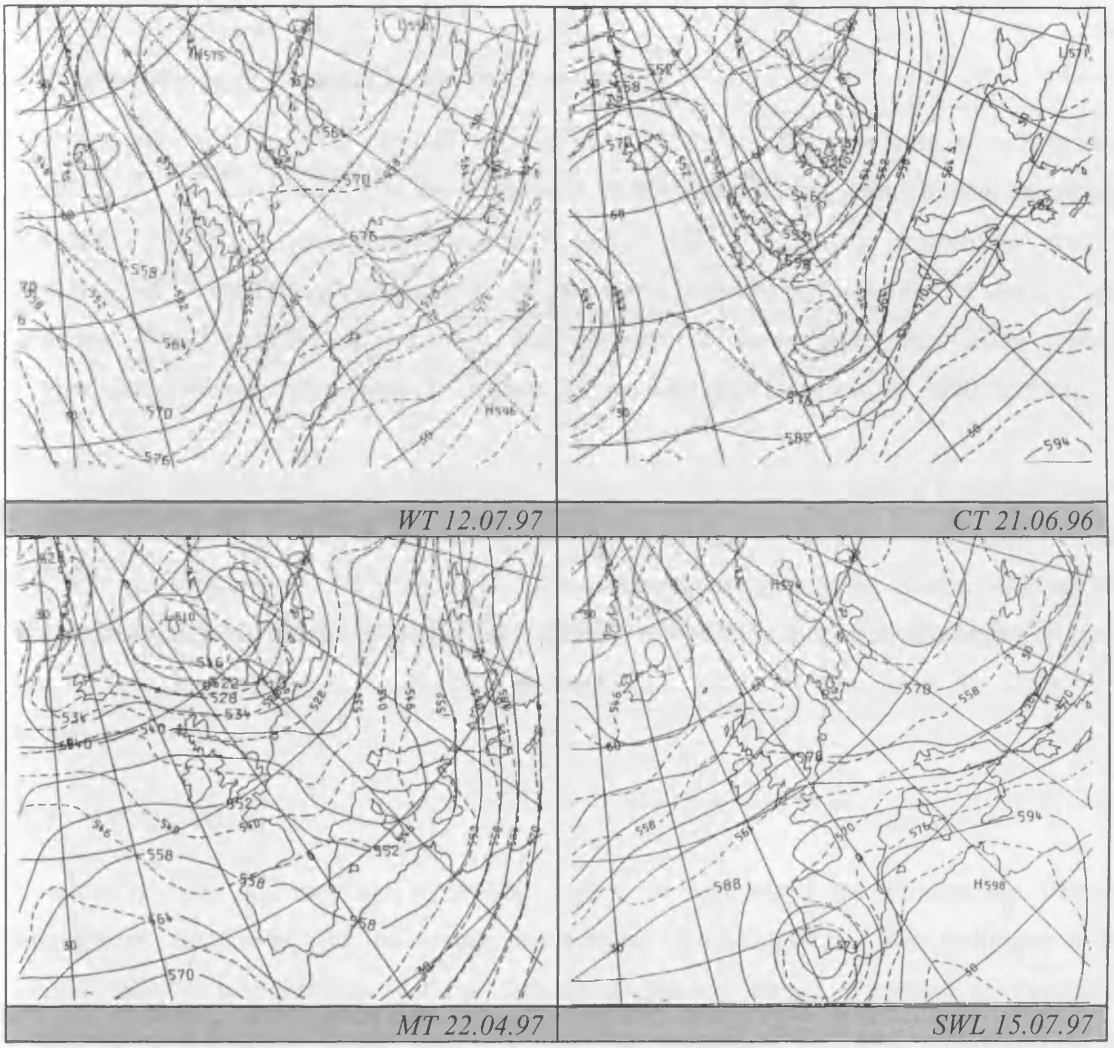
WT 12.07.97
CT 21.06.96
MT 22.04.97
SWL 15.07.97

3.5 Modification of 500MAN by kinematic information

The first real advance in a detailed understanding of day-to-day variability of mid-latitude weather was the identification of the importance of the movement of fronts, or the boundaries between different air masses (Barry and Chorley 1998). Kinematic approaches involve, primarily, the subjective identification of the motions of depressions (*appendix 3.4 and 3.5*) and attendant frontal surfaces and secondly, and comparatively less mobile, anticyclone activity. Consequently valuable insights can be gained from incorporating these within a static scheme.

In this study the procedures used by Flocas (1984) were employed to identify frontal incidence. All fronts (cold, warm or occluded) are grouped together and incidence of any deems that day 'frontal' in the catalogue. The incidence of fronts is incorporated into the synoptic analysis and the empirical models in later chapters. Incorporation of frontal information, although potentially crucial in addressing the non-stationarity problem, has only been undertaken by Wilby *et al* (1995) for the UK.

3.7 Conclusions

Synoptic climatology has one overriding goal - to understand the relationship between atmospheric circulation and the surface environment (Yarnal 1993). One technique is the classification of map patterns that can then be statistically related to surface environmental variables. Although in recent years this technique is increasingly being complemented by process-oriented and deterministic climate models, synoptic climatology still dominates climatic research. Manual procedures have a great deal of flexibility and work well when employed by skilled and knowledgeable operators. At each point in the classification an investigator can control the classification so as to fit known physical processes and therefore it is not an entirely 'black box' approach. On the other hand simple tests of replicability indicate that with respect to a large dataset, the benefits of speed and objectivity of index-to-class based models (*i.e.* SLPINDC and 500INDC) could render the manual catalogues redundant. This chapter has identified two manual methods for the Iberian area and an initial evaluation indicates that considerable knowledge and understanding of the behaviour of circulation in the region is afforded.

Manual typing aims to identify the prevailing air mass by examining wind direction and the connection between 500MAN and air mass is identified. Undoubtedly air mass climatology has had considerable influence on climate studies and consistent relationships can be found between air mass types and climatic elements. On the other hand consideration of air flow direction alone ignores key influential circulation characteristics like vorticity, flow strength and absolute isopleth values and these are captured better by objective procedures (PCA/CA methods).

One of the main advantages of any manual catalogue is the considerable meteorological skill and personal involvement that can be employed in its development and once a catalogue has been generated it can be revisited again when other applications are identified (for instance, the manual LWT catalogue has had the greatest number of applications of any synoptic method). The 500MAN catalogue developed in this study has been employed in two applications (Spellman 1998a, Spellman 2003).

Several disadvantages are commonly attached to manual methods and these can be identified in the development of these catalogues. Firstly, it is a time-consuming procedure. Over 14600 charts were individually examined for each catalogue and, in some instances, more than one chart for a particular day were used. The process is lengthened if corroboration is sought from an independent classifier. Secondly, the procedure is difficult to replicate. Simple tests of replicability indicate that some MSLP patterns are considerably harder to place in an undisputed class than smoother upper air patterns. The issue of replicability is well illustrated by *figure 3.5*, which depicts a synoptic pattern that could be classified as either WT or AR. This is one of the reasons why objective pattern recognition is favoured. Operator interpretation can vary over time.

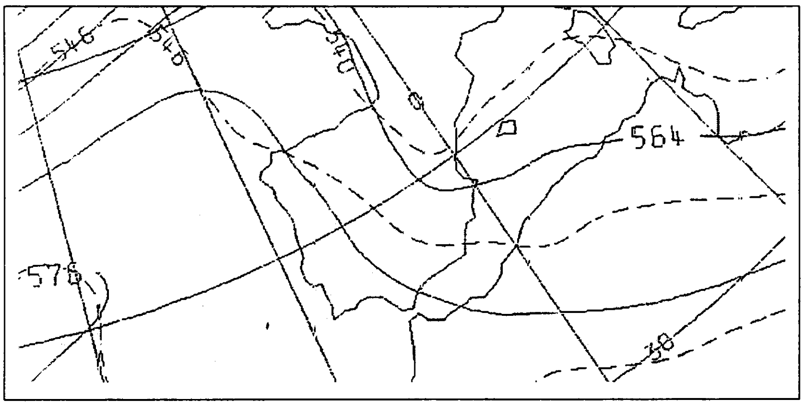

Figure 3.5 The above chart could be classified as either AR or MT.

Thirdly, overlap between classes can occur and is particularly noticeable between types such as

MT and AR or CR (*figure 3.6*). Ridge patterns over the peninsula are directly related to troughs occurring downstream to the east. On the other hand this need not be a problem as the occurrence of one flow type MT automatically dictates that CR is also present and hence association with any surface variable should be similar. Fourthly, significant regional variation may exist in the direction of airflow within the sample window. Regional variation of circulation pattern has been found to be less of a problem for the Iberian peninsula than for, say, the UK (Mayes 1996) due to the fact that the location is to the south of the main mid-latitude cyclone tracks and cyclonic systems are responsible for most regional flow differences (Lamb 1972). Regional differences in circulation are reduced at higher levels although some examples can be observed (*figure 3.7*).

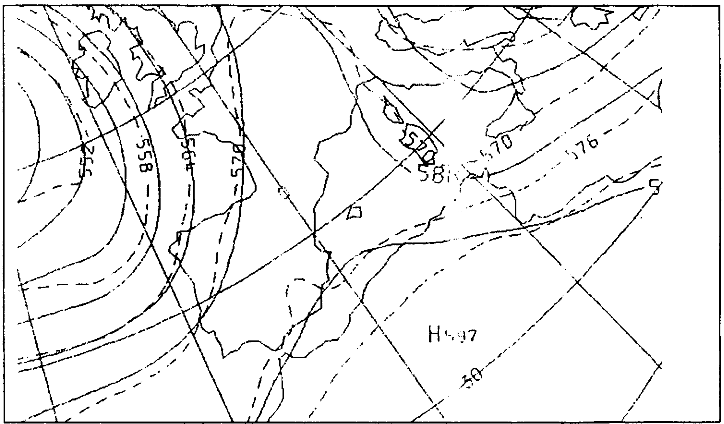

Figure 3.6 500hPa contour chart for 12th August 1997 represents a potential problem for classification. Isopleths over the peninsula display regional variation in curvature. Cyclonic to the north-west and anticyclonic to the south. The operator is confronted with a classification difficulty. Is this a trough or a ridge pattern? Furthermore what errors are introduced by the regional variation in synoptic mechanism with respect to the end use?

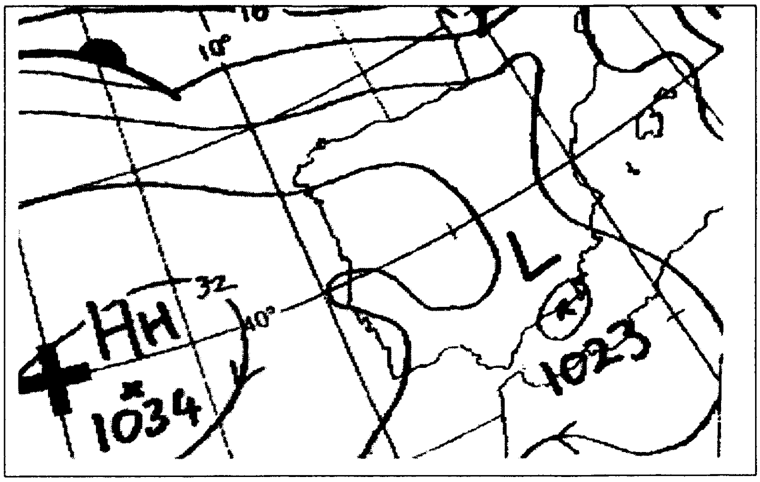

Figure 3.7 Regional variation in circulation characteristics 17.05.87.

Finally, the existence of different absolute values will affect the application of a synoptic system. The two charts depicted in *figures 3.8a* and *3.8b* can both be classified as CR patterns however *figure 3.8a* has significantly higher contour heights than *figure 3.8b*. The same air mass will be incident but lower contour heights (a function of steep tropospheric lapse rates) suggest greater atmospheric instability. This could result in cloud development and consequent precipitation. The procedure could be modified so as to incorporate absolute values however by raising the level of sophistication and difficulty of classification the overall rationale behind such taxonomic procedures is lost. Despite these comments the manual technique clearly advances an initial appreciation of modes of atmospheric circulation, its variability and persistence, much more so than the 'black box' automated procedures. In this respect, even if not judged as the 'optimal' classification technique, it is an extremely valuable exercise. The evaluation exercise in *section 3.5.1.1* (test of replicability) identifies that at this latitude subjectivity in classification has not proven to be a significant consideration.

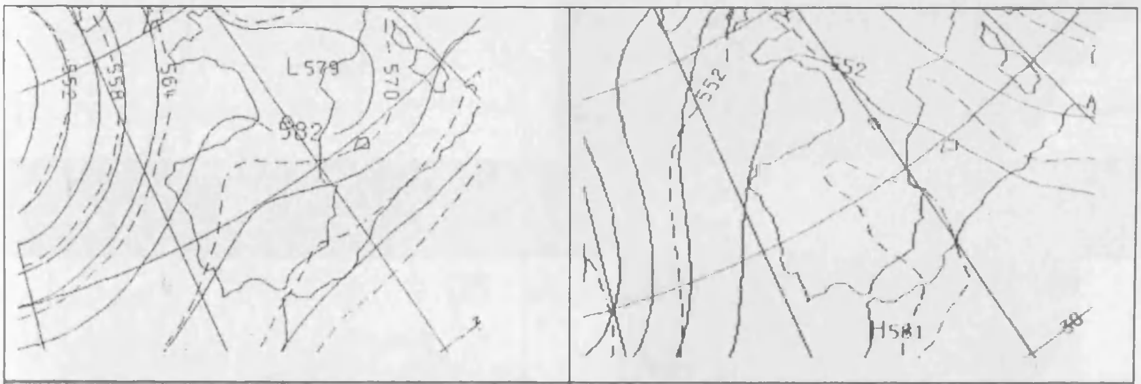

a.500hPa contour height 11.08.97 showing a CR pattern with a contour height of 588hPa over the central region of Spain.

b. 500hPa contour height chart for 6.02.95 showing a CR pattern with a contour height of 574 hPa over the central region of Spain.

Figure 3.8 Impact of absolute values of 500hPa contours. Nb. Dashed lines are thickness heights.

Manual scrutiny of surface charts is required if frontal information is to be included as this data is not amenable to a digital format. It is suggested that frontal incorporation will significantly reduce within-type class variability. This has been undertaken by Wilby *et al* (1995) for the UK and this present study represents the first attempt to do this for the Iberian area. The following cautionary points must be noted,

- Fronts do not have an equal incidence over the whole of the peninsula. One of the most common tracks is over the north-west quadrant, part of the trailing end of a front associated with a more northerly depression (*figure 3.9a*). These will not pass over much of the peninsula and often not over the Mediterranean and Balearics at all. Similarly fronts associated with Balearic depressions (*figure 3.9b)* will not affect rainfall in northern regions.

- Fronts generally arrive from the Atlantic but even when fronts have crossed the peninsula their precipitable water will be greatly reduced during passage (topography and the *meseta* will greatly reduce moisture).
- Fronts have different characteristics. They are warm, cold, occluded, stationary, fast moving, kata- and ana- but are necessarily classified as the same entity in this procedure.

Nevertheless detailed frontal information can clearly advance the success of this technique.

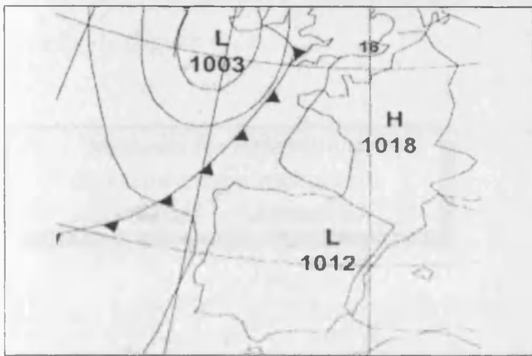

a. This trailing cold front will reach the north west of the peninsula but will not cross it. 12.07.97

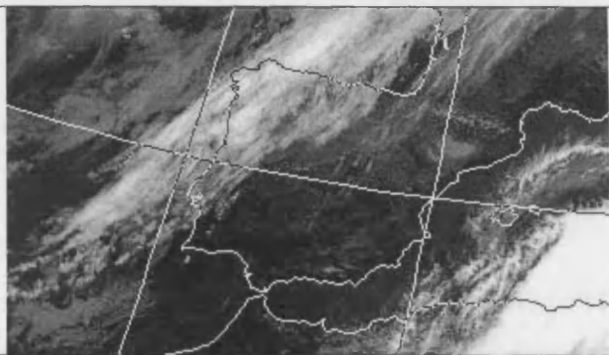

NOAA AVHRR Infrared image 12.07.97.

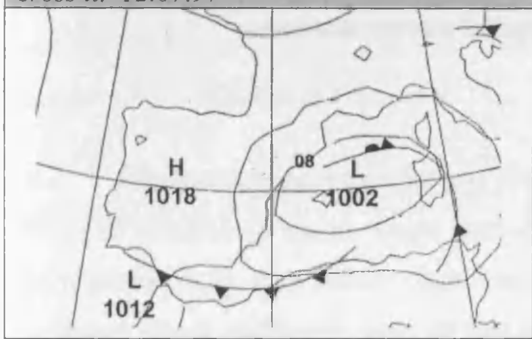

b. A depression in the Balearic region will move east and not affect central and western peninsula locations. 6.01.97

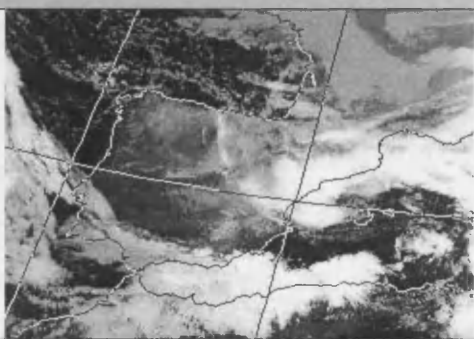

NOAA AVHRR Infrared image 6.01.97

Figure 3.9 Frontal differences in the peninsula region.

Chapter Four
Synoptic climatological methods
Static approaches: Daily models

4.1 Introduction

Automated circulation classification is more common than subjective map pattern identification due to the assumed objectivity and the speed at which a catalogue can be generated. Methods are, without exception, computer-based due to the huge quantities of data and the sophistication of analysis. The purpose of this chapter is to identify, describe and apply a range of automated methods (*figure 4.1*).

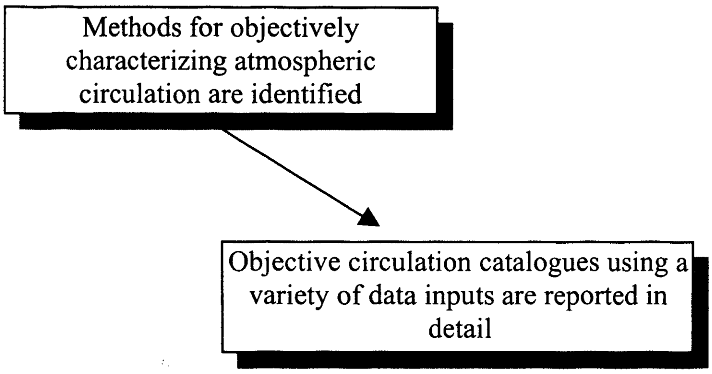

Figure 4.1 Outline of Chapter 4.

4.2 Eigenvector-based technique for synoptic classification

Synoptic climatology has no single methodological approach and a number of techniques have been proposed for map pattern classification. The eigenvector technique (see *chapter 2*) has remained almost unchanged since its first introduction to climatology and has become the most commonly used technique to derive a circulation catalogue (Richman 1986, Spellman 1998b).

Five objective catalogues are prepared by this PCA/CA technique: The four daily catalogues 500AUT, 500AUTR, SLPAUT and SLPAUTR and the monthly catalogue 500AUTM. In the pilot study THICKAUT and MULTIAUT also employed this technique.

4.3 Airflow index-to-class technique

The airflow index-to-class method generates 8 air flow index series - pressure (*p*), flow strength (*f*), flow direction (*dd*), southerly flow (*s*), westerly flow (*w*), southerly vorticity (*zs*), westerly vorticity (*zw*) and total vorticity (*z*) - that can either be used separately (Conway *et al* 1996, Spellman 2000a) or they can be combined to create nominal categories (*e.g.* Lindersen 2001) using simple rules. Jenkinson and Collinson (1977) note that an advantage of this technique is that it can be transferred to other mid-latitude locations and indeed a similar objective derivation of values of flow and vorticity can be found in an earlier paper by El Dessouky and Jenkinson (1975) for Egypt. Buishand and Brandsma (1997) have used a variant of the system to predict temperature and precipitation in the Netherlands and further applications have been described for Portugal (Trigo and Dacamara 1995), southern Spain (Goodess and Palutikof 1998), Sweden (Chen 2000), the Iberian Peninsula (Spellman 2000a, 2000b) and southern Scandinavia (Linderson 2001).

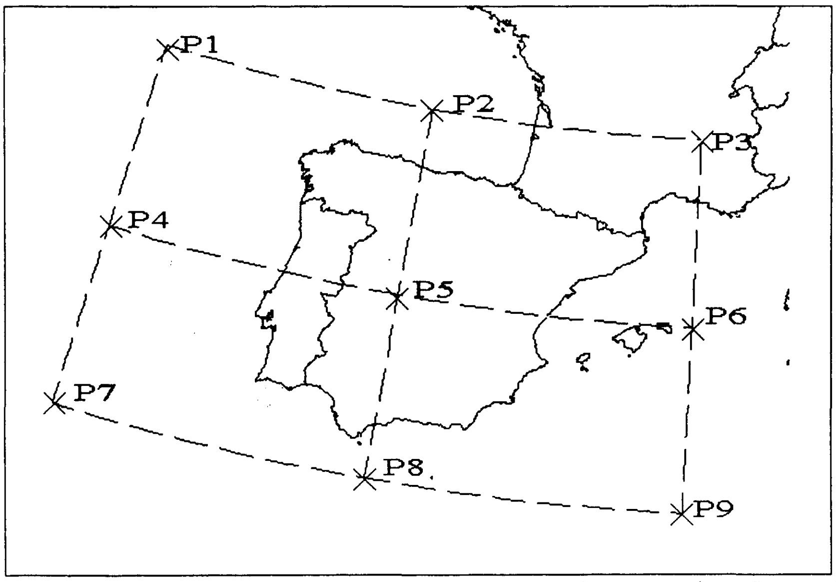

Figure 4.2 Locations of gridpoints for development of air flow indices.

Daily gridded MSLP (hPa) was taken to construct eight surface flow and vorticity indices (see *table 4.1*). The constants account for relative differences between gridpoint spacing (*figure 4.2*) in the east-west and north-south direction (recalculated using guidelines in El Dessouky and Jenkinson (1975)).

The mid-tropospheric catalogue was calculated using 500hPa contour height data and therefore the units are decametres (dm), rather than hectopascals (hPa), however, although strictly not comparable with the surface, values can be determined using the same equations.

Index	Definition
P	which is the MSLP over the area in hPa
W	which is the westerly component of geostrophic surface wind calculated as the pressure gradient between 35°N and 45°N
S	which is the southerly component of geostrophic wind surface wind calculated as the pressure gradient between 15°W and 5°E
Dd	which is the wind direction in degrees
F	which is the speed in metres per second of the wind (*i.e.* the surface geostrophic flow)
Zw	which is the westerly shear vorticity
Zs	which is the southerly shear vorticity
Z	which is the total shear vorticity
	1) $P = 0.0625\ [(P1 + P3 + P7 + P9) + 2\ (P2 + P4 + P6 + P8) + 4P5]$
	2) $W = 0.25\ [(P7 + 2P8 + P9) - (P1 + 2P2 + P3)]$
	3) $S = 0.653\ [0.25\ (P3 + 2P6 + P9) - 0.25\ (P1 + 2P4 + P7)]$
	4) $F \quad (W^2 + S^2)^{1/2}$
	5) $Dir = \tan^{-1} (W/S)$
	6) $ZW = 1.056\ [(P7 + 2P8 + P9) - (P4 + 2P5 + P6) - 0.951\ [(P4 + 2P5 + P6) - (P1 + 2P2 + P3)]$
	7) $ZS = 1.305\ [0.25(P3 + 2P6 + P9) - 0.25(P2 + 2P3 + P8) - 1.305\ [0.25\ (P2 + 2P3 + P8) - 0.25(P1 + 2P4 + P7)]$
	$Z = ZW + ZS$

Table 4.1 Air flow indices used in the airflow index method (flow units are geostrophic, expressed as hPa per 10° latitude at 40°N). Adapted from the original suite of equations developed by El Dessouky and Jenkinson 1975).

From the daily class-based catalogues obtained (SLPINDC and 500INDC), following the same rules as Jenkinson and Collison (1977), each day is assigned to a weather type as follows;

1) the direction of flow is $\tan^{-1}(W/S)$. 180° is added if W is positive. The direction of flow is determined using an eight point compass with 45° per sector.
2) if $|Z|$ is less than F a pure directional type based on flow direction in 1) results.
3) if $|Z|$ is greater than 2F then a cyclonic type results if $Z > 0$ and anticyclonic if $Z < 0$.
4) if $|Z|$ is between F and 2F then a hybrid type results depending on the sign of Z and flow direction.
5) if both F and $|Z|$ are less than 6 there is light indeterminate flow corresponding to Lamb's U.

The appropriateness of these rules to regions other than the British Isles has been discussed elsewhere and Goodess and Palutikof (1998) conclude that these threshold values can be retained for the Iberian region.

4.4 Development of circulation catalogues for the Iberian peninsula using MSLP

Classification of daily MSLP (hPa) was conducted using raw data (SLPAUTR) and standardized data (SLPAUT). As previously noted, in Mediterranean latitudes surface pressure fields can be difficult to classify in summer months when little variation can be detected. Consequently in both models the summer months were dominated by single pattern types (see *figure 4.3*). Investigation in the pilot study ruled out detailed discussion of these schemes.

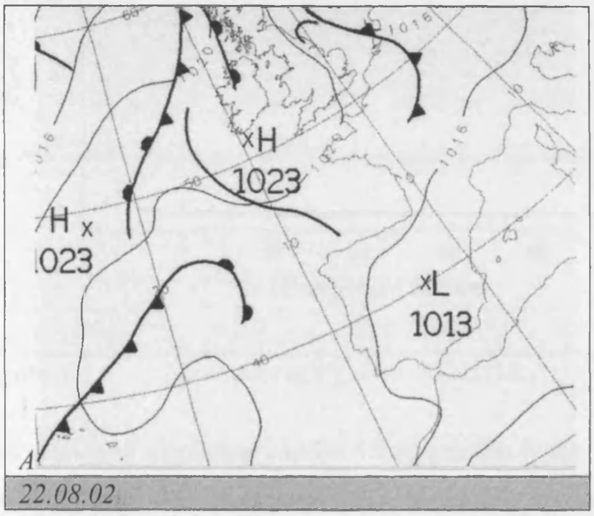

Figure 4.3 SLPAUT - Dominant SLPAUT pattern (a thermal low is present over the peninsula).

4.5 Development of circulation catalogues for the Iberian peninsula using 500hPa contour surface

Classification of daily maps of 500hPa contour height was conducted using raw data (500AUTR) and standardized data (500AUT).

4.5.1 Classification of the 500hPa surface using non-standardized data (500AUTR)

4.5.1.1 Method

Application of an unrotated[1] correlation matrix-based PCA lead to the identification of five principal components (*figure 4.4*) that together accounted for 98.2% of the total variance (*table 4.2*). A majority of the total original variance (73.9%) is explained by PC1.

[1] Rotation did not aid interpretation (see appendix 4.3)

	PC1	PC2	PC3	PC4	PC5
Eigenvalue	48.0	8.9	3.3	2.5	1.2
Proportion of total variance explained (%)	73.9	13.8	5.0	3.8	1.8
Cumulative proportion	73.9	87.7	92.7	96.5	98.2

Table 4.2 Eigenanalysis of PCA on 500AUTR .

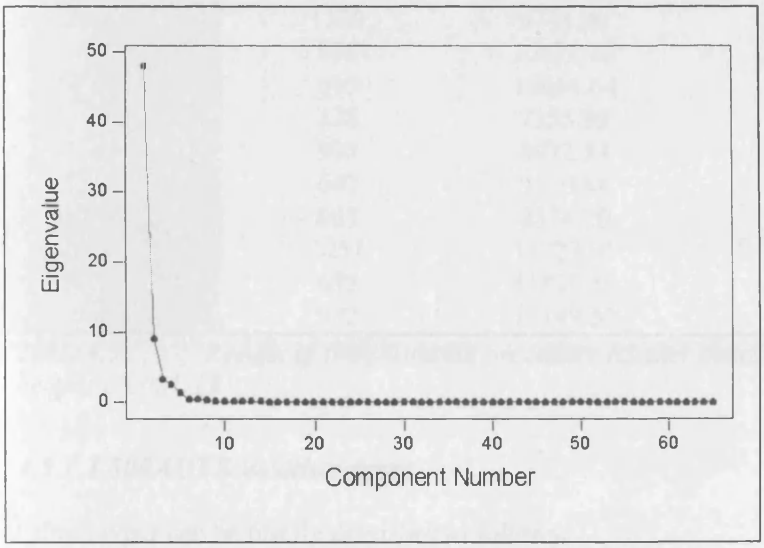

Figure 4.4 Scree plot of PCA on 500AUTR..

The clustering algorithm yielded 15 circulation types (*table 4.3* and *appendix 4.1*). Frequency is given in *figure 4.5,* mean patterns in the 500hPa contour field for each type are depicted in *figure 4.6* and *figure 4.7* gives examples of 500hPa charts (1200Z) for each type. The 500AUTR catalogue is included in this discussion because of its inherent description of actual flow patterns over the study area rather than because of its utility in explaining rainfall variability. Patterns in both surface and upper air level (particularly contour heights in this case) are strongly seasonally dependent, for instance types characterised by the highest 500hPa contour values will only occur in the summer months as 500hPa height is a function of air temperature in the lower troposphere. Consequently this scheme is not described in as much detail as the 500AUT scheme.

Cluster Number	No of observations	Within cluster sum of squares	Average distance from centroid	Maximum distance from centroid
1	1323	8634.26	2.42	7.45
2	1564	10997.64	2.53	6.54
3	775	8937.35	3.26	6.37
4	897	9697.66	3.14	8.51
5	1579	9384.17	2.29	5.79
6	1139	9741.80	2.80	5.89
7	876	10672.19	3.53	6.85
8	695	10634.64	3.77	7.70
9	378	7355.99	4.17	9.45
10	993	8972.34	2.87	6.75
11	647	9110.84	3.57	7.76
12	903	8374.20	2.92	6.80
13	1251	11723.91	2.93	6.79
14	653	11820.56	4.03	11.27
15	952	11149.59	2.82	7.33

Table 4.3 Results of the clustering procedure (cluster details) using raw 500hPa contour heights (500AUTR).

4.5.1.2 500AUTR weather types

Fifteen types can be briefly described as follows,

(a) Western trough patterns Types 1, 8 and 9 generally depict troughs with axes to the west of the peninsula. Types are differentiated by the absolute 500hPa surface heights (and therefore, indirectly, the season of occurrence). 500AUTR9 possesses the lowest mean heights (ranging between 538dm and 549dm over the peninsula) and 500AUTR1 the highest (577-585dm). 500AUTR1 displays low monthly frequencies in the winter half of the year (*figure 4.8* - virtually absent in January (RII – 0.1) and February (RII – 0.2)), this is a time when 500AUTR9 is comparatively common (the RPI of 500AUTR9 is 3.7 in February *figure 4.9*). 500AUTR9 trough axes often lie over the west or even central parts of the region.

(b) Eastern trough patterns - Trough features lying to the east of the peninsula are typified by Types 4, 6, 11, 12 and 14. Again the primary difference relates to the height of the 500hPa pressure surface. The example of 500AUTR11 (*figure 4.7k*) shows a tight gradient across the peninsula which brings north westerlies towards a deep mid-Mediterranean trough. A similar pattern is observed on 16th October 1996 under 500AUTR4 but mean 500hPa height is greater.

(c) Zonal patterns – Type 2, 3 and 12 (northerly) and type 7 (southerly) depict zonal patterns. 3 and 12 both have steeper contour gradients than 2, and 500AUTR3 has lower heights than 500AUTR12. A good example of zonal flow is depicted by *figure 4.7l,* in this case very shallow wave features sets up a weak north westerly across Spain.

(d) Ridges – 500AUTR5 days are typified by strong ridge patterns with a mean of 586dm over the peninsula. It is illustrated by the example of 13th August 1997 (*figure 4.7e*) where the 594dm contour crosses the region. This type dominates the circulation of the high summer (*figure 4.8*) with 49% of July days (RII 4.6) and 42% of August days (RII 3.9). In 500AUTR7 the axis of the ridge is to the east (*figure 4.7g*).

(e) Slack patterns – 500AUTR10 and 500AUTR15 depict very little gradient in the 500hPa surface. There is an average 500hPa height of 570dm in 500AUTR10 and 560dm in 500AUTR12. A good example of 500AUTR10 shows the peninsula lying in a col between areas of low heights to the west and east. To the north (around 60°N) there is strong zonal flow. 500AUTR15 (15th February 1996) occurs between a north-eastern extension of the Azores anticyclone and a retrogressive trough over the Gulf of Lyons (*figure 4.7o*).

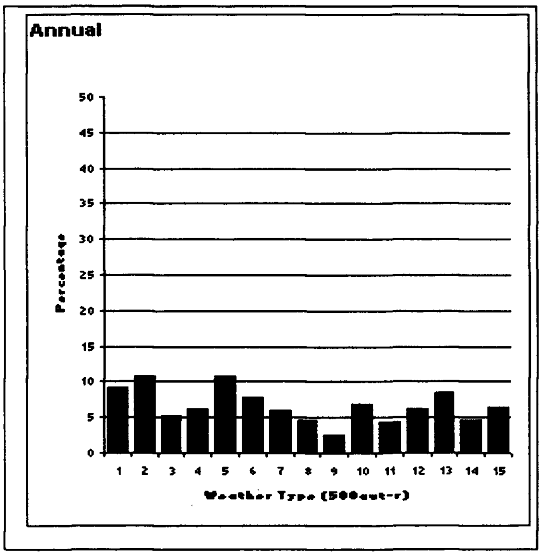

Figure 4.5 Percentage occurrence of each 500AUTR weather type.

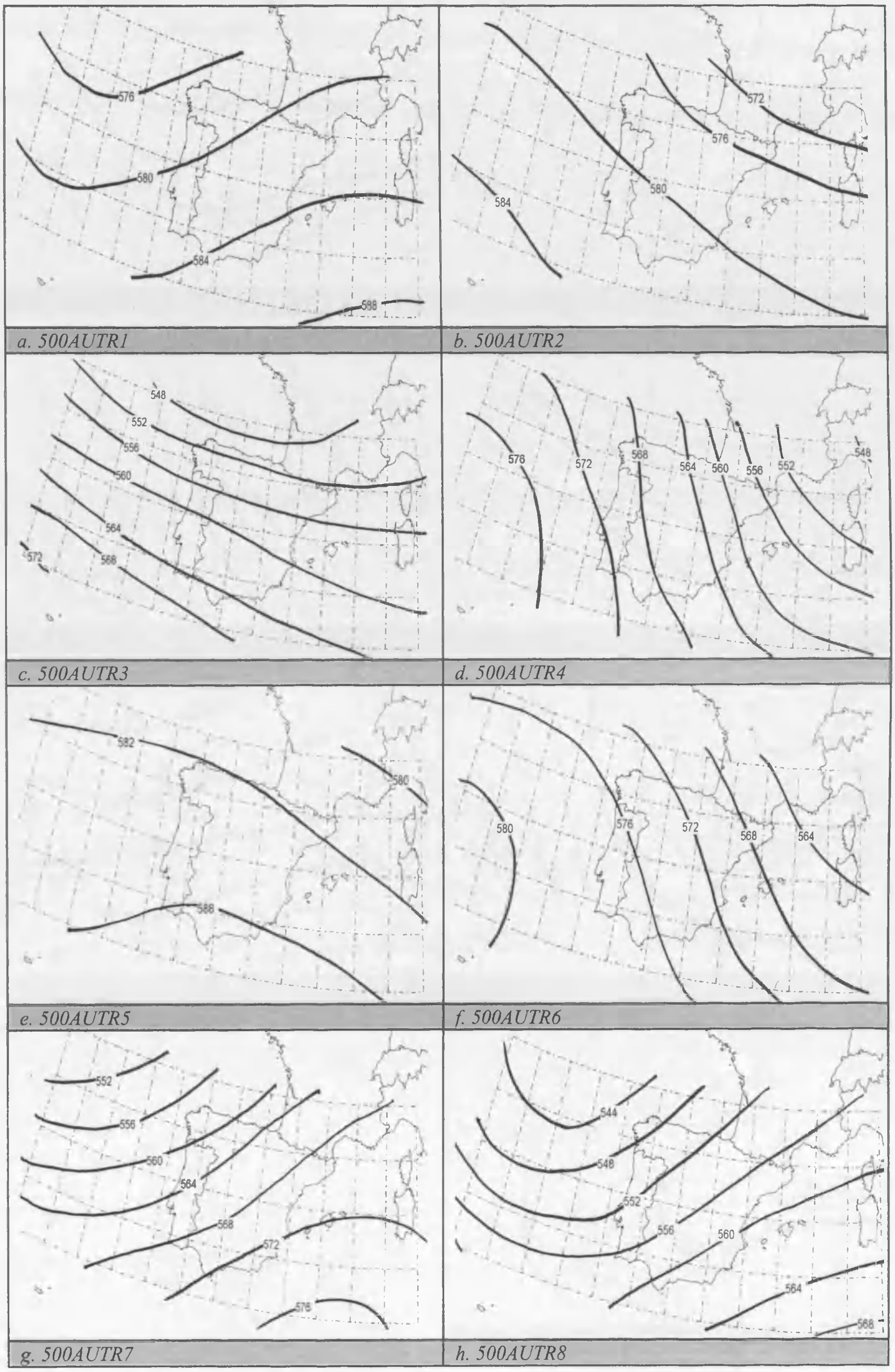

a. 500AUTR1 b. 500AUTR2 c. 500AUTR3 d. 500AUTR4 e. 500AUTR5 f. 500AUTR6 g. 500AUTR7 h. 500AUTR8

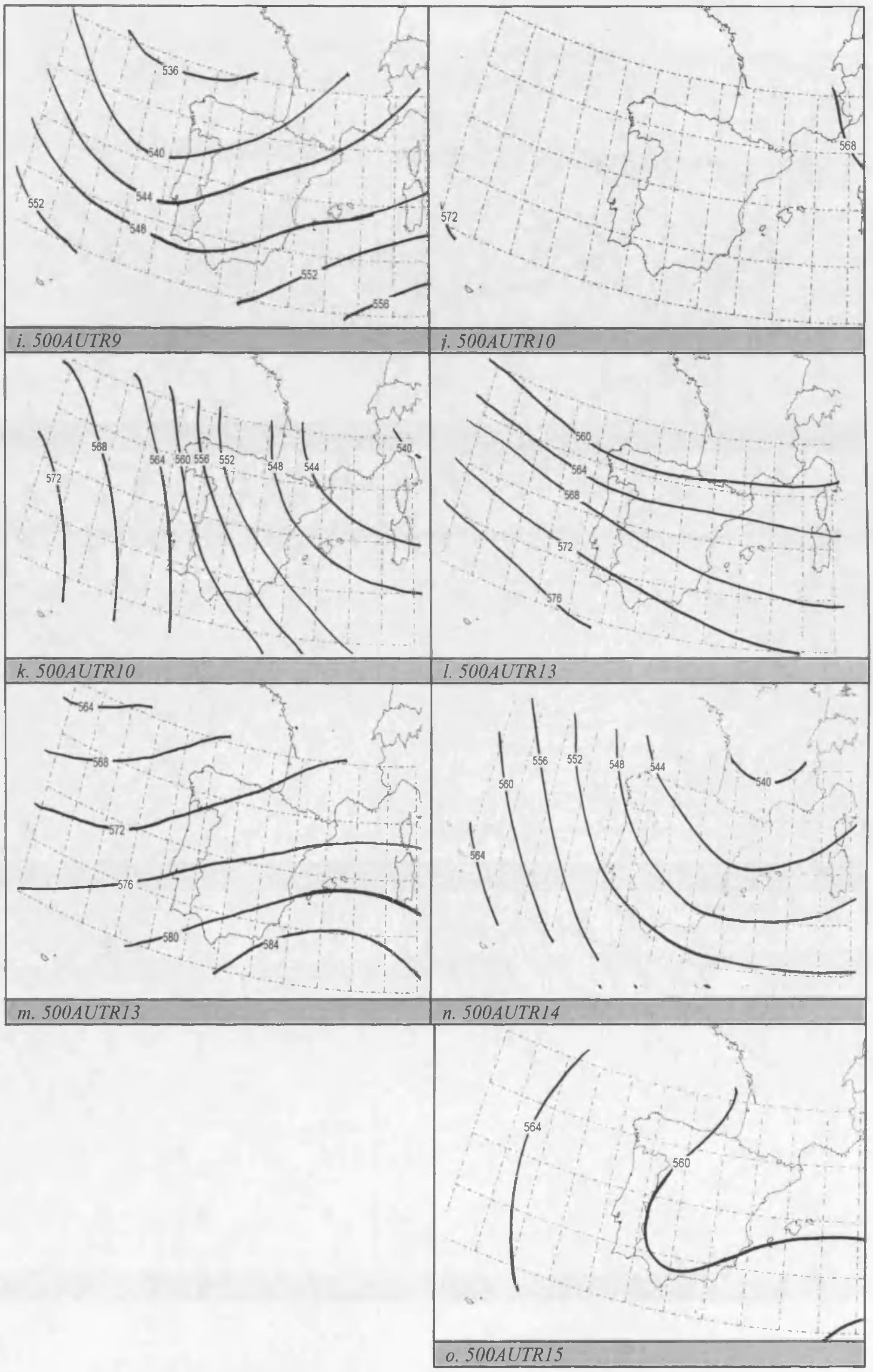

Figure 4.6 500AUTR weather types. Charts show mean contour heights in decametres.

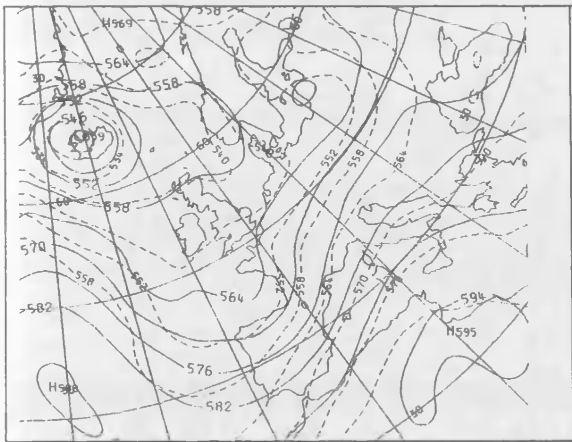

a. 500AUTR1 16.06.97

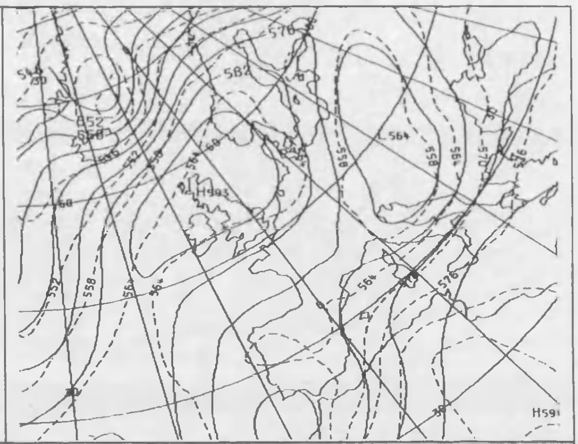

b. 500AUTR2 25.06.96

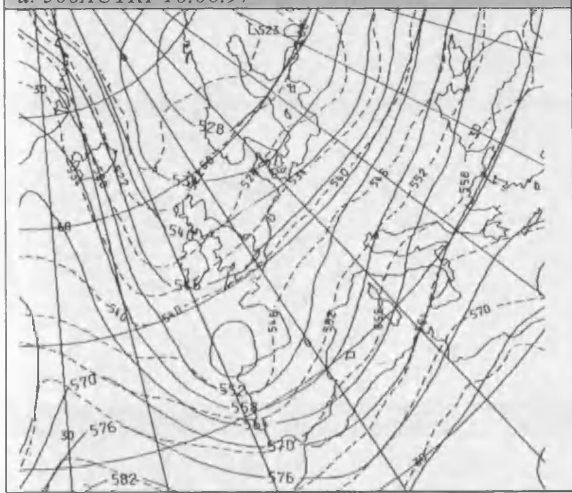

c. 500AUTR3 11.05.95

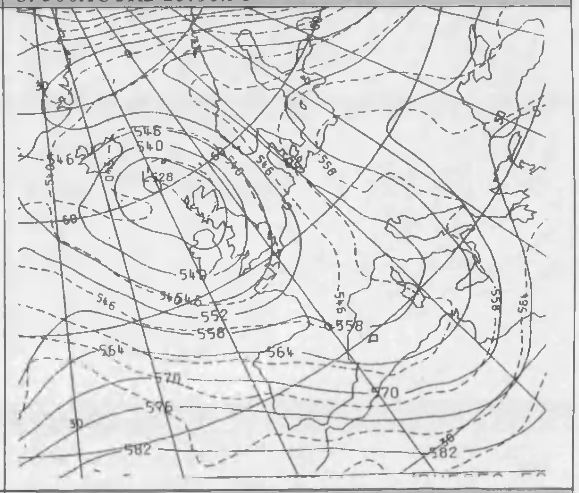

d. 500AUTR4 16.10.96

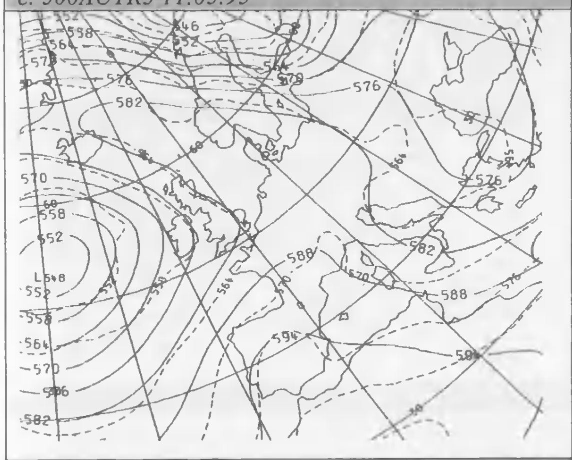

e. 500AUTR5 13.08.97

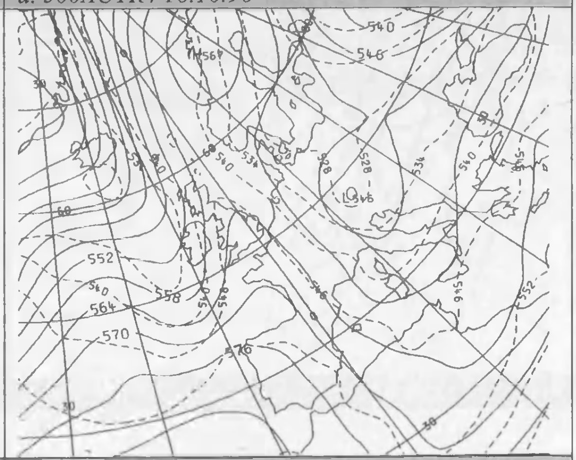

f. 500AUTR6 03.12.95

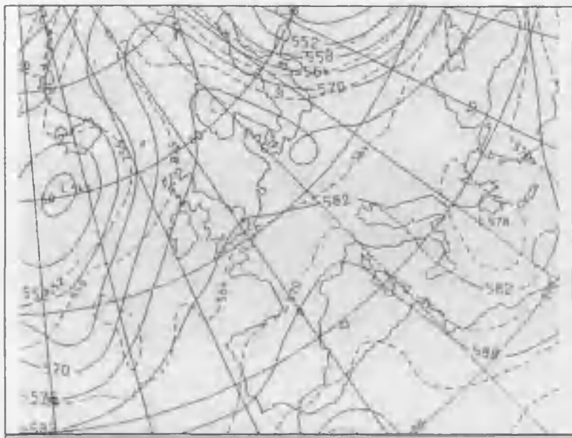

g. 500AUTR7 15.08.97

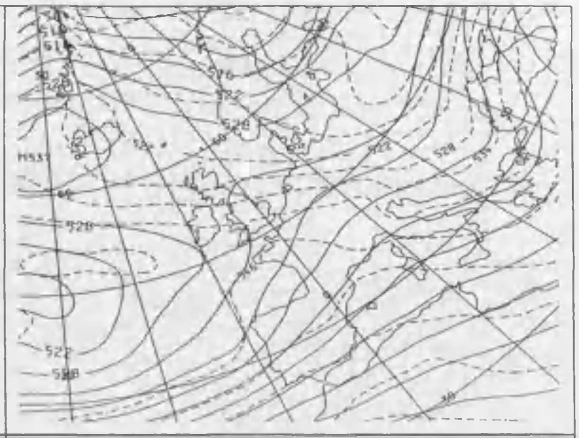

h. 500AUTR8 30.12.97

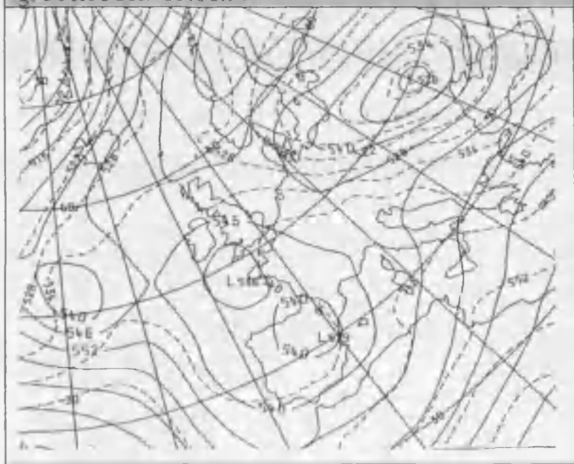

i. 500AUTR9 24.01.96

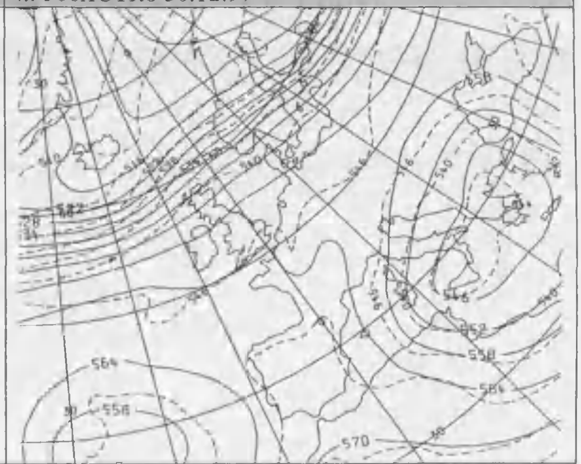

j. 500AUTR10 06.06.96.

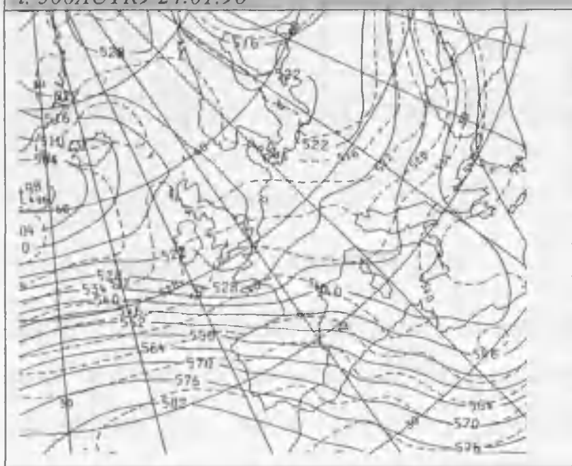

k. 500AUTR11 07.02.96

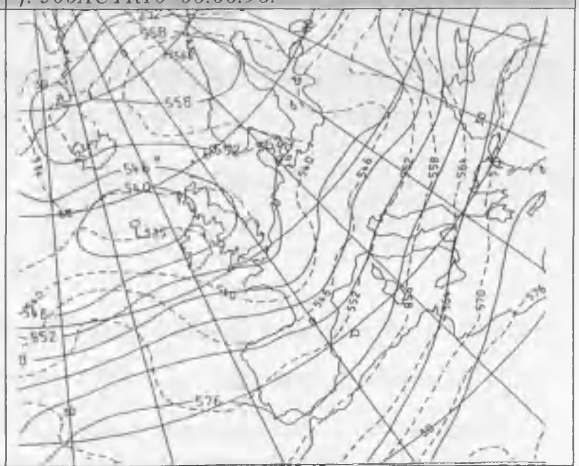

l. 500AUTR12 18.01.96

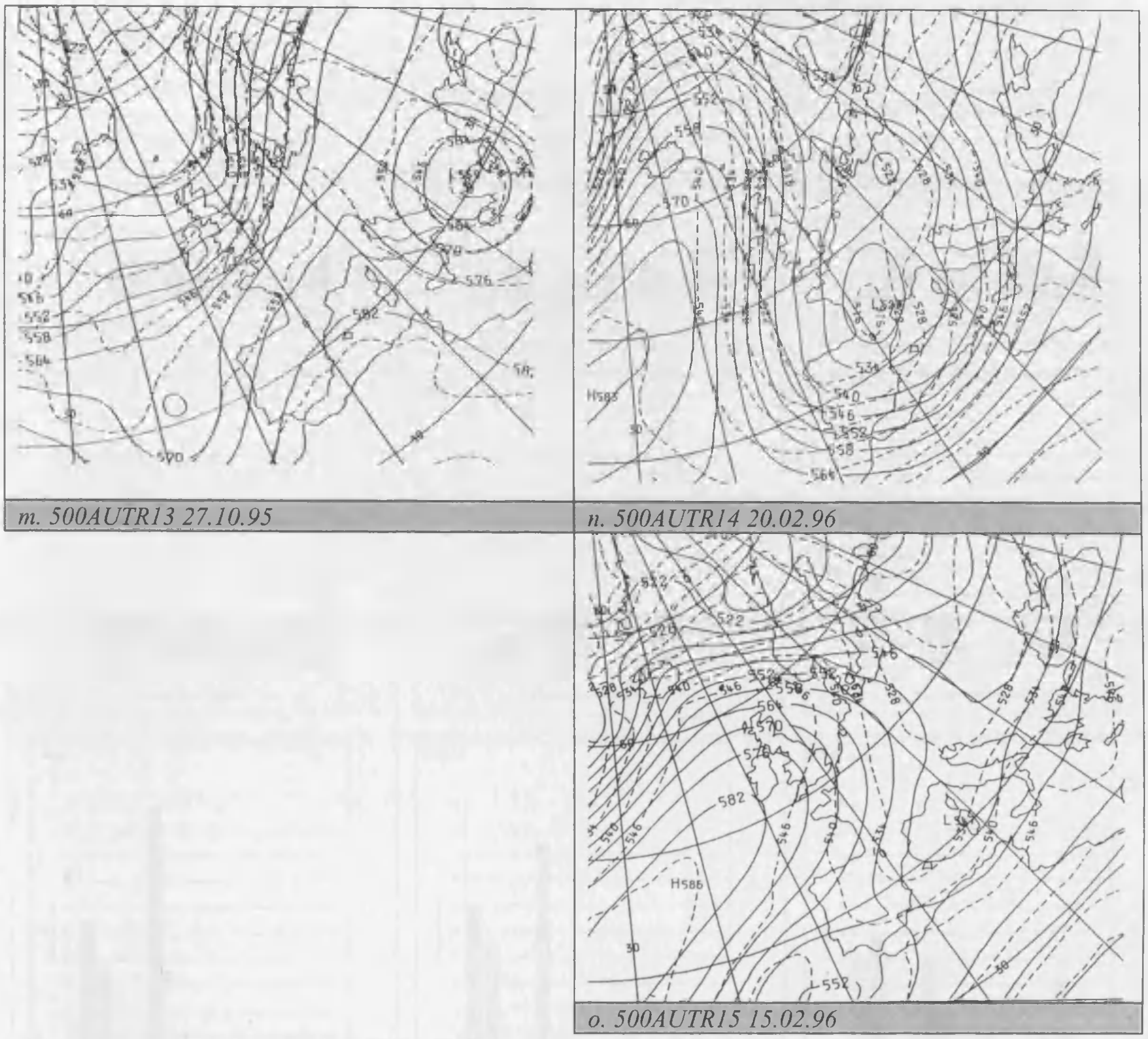

m. 500AUTR13 27.10.95

n. 500AUTR14 20.02.96

o. 500AUTR15 15.02.96

Figure 4.7 Examples of 500AUTR weather types. Isopleths are recorded in decametres.

4.5.1.3 Incidence of 500AUTR types

Relative Incidence Index (RII) scores are calculated for each 500AUTR weather type. The RII score is a simple calculation that indicates whether a particular weather type is over or under represented in any month compared to its overall frequency of occurrence. It is calculated for each month as in *equation 4.2*.

$$RII = \frac{\text{Percentage frequency of occurrence during month } i}{\text{Percentage frequency of occurrence during year}} \qquad (Eqn\ 4.2)$$

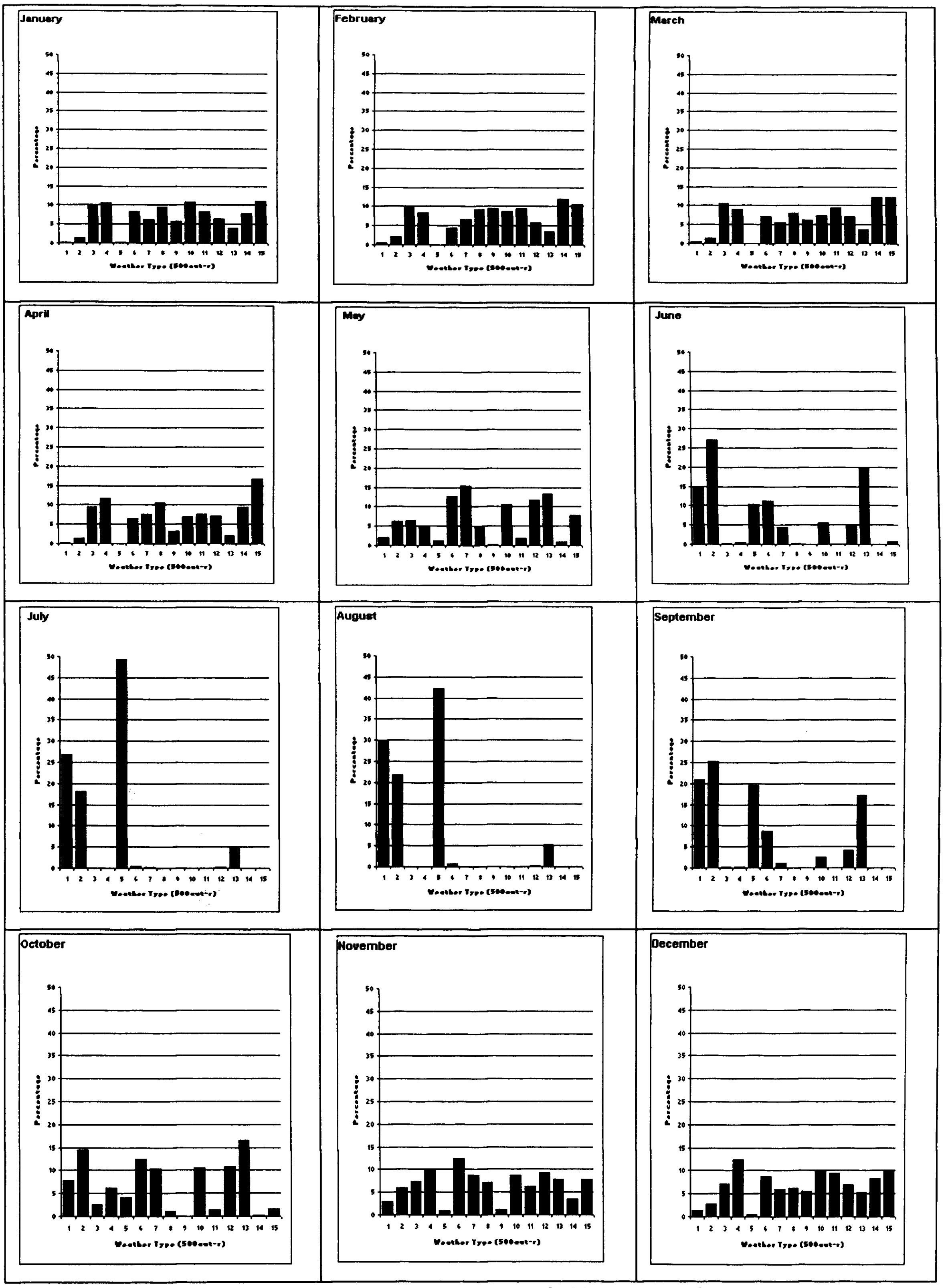

Figure 4.8 *Mean monthly percentage occurrence of 500AUTR weather types.*

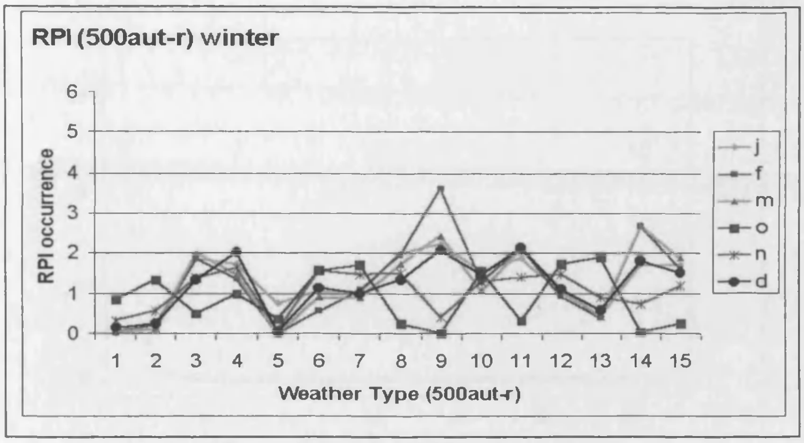

Figure 4.9 *RII scores of 500AUTR weather types (winter). Points are connected to emphasize variability.*

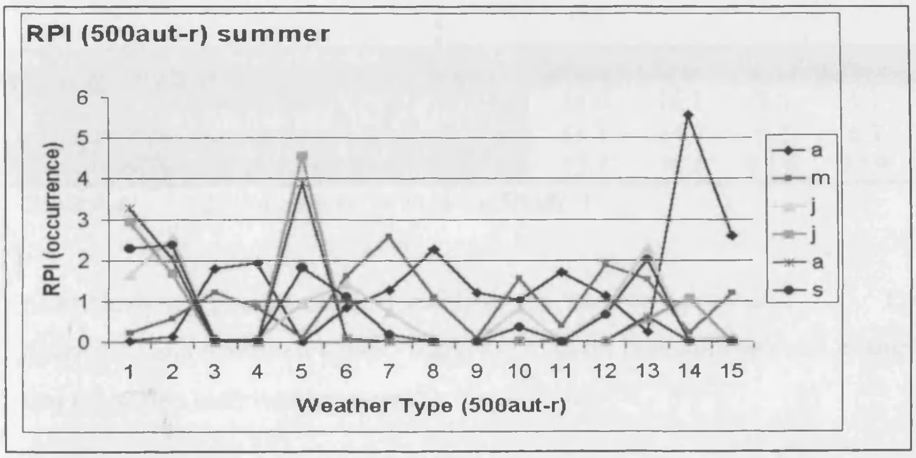

Figure 4.10 *RII scores of 500AUTR weather types (summer). Points are connected to emphasize variability.*

4.5.2 Classification of the 500hPa surface using standardized data (500AUT)

4.5.2.1. Method

Application of an unrotated correlation-matrix based PCA lead to the identification of five principal components (*figure 4.11*) that together account for 96.4% of the total variance (*table 4.4*).

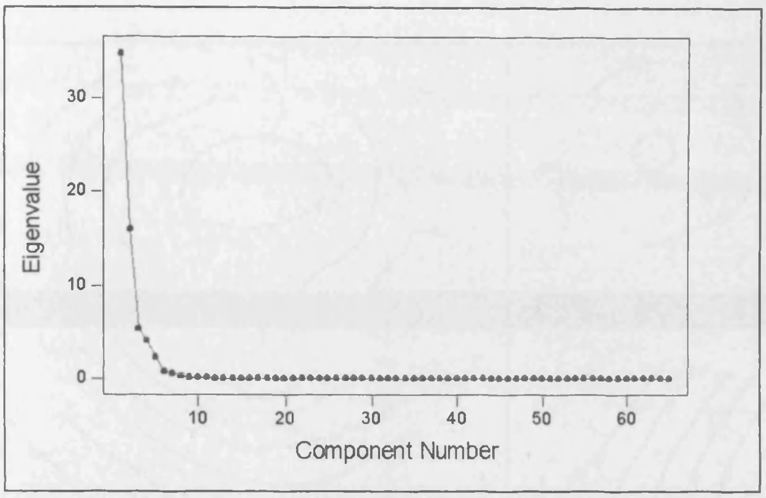

Figure 4.11 *Scree plot of PCA on 500AUT.*

	PC1	PC2	PC3	PC4	PC5
Eigenvalue	34.9	16.1	5.3	4.1	2.3
Proportion of total variance explained (%)	53.7	24.7	8.2	6.3	3.5
Cumulative proportion	53.7	78.4	86.6	92.9	96.4

Table 4.4 *Eigenanalysis of PCA on 500AUT.*

After clustering this catalogue consists of ten weather types *(table 4.5*). These are depicted in *figure 4.12* and described below. *Figure 4.13* gives randomly selected examples of 1200Z charts that fall within each weather type.

Cluster Number	No of observations	Within cluster sum of squares	Average distance from centroid	Maximum distance from centroid
1	1329	20200.34	3.69	10.15
2	2018	30549.27	3.72	9.68
3	1609	26077.21	3.85	8.93
4	1379	31175.24	4.51	13.86
5	1296	31640.69	4.71	12.40
6	1198	23935.85	4.25	12.70
7	1920	30878.21	3.80	11.72
8	739	21472.53	5.05	13.38
9	1837	31329.93	3.94	9.85
10	1295	23625.09	4.06	10.64

Table 4.5 *Results of the clustering procedure (centroid distances (500AUT)).*

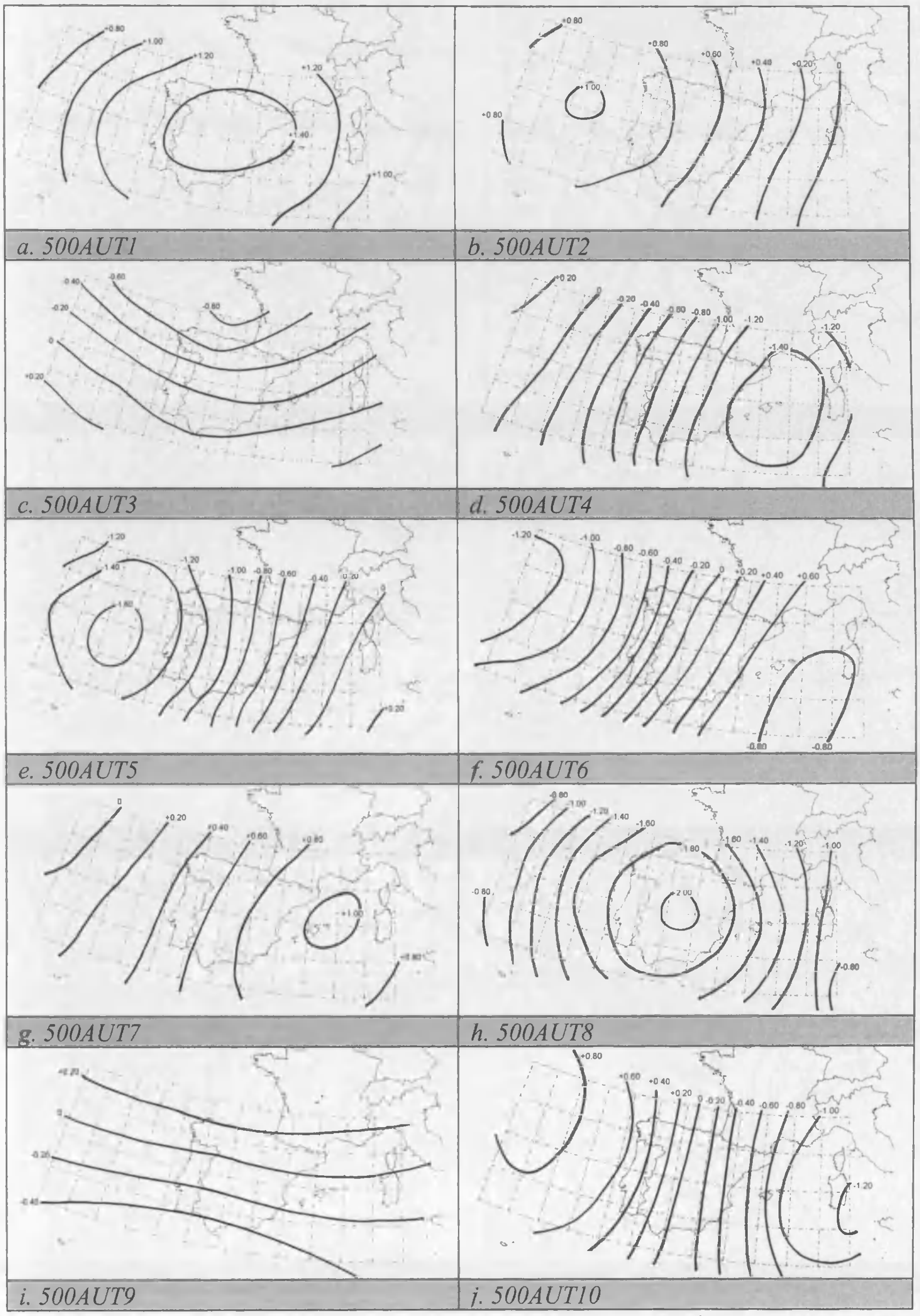

Figure 4.12 500AUT weather types- standardized contour heights.

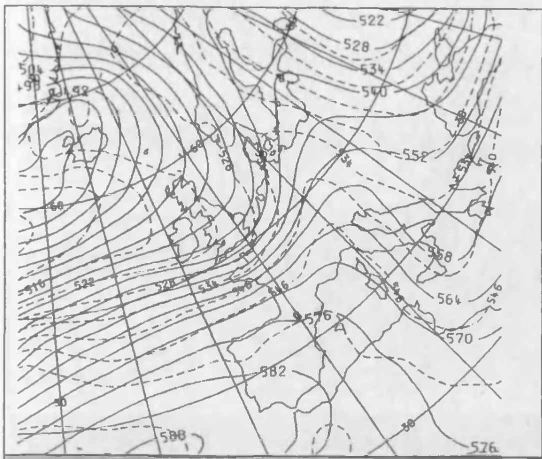

a. 500AUT1Winter

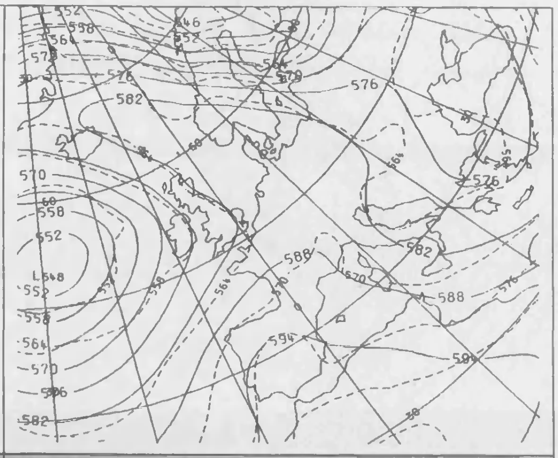

b. 500AUT1Summer

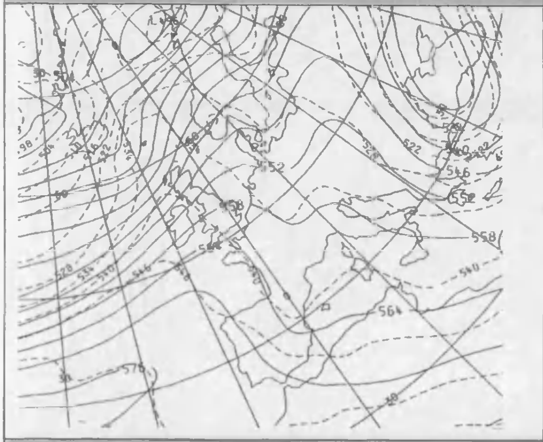

c. 500AUT2Winter

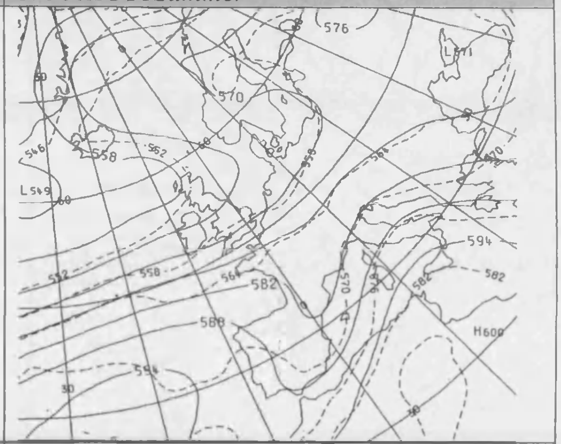

d. 500AUT2Summer

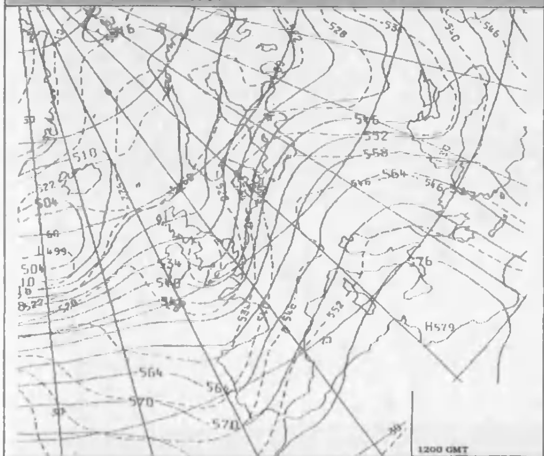

e. 500AUT3Winter

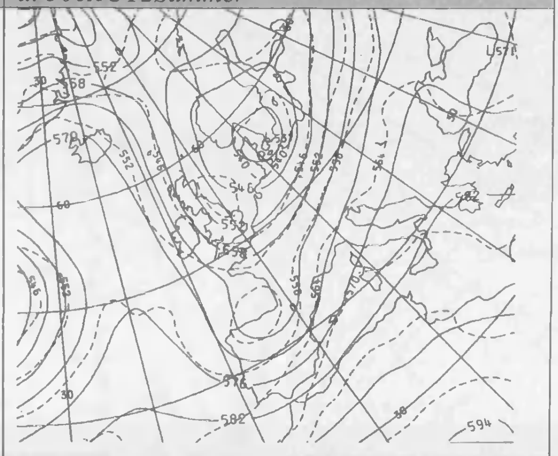

f. 500AUT3Summer

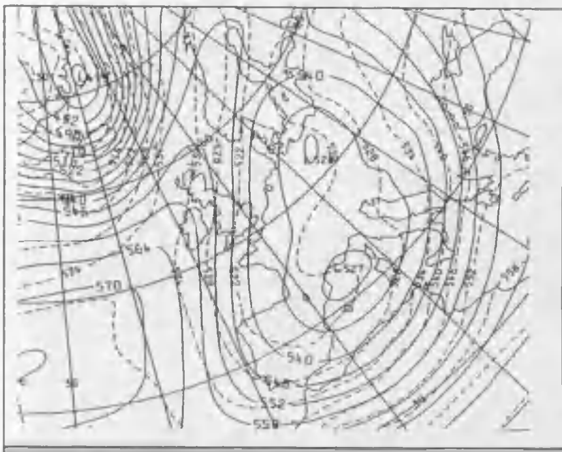

g. 500AUT4Winter

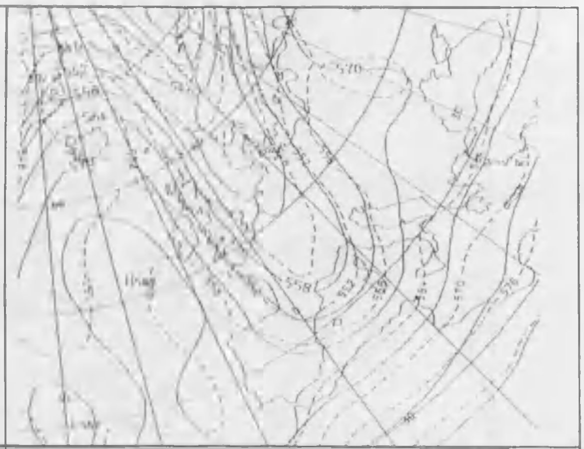

h. 500AUT4Summer

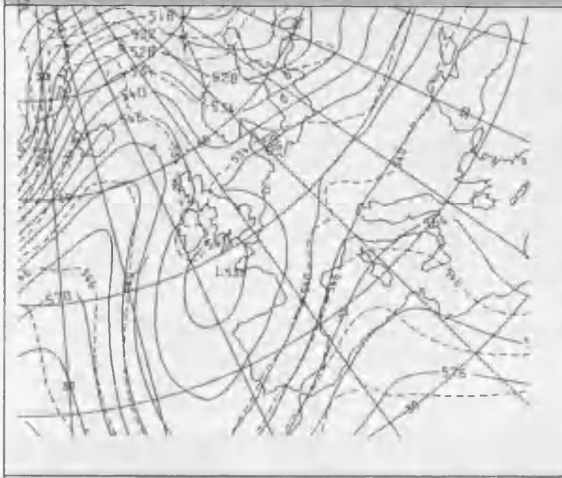

i. 500AUTR5Winter

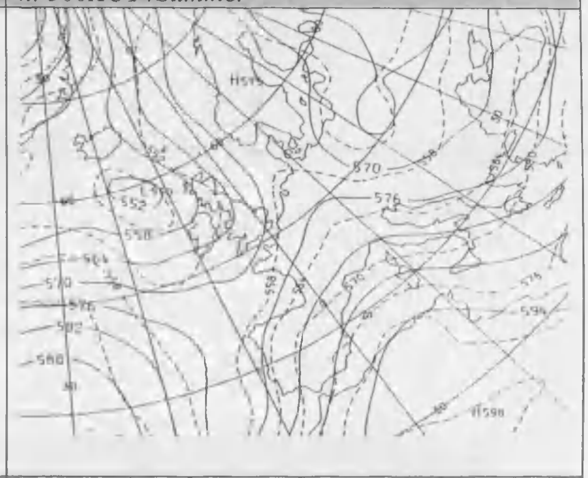

j. 500AUTR5Summer

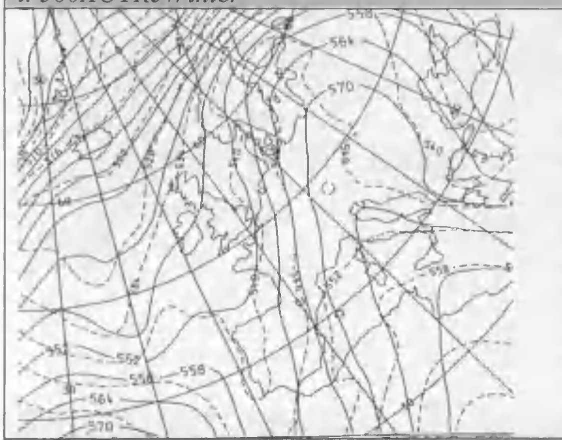

k. 500AUTR6Winter

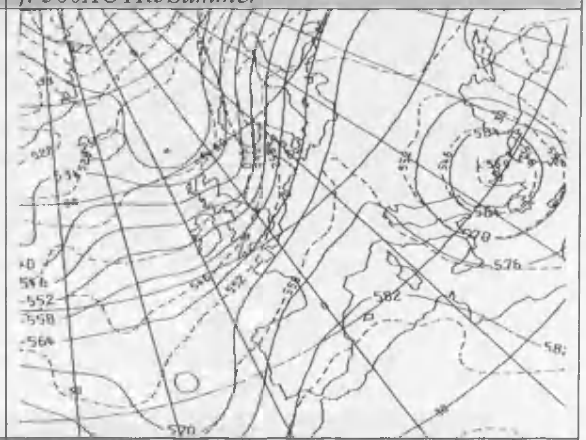

l. 500AUTR6Summer

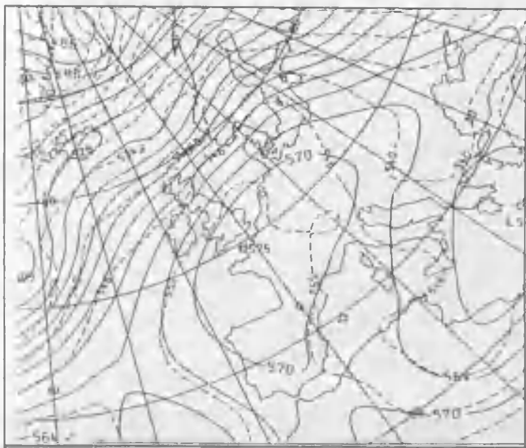

m. 500AUTR7Winter

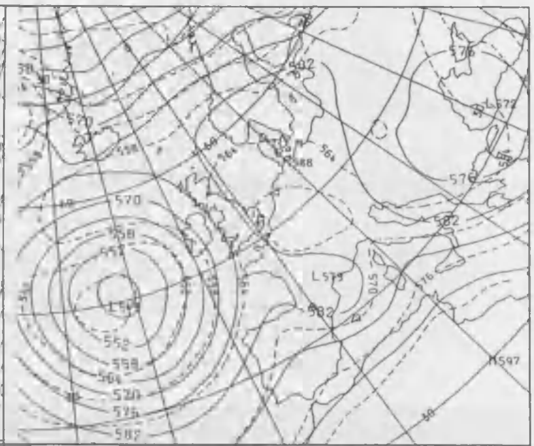

n. 500AUTR7Summer

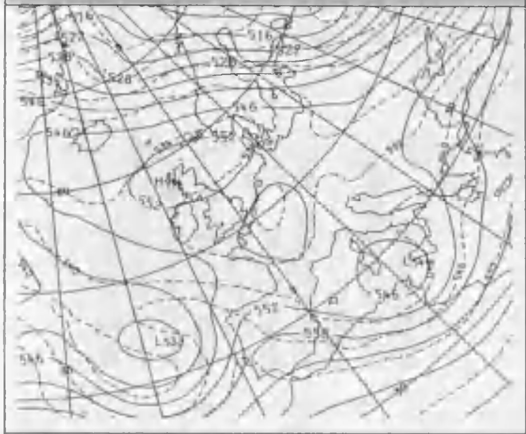

o. 500AUTR8Winter

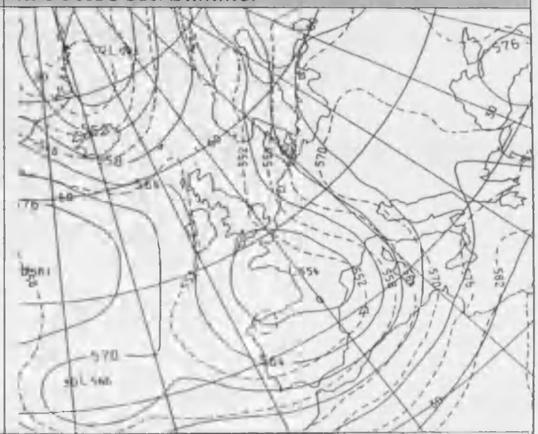

p. 500AUTR8Summer

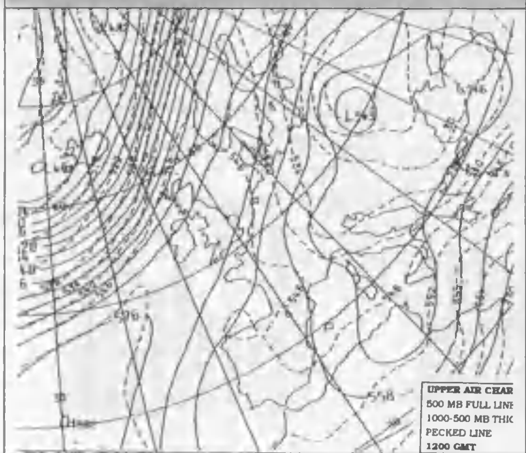

q. 500AUTR9Winter

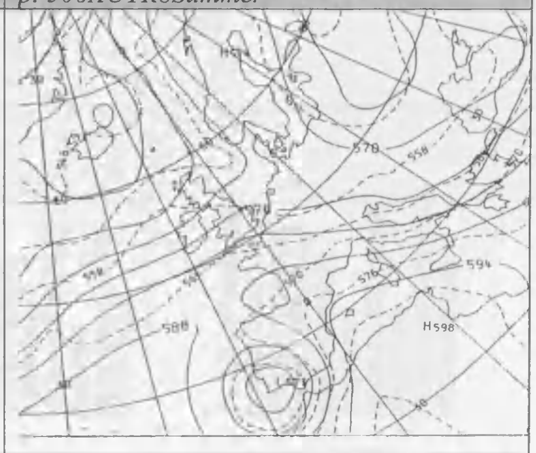

r. 500AUTR9Summer

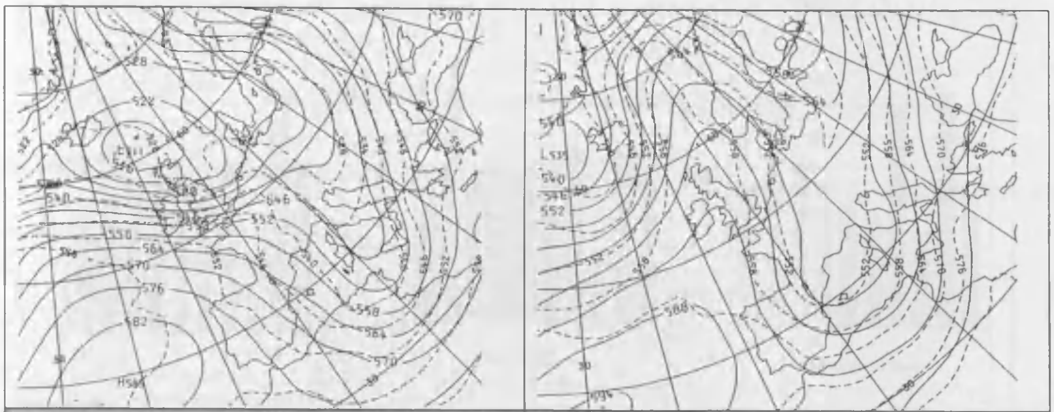

s. 500AUTR10Winter | *t. 500AUTR10Summer*

Figure 4.13 *Examples of 500AUT weather types. Isopleths are recorded in decametres.*

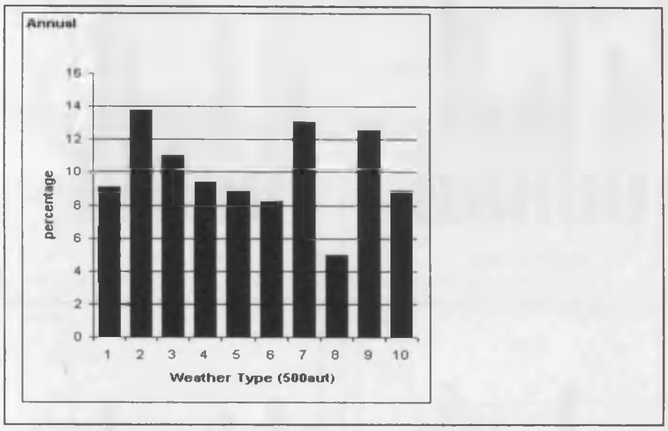

Figure 4.14 *Percentage occurrence of 500AUT weather types.*

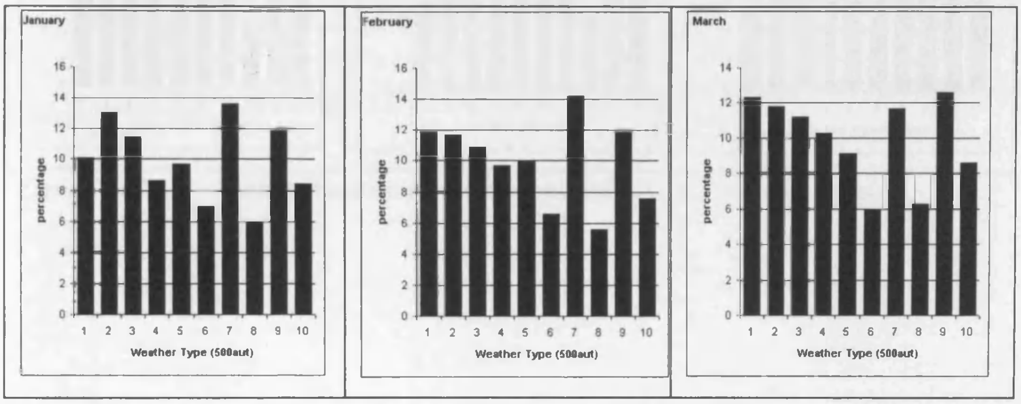

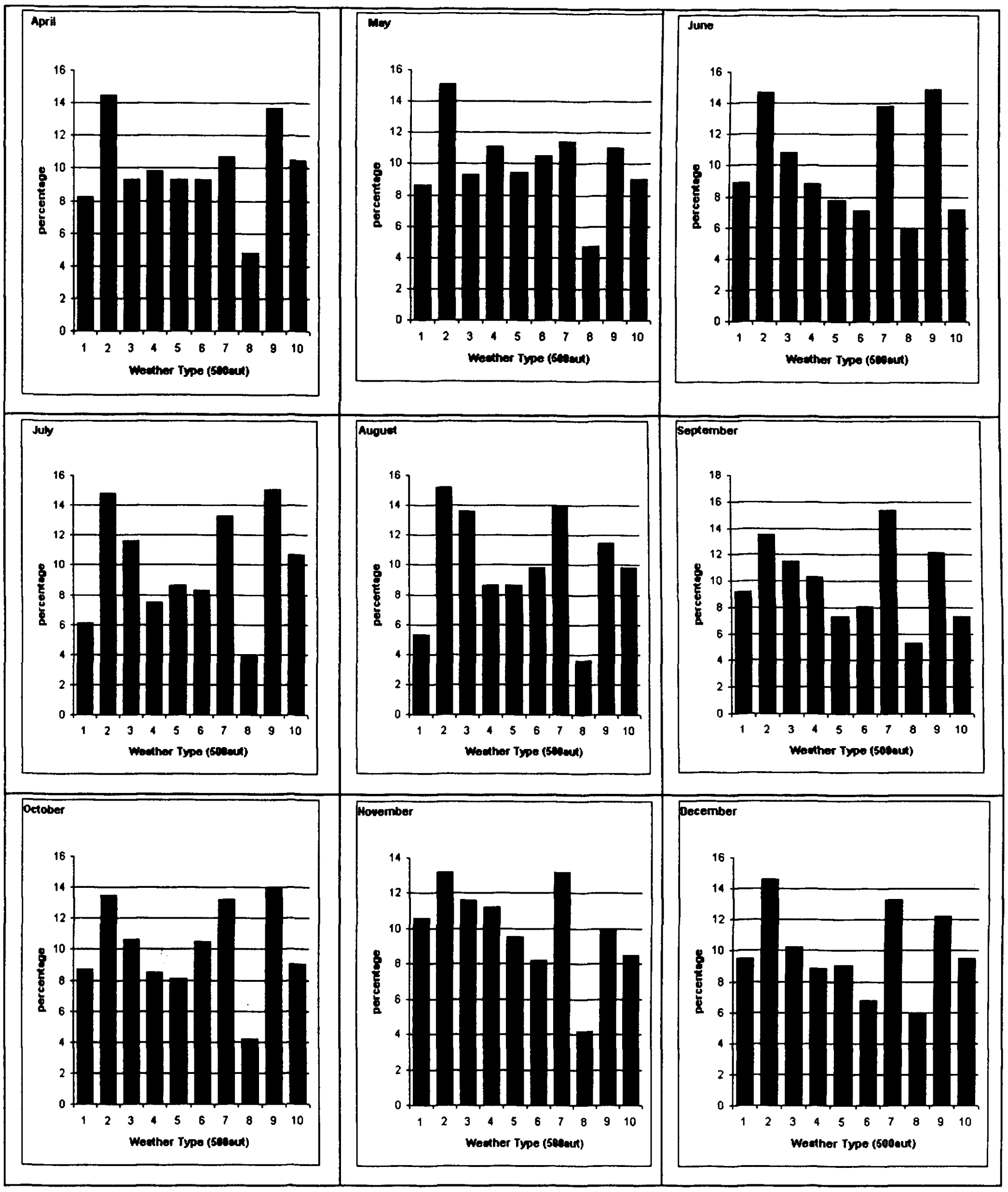

Figure 4.15 Monthly frequency of occurrence of 500AUT weather types.

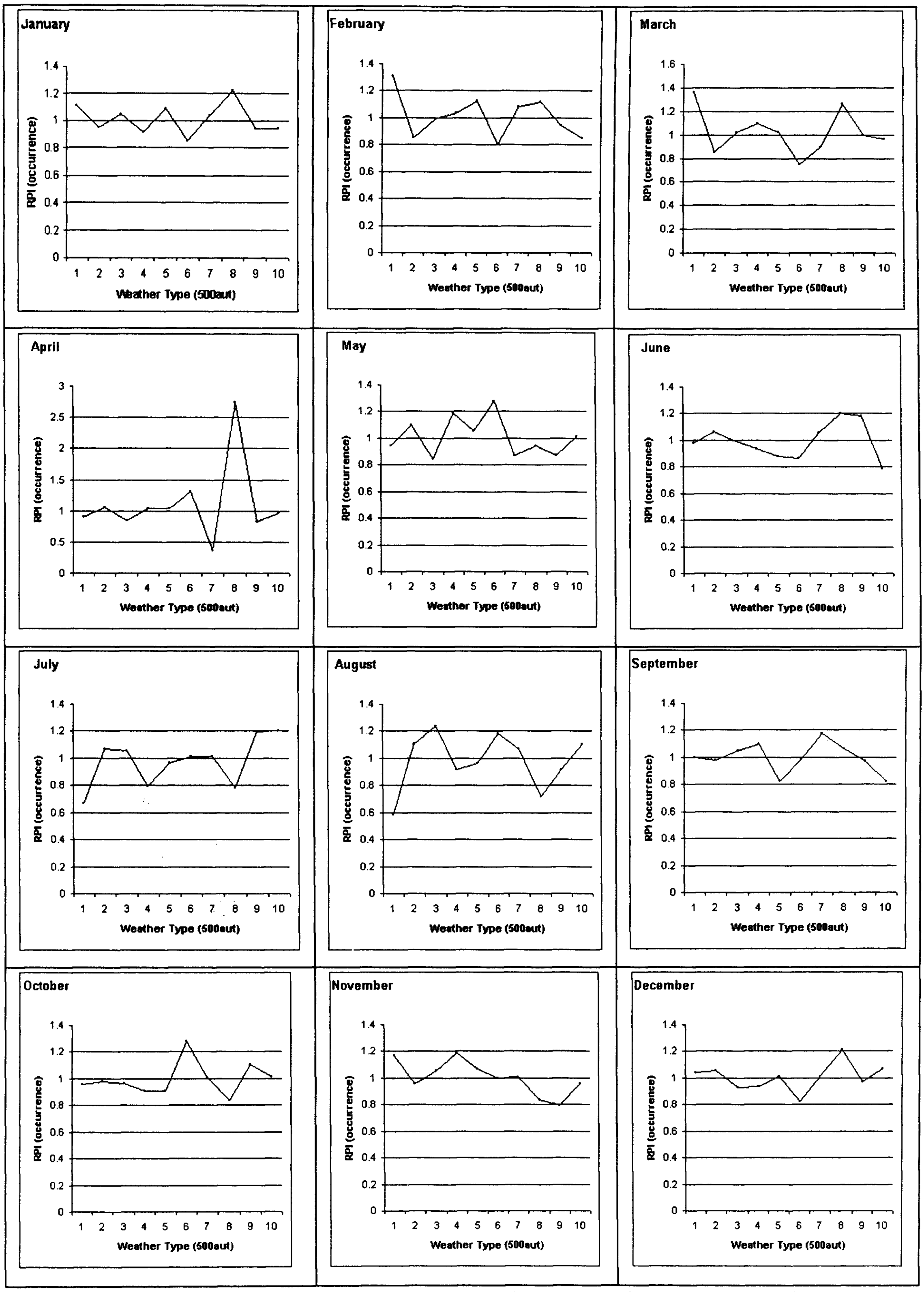

Figure 4.16 Monthly RII scores for 500AUT (connecting lines are inserted to emphasize variability).

4.5.2.2 500AUT weather types

Characteristics of the 500AUT scheme are described as,

500AUT1 The peninsula and the Balearic Islands are under the influence of positive anomalies (>1.20 standard deviates (SD)) and therefore this is essentially a strongly anticyclonic circulation mode. It has a greater occurrence in the winter months (9% of all incidences – *figure 4.15*). Both examples of this type show well-developed ridge patterns over the peninsula (*figures 4.13a, b*).

500AUT2 is typified by a pattern displaying a 1SD positive anomaly (and hence anticyclonicity) to the west of the peninsula. There is a slow fall in standardized heights towards the east but the field remains positive. 500AUT2 days are more common in the summer months (*figure 4.15*). Examples depict weakly developed troughs over the east of the peninsula and an extension of the Azores anticyclone towards Portugal *(figures 4.13c, d).* It is the most common type with an annual prevalence of 13.9%.

500AUT3 This type depicts a trough formation of slightly negative anomalies. The trough axis lies on the central meridian crossing the peninsula (5°W). This can be interpreted as northerly zonal pattern. The examples illustrate upper air troughs lying to the north *(figures 4.13e, f).*

500AUT4 This is typified by a region of large negative anomalies (>-1.40SD) over the Balearic region and the east Mediterranean coast and occurs when the upper wave form tends towards retrogression. The winter example *(figure 4.13g)* shows a large and deep region of cyclonicity to the north-east over central Europe and the Azores ridge extending towards the British Isles.

500AUT5 This weather type is described by negative anomalies to the west of the Portuguese coast. There is then a steep gradient towards the eastern coast yet the entire peninsula displays negative departures. Examples depict western troughs with north-east to south-west axes *(figures 4.13i,,j).*

500AUT6 Under this predominantly summer type there is a north-west to south-east division between positive and negative anomalies. Highest positive anomalies (+0.8SD) lie to the south-east. The actual examples of this type *(figures 4.13k, l)* show western troughs which although similar in form to *500AUT5,* it displays higher contours. It represents a southerly zonal air flow.

500AUT7 There are positive anomalies (+1.0SD) (anticyclonicity) centred over the Balearic region and the Gulf of Lyons. Isopleths are approximately aligned with the longitude. Examples show well-developed ridge patterns over the peninsula *(figures 4.13m, n)*.

500AUT8 This is the least frequent type (5.1%). The cyclonic pattern depicts very low contour heights (-2.0SD) in the centre of the peninsula with isopleths radiating out to a highest value of –1.50SD in the Balearic region. It is unusually common in April months (*figure 4.16*) displaying the highest RII statistic (2.7) of any of the weather types.

500AUT9 The mean isopleth pattern is zonal but with little variation from 'normal' contour height. +0.20SD is aligned with 43°N (along the north coast), 0.00 SD with 41°N, -0.20SD with 39°N and –0.40SD with 37°N (although with distinct anticyclonic curvature). The isopleth to the south displays a slight ridge formation and to the north there is a trough. The examples from both seasons *(figures 4.13q, r)* show retrogressive patterns with a well-developed cut-off low pressure centre (*'gota fria')* south-west in the summer instance.

500AUT10 This meridional pattern displays negative standard deviates in the Balearic region reaching –1.0 SD over Menorca and positive deviates to the west at its highest +0.5 SD in the northeast . The 0.0 SD isopleth follows about 6°W. Both examples (*figures 4.13s, t*) show ridges to the west and troughs to the east of the peninsula.

The evaluation of circulation type-rainfall association in the next chapter indicates that classes in the 500AUT system strongly discriminate between rainfall totals. Some additional aspects of this synoptic catalogue are described and illustrated. In the following sections however these should be regarded as preliminary work that would require more sophisticated analysis that is beyond the scope of this study.

4.5.2.3 Examination of time series of 500AUT

Significant temporal trends emerge in the frequency of certain weather types (*figure 4.17*). The annual frequencies of *500AUT1* increases significantly ($p<0.050$) over the period 1958-1997, as does *500AUT7*. These are both types associated with positive anomalies in 500hPa heights over the entire peninsula. In contrast *500AUT4*, characterised by large negative anomalies, displays a significant ($p<0.050$) decrease over the period. This suggests increases in temperature and anticyclonicity and decreases in cyclonicity during the study period.

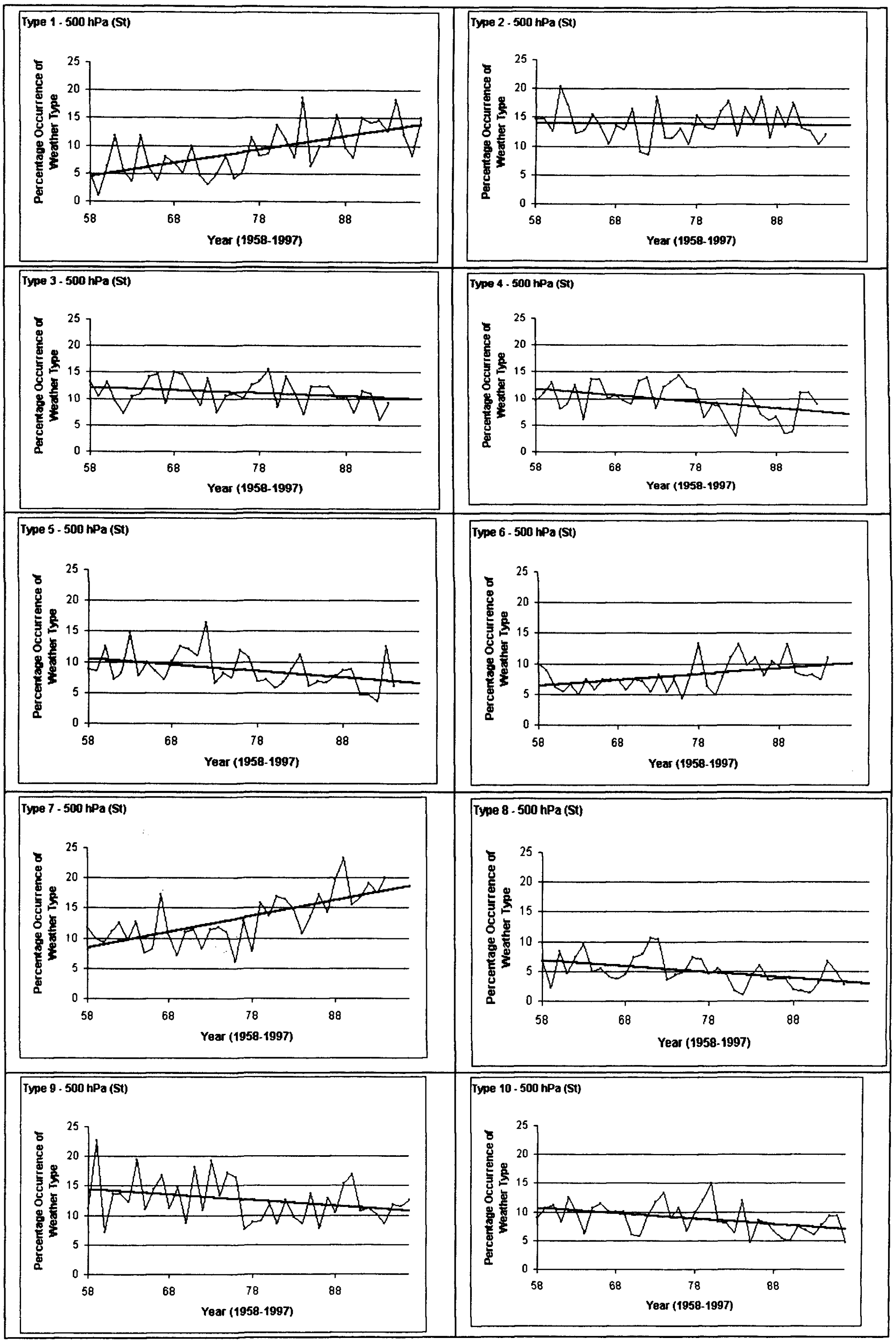

Figure 4.17 Time series of annual frequencies of 500AUT weather types.

4.5.2.4 Probability assessment of 500AUT weather types

The probability of a given weather type is given by its percentage frequency of occurrence (*figure 4.14*). Transition probabilities, on the other hand, can be defined as the probability that any chosen weather type follows another. El-Kadi and Smithson (2000 p1357) note that this can aid the interpretation of which patterns are persistent and which are more transitional in nature. They comment that it is necessary to '...*fully understand the statistical climatology*...' of atmospheric circulation patterns, in addition interrelationships between weather types can be examined. Finally transition matrices are employed in the development of stochastically derived weather type catalogues.[2]

	500AUT Weather Types									
Duration (days)	**1**	**2**	**3**	**4**	**5**	**6**	**7**	**8**	**9**	**10**
5	6	11	3	7	3	0	7	4	8	4
6	4	3	3	3	4	3	1	4	6	1
7	0	3	0	2	2	1	2	2	5	0
8	1	4	0	1	1	1	0	0	1	0
9	0	0	0	0	0	0	0	0	0	0
10	0	2	0	1	0	0	0	0	0	0
10+	1	0	0	0	0	0	0	0	2	0

Table 4.6 Day–to-day duration of 500AUT weather types for a sample ten years in the period 1958-1997.

Weather type persistence can be described by duration or the number of consecutive days of any type. *Table 4.6* gives duration statistics for consecutive periods of 5 days or more for a sample of ten years. Longest duration can be seen, as expected, for the anticyclonic *500AUT2* yet *500AUT4*, which is strongly cyclonic, also records a considerable number of consecutive days. Least duration occurs in types 3, 6 and 10 suggesting they are transitional modes of atmospheric circulation. The longest durations in the sample of 15 days is recorded under the zonal *500AUT9*.

Transitional probabilities are given in *table 4.7* and *4.8*. The probability of a weather type, for instance the occurrence of *500AUT1* is *p(WT1) = r/n* where *r* is the relative frequency and *n* is the total frequency of all weather types (*i.e.* the daily series). The full dataset represents a probability of 1. The conditional probability of *500AUT2* therefore given that *500AUT1* occurred the day before is for the whole period, 0.129 in winter and 0.166 in summer. In winter WTs with the

[2] A Monte-Carlo ('weather generator') method was employed in this project but results are not given here.

greatest persistence are recorded by 1, 5 and 8. *500AUT8* is a cyclonic type and hence it is probably unlikely that 3-day transition probability is high.

	Followed by									
	1	2	3	4	5	6	7	8	9	10
1	0.643	0.129	0.015	0.000	0.000	0.009	0.198	0.000	0.003	0.003
2	0.145	0.479	0.061	0.005	0.001	0.003	0.137	0.000	0.064	0.106
3	0.004	0.064	0.397	0.117	0.086	0.088	0.057	0.035	0.045	0.106
4	0.000	0.006	0.109	0.502	0.056	0.005	0.000	0.078	0.085	0.160
5	0.000	0.000	0.098	0.055	0.536	0.062	0.002	0.143	0.105	0.003
6	0.002	0.019	0.136	0.000	0.157	0.470	0.132	0.002	0.083	0.000
7	0.117	0.115	0.080	0.000	0.004	0.109	0.509	0.000	0.059	0.008
8	0.000	0.000	0.003	0.248	0.150	0.006	0.000	0.552	0.011	0.006
9	0.006	0.109	0.052	0.039	0.048	0.058	0.061	0.005	0.559	0.061
10	0.009	0.215	0.113	0.129	0.004	0.005	0.021	0.002	0.078	0.424

Table 4.7 Day-to-day transition sequences of 500AUT weather types for the winters (1958-1997).

	Followed by									
	1	2	3	4	5	6	7	8	9	10
1	0.588	0.166	0.005	0.000	0.000	0.012	0.202	0.000	0.012	0.014
2	0.099	0.537	0.045	0.010	0.001	0.008	0.114	0.000	0.086	0.099
3	0.005	0.087	0.404	0.081	0.069	0.080	0.086	0.037	0.059	0.091
4	0.000	0.011	0.087	0.504	0.056	0.005	0.003	0.076	0.097	0.161
5	0.000	0.002	0.140	0.066	0.513	0.116	0.019	0.089	0.054	0.002
6	0.007	0.014	0.125	0.000	0.121	0.515	0.173	0.007	0.046	0.000
7	0.117	0.127	0.084	0.001	0.010	0.097	0.477	0.000	0.075	0.011
8	0.000	0.003	0.050	0.225	0.174	0.000	0.003	0.522	0.022	0.000
9	0.002	0.069	0.065	0.067	0.065	0.056	0.078	0.011	0.541	0.046
10	0.008	0.196	0.061	0.124	0.003	0.006	0.008	0.008	0.121	0.464

Table 4.8 Day-to-day transition sequences of 500AUT weather types for the summers (1958-1997).

	(a)Persistence		(b)Followed by	
	Winter	Summer	Winter	Summer
1	0.643	0.588	7	7
2	0.479	0.537	1	7
3	0.397	0.404	4	10
4	0.502	0.504	10	10
5	0.536	0.513	8	3
6	0.470	0.515	5	7
7	0.509	0.477	1	2
8	0.552	0.522	4	4
9	0.559	0.541	2	7
10	0.424	0.464	2	2

Table 4.9 (a) Persistence of weather types by season and for the whole period of 1958-1997 and (b) Strongest conditional probabilities from one weather type to another.

4.5.2.5 Association with kinematic features

Incorporation of kinematic information has been identified as one way by which non-stationarity (or within-type variability) of weather types may be reduced, given that frontal incidence considerably raises the possibility of rainfall. It cannot be assumed that this frontal incidence passage is independent of prevailing weather type, in fact *table 4.10* indicates the different probabilities of frontal passage associated with each 500AUT type. Highest frontal incidence is in winter and weather type association is consistent in both seasons. Probabilities for *500AUT3* and *500AUT4* which represent travelling systems to the north and west clearly suggest trailing fronts across the peninsula. Summer ridge patterns such as *500AUT1* and *500AUT2* have expected low frontal incidence.

	All year	Summer	Winter
1	0.169	0.146	0.186
2	0.212	0.160	0.263
3	0.514	0.410	0.620
4	0.326	0.273	0.377
5	0.532	0.430	0.642
6	0.435	0.394	0.487
7	0.237	0.200	0.272
8	0.383	0.362	0.399
9	0.183	0.125	0.251
10	0.268	0.177	0.366

Table 4.10 Probability of any front crossing the Iberian peninsula under each 500AUT weather type.

4.6 Development of circulation catalogues for the Iberian peninsula using SLPINDC

SLPINDC consists of the same 27 circulation types as SLPMAN (*section 3.5.1*). The annual, seasonal and monthly frequencies of each type in the SLPINDC scheme are given in *table 4.11*. Considerable differences in incidence of each type occur during the year. In winter the dominant weather type is anticyclonic (A) for both dynamic and thermal reasons. The Azores anticyclone migrates to a position over the peninsula (*figure 4.18a*). Hybrid anticyclonic types arise when there is a strong negative vorticity but a distinct direction of flow is observed. The most common hybrid type is anticyclonic westerly (AW) which occurs when the system is situated over the Azores region (*figure 4.18b*). Pure or hybrid A types can also be due to the southward extension of the Eurasian continental anticyclone (*e.g.* anticyclonic easterly AE) in *figure 4.18c*, although this is less common and occurs predominantly during the winter half of the year. Cyclonic (C) weather types are also relatively frequent. In winter months C types result from travelling Atlantic depressions entering the Mediterranean areas from the Atlantic either across the peninsula or via the Strait of Gibraltar/Alboran Channel (*figure 4.18d*) to the south or across the Bay of Biscay and via the Garonne-Carcassonne gap to the north.

On some occasions C types will be the result of a depression that fronts within the western Mediterranean basin itself (*figure 4.18e*) The Catalano-Balearic region is an important area for such cyclogenesis. In summer C is the most common type but nearly all incidences involve shallow thermal lows rather than deep mobile systems (*figure 4.18f*). These occur either as northwards extensions of the vast surface low pressure system that dominates the central Sahara during the warm season or, more often, as a thermal low over the Iberian plateau itself. Both form after strong surface heating under clear stable atmosphere and are therefore relatively shallow features. Air rises usually by only about 1000 metres and then meets the subsiding air of the Azores anticyclone above.

The incidence of pure directional types will depend on the relative positions of low and high pressure areas with respect to the peninsula. Westerly (W), northwesterly (NW) and northerly (N) types are associated with the movement of depressions to the north of the peninsula, often under well-developed zonal flow patterns (*figure 4.18g*). These cause incursions of moist, cool and often unstable polar air into the region. Atlantic types (W, NW and N) show greater frequency during the winter months. North-easterly types (NE (*figure 4.18h*) bring continental air when high pressure extends on a south west to northeast axis across northern Europe. As result these are common when blocking patterns are present in northern latitudes. NE is the second most frequent types in the summer. Easterly flow (*figure 4.18i*) occurs when an anticyclone dominates central Europe, either as an extension of the Azores or the Eurasian anticyclone. The original continental air mass is gradually modified (warmed, moistened and become more unstable) to a Mediterranean air mass. This weather type will be accompanied by *Tramontana* and *Levante* winds (Tout and Kemp 1985) along the Mediterranean coast. The least frequent directional types come from the south (S, SE, SW). South-westerly patterns are associated with northward-moving depressions steered by meridional patterns in the upper air flow. S types are quite unusual but can arrive on the western flank of a high pressure system in the central Mediterranean.

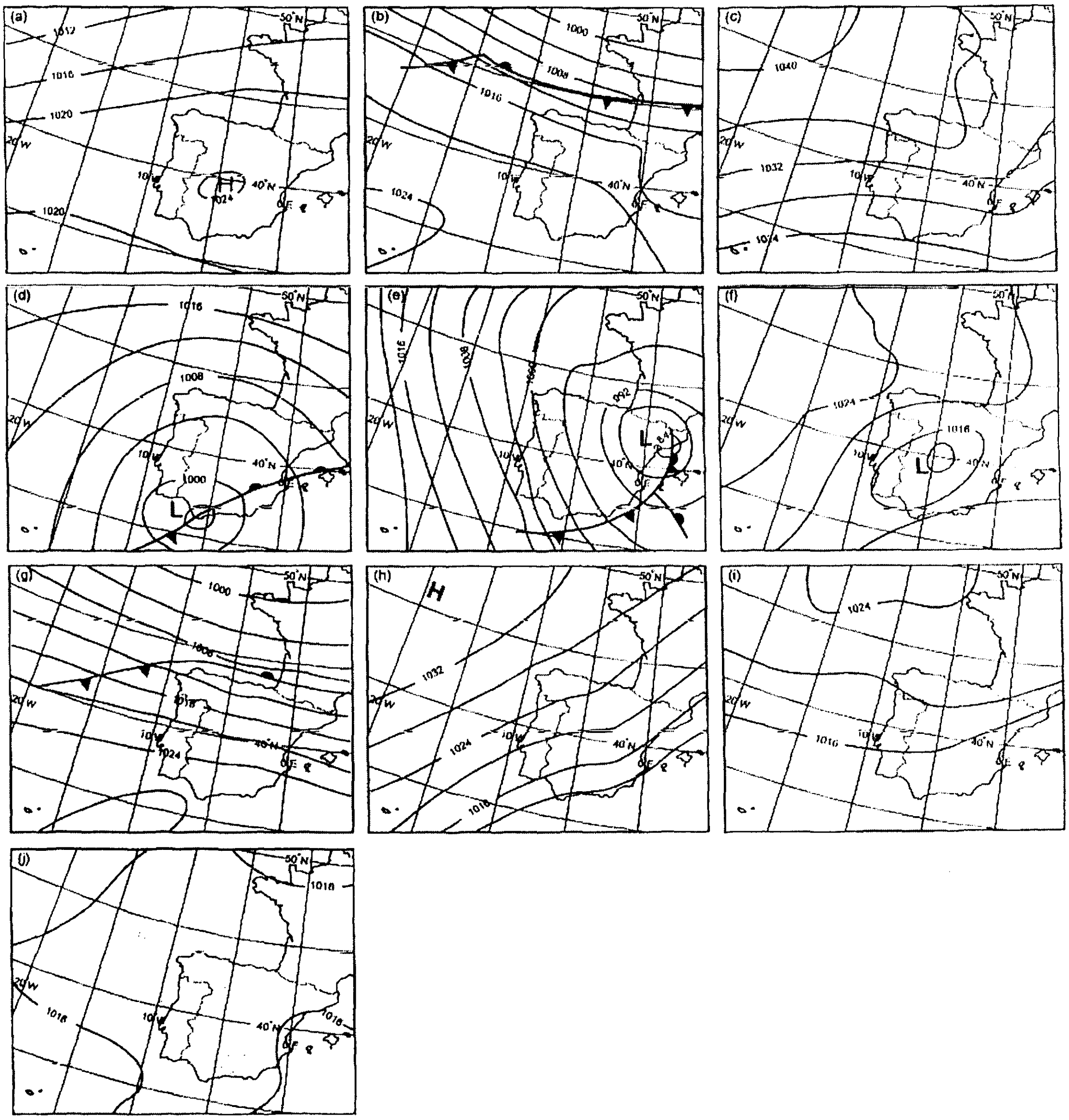

Figure 4.18 Examples of typical synoptic charts associated with SLPINDC: (a) anticyclonic, 14 November 1994; (b) anticyclonic westerly, 12 November 1987; (c) anticyclonic easterly, 21 March 1966; (d) cyclonic, 15 December 1995; (e) cyclonic, 30 January 1986; (f) cyclonic, 29 July 1970; (g) westerly, 30 December 1994; (h) north-easterly, 17 January 1994; (i) easterly, 23 December 1970; j) unclassified, 16 October 1994.

The third most frequent type overall is the unclassified (U) type (*figure 4.18j*), where surface flow is very light and indeterminate. It is worthwhile comparing the relative infrequency of this type in the British Isles region (annual 3.9 per cent, winter 3.4 days, spring 3.9 days, summer 3.5 days, autumn 3.6 days) with Iberia (annual 18.1 per cent, winter 4.6 days, spring 13.9 days, summer 25.3 days, autumn 16.3 days). U types have very slack pressure gradients and are most common in summer when strong anticyclonicity aloft is in control. Under the manual synoptic catalogue of Paricio and Nadal (1979) this type is known as '*Pantano barometrico*'.

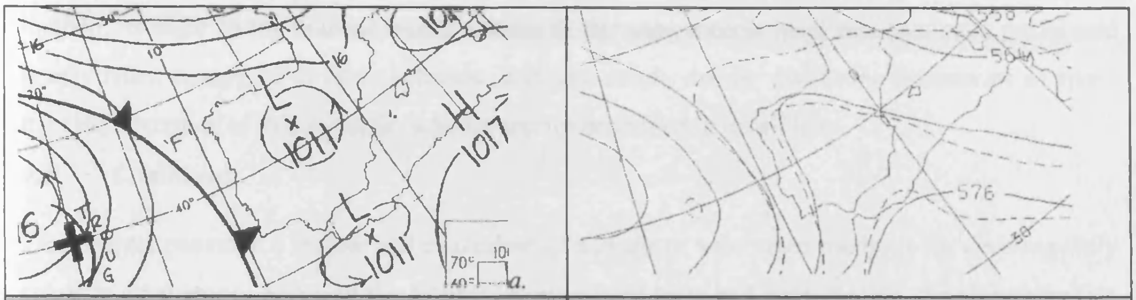

MSLP chart | b. 500hPa Chart

Figure 4.19 (a) A thermal low pressure centre at surface capped by (b) a ridge feature at 500hPa 16.05.97.

Weather Type SLPINDC	Annual	Spring	Summer	Autumn	Winter
A	23.34	19.31	8.35	28.42	37.79
ANE	1.51	1.63	1.38	1.26	1.78
AE	1.76	1.74	0.90	2.07	2.36
ASE	0.71	0.82	0.06	1.03	0.93
AS	0.59	0.42	0.00	1.06	0.90
ASW	1.54	1.57	0.31	1.48	2.83
AW	2.49	2.39	0.67	2.63	4.35
ANW	1.81	2.05	0.93	1.90	2.39
AN	1.13	1.18	0.70	1.15	1.49
NE	6.65	8.35	9.65	4.81	3.71
E	4.26	4.89	4.87	4.69	2.51
SE	0.81	0.90	0.53	0.87	0.90
S	0.47	0.51	0.14	0.59	0.67
SW	1.86	1.52	0.20	2.32	3.44
W	4.31	4.67	0.84	4.44	7.38
NW	3.76	4.58	1.72	3.21	5.60
N	3.46	4.61	2.73	3.38	3.09
C	15.18	16.22	25.67	10.87	7.70
CNE	2.82	2.64	6.72	1.31	0.53
CE	1.08	0.98	2.14	0.92	0.26
CSE	0.18	0.08	0.22	0.20	0.20
CS	0.11	0.06	0.00	0.14	0.23
CSW	0.25	0.25	0.06	0.36	0.32
CW	0.41	0.48	0.11	0.36	0.70
CNW	0.68	1.04	0.70	0.50	0.47
CN	1.43	1.69	2.64	0.67	0.70
U	16.63	15.15	27.62	18.47	4.84

Table 4.11 Frequency of incidence of SLPINDC.

4.7 Development of circulation catalogues for the Iberian peninsula using 500INDC

Index series for the 500hPa catalogue can be converted into weather type classes using the same method. Similar to the manual typing system at this atmospheric level this catalogue performed poorly when compared to other schemes, and as a result, mainly due to the limitations of space the characteristics of this synoptic scheme are not described in detail here.

4.8 Comment

This chapter provides a review and evaluation of a range of automated methods for deriving daily synoptic catalogues. Some of the techniques employed have had considerable use elsewhere (*i.e.* SLPAUT, 500AUT) but have not been developed for Spain. Other models have made infrequent appearances in the literature but not for this location (THICKAUT, MULTIAUT) or atmospheric level (500INDC).

Techniques are subdivided on the basis of,

(i) Various traditional approaches (PCA/CA-based and those based on airflow indexing)

(ii) Surface and mid-tropospheric level.

(iii) Standardized and unstandardized data input.

500AUTR is described because it provides a good characterization of basic atmospheric flow patterns over Spain. Only a limited comparison can be made between classes in this scheme and the manual classification 500MAN due to the fact that the former also takes into account absolute contour heights (not just isoplethic alignment). Consequently two ZN patterns emerge, 500AUTR3 (a winter ZN – low contour heights) and 500AUTR13 (a summer ZN – raised contour heights) and two WT patterns (500AUTR8 and 500AUTR9). 500AUT is subsequently derived using standardized heights to counteract the problem that the 500AUTR scheme perhaps is only really showing gross seasonal changes rather than true circulation features (Bárdossy 1998 – *pers. comm.*). Whether this distinction is important with respect to precipitation modelling is investigated in *chapter 6.*

The so-called 'Jenkinson-Collison' method is used to develop SLPINDC and 500INDC. Unlike the PCA/CA models these catalogues are constructed independently of absolute isoplethic values and thus represent basic wind direction rather like the quasi-air mass manual methods, SLPMAN and 500MAN. *Section 3.5.1.1* states that there is little difference between the manual and automated classifications but whether consideration of actual contour height or mere flow direction is crucial is addressed in *chapter 6.*

Goodess and Palutikof (1998) demonstrated the use of an index-to-class method for investigating rainfall in south-east Spain but failed to recognize that mid-tropospheric flow may have stronger association with rainfall occurrence. Consequently 500INDC (and 500IND) are investigated in this study. Daily index based models were not created partly due to problems that are created by a highly skewed precipitation distribution. The application of ANNs, which are distribution-free could, in the future, have great potential with respect to this.

In an evaluation of the synoptic catalogue generation automated methods prove to have clear advantages over manual methods in terms of time of development., but have one important disadvantage relating to the opportunity that the manual classifier can identify 'rogue patterns'. Some crucial but infrequent synoptic patterns, for instance, SEL patterns, which produce high rainfall in eastern areas, are not segregated by automated methods. SEL is 'lumped' within a less extreme eastern trough pattern. This is a clear disadvantage when dealing with significant precipitation events and further analysis could indicate that this devalues the automated output considerably. Whether automated systems are actually better modellers than manual methods will be demonstrated in *chapter 6.*

Three preliminary studies are undertaken that warrant further analysis beyond this project. The incorporation of frontal information would appear to be crucial for solving non-stationarity problems if the catalogue could attain higher resolution without a prohibitive increase in complexity. Secondly, some basic time series are investigated and results indicate the potential merits of further work. Finally the dynamics of the synoptic catalogue, such as type duration, persistence and transition need to be investigated with respect to change over time and how these affect the nature of circulation-precipitation association but once again more in-depth study goes beyond the space restrictions of this thesis.

Evaluation of the Iberian daily models indicate that statistical procedures yield clearly defined circulation catalogues which incorporate the main features of atmospheric movement and successfully differentiate between common modes of circulation.

Chapter Five
Synoptic climatological methods
Static Approaches: Monthly models

5.1 Introduction

This chapter introduces and describes a range of automated monthly synoptic catalogues. Catalogues are both index and class-based (*figure 5.1*).

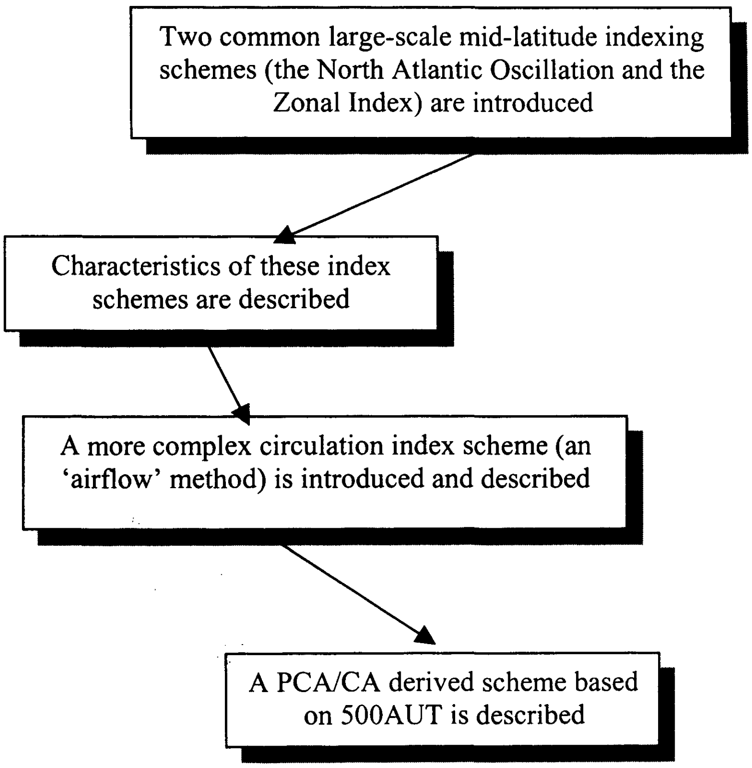

Figure 5.1 Outline of Chapter 5.

5.2 Indexing Methods

Atmospheric indexing schemes include the Murray and Lewis PCSM indices (Murray and Lewis 1966), the (El Niño) Southern Oscillation Index (SOI) (Rasmusson and Wallace 1983, Allan *et al* 1996), the East Atlantic Jet (EAJET) (Bell 1998), the West Pacific (WP) pattern (Wallace and

Gutzler 1981), the Pacific North American (PNA) pattern (Barnston and Livezey 1987) and the Tropical Northern Hemisphere (TNH) pattern (Mo and Livezey 1986).

An index value is the distillation of atmospheric circulation characteristics into a single number. Series may be calculated for various spatial and temporal resolutions, but are most commonly associated with monthly and annual time periods. The continuous nature of index data means that the artificial delimitation of class boundaries is not an issue, and, furthermore, they allow the use of restrictive, but powerful, parametric statistical techniques that require smooth data distributions. Indexing methods relevant to this study include, in order of computational complexity, the North Atlantic Oscillation Index (NAOI), the Zonal Index (ZI) and an airflow indexing method originally developed by El Dessouky and Jenkinson (1975).

5.2.1 Pilot Study

A pilot study was undertaken to assess the performance of 12 index catalogues (*table 5.1*). Models were divided by level, index grid and the technique for relating predictor and predictand. In these early stages the performance of a sample of the ZI and the NAOI based on the 500hPa was poor and further analysis was not undertaken. Furthermore the modelling of rainfall–circulation links by an ANN-based transfer function (back propagation, see *appendix 5.3*) did not improve on linear models. Preliminary results of this pilot study are given in *appendix 5.1*.

Index	Level	Linear Regression	Non-linear ANN
NAOI	Surface	**NAOI**	NAOIANN
	500hPa	500NAOI	500NAOIANN
ZI	Surface	**ZI**	ZIANN
	500hPa	500ZI	500ZIANN
Airflow technique	Surface	**SLPIND**	SLPINDANN
	500hPa	**500IND**	500INDANN

*Table 5.1 Index catalogues evaluated in pilot study (those in **bold** are reported in this thesis).*

5.3 The North Atlantic Oscillation Index (NAOI)

The North Atlantic Oscillation Index (NAOI) (*figure 5.2*) was first described by Walker (1924) and then by Walker and Bliss (1930 p53) as '...the tendency for pressure to be low near Iceland in winter when it is high near the Azores and south west Europe'. NAOI temporal variability and its relationship to surface meteorological variables (*e.g.* Hurrell 1995, Hurrell and Van Loon 1997, Stephenson *et al* 2000, Trigo *et al* 2002) and other environmental variables (*e.g.*

agricultural yields in Spain (Gimeno *et al* 2002)) has been widely discussed. It is defined as the difference in sea level barometric pressure (hPa) between the two 'centres of action' that control the weather of western Europe; the 'Azores High' (as represented by Ponta Delgada at 37.8°N, 25.7°W) and the 'Icelandic Low' (Stykkisholmur at 65.1°N, 22.7°W) (*figure 5.3*). The index is presented as a series of standardized values. The North Atlantic pressure gradient affects the strength of the North Atlantic zonal westerlies. The 'normal' situation (a NAOI value of 0.0) results in westerly flow.

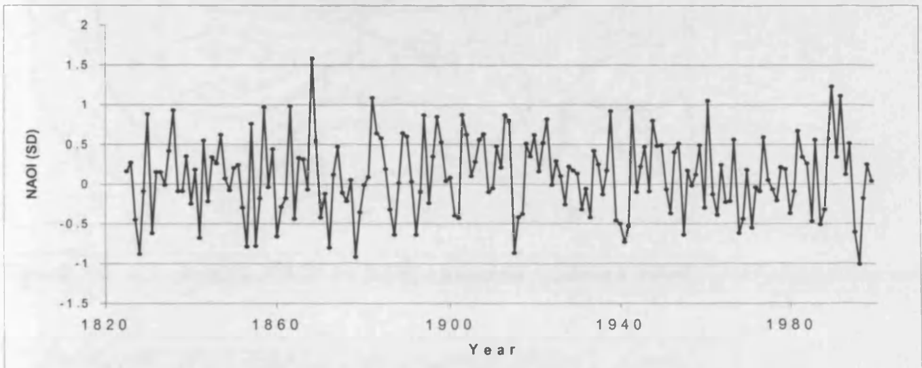

Figure 5.2 Annual values of the NAOI 1822-2000.

Figure 5.3 Location of stations used to calculate the NAOI.

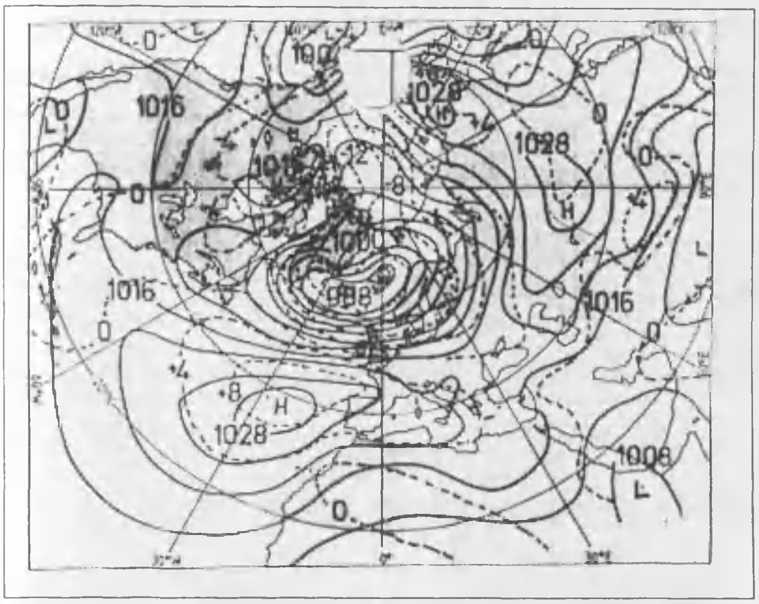

Figure 5.4 *A high NAOI (+3.68) situation – March 1994.*

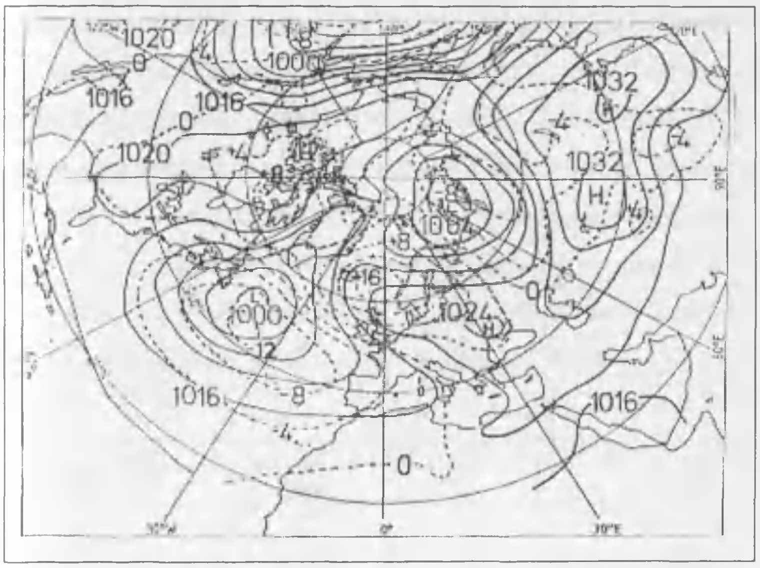

Figure 5.5 *A low NAOI (-3.0) situation – December 1995.*

Figure 5.4 represents a strengthened 'normal' pressure gradient, hence a vigorous westerly flow, and a strongly negative NAOI implies retrogressive or easterly flow of air (*figure 5.5)*. Positive NAOI values represent either a deepening of the Icelandic Low or a strengthening of the Azores High. The fundamental mechanisms determining the evolution of the NAOI are far from understood (Stephenson *et al* 2000) and it is not clear whether the NAOI is simply due to the aggregation of stochastic weather elements or whether ocean dynamics in the North Atlantic play an active role.

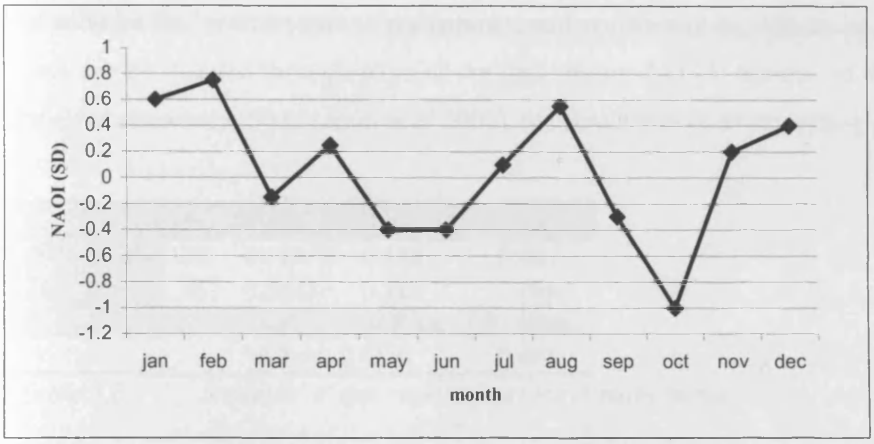

Figure 5.6 *Mean monthly values of the NAOI 1822-2000.*

The mean monthly values are shown in *figure 5.6* and notable months are October (strongly negative) and February and August (positive). Smoothed time series plots of annual sets indicate that certain periods display distinct modes of circulation. For instance, *figure 5.7* indicates four distinct primary phases in the annual NAOI that can be summarized by;

(i) low NAOI values at the end of the nineteenth century,
(ii) a strengthened NAOI in the first few decades of the twentieth century (1900-1930),
(iii) a steady reduction in the NAOI to the early seventies,
(iv) a recent shift to positive values.

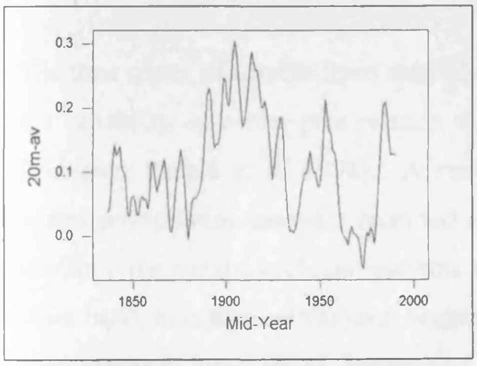

Figure 5.7 *20-year moving averages of annual NAOI series values 1822-2000.*

Although a test for a 'climatic jump' (see *appendix 2.4*) in NAOI values (assuming a Gaussian distribution and employing Student's 't' test (*table 5.2*) indicates no significant 'switches' in the

NAOI time series (*p<0.050*), the years 1920-2000 can be examined and a statistically significant reversal of trend emerges. 1920 is chosen because it represents the period when the annual NAOI was strongest in the early twentieth century and, after scrutiny, of the original time series 1967 is taken to be the 'switch year'. Two opposite and statistically significant (at *p<0.050*) linear trend lines can be inserted through plots of the data (*figure 5.8*). At the end of the 1990s, as has been reported elsewhere (Stephenson *et al* 2000), the NAOI was in a very strong positive phase.

	N	mean	SD	SE mean
1920-1966	47	0.111	0.438	0.064
1967-2000	33	0.067	0.111	0.088
		DF	**T-value**	**P-value**
		62	0.41	0.685

Table 5.2 Students' t' test result of test for climatic jump.

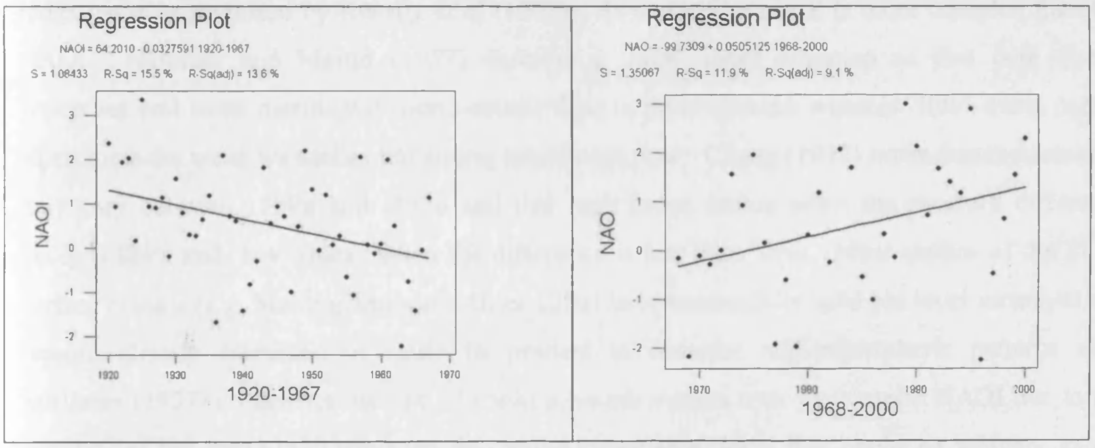

Figure 5.8 Significant reversal of trends in the NAOI time series.

The time series of standardized monthly NAOI values has proved valuable in the explanation of the variability of winter precipitation in western Europe (Lamb and Peppler 1987, Hurrell 1995, Rodriguez-Puebla *et al* 1998). A strong statistical correlation exists between the NAOI and winter precipitation amounts recorded at northern European stations. One reason for this is the tendency for zonal circulation patterns to 'push' cyclonic disturbances further south and, on the other hand, negative correlations suggest that blocking patterns will increase rainfall amounts in Mediterranean locations as depressions and frontal disturbances are 'forced' to the south of the block. Almerza and Lopez (1996) demonstrate that positive index values cause the Azores anticyclone to encroach upon the Iberian Peninsula giving low precipitation whereas negative NAOI values bring humid air from the west and south-west and abundant precipitation. This can be demonstrated by the examples in *figures 5.3* and *5.4*. The high index situation of March 1994 lead to widespread low rainfall across the peninsula (for instance at grid point 10 - total 2.6 mm, z-score -1.45, and at grid point 2 – total 19.1 mm, z-score -1.48), and the low index pattern on December 1995 was very wet (grid point 6 – total 112.7 mm, z-score +2.19 and grid point 9 – total 207.1 mm, z-score +2.14).

5.4 The Zonal Index

The Zonal Index (*ZI*) is one of the most frequently used parameters for describing the mode of circulation over the mid-latitudes (Spellman 1997). The index is defined as the MSLP difference (hPa) between latitudes 35°N and 55°N (Makrogiannis *et al* 1984). It is therefore centred on the region of maximum westerly circulation and so the mean pressure difference is nearly proportional to the mean wind component of this zone (Makrogiannis *et al* 1991). It relates to the index cycle as proposed by Rossby *et al* (1939). As a consequence it is more complex than the NAOI. Haltimer and Martin (1957) describe a 'high' index situation as that with strong westerlies and weak meridional (north-south) flow in mid-latitudes, whereas 'low' index occurs when there are weak westerlies but strong meridional flow. Chang (1972) notes that the actual *ZI* may vary between 15hPa and -5hPa and that high index occurs when the pressure difference exceeds 8hPa and 'low index' when the difference is less than 3hpa. Most studies of the *ZI* on surface climate (*e.g.* Makrogiannis and Giles 1980) have successfully used sea level series yet, for reasons already discussed, it could be prudent to consider mid-tropospheric patterns also. Spellman (1997) comments that the ZI could have advantages over the simpler NAOI due to the inability of the latter to distinguish downwind circulation detail that could be relevant to the eastern side of the peninsula.

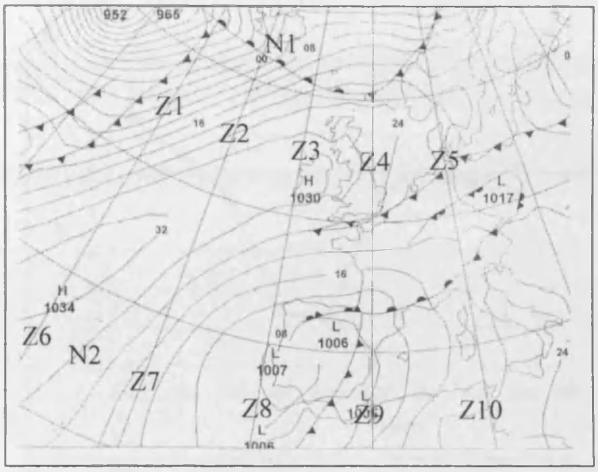

Figure 5.9 Grid points used in the calculation of the NAOI (N1, N2) and the calculation of the ZI (Z1-Z6).

In this study ZI values are calculated for the period 1945-1995 for the larger sector 55°N -35°W and 30°W-10°E (*figure 5.9*). A significant area upwind of the Iberian Peninsula is included. A time series (1958-2000) is shown in *figure 5.10* which, similar to the NAOI, depicts an upward trend in the data in the second half of this time period.

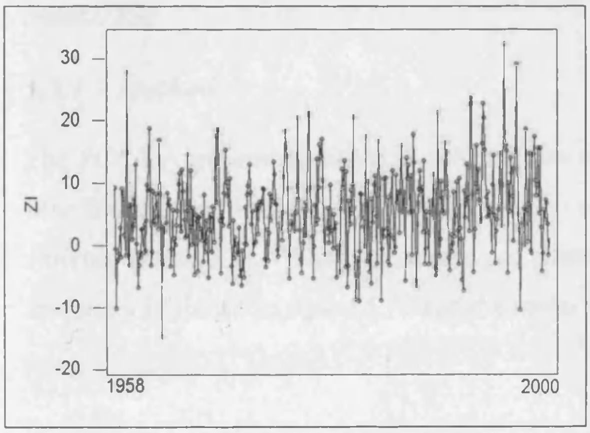

Figure 5.10 ZI values 1958- 2000.

A strong asymmetrical seasonal pattern can be observed in mean monthly ZI values - highest values occur in December and January (ZI ~ +9.0) and lowest (negative mean values) in April and May (ZI ~ -1.0) (*figure 5.11*). It can be inferred that over the entire sector strong westerlies control mid-winter circulation and late spring sees significant retrogressive patterns. The other months of the year are characterised by westerly patterns of similar strength (ZI +6.0).

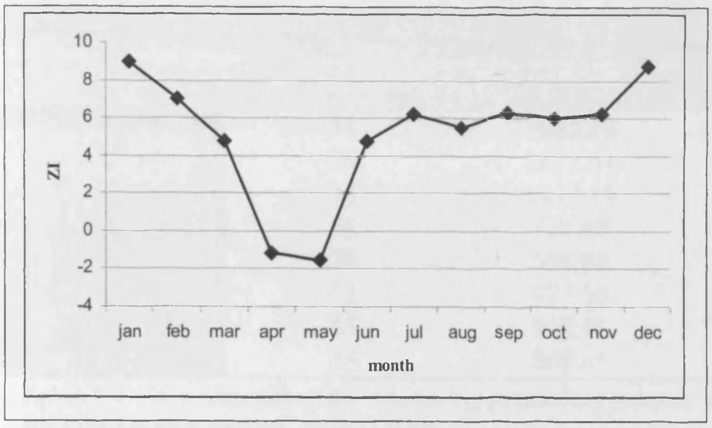

Figure 5.11 *Mean monthly values of the ZI.*

The role of these large-scale patterns can be examined using regression equations and Artificial Neural Networks (ANN). However ANN techniques were discarded at an early stage as they were found to not improve on the accuracy of estimation (see Spellman 1999).

5.5 Development of circulation catalogues using 500hPa contour surface - 500AUTM

5.5.1 Method

The PCA/CA generated 500AUT scheme described in *section 4.2* can be created for a monthly time frame. Application of PCA generates 5 components that account for 98.8% of the original variance (*table 5.3*). When the scores are clustered 8 monthly weather types emerge (*table 5.4*) frequency is shown in *figure 5.12* and the mean 500hPa surfaces are shown in *figure 5. 13.*

	PC1	PC2	PC3	PC4	PC5
Eigenvalue	41.1	13.5	5.2	2.0	1.4
Proportion of total variance explained (%)	64.2	21.1	8.1	3.2	2.3
Cumulative proportion	64.2	85.3	93.4	96.6	98.8

Table 5.3 *Eigenanalysis of PCA on monthly 500hPa data.*

Cluster Number	No of observations	Within cluster sum of squares	Average distance from centroid	Maximum distance from centroid
1	73	1082.18	3.63	6.91
2	108	1872.64	3.97	7.89
3	76	1157.18	3.71	7.48
4	55	722.49	3.52	6.16
5	28	594.83	4.39	8.34
6	52	977.56	4.18	7.88
7	45	912.41	4.22	9.44
8	38	809.65	4.27	8.72

Table 5.4 Results of the clustering procedure (cluster details) using monthly standardized 500hPa contour heights (500AUTM).

5.5.2 500AUTM weather types

500AUTM1 Slightly positive anomalies to the north-west (maximum +0.2SD) and slightly negative to the south-east (maximum –0.2SD).

500AUTM2 This is the commonest type (22.7% of months *figure 5.12*). A pool of positive anomalies (+0.3 SD) is located over the Balearic region. The rest of the peninsula displays slightly positive anomalies decreasing to the west.

500AUTM3 Virtually all of the peninsula displays positive anomalies of about +0.3SD. These are marginally lower in the north-east corner.

500AUTM4 Relatively strong positive departures off the west coast of the peninsula (>+ 0.5SD).

500AUTM5 This relatively uncommon (5.9%) pattern displays high negative anomalies (-0.9SD) centred on the Balearic Islands. Anticyclonic.

500AUTM6 This includes generally negative anomalies everywhere but lowest values occur in the north west province (-0.4SD) and rising to mean contour heights along the eastern Mediterranean coasts.

500AUTM7 Generally cyclonic. Positive anomalies which are highest centred on the eastern parts of the peninsula. All of Spain is above +0.65SD.

500AUTM8 The peninsula is dominated by negative anomalies between -0.75 in the west and -0.55 near the Balearics. Anticyclonicity.

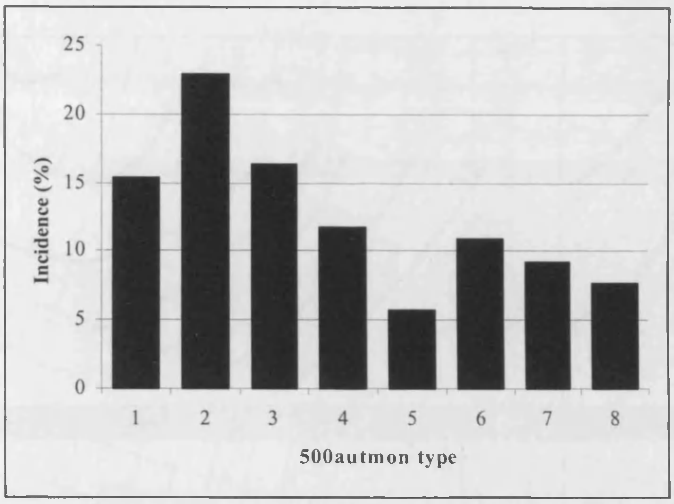

Figure 5.12 Annual frequency of 500AUTM weather types.

Next page Figure 5.13 500AUTM mean contour heights.

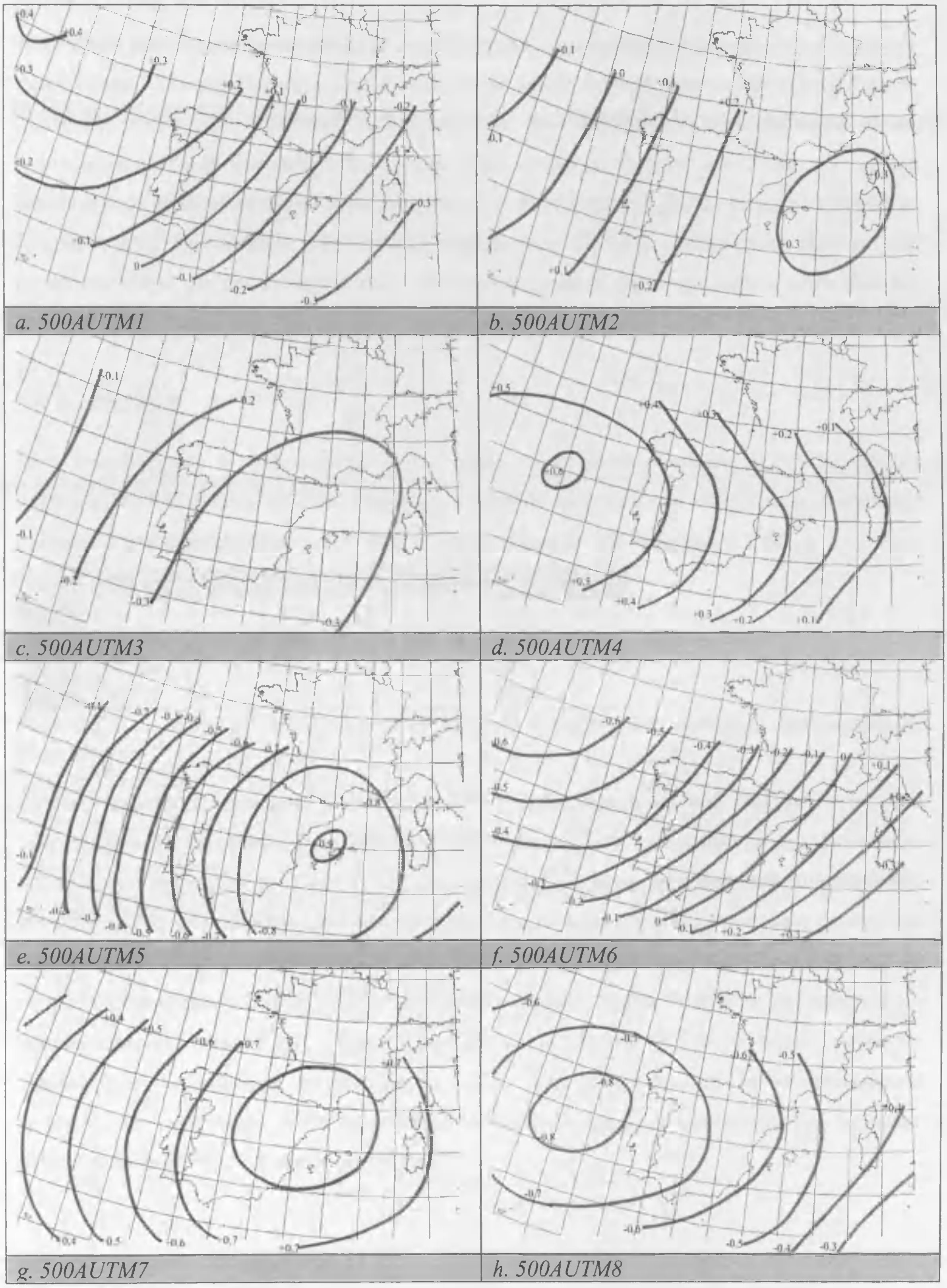

a. 500AUTM1

b. 500AUTM2

c. 500AUTM3

d. 500AUTM4

e. 500AUTM5

f. 500AUTM6

g. 500AUTM7

h. 500AUTM8

5.6 Air Flow Indexing

The airflow index method introduced in *section 4.3* can also be employed to produce circulation index values. The disadvantages that arise from the use of discrete weather type classifications (especially within-type variability in intensity and flow strength) can be addressed by an examination of the airflow indices themselves. This allows for detailed description and perhaps more rigorous analysis of the association between climate variables and atmospheric circulation features and the development of models (*e.g.* regression or ANN) by which climate elements can be estimated from airflow characteristics. This method is much more regionally specific than the ZI and NAOI meaning that data requirements are greater.

5.6.1 SLPIND

Mean monthly plots of surface-based airflow index values (from which the SLPINDC weather types are derived) display seasonal changes. Descriptive summaries of airflow indices are listed in *table 5.5* and monthly means of *P, W, S, F* and *Z* indices are given in *figure 5.14.*

	P	W	S	F	ZW	ZS	Z
Mean	1017.64	0.20	-1.73	7.13	-3.41	0.41	-3.00
SD	5.71	6.48	4.81	4.16	12.34	6.24	15.09
Min	989.96	-22.98	-19.82	0.07	-49.92	-30.87	-55.30
Max	1038.79	30.24	25.03	31.53	61.95	29.00	75.55

Table 5.5 Monthly characteristics of SLPIND. SD-Standard deviation; Max-maximum; Min–minimum.

The key features of the annual variation are firstly, a domination of high pressure in the cold season (*figure 5.14a*) partly due to the cool temperatures over the high plateau causing subsidence in the lower troposphere. This is replaced by lower pressure in spring and autumn when travelling Atlantic depressions are most frequent. In the summer months the Azores anticyclone dominates the circulation of the region however the existence of strong surface heating leads to relative low pressure at surface. The switch from a westerly regime in autumn and winter to an easterly flow in summer and spring (*figure 5.14b)* is accompanied by a weaker southerly component in the middle of the year (*figure 5.14c*). This is explained by the well-pronounced expansion and contraction of the circumpolar vortex and subsequent displacement of the upper westerlies from winter to summer (Perry 1997).

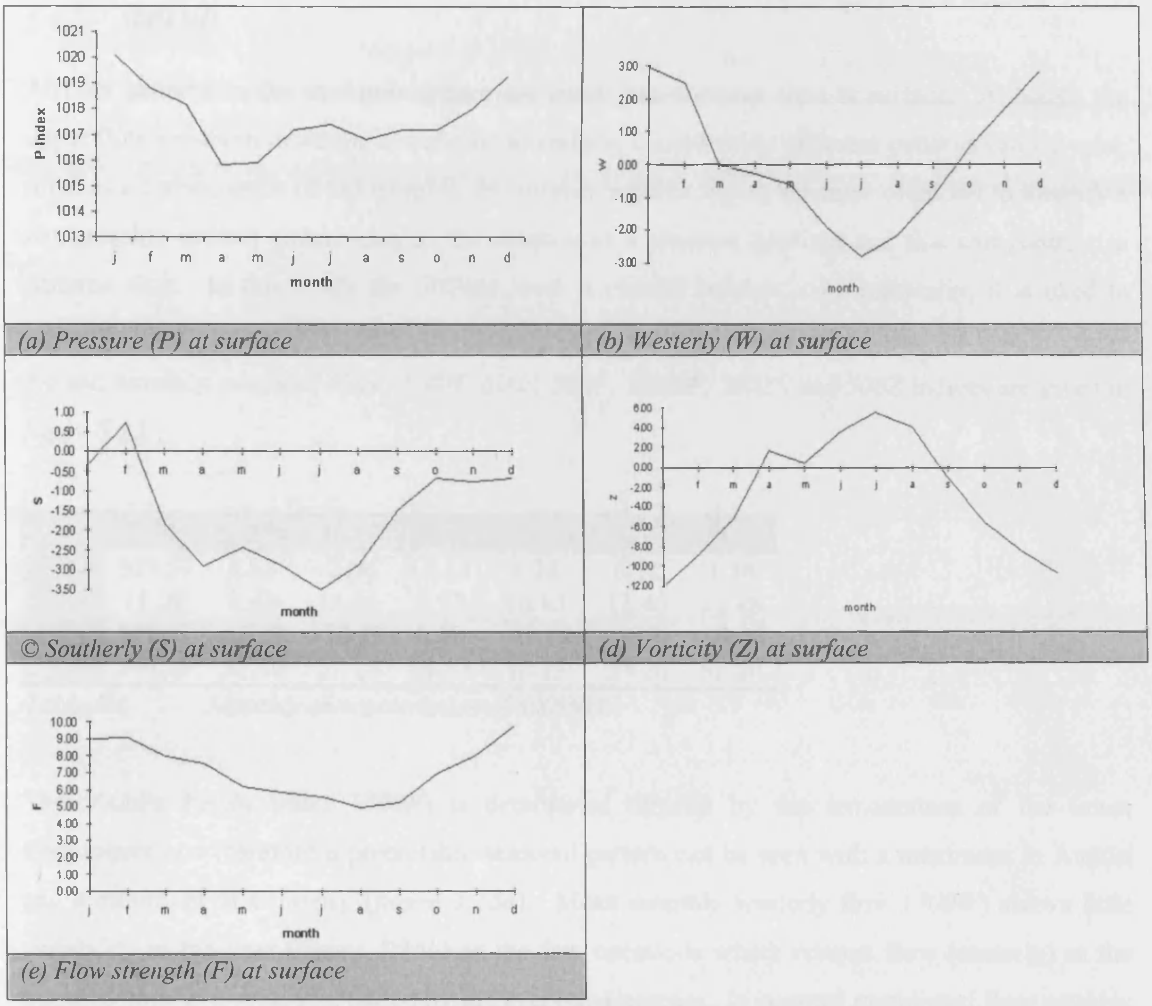

(a) Pressure (P) at surface

(b) Westerly (W) at surface

© Southerly (S) at surface

(d) Vorticity (Z) at surface

(e) Flow strength (F) at surface

Figure 5.14 Mean monthly values SLPIND (from Spellman 2000b).

Strong anticyclonicity (negative Z values) in winter is replaced by cyclonicity in the summer months (*figure 5.14d*). Although on average there are between one and three travelling low pressure systems passing through the region between June and September this cyclonicity is actually a consequence of the near-surface establishment of thermal low pressure systems due to strong surface heating. This occurs despite the strengthening of anticyclonic patterns aloft. As a consequence of a hemispheric reduction in the pole-to-equator temperature gradient surface geostrophic flow is weaker in the summer half of the year (*figure 5.14e*).

5.6.2 500IND

Airflow patterns in the mid-troposphere are much less complex than at surface. Although the upper flow serves to drive the circulation at surface, considerably different patterns can co-exist, often as a consequence of topography. In summer weather typing schemes often fail to identify a recognisable surface pattern due to the absence of a pressure gradient and this can contrast to patterns aloft. In this study the 500hpa level is chosen because, conventionally, it is used to represent upper atmospheric patterns. Descriptive summaries of airflow indices are listed in *table 5.6* and monthly means of *500P, 500W, 500S, 500F, 500ZW, 500ZS* and *500Z* indices are given in *figure 5.15.*

	500P	500W	500S	500F	500ZW	500ZS	500Z
Mean	569.57	9.88	-2.94	17.33	1.38	0.12	1.50
SDev	11.28	8.43	14.66	9.57	16.85	11.40	22.48
Min	532.52	-17.28	-58.79	0.08	-67.08	-36.93	-63.43
Max	593.79	51.40	51.18	59.53	80.15	55.20	98.86

Table 5.6 Monthly characteristics of 500IND.

The 500hPa height index (*500P*) is determined directly by the temperature of the lower troposphere and therefore a predictable seasonal pattern can be seen with a maximum in August and a minimum in February (*figure 5.15a*). Mean monthly westerly flow (*500W*) shows little variability in the year (*figure 5.15b*) as the few occasions where reverse flow (easterly) in the upper atmosphere occurs is hidden by the averaging process. In contrast meridional flow patterns show a swing from winter northerly to summer southerly flow (*500S - figure 5.15c*). Upper flow (*500F - figure 5.15d)* is, at all times of the year, stronger than at surface and decreases in the summer months. Finally the pattern in vorticity (*500Z - figure 5.15e)* more clearly reflects hemispheric changes in circulation. There is a strengthening in early summer and autumn and slight anticyclonicity in high summer as the Azores anticyclone starts to dominate. Vorticity is negative in January as a consequence of low level subsidence due to contact winter cooling over the high altitude continentality of the Peninsula. *Table 5.7* lists PPM correlation coefficients between upper and low level flow. Virtually all are significantly positively related at $p<0.050$ and this relationship is stronger in the winter months.

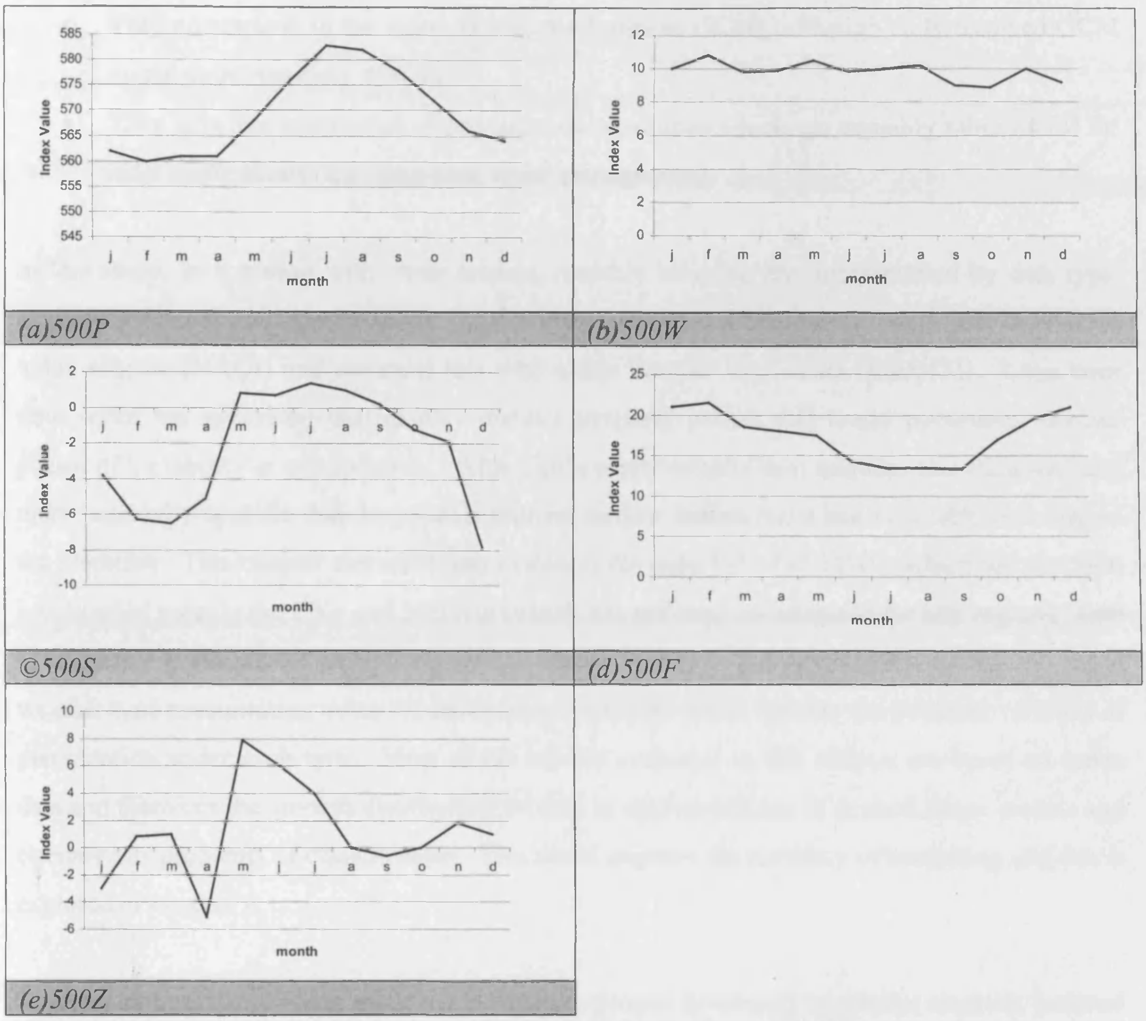

Figure 5.15 Mean monthly values of 500IND (from Spellman 2000b).

	P	W	S	F	ZW	ZS	Z
Summer	**0.536**	**0.606**	**0.481**	**0.479**	**0.458**	0.157	**0.349**
Winter	**0.525**	**0.835**	**0.555**	**0.706**	**0.752**	**0.507**	**0.703**
Year	**0.546**	**0.781**	**0.439**	**0.693**	**0.750**	**0.494**	**0.685**

*Table 5.7 PPM correlation coefficients between SLPIND and 500IND. **Bold** values are significant at $p<0.050$ (from Spellman 2000b).*

5.7 Conclusions

Monthly synoptic schemes sacrifice the valuable process-related temporal resolution of daily catalogues, however they have two main advantages over daily models,

- They correspond to the more reliable resolution of GCMs (although daily resolved GCM output is increasingly available[1]).
- They generate summaries of precipitation conditions which are arguably more useful for most applications (*e.g.* long-term water management).

In this study, in common with other models, monthly schemes are differentiated by data type, atmospheric level and spatial scale. The project evaluates a commonly employed large-scale index scheme (NAOI) and contrasts this with a less familiar large-scale index (ZI). Long term time series are generated that display distinct temporal phases that could potentially explain phases of variability in precipitation. Although less problematic than nominal classifications and more regionally specific than large-scale indices, airflow indices have had very little coverage in the literature. This chapter therefore also evaluates the potential of SLPIND (which has not been investigated outside the UK) and 500IND (which has not been investigated for any region). One of the main problems of modelling using weather typing is the requirement to use the mean weather type precipitation value for calibrating the model which ignores the potential variance of precipitation under each type. Most of the models evaluated in this chapter are based on index data and therefore the smooth distribution permits an appropriate use of general linear models and circumvents problems of classification. This could improve the accuracy of modelling and this is explored in *chapter 6.*

To contrast with these index models a monthly catalogue developed by similar methods outlined in *chapter 4* is also generated. It is highly unusual for monthly schemes to be created by PCA/CA however there is no reason why this should be the case.

The NAOI and the ZI increases in value and therefore, indirectly, there is an increase the Mediterranean anticyclonicity particularly in the final two decades of the study period. This agrees with the circulation trends indicated by 500AUT, which show an increase in anticyclonicity in this period. It could be that the decreases in rainfall identified in *section 1.2* could be related to this. Circulation-rainfall links are explored in *chapter 6.*

[1] Daily GCM output from CCCMA became available in early 2003.

Chapter Six
Evaluation of synoptic models

6.1 Introduction

The aim of each synoptic model is to capture a stable circulation-precipitation relationship. Relative model performance can be evaluated by statistical procedures (*i.e.* split-sampling and the use of validation statistics (Spellman 1999)). This chapter examines the performance of synoptic models (*figure 6.1*).

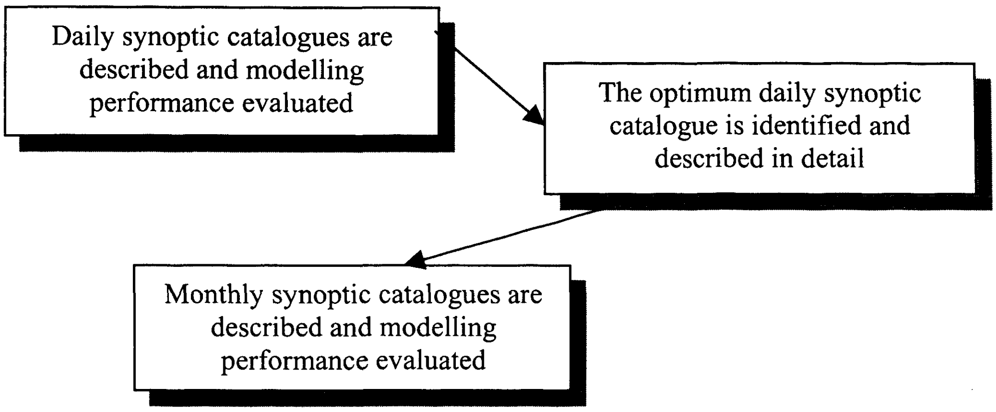

Figure 6.1 Outline of Chapter 6.

6.2 Examining the performance of daily class-based synoptic methods

Quantification of the strength of the relationship between circulation pattern and precipitation can be performed by a simple relative performance index (*RPI*) (*eqn 6.1*). This scores the relative contribution of a particular weather type to the total rainfall amount at a location, and is thus independent of total expected amounts. Effectively it is the ratio of the mean daily rainfall (mm) under weather type *i*, and the climatological mean daily rainfall (mm) (Zhang *et al* 1997).

$$RPI = \left(\frac{Ri}{ni} \Big/ \frac{R}{n} \right). \quad (Eqn\ 6.1)$$

Where *ni* is the number of occurrences of pattern *i*, *Ri* is the total amount of rain (mm) falling in *ni* type days, and *R* is the total precipitation (mm) falling during the entire sample period of *n* days. *RPI* is therefore a normalized mean rainfall intensity for type *i* which considers the probability of rainfall occurrence conditional upon type *i* and also the intensity of rainfall within that pattern.

If the weather type has little contribution to rainfall then *RPI (i)* will be less than 1. *RPI* values greater than 1 indicate an increasing contribution of that type to rainfall. When the *RPI* is close to 1 it means that that type supplies rainfall totals near to the climatological mean. In order to illustrate differences in *RPI* values under each classification scheme seven rainfall locations (*figure 6.2*) – Badajoz (APAA3d), Burgos (APAA2d, east), Mahon (APAA6d). Malaga (APAA3d), Murcia (APAA4d), Salamanca (APAA2d, west) and Santander (APAA5d) – are selected. These stations all have a limited amount of missing data and are representative of the covariant rainfall affinity areas (noted in parenthesis) described in *section 2.10.* A representative station in the north-west quadrant (APAAd1) is not listed due to dataset problems.

A one-way analysis of variance (ANOVA) (*appendix 6.1*) test was applied to,

(*i*) the *RPI* values to investigate if significant differences existed between the mean values recorded at all sites under each weather type and,

(*ii*) the daily rainfall amounts at each station to investigate how catalogues discriminated between each site.

Due to the fact that ANOVA will only indicate that at least one significant difference exists between weather type rainfall response a *post hoc* test (Fisher's Least Significant Difference (LSD) test) was applied to identify which types are significantly different from which (Dytham 1999). This yields a critical mean difference required for two groups to be deemed different at the chosen level of significance ($p<0.050$). In this test the least significant difference is calculated for each pairs of means *(eqn 6.2),*

$$LSD_{A.B} = qSE_{A.B} \; (Eqn\ 6.2)$$

where the standard error is calculated in *eqn 6.3,*

$$SE_{A.B} = \sqrt{\frac{MS_{within}}{2}\left[\frac{1}{n_A}+\frac{1}{n_B}\right]} \quad (Eqn\ 6.3)$$

and $LSD_{A.B}$ is the least significant difference between the means of samples A and B, n_A and n_B are the number of items in samples A and B and q is the value obtained from q distribution tables (Wheater and Cook 2000).

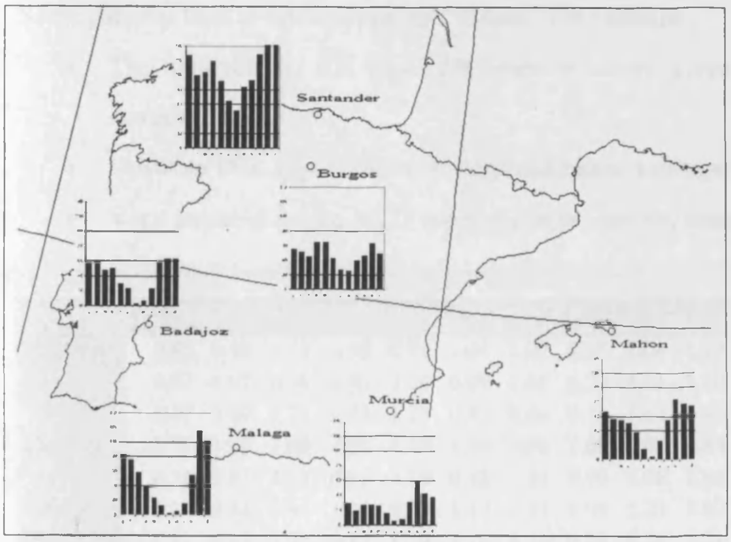

Figure 6.2 Stations chosen to illustrate circulation-rainfall association.

These methods provided an appropriate preliminary assessment of the discriminatory power of each synoptic catalogue. More rigorous split-sampling validation was later applied to evaluate refined versions of optimal catalogues.

6.3 Evaluating the performance of daily synoptic models

6.3.1 SLPMAN

ANOVA of the mean rainfall recorded under each SLPMAN weather type is reported in *appendix 6.2.* SLPMAN can be substituted satisfactorily by an objective method (SLPINDC) and therefore further comments are not made here.

6.3.2 500MAN

Rainfall modelling under 500MAN yields both expected and unexpected results (*table 6.1* and *6.2*). Of the former, for instance, the *RPI* associated with SEL (*3*) patterns is relatively high for

Mahon (1.25) and Murcia (1.23) and lower for those locations which are geographically remote from the synoptic source of precipitation (*e.g.* Salamanca – 0.97). Similarly RMT (*16*) patterns, which lead to cold air flow from the north-east, gives high rainfall in Mahon (2.36), as it destabilizes over the Mediterranean, and less at inland peninsula locations such as Burgos (0.77) which is sheltered by the Pyrenees. Finally WT (*7*), favours rainfall to the west of the peninsula but is unimportant in eastern locations like Mahon (0.64) and Santander (0.79).

Some patterns lead to unexpected *RPI* values. For instance,

- The anticyclonic CR type (*10*) leads to above average rainfall in Badajoz (1.13) and Burgos (1.10).
- Unstable PCL types lead to widespread below average rainfall (*e.g.* Salamanca 0.69).
- Very unstable Arctic MCT types result in very dry conditions (*e.g.* Santander 0.66).

	1	2	3	4	5	6	7	8	9	10	11	12	13	14	15	16
Badajoz	0.60	0.92	1.11	0.93	0.93	1.04	1.07	0.85	1.04	1.13	1.19	1.10	0.72	0.56	0.86	1.26
Burgos	0.97	0.97	0.99	0.92	1.20	0.99	1.06	0.77	0.91	1.10	0.88	1.14	0.89	1.13	0.89	0.77
Mahon	0.40	0.89	1.25	0.83	1.25	0.95	0.64	0.75	1.13	0.88	1.35	1.05	0.63	0.80	1.10	2.36
Malaga	0.78	1.10	1.03	1.01	1.10	1.14	1.03	1.08	1.07	0.84	1.01	1.06	0.66	0.90	0.83	0.95
Murcia	0.74	0.87	1.14	0.95	1.10	0.92	1.03	0.90	1.08	0.96	0.93	1.13	0.99	1.04	0.98	0.70
Salamanca	1.14	0.64	0.97	1.05	0.85	1.10	1.31	0.70	1.20	0.82	1.10	1.16	0.57	0.83	1.12	1.06
Santander	0.92	0.93	1.23	0.87	1.19	1.14	0.79	0.71	0.70	1.01	1.03	1.17	0.66	0.64	1.02	1.19

1 RCT; 2 PCL; 3 SEL; 4 AR; 5 ZN; 6 CT; 7 WT; 8 SWL; 9 MT; 10 CR; 11 PL; 12 ZS; 13 MCT; 14 LN; 15 MR; 16 RMT

Table 6.1 RPI scores for 500MAN.

	Badajoz	Burgos	Mahon	Malaga	Murcia	Salamanca	Santander
Maximum	1.26	1.20	2.36	1.14	1.14	1.31	1.23
Minimum	0.56	0.77	0.40	0.66	0.70	0.57	0.64
Sdev	0.20	0.13	0.44	0.14	0.13	0.22	0.20
COV (%)	21	13	43	14	13	22	22

Table 6.2 Descriptive statistics of RPI values for 500MAN

Source	DF	SS	MS	F	P-value
Factor	15	1.74	0.12	2.84	0.001
Error	96	3.91	0.04		
Total	111	5.65			

Table 6.3 ANOVA of RPI scores for 500MAN.

	F	P-value
Badajoz	1.63	0.058*
Burgos	1.54	0.083*
Mahon	1.27	0.213*
Malaga	1.28	0.208*
Murcia	2.32	0.003
Salamanca	1.17	0.285*
Santander	1.54	0.082*

Table 6.4 *ANOVA of 500MAN. * Not significant at p<0.050.*

Tables 6.2, 6.3 and 6.4 indicate the discrimination between mean rainfall amounts at each site under each weather type. It is relatively poor when compared to other schemes. RPI is variable, suggesting good discrimination, in Mahon (Coefficient of Variability[1] - 43%) but much less so elsewhere (*e.g.* Burgos and Murcia 13%).

Figure 6.3 gives a hypothetical example of a 10-class catalogue in which all classes show significant differences from each other (in this case a mixture of 'greater than ' and 'less than' differences) after application of the Fisher's LSD test. *Figure 6.4* indicates the limited amount of significant differences between RPI at all sites.

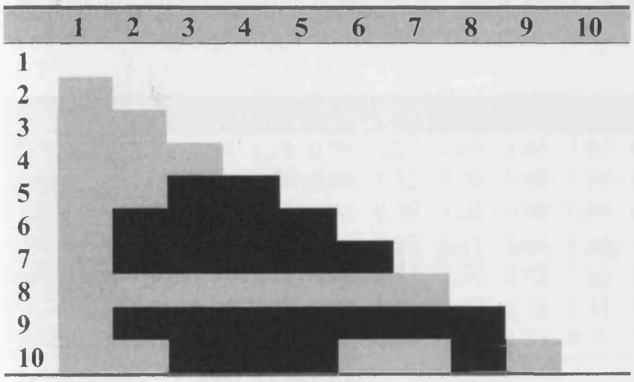

Figure 6.3 *A multiple comparison diagram depicting a situation where the mean values of 10 classes all display significant differences from the mean values of each other class. When the RPI value of the circulation type in the column is significantly lower than the type in the row then the cell is shaded in grey. If the RPI value of the type in the column is significantly higher than the row type then the cell is shaded black.*

[1] Standard deviation/mean – a comparative (unit free) measure of variability.

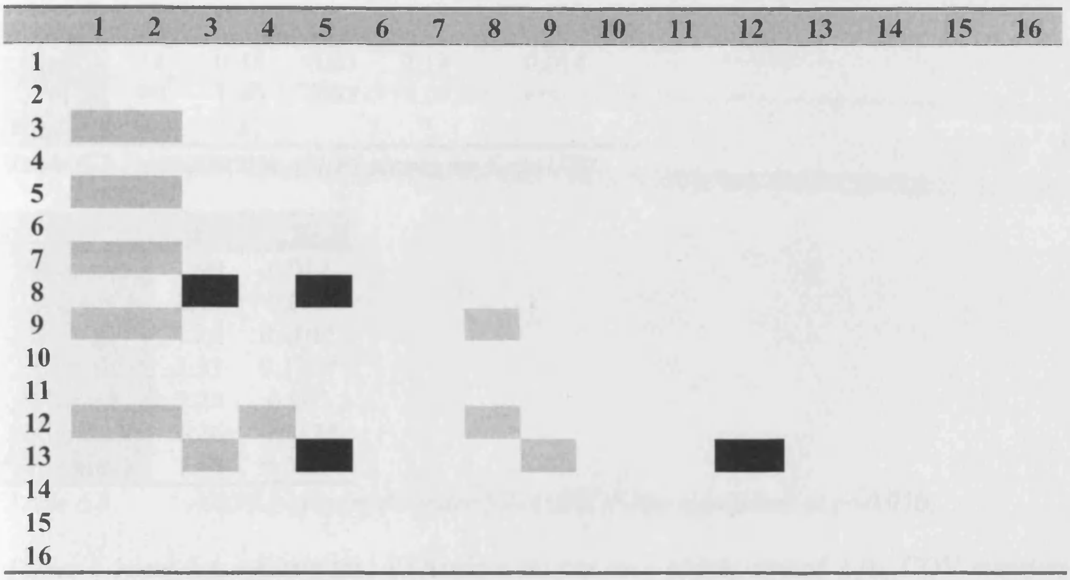

Figure 6.4 *Fisher's Pairwise Comparisons between RPI values of 500MAN weather types.*

6.3.3 500AUTR

Table 6.5 lists RPI scores under 500AUTR. Some expected associations emerge - eastern trough patterns (6, 12) are important for rainfall in eastern locations, zonal southerlies (7) lead to wetter days in the west and dry conditions are associated with the slack *500AUTR15*. On the other hand, the strongly anticyclonic 5 is not as dry as expected (*e.g.* Burgos 1.12).

	1	2	3	4	5	6	7	8	9	10	11	12	13	14	15
Badajoz	1.01	0.90	1.10	0.96	1.07	0.93	1.04	1.07	0.85	1.04	0.95	1.20	0.87	0.96	0.99
Burgos	1.00	1.10	0.99	0.88	1.12	1.20	0.99	1.06	0.77	0.91	0.95	0.88	0.90	1.00	0.93
Mahon	1.06	1.00	1.26	0.94	0.79	1.25	0.95	0.64	0.74	1.13	0.95	1.35	1.06	0.81	0.92
Malaga	0.93	1.03	1.03	1.00	0.97	1.11	1.14	1.03	1.08	1.05	1.00	1.01	0.84	0.99	0.86
Murcia	0.97	1.01	1.14	0.96	0.95	1.10	0.92	1.03	0.90	1.08	0.96	0.93	1.00	1.03	0.98
Salamanca	0.96	0.88	0.97	0.93	0.83	0.85	1.10	1.31	0.70	1.20	1.22	1.10	1.02	1.14	1.21
Santander	1.00	0.99	1.23	0.86	1.00	1.19	1.15	0.79	0.71	0.70	1.10	1.03	0.99	0.77	1.06

Table 6.5 *RPI scores under 500AUTR.*

	Badajoz	Burgos	Mahon	Malaga	Murcia	Salamanca	Santander
Maximum	1.20	1.20	1.35	1.14	1.14	1.31	1.23
Minimum	0.85	0.77	0.64	0.84	0.90	0.70	0.70
Sdev	0.09	0.11	0.20	0.08	0.07	0.17	0.17
COV (%)	9	11	20	8	7	17	18

Table 6.6 *Descriptive statistics of RPI values under 500AUTR.*

Source	DF	SS	MS	F	P-value
Factor	14	0.48	0.03	2.19	0.014
Error	90	1.40	0.02		
Total	104	1.87			

Table 6.7 *ANOVA of RPI scores for 500AUTR.*

	F	P
Badajoz	1.99	0.012
Burgos	1.71	0.043
Mahon	1.29	0.201*
Malaga	1.33	0.173*
Murcia	2.28	0.003
Salamanca	1.26	0.217*
Santander	1.12	0.088*

Table 6.8 *ANOVA of rainfall under 500AUTR. * Not significant at p<0.050.*

Tables 6.5 and *6.6* indicate that RPI values do not vary widely around 1.0. COV statistics are considerably lower than for 500MAN. *Tables 6.7* and *6.8,* which list ANOVA results, suggest that discrimination is not entirely successful. *Figure 6.5* depicts that discrimination under *500AUTR* is limited but *500AUTR9* is quite distinctive.

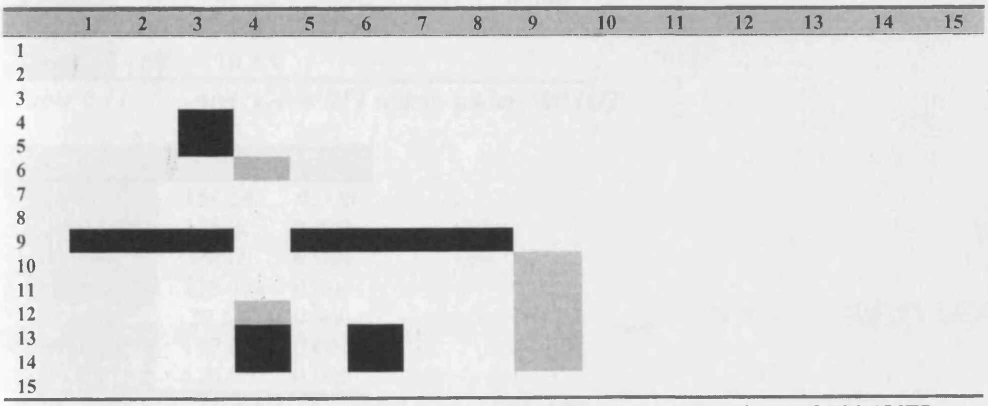

Figure 6.5 *Fisher's Pairwise Comparisons between RPI values of 500AUTR weather types.*

6.3.4 500AUT

RPI statistics under 500AUT are summarized in *tables 6.9* and *6.10.* There is considerably more variability in RPI between types at each site, as confirmed by the COV statistics in *table 6.9* and ANOVA in *tables 6.11* and *6.12.* Notable rainfall signatures *(figure 6.6)* can be summarized as,

- Widespread dry conditions under anticyclonic *500AUT1* (especially in the south) and *500AUT2.*
- Widespread wet conditions under cyclonic *500AUT8* (especially in the south).

- Very wet conditions in the south-west under *500AUT5*.
- Dry conditions in the east under *500AUT6*.

	1	2	3	4	5	6	7	8	9	10
Badajoz	0.07	0.10	1.16	0.64	3.26	2.64	0.47	2.10	0.90	0.12
Burgos	0.09	0.31	0.42	1.74	1.57	0.50	0.77	2.12	2.43	0.48
Mahon	0.22	0.60	1.63	1.97	1.17	0.73	0.50	2.49	0.52	1.25
Malaga	0.04	0.10	0.44	0.70	4.78	1.09	0.35	3.30	1.25	0.13
Murcia	0.07	0.55	1.02	2.87	0.81	0.22	0.25	3.01	1.19	1.77
Salamanca	0.16	0.24	1.42	0.99	2.90	1.81	0.70	1.96	0.60	0.45
Santander	0.18	0.18	1.26	0.71	2.86	2.17	0.74	1.95	0.85	0.23

Table 6.9 *RPI scores under 500AUT.*

	Badajoz	Burgos	Mahon	Malaga	Murcia	Salamanca	Santander
Maximum	3.26	2.43	2.49	4.78	3.01	2.90	2.86
Minimum	0.07	0.09	0.22	0.04	0.07	0.16	0.18
Sdev	1.14	0.84	0.73	1.58	1.06	0.88	0.93
COV (%)	99	81	66	130	90	79	84

Table 6.10 *Descriptive statistics of RPI values under 500AUT.*

Source	DF	SS	MS	F	P-value
Factor	9	41.23	4.58	9.37	0.000
Error	60	29.32	0.49		
Total	69	70.55			

Table 6.11 *ANOVA of RPI scores under 500AUT.*

	F	P
Badajoz	154.54	0.000
Burgos	128.82	0.000
Mahon	69.82	0.000
Malaga	118.33	0.000
Murcia	37.52	0.000
Salamanca	127.01	0.000
Santander	126.00	0.000

Table 6.12 *ANOVA of rainfall under 500AUT.*

Results of the Fisher's LSD test are depicted in *figures 6.7* for all sites and *figures 6.8* to *6.14* for individual locations. Excellent discrimination is identified for Burgos and Badajoz. Lesser but nonetheless successful discrimination is seen at eastern Mediterranean locations.

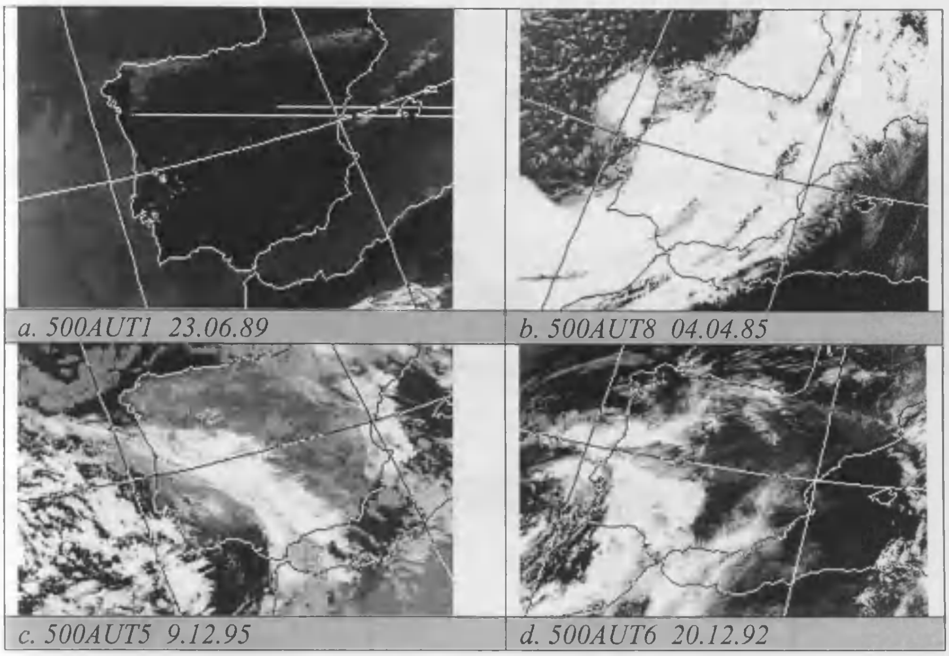

Figure 6.6 Daytime satellite NOAA 9 AHHRR of selected weather types (channel 4 - thermal infra-red, 10.3-11.3μm).

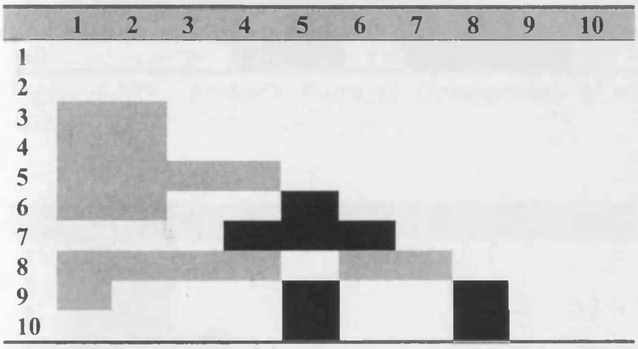

Figure 6.7 Fisher's Pairwise Comparisons between RPI values of weather types under 500AUT.

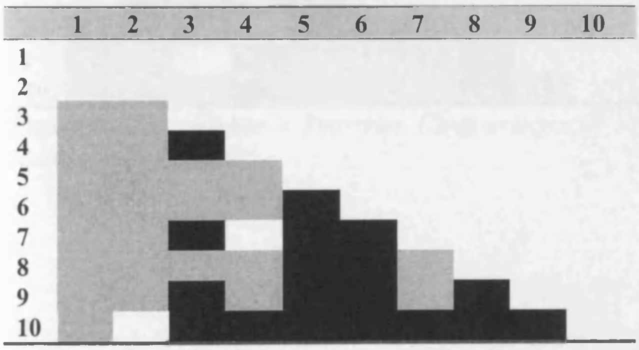

Figure 6.8 Fisher's Pairwise Comparisons between rainfall amounts under 500AUT at Badajoz.

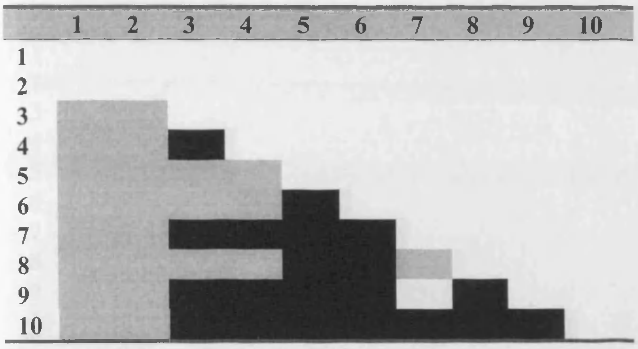

Figure 6.9 Fisher's Pairwise Comparisons of rainfall to weather type under 500AUT at Burgos.

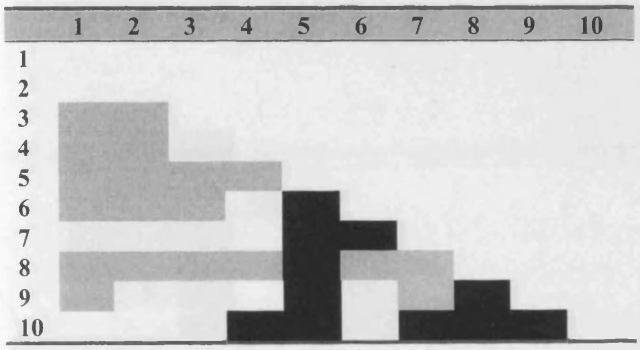

Figure 6.10 Fisher's Pairwise Comparisons of rainfall to weather type under 500AUT at Malaga.

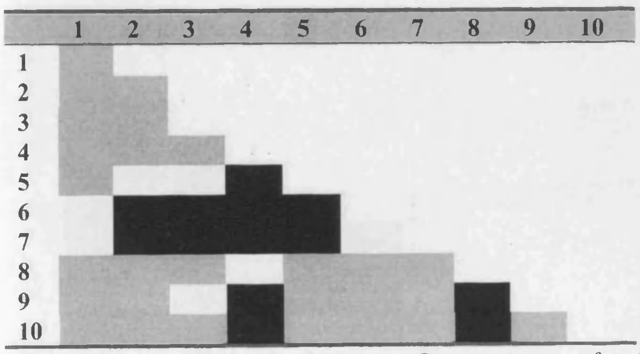

Figure 6.11 Fisher's Pairwise Comparisons of rainfall to weather type under 500AUT at Mahon.

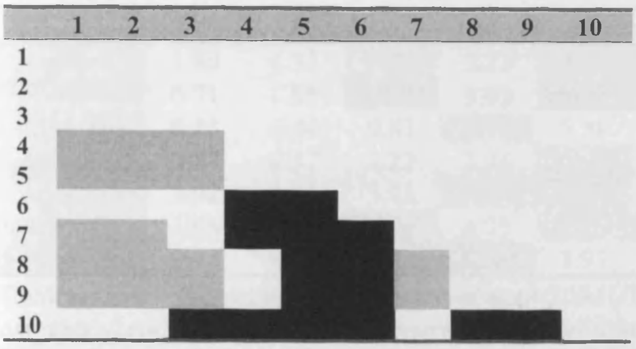

Figure 6.12 *Fisher's Pairwise Comparisons of rainfall to weather type under 500AUT at Murcia.*

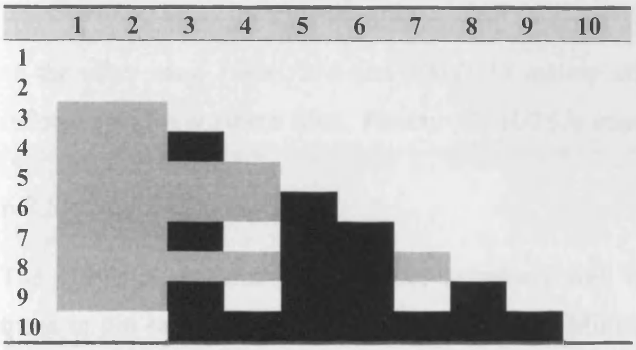

Figure 6.13 *Fisher's Pairwise Comparisons of rainfall to weather type under 500AUT at Salamanca.*

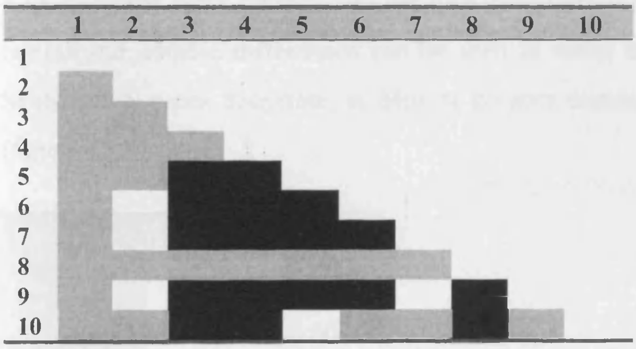

Figure 6.14 *Fisher's Pairwise Comparisons of rainfall to weather type under 500AUT at Santander.*

6.3.4.1 Further comments on 500AUT

Given that 500AUT is the better performing daily synoptic model some further comments are made on this scheme. High rainfall amounts at each location can be arbitrarily defined as daily rainfall totals in the top decile of the range.

	1	2	3	4	5	6	7	8	9	10
Badajoz	1.00	0.33	11.63	5.32	29.90	25.58	4.98	10.63	10.30	0.33
Burgos	0.71	1.90	13.30	9.03	31.35	14.96	9.03	9.03	7.84	2.85
Mahon	0.43	6.44	9.87	27.47	5.58	2.15	1.29	13.73	18.45	14.59
Malaga	0.57	0.57	2.27	3.98	49.43	7.95	3.41	18.18	12.50	1.14
Murcia	1.02	3.05	3.05	20.30	13.71	2.54	10.15	10.66	31.47	4.06
Salamanca	1.68	1.68	10.61	4.75	30.73	20.11	8.66	8.66	11.45	1.68
Santander	0.92	6.61	18.59	22.43	8.91	4.30	4.92	16.59	5.22	11.52

Table 6.13 Percentage occurrence of each 500AUT type in the top 10% of rain day rainfall amounts at each site (shaded cells represent greater than 10% incidence in top 10%).

Consistent and clear relationships can be seen between high rainfall amounts and weather type in *table 6.13*. *500AUT1* and *2* are responsible for few high rainfall events at any of the sites. *500AUT5* is associated with extreme rainfall amounts in all locations bar the east of the country, on the other hand *500AUT10* and *500AUT4* mainly affect the east. *500AUT8* and *9* have less influence on the northern sites. Finally *500AUT6* is important for inland sites.

6.3.5 SLPINDC

The SLPINDC scheme discriminates extremely well (*table 6.14*) between all locations except those in the eastern Mediterranean (Mahon and Murcia). It is only marginally less successful than 500AUT, although the reduced number of classes of the latter scheme gives it a practical advantage. Due to the high numbers of classes in SLPINDC RPI values are not listed but *table 6.15* illustrates some rainfall-weather type characteristics. C-types are responsible for widespread rainfall but notable differences can be seen in terms of rainfall-relevant air flow direction - at Santander N-types dominate, at Murcia E-types dominate and at Salamanca W-types dominate (*figure 6.15*).

	F	P-value
Badajoz	70.38	0.000
Burgos	46.53	0.000
Mahon	10.42	0.000
Malaga	21.55	0.000
Murcia	10.64	0.000
Salamanca	48.14	0.000
Santander	49.90	0.000

Table 6.14 ANOVA of rainfall under SLPINDC.

Six wettest SLPINDC types at each site						
Badajoz	**Burgos**	**Mahon**	**Malaga**	**Murcia**	**Salamanca**	**Santander**
SW	SW	CS	CS	CSE	SW	NW
S	CW	CNW	SW	C	CW	CNW
CSW	CS	N	SE	CE	W	ANW
CS	CSW	CW	S	E	CSW	N
AS	C	CN	CW	CNE	ASW	AN
CW	S	CSE	CSE	AE	S	CN

Table 6.15 Wettest SLPINDC weather types.

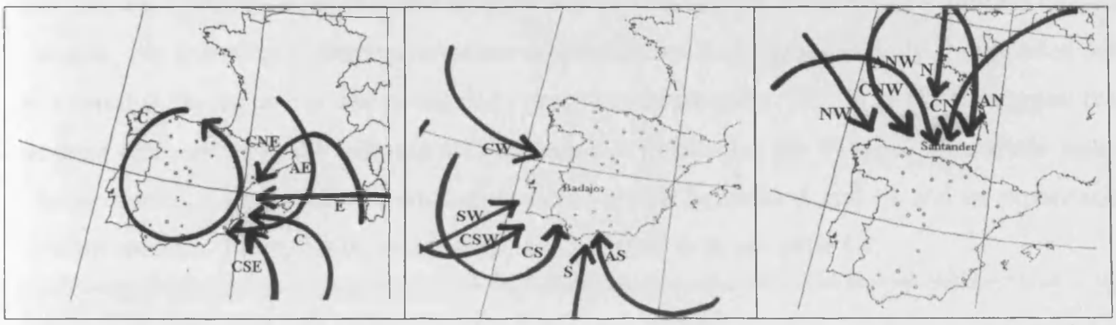

Figure 6.15 Schematic representation of variable airflow contribution to wet days at Badajoz, Murcia and Santander.

6.4 *Modelling daily rainfall amounts using the 500AUT scheme*

The 500AUT model is most discriminatory of rainfall patterns. The performance of this synoptic catalogue can then be tested using calibration and validation method where the relationship between weather type and precipitation can then be defined either deterministically or stochastically (see *table 1.1*).

(a) *Weather Type (WT)* model in which the mean value of daily rainfall is assigned given the prevailing 500AUT weather type.

(b) *Stochastic Weather Type (SWT)* model in which a value is derived stochastically from the rainfall frequency distribution of each weather type.

Both of these approaches can be modified using kinematic information,

(c) *Weather Type (Fronts) (WTF)*.

(d) *Stochastic Weather Type (Fronts) (SWTF)*.

6.4.1 *Model calibration – WT Model*

The catalogue is divided into an approximately equal calibration (8000 days) and validation (6610 days) dataset. The former fixes the mean daily rainfall statistics to be used in the *WT* model. The validation set then takes the mean value of each circulation type and is therefore the rainfall for that day (Yarnal 1993).

6.4.2 *Model calibration – SWT Model*

Rainfall under each type is simulated by randomly drawing from the full frequency distribution of the calibration set using an appropriate model. On each successive daily time step t precipitation amounts are modelled using the product of an exponential random number and a uniform random variable. An exponential distribution alone underestimates the variance in daily precipitation and as a result is inadequate in describing daily precipitation amounts. Hay *et al* (1991) suggest that an error term added to the exponential distribution will increase the variance around the mean. The error term is a product of a uniform random variable between -1 and +1 and an exponential random variable. Precipitation amounts *(P)* are modelled as in *equation 6.4*,

P = (Ii (-lnR)(1-e) (Eqn 6.4)

where *Ii* is the daily amount of precipitation (mm per day) for wet days for the given weather type *I*, *R* is a uniform random variable between 0 and 1, and *e* is the error term, a uniform random variable between -1.0 and +1.0. This could permit the assignment of more realistic 'typical' values of rainfall under each circulation type. The aim is to develop possibilities of the entire theoretical rainfall likelihood rather than rely only on historical occurrences.

6.4.3 *Model calibration - WTF/SWTF Models*

Once the prevailing weather type is identified these models then determine the presence or absence of weather fronts based on frontal probabilities. Frontal information increases the number of 500AUT classes to 20. *Table 6.16* displays the significant variability in frontal probability between classes and also between seasons.

	Probability of frontal incidence Calibration			Probability of front Test		
Weather	All year	Winter	Summer	All year	Winter	Summer

type						
1	0.169	0.186	0.175	0.168	0.203	0.119
2	0.212	0.263	0.247	0.215	0.268	0.160
3	0.514	0.620	0.561	0.475	0.569	0.382
4	0.326	0.377	0.357	0.322	0.367	0.282
5	0.532	0.642	0.587	0.528	0.628	0.435
6	0.435	0.487	0.459	0.541	0.683	0.407
7	0.237	0.272	0.245	0.284	0.316	0.253
8	0.383	0.399	0.392	0.387	0.443	0.333
9	0.183	0.251	0.219	0.206	0.275	0.145
10	0.275	0.366	0.331	0.289	0.342	0.238

Table 6.16 Probability of frontal incidence in calibration and test datasets.

6.5 *Evaluating results - Testing group differences*

Evaluation examines the degree to which weather types are different from one another with respect to their rainfall characteristics. In a series of articles Wilmott (1981 and Wilmott *et al* 1985) appraised several measures of evaluation in order to establish *'...the degree to which model-predicted values approach a linear function of the reliable observations'* (Wilmott *et al* 1985 p8995).

PPM Correlation Coefficient *'r'*, the coefficient of determination r^2, and tests of their significance are commonly used for determining model performance. Nevertheless Wilmott states that these are inadequate and recommends the following set of indices for comparing predicted and observed values, the mean bias error (*MBE*), the mean absolute error (*MAE*), the root mean square error (*RMSE*)[2] and Wilmott's index of agreement (*d*).

MBE is the average of all the residuals and is calculated by *eqn 6.5,*

$$MBE = N^{-1}\sum_{i-1}^{N}(P_i - O_i) \quad \textit{(Equation 6.5)}$$

MAE and *RMSE* estimate the average error (*eqn 6.6 and 6.7*),

$$MAE = N^{-1}\sum_{i=1}^{N}\left|P_i - O_i\right| \quad \textit{(Equation 6.6)}$$

[2] Components of RMSE (systematic and unsystematic RMSE are not calculated here)

and $RMSE = \left[N^{-1}\sum_{i=1}^{N}\left(P_i - O_i\right)^2\right]^{0.5}$ *(Equation 6.7)*

O and P are the observed and model-predicted variables, respectively, and N is the number of observations. The *MAE* is the actual absolute average error and hence yields more information than the *MBE*, while the *RMSE* is a high estimate of the *MAE* although the results are clearly similar.

Wilmott developed a measure (d -the Index of Agreement) that reflects the relative degree to which predicted values approach observed values *(eqn 6.8)*,

$d = 1 - \dfrac{N(RMSE)^2}{PE}$ *(Equation 6.8)*

where the potential error variance is *(eqn 6.9)*,

$PE = \sum_{i=1}^{N}[|P_i| - |O_i|]^2$ *(Equation 6.9)*

Wilmott's d varies between 0.0 and 1.0. 1.0 represents perfect agreement between observed and predicted values and 0.0 expresses perfect disagreement. There is no absolute value that *'d'* must reach in order for the results to be deemed significant. Instead the output is evaluated on subject and contextual knowledge.

In this review, in the interests of brevity, not all model performance statistics are listed for all models. The two main measures *RMSE* (which allows inter-model comparison) and the d statistic (which is unit-free and therefore can allow inter-site comparison also) are listed for all models. *MBE, MAE,* r and r^2 are quoted for the better performing monthly models.

6.6 *Overview of relative performance daily models*

Table 6.17 lists validation statistics for each of the 500AUT models. Model performance varies depending on season, location and which metric is used. *d* statistics are impressively high. A consistent response is difficult to identify but it would seem that,

- Weather type models perform better than stochastic models at marginally more locations.
- Western and northern locations are better estimated than eastern.
- Winter accuracy of the model is higher than that of summer.
- Western locations improve with the addition of frontal information.

	WT	WTf	WTst	WTstf
Badajoz	4.86	**4.21**	4.77	4.23
Burgos	4.01	3.64	3.87	**3.63**
Mahon	**5.28**	6.77	6.98	7.87
Malaga	**9.14**	9.21	10.24	10.54
Murcia	**4.68**	6.39	5.98	6.77
Salamanca	2.98	**2.79**	3.21	3.01
Santander	6.41	6.14	5.14	**4.88**

RMSE statistics winter

	WT	WTf	WTst	WTstf
Badajoz	3.60	3.12	3.51	**3.04**
Burgos	3.24	**2.97**	3.10	3.04
Mahon	**4.53**	4.77	4.88	5.00
Malaga	**2.85**	3.11	2.98	3.15
Murcia	4.57	**3.13**	4.87	3.25
Salamanca	3.30	**3.13**	3.22	3.16
Santander	5.13	6.52	**5.01**	6.31

RMSE statistics summer

	WT	WTf	WTst	WTstf
Badajoz	0.89	**0.92**	0.90	0.91
Burgos	0.79	0.83	0.85	**0.89**
Mahon	0.72	0.68	0.76	**0.77**
Malaga	0.79	**0.83**	0.64	0.71
Murcia	**0.78**	0.68	0.71	0.69
Salamanca	0.91	**0.93**	0.88	0.85
Santander	0.84	0.88	0.85	**0.89**

d statistics winter

	WT	WTf	WTst	WTstf
Badajoz	0.85	**0.87**	0.83	0.85
Burgos	0.79	0.81	0.82	**0.86**
Mahon	0.58	0.61	0.73	**0.74**
Malaga	0.63	0.71	0.70	**0.76**
Murcia	**0.69**	0.61	0.63	0.65
Salamanca	0.81	**0.86**	0.81	0.79
Santander	0.83	0.79	**0.89**	0.88

d statistics summer

Table 6.17 Model performance statistics for 500AUT.

6.7 *Examining the performance of monthly class-based synoptic methods (500AUTM)*

6.7.1 RPI values

RPI values for classes under the 500AUTM classification are listed in *table 6.18* and descriptive statistics in *table 6.19*. Variation in RPI values is considerably less than for 500AUT (COV – 4%-16%) reflecting the reduction in temporal resolution. ANOVA (*table 6.20*) gives mixed results. Performance is good for central sites but poorer in the eastern sites.

	1	2	3	4	5	6	7	8
1	0.83	0.95	1.01	0.90	1.12	1.09	0.98	1.42
2	0.90	0.94	1.12	1.03	1.23	0.90	0.91	1.56
3	0.82	0.97	1.14	1.01	1.22	0.96	0.94	1.10
4	0.74	0.97	1.07	1.00	1.17	1.14	0.86	1.31
5	0.76	1.00	0.99	0.86	1.17	1.17	0.84	1.56
6	0.76	1.03	1.03	1.00	1.16	1.05	0.79	1.36
7	0.75	1.04	1.09	0.90	1.18	1.09	0.80	1.32
8	1.03	0.94	1.08	1.01	1.23	0.83	0.91	1.28
9	0.71	0.96	0.98	0.85	1.26	1.19	0.69	1.86
10	0.79	0.91	1.06	0.88	1.17	1.09	0.69	1.84
11	0.91	0.95	1.00	1.05	1.03	1.10	0.82	1.31

Table 6.18 RPI values of weather types under 500AUTM.

	1	2	3	4	5	6	7	8
Maximum	1.03	1.04	1.14	1.05	1.26	1.19	0.98	1.86
Minimum	0.71	0.91	0.98	0.85	1.03	0.83	0.69	1.10
Sdev	0.09	0.04	0.05	0.08	0.06	0.11	0.09	0.24
COV	12	4	5	8	5	11	11	16

Table 6.19 Descriptive statistics of RPI values under 500AUTM.

	F	P
1	2.36	0.023
2	2.55	0.014
3	2.80	0.007
4	2.56	0.013
5	3.30	0.002
6	2.79	0.007
7	2.03	0.050
8	0.78	0.602
9	5.12	0.000
10	4.63	0.000
11	0.79	0.599

Table 6.20 ANOVA of mean rainfall of 500AUTM weather types recorded at gridpoint locations.

Fisher's LSD test (*figure 6.16*) depicts the poor discrimination between classes when compared to the daily model (*figure 6.7*). Two eastern gridpoints, 8 and 11, show no significant differences at all.

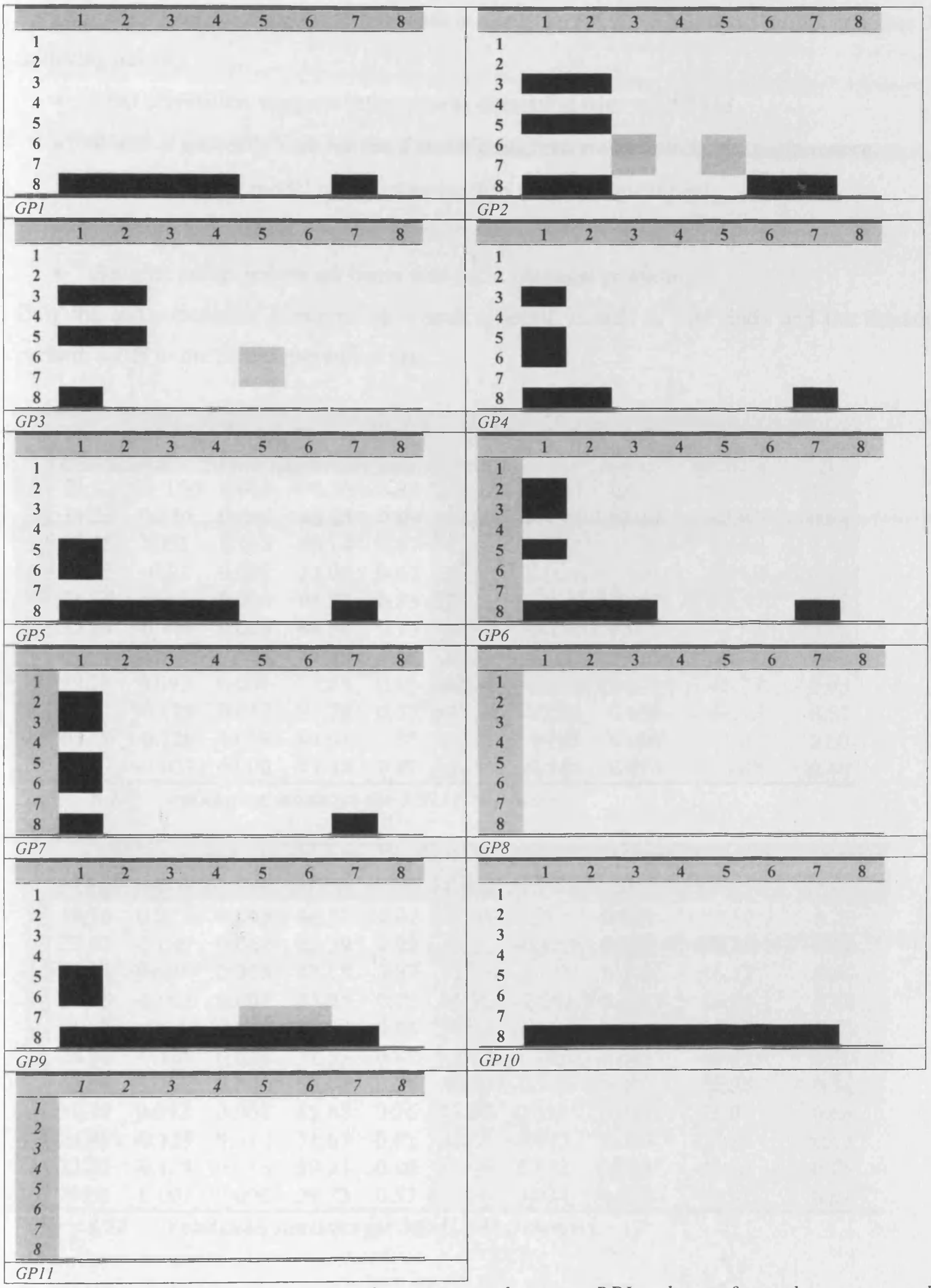

Figure 6.16 Fisher's Pairwise Comparisons between RPI values of weather types under 500AUTM.

Validation statistics for 500AUTM are listed in *tables 6.21-6.22.* Scrutiny of results indicates the following points,

- PPM correlation suggests little value to estimating with 500AUTM.
- *RMSE* is generally high but the *d* statistic suggests reasonable model performance.
- The mean value model performs better than the stochastic model.
- Northern and western sites are more closely related to this scheme than eastern sites.
- Summer model results are better than those obtained in winter.

Only the last conclusion is surprising - most synoptic models in this study and the literature perform better in the cooler part of the year.

	Mean					Stochastic				
	MAE	*r*	r^2	*RMSE*	*d*	*MAE*	*r*	r^2	*RMSE*	*d*
1	74.37	-0. 150	0.049	99.23	0.83	138.15	-0.043	0.002	107.99	0.69
2	34.28	0.150	0.064	46.55	0.89	56.86	0.119	0.014	42.07	0.84
3	29.55	0.03	0.058	40.14	0.87	46.37	0.003	0.000	36.90	0.79
4	52.45	-0.02	0.002	73.03	0.67	76.91	0.064	0.004	56.68	0.63
5	71.34	-0.11	0.020	95.53	0.73	121.95	0.019	0.000	96.54	0.57
6	35.69	-0.168	0.028	46.58	0.73	53.88	-0.139	0.019	42.84	0.66
7	62.11	0.062	0.004	73.29	0.48	74.02	-0.242	0.059	62.68	0.47
8	59.24	0.092	0.008	77.85	0.65	83.98	-0.129	0.017	63.77	0.63
9	73.37	-0.129	0.017	97.78	0.57	105.20	-0.016	0.000	84.15	0.52
10	65.49	-0.128	0.016	83.95	0.57	85.52	-0.005	0.000	65.61	0.60
11	33.67	-0.001	0.000	43.44	0.47	46.09	-0.264	0.070	35.62	0.40

Table 6.21 Validation statistics for 500AUTM (winter).

	Mean					Stochastic				
	MAE	*r*	r^2	*RMSE*	*d*	*MAE*	*r*	r^2	*RMSE*	*d*
1	39.10	0.277	0.049	46.77	0.92	73.98	0.253	0.064	91.57	0.79
2	27.02	0.180	0.064	36.39	0.92	40.31	-0.170	0.029	50.78	0.86
3	35.13	0.005	0.058	42.18	0.87	37.78	0.007	0.000	46.52	0.85
4	38.48	-0.008	0.002	53.05	0.75	41.95	-0.044	0.002	56.31	0.74
5	31.73	-0.11	0.020	38.30	0.88	58.01	-0.173	0.030	79.07	0.55
6	24.36	-0.168	0.028	31.53	0.83	32.63	-0.025	0.001	41.45	0.70
7	45.96	0.062	0.004	55.59	0.57	44.98	-0.012	0.000	55.55	0.58
8	31.79	0.092	0.008	45.85	0.76	43.04	0.134	0.018	56.06	0.66
9	24.98	-0.129	0.017	31.65	0.81	33.69	0.063	0.004	43.83	0.68
10	22.70	-0.128	0.016	30.33	0.80	34.49	0.152	0.023	40.10	0.75
11	20.68	-0.001	0.000	29.72	0.57	21.88	0.094	0.009	30.51	0.61

Table 6.22 Validation statistics for 500AUTM (summer).

6.8 Examining the performance of monthly index-based synoptic methods using correlation and regression techniques

6.8.1 North Atlantic Oscillation Index

PPM correlation coefficients between the monthly NAOI and grid point rainfall amounts are listed in *table 6.23.* Almost everywhere highly significant negative relationships are recorded and the association is strongest in central and southern meseta regions (3, 5, 6, 9 and 10). Two eastern areas (8, 11) show a positive association in the summer months. Overall the association is strongest in winter months.

	1	2	3	4	5	6	7	8	9	10	11
Year	**-0.257**	**-0.335**	**-0.399**	**-0.309**	**-0.356**	**-0.490**	**-0.300**	**-0.187**	**-0.393**	**-0.426**	**-0.251**
Summer	**-0.203**	**-0.245**	**-0.298**	**-0.258**	**-0.220**	**-0.312**	**-0.252**	**0.191**	**-0.242**	**-0.230**	**0.245**
Winter	**-0.391**	**-0.445**	**-0.482**	**-0.368**	**-0.611**	**-0.648**	**-0.355**	**-0.255**	**-0.611**	**-0.648**	**-0.301**

*Table 6.23 PPM correlation coefficient between the NAOI and grid point rainfall amounts (**bold** figures represent significant at $p<0.050$).*

6.8.1 Zonal Index

Table 6.24 indicates significant (at $p<0.050$) PPM correlation coefficients. A pattern emerges whereby there is a shift in correlation between west and east and north-west and south. The strongest ZI control can be seen in winter however summer association is related to the three western grid points (1, 5 and 9). This association is stronger than that for the NAOI. Some eastern grid points (7, 8, 11) are not significantly correlated to rainfall amounts in any season.

	1	2	3	4	5	6	7	8	9	10	11
Year	**-0.197**	**-0.220**	**-0.289**	-0.087	**-0.246**	**-0.339**	-0.025	-0.031	**-0.190**	**-0.238**	-0.039
Summer	**-0.405**	**-0.286**	**-0.257**	-0.110	**-0.460**	**-0.366**	-0.045	0.113	**-0.407**	**-0.329**	**0.173**
Winter	**-0.377**	**-0.326**	**-0.330**	-0.157	**-0.436**	**-0.460**	-0.087	-0.069	**-0.399**	**-0.470**	-0.095

*Table 6.24 PPM correlation coefficients of association between ZI and annual and seasonal gridpoint rainfall amounts (**bold** figures represent significant at $p<0.050$).*

6.8.3 Evaluating NAOI and ZI

Model performance statistics for the NAOI and ZI models are given in *tables 6.25 - 6.26.* According to r^2 values NAOI is better than the ZI yet *d* statistics give contrary results.

	NAO					ZI				
	MAE	*r*	r^2	*RMSE*	*d*	*MAE*	*r*	r^2	*RMSE*	*d*
1	86.80	0.460	0.212	93.67	0.83	82.55	0.401	0.161	90.22	0.83
2	27.28	0.491	0.241	34.74	0.95	27.81	0.371	0.138	36.07	0.94
3	34.87	0.428	0.183	42.57	0.89	36.70	0.335	0.112	45.02	0.88
4	39.83	0.206	0.042	58.50	0.80	42.13	0.062	0.004	61.22	0.77
5	60.27	0.560	0.314	67.51	0.84	54.97	0.431	0.186	61.19	0.85
6	19.81	0.605	0.366	25.50	0.94	22.30	0.430	0.185	27.91	0.91
7	52.39	0.092	0.008	62.46	0.62	54.05	-0.061	0.004	64.47	0.57
8	29.70	0.010	0.000	40.36	0.89	29.61	0.000	0.000	42.01	0.87
9	46.48	0.554	0.307	52.55	0.80	41.18	0.369	0.136	45.92	0.82
10	36.69	0.615	0.378	43.57	0.85	36.98	0.451	0.203	40.11	0.85
11	73.52	-0.057	0.003	93.89	0.17	19.99	-0.043	0.002	28.51	0.74

Table 6.25 Validation statistics for NAO and ZI (winter).

	NAO					ZI				
	MAE	*r*	r^2	*RMSE*	*d*	*MAE*	*r*	r^2	*RMSE*	*d*
1	61.38	0.243	0.059	72.86	0.94	58.73	0.082	0.007	72.38	0.94
2	25.80	0.278	0.077	34.60	0.95	27.66	0.135	0.018	37.99	0.94
3	26.01	0.385	0.148	35.96	0.91	28.99	0.096	0.009	39.33	0.88
4	49.35	0.265	0.070	71.73	0.75	53.42	-0.027	0.001	75.74	0.70
5	42.55	0.408	0.166	54.08	0.95	47.11	0.289	0.084	61.63	0.92
6	20.48	0.454	0.206	27.09	0.94	26.08	0.291	0.085	34.58	0.88
7	63.56	0.262	0.069	74.09	0.57	66.33	-0.134	0.018	76.67	0.51
8	47.53	0.180	0.032	68.59	0.81	51.82	0.003	0.000	71.84	0.78
9	43.67	0.356	0.127	58.28	0.91	51.63	0.293	0.086	70.24	0.84
10	32.31	0.360	0.130	45.40	0.93	40.87	0.202	0.041	56.74	0.86
11	88.93	-0.316	0.100	106.19	0.25	31.39	0.128	0.016	41.82	0.63

Table 6.26 Validation statistics for NAO and ZI (summer).

6.9 Air Flow Indices

6.9.1 SLPIND

PPM correlation coefficients between the monthly surface airflow indices and gridpoint rainfall are listed in *table 6.27.* The following points can be made with respect to the association with monthly rainfall,

- Pressure (*P*) association is strongly significant (at $p<0.050$) in all areas (negative).
- Vorticity (*Z*) association is significant (at $p<0.050$) in all areas (positive).
- *W* association decreases in an easterly direction.
- *S* association decreases from southwest to northeast.
- The strength of flow (*F*) increases rainfall amounts except in Mediterranean locations.

	P	W	S	ZW	ZS	Z	F
1	**-0.684**	**0.797**	**0.187**	**0.263**	-0.071	**0.211**	**0.605**
2	**-0.650**	**0.564**	**-0.198**	**0.347**	0.117	**0.359**	**0.549**
3	**-0.647**	**0.464**	-0.032	**0.372**	**0.190**	**0.409**	**0.435**
4	**-0.482**	**0.173**	0.083	**0.415**	**0.289**	**0.486**	0.086
5	**-0.745**	**0.655**	**0.352**	**0.411**	-0.128	**0.325**	**0.514**
6	**-0.765**	**0.524**	**0.289**	**0.529**	0.015	**0.488**	**0.425**
7	**-0.285**	-0.079	0.096	**0.371**	**0.207**	**0.413**	-0.070
8	**-0.240**	0.048	**-0.239**	**0.272**	0.074	**0.275**	0.160
9	**-0.716**	**0.448**	**0.457**	**0.499**	-0.144	**0.402**	**0.400**
10	**-0.699**	**0.388**	**0.353**	**0.553**	-0.082	**0.476**	**0.392**
11	**-0.223**	-0.105	0.111	**0.311**	0.124	**0.327**	-0.012

*Table 6.27 PPM Correlation Coefficients between SLPIND and gridpoint rainfall amounts (mm) – all data. Figures in **bold** indicate significant correlation at p<0.050.*

6.9.2 500IND

PPM correlation coefficients between the 500hPa indices and gridpoint rainfall are listed in *table 6.28*. The following points can be made with respect to association with monthly rainfall,

- Pressure (*500P*) association is significant (at $p<0.050$) in western and central areas (negative) but not in Mediterranean locations. *500P* is not as closely related as *P* to rainfall.
- Vorticity (*500Z*) association is significant (at $p<0.050$) in all areas (positive). The association is strongest towards the eastern part of the peninsula and stronger than surface *Z*.
- *500W* association decreases in an easterly direction and this is similar to surface *W*.
- *500S* association decreases from southwest to northeast.
- The strength of flow (*500F*) increases rainfall amounts except in Mediterranean locations. In fact a significant negative relationship (emphasizing eastern flow strength) is found at gridpoint 11. Generally *500F* is not as influential as *F*.
- *500ZS* is considerably more important than *S*.

	5P	5W	5S	5F	5ZW	5ZS	5Z
1	**-0.445**	**0.775**	**0.215**	**0.511**	**0.246**	**0.233**	**0.316**
2	**-0.449**	**0.596**	0.137	**0.622**	**0.270**	**0.552**	**0.469**
3	**-0.395**	**0.480**	**0.273**	**0.440**	**0.315**	**0.532**	**0.494**
4	**-0.200**	0.140	**0.215**	0.091	**0.418**	**0.542**	**0.584**
5	**-0.448**	**0.674**	**0.300**	**0.380**	**0.429**	**0.189**	**0.449**
6	**-0.429**	**0.561**	**0.350**	**0.286**	**0.498**	**0.326**	**0.563**
7	-0.013	-0.077	**0.274**	-0.135	**0.330**	**0.477**	**0.478**
8	-0.100	0.036	-0.120	**0.205**	**0.297**	**0.455**	**0.443**
9	**-0.447**	**0.472**	**0.369**	**0.210**	**0.532**	0.087	**0.488**
10	**-0.465**	**0.427**	**0.269**	**0.238**	**0.551**	0.159	**0.535**
11	0.027	-0.099	0.160	**-0.173**	**0.268**	**0.407**	**0.402**

Table 6.28 PPM Correlation Coefficients between 500IND and gridpoint rainfall amounts (mm) – all data. Figures in ***bold*** *indicate significant correlation at $p<0.050$.*

6.9.3 Validation of index models

Stepwise regression is employed to determine significant independent variables for the estimation of rainfall at each gridpoint.

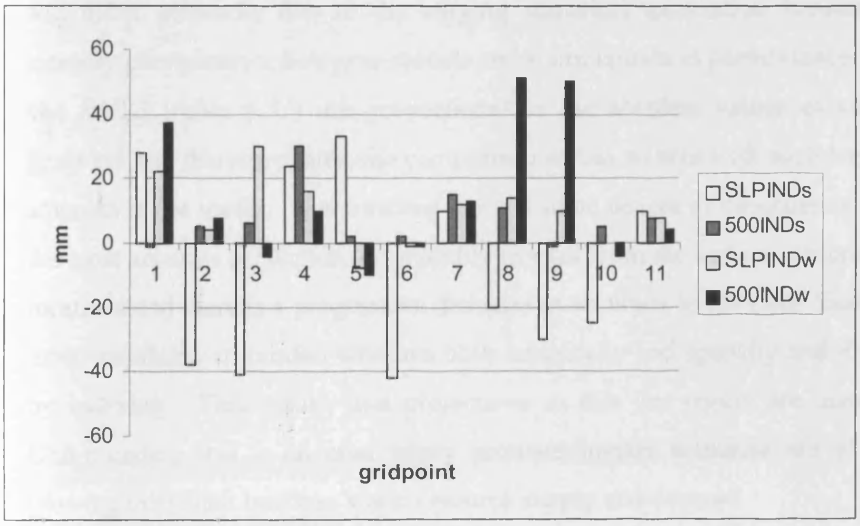

Figure 6.17 MBE of SLPIND and 500IND. s – summer; w – winter.

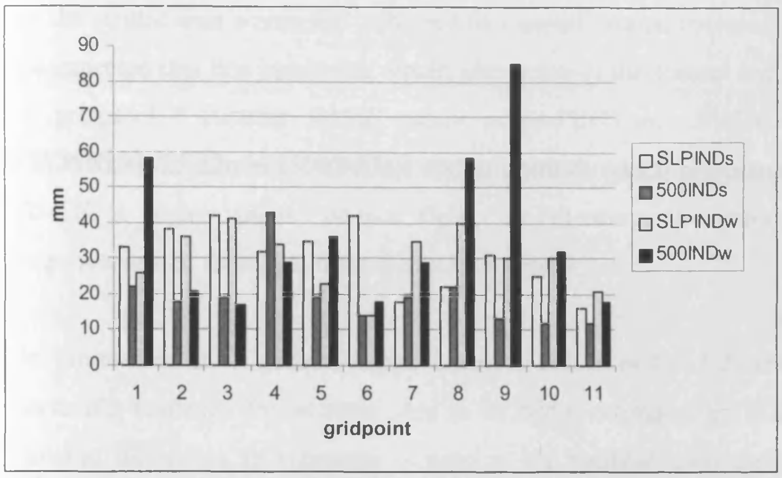

Figure 6.18 *MAE of SLPIND and 500IND. s – summer; w – winter.*

Figure 6.17 shows the *MBE* of models at each location. The SLPINDs model repeatedly underestimates the precipitation amounts, more so than any other model (these are more likely to overestimate totals). The ability of models to capture the variance of rainfall at each gridpoint will differ markedly due to the varying statistical association between air flow indices and monthly precipitation, however models show similarities in performance. Both *MAE* (*figure 6.18)* and *RMSE* (*table 6.31*) are proportional to the absolute values of observed rainfall at each gridpoint and therefore inter-site comparison across an area with such large differences in rainfall amounts is not useful. Nevertheless there is some degree of consistency with models. In general the most accurate predictions of monthly rainfall from the airflow indices are achieved in western locations and there is a progressive decrease in accuracy to the east. Eastern locations display far more variability in rainfall amounts both temporally and spatially and this is less easy to capture by indexing. This means that projections in this dry region are made with less confidence. Unfortunately this is an area where accurate impact scenarios are of most value due to the growing mismatch between water resource supply and demand.

Seasonal contrasts in model performance are as expected. Overall winter rainfall amounts display a marginally better relationship to index values at each level. An examination of the spatial variation of error measures shows that better estimates in the east of the peninsula are provided by winter models yet the reverse is demonstrated at western sites.

Generally in summer there is an improvement in estimates from the application of the upper air series. If gridpoint 4 is omitted (here the use of upper air flow leads to a decrease in accuracy) the mean difference in *RMSE* is 15.40mm with a range between 1.14mm and 31.28mm. The greater importance of surface air circulation at grid point 4 is explained by the fact that this is peripheral to the central area where the influence of thermal related cyclonicity is most important. It could be expected that this behaviour would also occur at the coastal and island points 7 and 8. Indeed at gridpoint 7 summer *RMSE* values of SLPIND and 500IND are very similar (26.36mm (SLPINDs), 25.22mm (500INDs)) and at point 8, which represents the Balearics area, although *RMSE* is higher under surface flow, the measure of agreement *d* indicates a marginal improvement in estimates from the surface model.

In winter there is no general improvement in *RMSE* or the *d* statistics provided by 500IND. Yet there is a tendency for western sites to be better estimated by SLPIND than eastern sites. The greatest difference in estimates is seen at the furthest south-east gridpoint 9 at which *RMSE* values are 40.26mm (SLPINDw) and 104.96mm (500INDw) and this discrepancy is further illustrated by the large difference in *d*.

	SLPIND						500IND				
	MAE	*RMSE*	*r*	r^2	*d*		*MAE*	*RMSE*	*r*	r^2	*d*
1	33.4	39.9	0.79	0.62	0.80	1	22.8	32.1	0.75	0.56	0.88
2	38.6	46.4	0.47	0.22	0.61	2	17.2	21.9	0.68	0.46	0.82
3	42.9	49.3	0.43	0.19	0.56	3	17.8	22.2	0.59	0.35	0.76
4	33.9	40.7	0.24	0.06	0.47	4	42.7	43.0	0.18	0.03	0.44
5	35.6	40.8	0.79	0.63	0.73	5	18.9	26.8	0.74	0.55	0.88
6	42.4	47.6	0.49	0.24	0.52	6	12.8	16.3	0.73	0.54	0.86
7	17.9	26.4	0.28	0.08	0.48	7	19.2	25.2	0.53	0.28	0.68
8	23.4	34.0	0.09	0.01	0.68	8	23.5	27.3	0.43	0.19	0.61
9	30.8	36.5	0.69	0.47	0.67	9	12.0	17.1	0.78	0.61	0.90
10	25.7	32.2	0.57	0.33	0.69	10	11.4	14.7	0.79	0.63	0.89
11	15.5	20.1	0.26	0.07	0.56	11	11.1	15.3	0.59	0.35	0.74

Table 6.29 Model performance statistics (summer)

	SLPIND						500IND				
	MAE	*RMSE*	*r*	r^2	*d*		*MAE*	*RMSE*	*r*	r^2	*d*
1	35.3	43.3	0.89	0.79	0.24	1	58.7	69.9	0.71	0.36	0.81
2	34.0	43.5	0.12	0.02	0.54	2	20.8	26.9	0.73	0.55	0.85
3	37.7	43.1	0.26	0.08	0.51	3	16.4	22.9	0.69	0.57	0.82
4	33.2	40.5	0.49	0.24	0.69	4	28.8	35.5	0.60	0.31	0.75
5	26.9	37.1	0.87	0.75	0.38	5	35.5	50.4	0.74	0.30	0.80
6	15.2	19.6	0.82	0.68	0.03	6	17.5	22.8	0.75	0.66	0.88
7	32.9	41.6	0.37	0.14	0.67	7	28.5	35.5	0.56	0.59	0.73
8	36.2	46.4	0.35	0.12	0.64	8	57.8	64.9	0.55	0.11	0.57
9	32.1	40.3	0.81	0.50	0.87	9	84.5	105	0.00	0.00	0.46
10	29.0	38.3	0.77	0.53	0.85	10	31.7	44.0	0.66	0.44	0.84
11	19.7	25.0	0.34	0.47	0.64	11	17.3	22.4	0.47	0.22	0.65

Table 6.30 Model performance statistics (winter).

6.10 Comment

In this chapter the evaluation of a range of synoptic model performance is undertaken by split-sampling procedures and the application of validation statistics. Evaluation of such a large number of models is uncommon in the literature and has not been undertaken for the Iberian peninsula region. Comments are divided on the basis of temporal framework.

6.10.1 Daily model summary

Scrutiny of validation statistics (*table 6.17*) indicates that daily model performance varies between weather type - no scheme consistently improves performance for all sites yet some patterns do emerge,

- Stochastic modelling performs poorer for drier sites (Mahon, Murcia), reflecting the limits of the data distributions upon which to calibrate the models.
- Stochastic modelling performs marginally better in summer than in winter, although this outcome requires further corroboration.
- Frontal models perform well at wetter western locations (Badajoz, Salamanca and Burgos), but are less useful at Mediterranean sites. This is a consequence of the frontal catalogue method as a significant number of fronts do not reach the Mediterranean or, when they do, rainfall is considerably reduced after passage across the peninsula.

The performance of the 500AUT therefore depends entirely on the season and location under consideration. Consequently this synoptic technique should not be employed on a peninsula-wide basis but should be modified to fit whichever subregion is being considered (for instance, WTf is optimum for the west). This study shows that the incorporation of both frontal information and stochastic models are useful depending on location because there are differences in process (*i.e.* the relative importance of frontal rainfall as opposed to other sources) and differences in rainfall distributions.

6.10.2 Monthly model summary

Table 6.31 lists model performance statistics for all the monthly models – the two best performing models for each gridpoint are highlighted. Again the better performing model depends on which sub-region of the study area is considered and what time of year. Validation statistics give contrasting results - although the NAOI and ZI consistently display the highest the *d* statistics, *RMSE* errors are generally less for the more complex index measures. The latter are suitable metrics of comparison given that the same calibration and test data is used for each model.

Results can be summarized as follows,

- PPM correlation coefficients indicate a stronger relationship between the simple NAOI and Spanish rainfall rather then the more complex ZI (the latter is not significantly associated with many eastern regions.
- Correlation also indicates a stronger control in winter than summer by these large-scale indices.
- With respect to validation statistics in virtually all instances the class-based 500AUTM and 500AUTMR perform poorly.
- The *d* statistic suggests that NAOI and ZI are the better models but this is not agreed by RMSE values.
- On the basis of RMSE the best models are the IND models.
- In winter 500IND is marginally better than SLPIND in eastern locations suggesting that in winter mid-tropospheric flow patterns are suited to modelling in eastern areas and surface flow in western areas.
- ZI performs better for south-eastern sites.
- With respect to RMSE in summer 500IND is consistently the best performer at all sites and other models are also useful but not consistently so. SLPIND also performs well in the east.

Overall *RMSE* results indicate that index models are most suited to the modelling of rainfall however *d* statistics indicate that large-scale catalogues perform well particularly at western sites. Some cautionary notes are proposed. A major limitation of this type of analysis is the lack of sufficient data to both calibrate and test models. This is less of a problem for daily models given the increased number of events. In this study the calibration problems are exacerbated when monthly models are subdivided by season.

Synoptic modelling of rainfall over the Iberian peninsula using these methods yields results that can adequately utilized for downscaling purposes. Evaluation suggests that the synoptic mechanism-precipitation association varies across the peninsula and between summer and winter seasons. Consequently models are both spatially and temporally specific. Results are good but are likely to be improved with increasing periods on which to calibrate the models.

	500AUTM	500AUTMR	NAO	ZI	SLPIND	500IND
1	**0.83**	0.69	**0.83**	**0.94**	0.24	0.81
2	0.89	0.84	**0.95**	**0.94**	0.54	0.85
3	0.87	0.79	**0.89**	**0.88**	0.51	0.82
4	0.67	0.63	**0.80**	0.70	0.69	**0.75**
5	0.73	0.57	**0.84**	**0.92**	0.38	0.80
6	0.73	0.66	**0.94**	**0.88**	0.03	**0.88**
7	0.48	0.47	0.62	0.51	**0.67**	**0.73**
8	0.65	0.63	**0.89**	**0.78**	0.64	0.57
9	0.57	0.52	0.80	**0.84**	**0.87**	0.46
10	0.57	0.60	**0.85**	**0.86**	**0.85**	0.84
11	0.47	0.40	0.17	0.63	**0.64**	**0.65**

Table 6.31 Comparison of d statistic (winter).

	500AUTM	500AUTMR	NAO	ZI	SLPIND	500IND
1	99.23	107.99	93.67	90.22	**43.3**	**69.9**
2	46.55	42.07	**34.74**	36.07	43.5	**26.9**
3	40.14	36.90	**42.57**	45.02	43.1	**22.9**
4	73.03	56.68	58.50	61.22	**40.5**	**35.5**
5	95.53	96.54	67.51	61.19	**37.1**	**50.4**
6	46.58	42.84	25.50	27.91	**19.6**	**22.8**
7	73.29	62.68	62.46	64.47	**41.6**	**35.5**
8	77.85	63.77	**40.36**	**42.01**	46.4	64.9
9	97.78	84.15	52.55	**45.92**	**40.3**	105
10	83.95	65.61	43.57	**40.11**	**38.3**	44.0
11	43.44	35.62	93.89	28.51	**25.0**	**22.4**

Table 6.32 Comparison of RMSE (winter).

	500AUTM	500AUTMR	NAO	ZI	SLPIND	500IND
1	0.92	0.79	**0.94**	**0.94**	0.80	0.88
2	0.92	0.86	**0.95**	**0.94**	0.61	0.82
3	0.87	0.85	**0.91**	**0.88**	0.56	0.76
4	**0.75**	0.74	0.75	0.70	0.47	0.44
5	0.88	0.55	**0.95**	**0.92**	0.73	0.88
6	0.83	0.70	**0.94**	**0.88**	0.52	0.86
7	0.57	0.58	0.57	0.51	0.48	**0.68**
8	0.76	0.66	**0.81**	**0.78**	0.68	0.61
9	0.81	0.68	**0.91**	0.84	0.67	**0.90**
10	0.80	0.75	**0.93**	0.86	0.69	**0.89**
11	0.57	0.61	0.25	**0.63**	0.56	**0.74**

Table 6.33 Comparison of d statistic (summer).

	500AUTM	500AUTMR	NAO	ZI	SLPIND	500IND
1	46.77	91.57	72.86	72.38	**39.9**	**32.1**
2	36.39	50.78	**34.60**	37.99	46.4	**21.9**
3	42.18	46.52	**35.96**	39.33	49.3	**22.2**
4	53.05	56.31	71.73	75.74	**40.7**	**43.0**
5	38.30	79.07	54.08	61.63	**40.8**	**26.8**
6	31.53	41.45	**27.09**	34.58	47.6	**16.3**
7	55.59	55.55	74.09	76.67	**26.4**	**25.2**
8	45.85	56.06	68.59	71.84	**34.0**	**27.3**
9	**31.65**	43.83	58.28	70.24	36.5	**17.1**
10	**30.33**	40.10	45.40	56.74	32.2	**14.7**
11	29.72	30.51	106.19	41.82	**20.1**	**15.3**

Table 6.34 Comparison of RMSE (summer).

Chapter Seven
Downscaling from empirical models

7.1 Introduction

In this chapter selected synoptic methods are described as part of an empirical downscaling approach (*figure 7.1*).

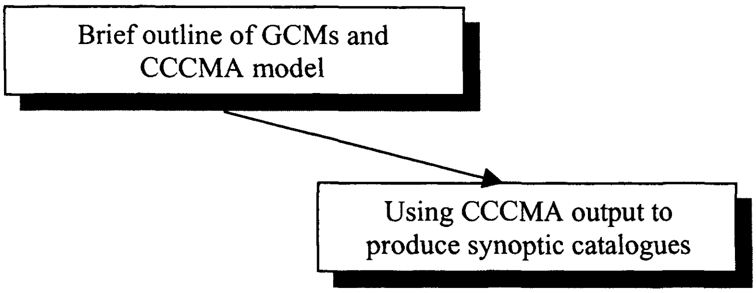

Figure 7.1 Outline of Chapter 7 .

7.2 Empirical Downscaling

Downscaling aims to identify consistent circulation-environment relationships that can then be used to model precipitation under a perturbed climate. Models are only valid for a certain range of possible climates. If the climate is too different from the current regime (*e.g.* the Ice Age) the models are not applicable (Dehn *et al* 2000).

The success of downscaling depends on,

- The existence of homogeneity in precipitation-circulation response (stationarity).
- Sufficient and accurate calibration data for synoptic models.
- Realistic GCM output.

7.3 GCM Output

GCMs simulate the climate system using mathematical equations that describe the Earth's radiation budget, its translation into heat and motion, and the operation of the water cycle. GCMs integrate the main climatic processes and calculate the adjustments and readjustments of system elements (the atmosphere, the lithosphere, the cryosphere and the hydrosphere) as they respond to an initial perturbance. The ability to model 'transient change' that is, the behaviour of the climate system while it is changing rather than after it has changed, is very important. Transient change modelling provides a more realistic approximation of the variability of the climate system.

Coupled atmospheric-ocean general circulation models (AOGCMs) are atmospheric GCMs that are fully integrated with models of the ocean processes. In 2002 there were more than 20 of these models in use or under development around the world.

7.3.1 Global rainfall prediction from CCCMA

With respect to global rainfall changes the CGCM1 experiments project an increase of about 1% by 2050 for the GHG+A (greenhouse gases and aerosols) runs and more than 2% for the GHG only scenario (CCCMA 2002). By 2100 these estimates rise to 4.5% and 7% respectively *(figure 7.2)*. Increases occur primarily over the oceans (where surface moisture is readily available) and over land masses in the higher latitudes of the Northern Hemisphere. Elsewhere, average precipitation over land changes little or decreases. Increased temperature and evaporation will lead to almost all land areas experiencing a decrease in average soil moisture, particularly in summer. The type of precipitation over the Northern Hemisphere also changes as the climate warms, becoming significantly more intense.

While global averages and patterns give an indication of the expected magnitude and general characteristics of climate change, impacts of climate change will be experienced at the local and regional levels. Regional changes, though, could be quite different from the global averages but are generally less reliable and should be treated with greater caution. Model intercomparisons are especially important at this level as a way of estimating the degree of uncertainty in the results. CGCM1 projects that Southern Europe could experience precipitation decreases in excess of 30%. Projected changes over the mid to high latitudes of the Northern Hemisphere are more moderate, in general remaining within 10% of present levels until after 2050. Most of the increases occur during winter. Such trends are consistent with both an increased flow of moisture northward from the tropics and a transition to a more maritime climate as sea ice cover over water bodies decreases.

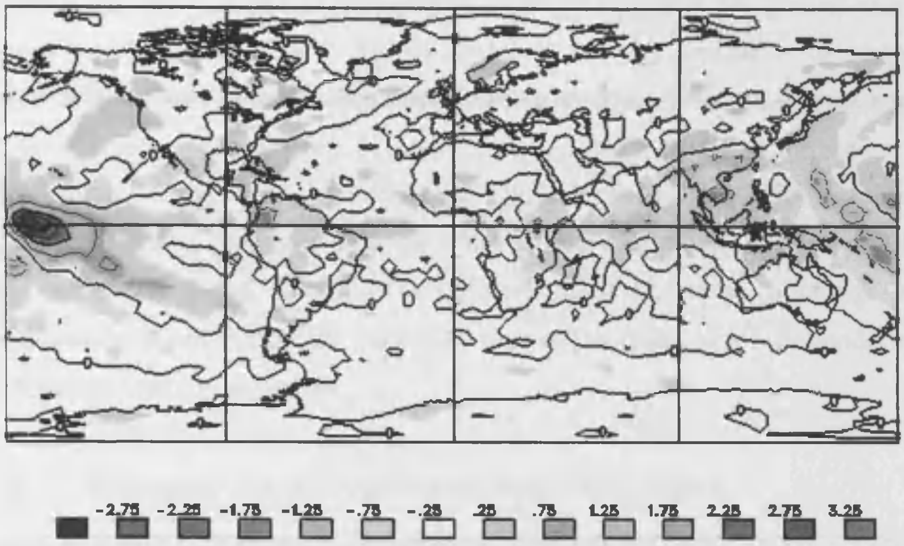

a.CGCM2 GHGA Precipitation (mm/day) difference between 2040-2060 and 1975-1995

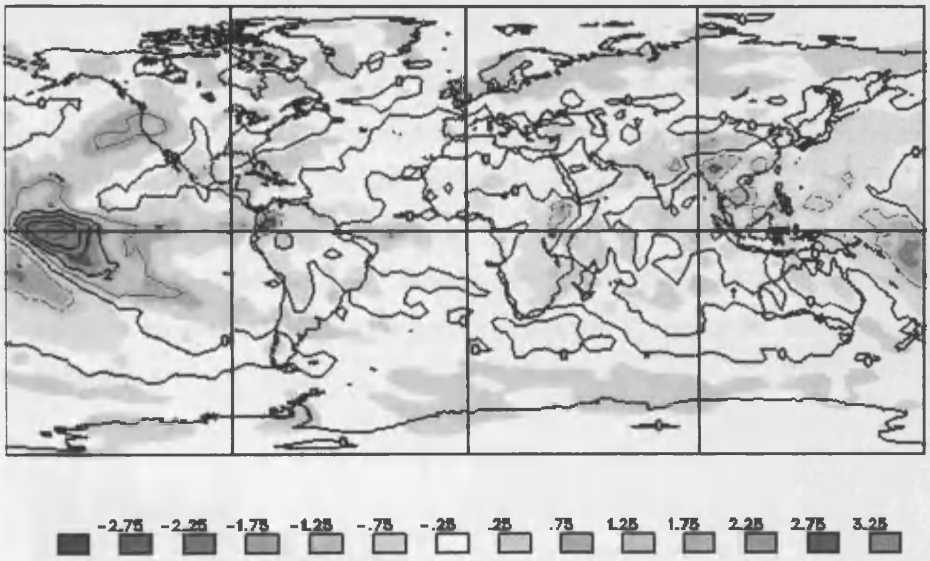

b.CGCM2 GHGA Precipitation (mm/day) difference between 2080-2100 and 1975-1995

Figure 7.2 Global precipitation scenario output from CCCMA (CCCMA 2003).

As CGCM1 and CGCM2 experiments successfully reproduce the general characteristics of the global climate since 1900 it can be assumed that the simulation of climatic processes is reasonably accurate. Future projections however are approximations and not a precise forecast of future conditions. The accuracy of the projections depend, in part, on the accuracy of assumptions about future changes in greenhouse gases and aerosols as well as the precision with which it simulates climatic processes such as water vapour and cloud response or changes in ocean circulation. If concentrations of greenhouse gases and aerosols change at rates that are significantly different from the estimates used in the model, then the model's projections will become increasingly unrealistic.

7.4 *Developing synoptic catalogues from GCM output*

Monthly MSLP and 500hPa contour height sets (2001-2100) were obtained from the CGCM2 model for relevant grid points.

7.4.1 *Future NAOI (NAOIFUT)*

GCM output was used to project a NAOI time series (NAOIFUT). The depiction of the time series (*figure 7.3*) reveals an abrupt decrease in the NAOI when the historical time series is replaced by modelled data. Scrutiny of historical gridpoint data reveals that the CCCMA output underestimates MSLP values to the west of the Iberian peninsula, or, more accurately the gridpoint used to calculate the 'Azores' value of the NAOI. The inaccuracy of the modelled output limits the success of any downscaling exercise. Comment on this exercise are made in the final chapter.

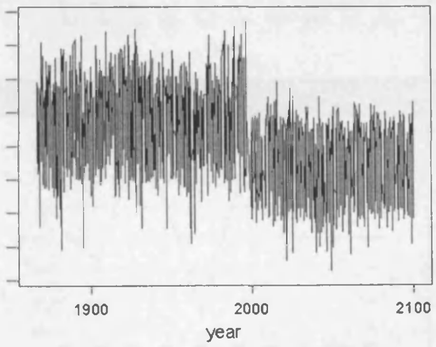

Figure 7.3 Time series plot of the NAOI using data standardized against the period 1860-2100. The shift around the year 2000 indicates the change from observed to modelled data.

7.4.2 *Future 500IND (500INDFUT)*

Airflow indices were calculated using the modelled 500hPa contour heights. CGCM2 models the peninsula area slightly more successfully than the Azores region. Time series (decadal means 2001-2100) of air flow index data are depicted in *figure 7.4.* Time series can be summarized as follows,

- A linear increase in 500hPa contour height of just above 80 metres from 2001-2100 (significant at $p<0.050$, r^2 0.94). This is expected given the projected increase in the air temperature of the lower troposphere.
- An initial drop from 2001-2010 to 2011-2020 but then a quasi-linear increase in westerly flow ($p<0.050$, r^2 0.91).
- Variability in *500S* but no significant trend.
- A decrease from the first decade to the second but then a linear increase ($p>0.050$, r^2 0.91) in flow strength (*500F*). The trend (and values) are very similar to that of *500W*.
- A decrease in total vorticity (*500Z*) from 2030-2100 (decrease in *500ZW* but no change in *500ZS*). In other words a shift towards greater anticyclonicity.

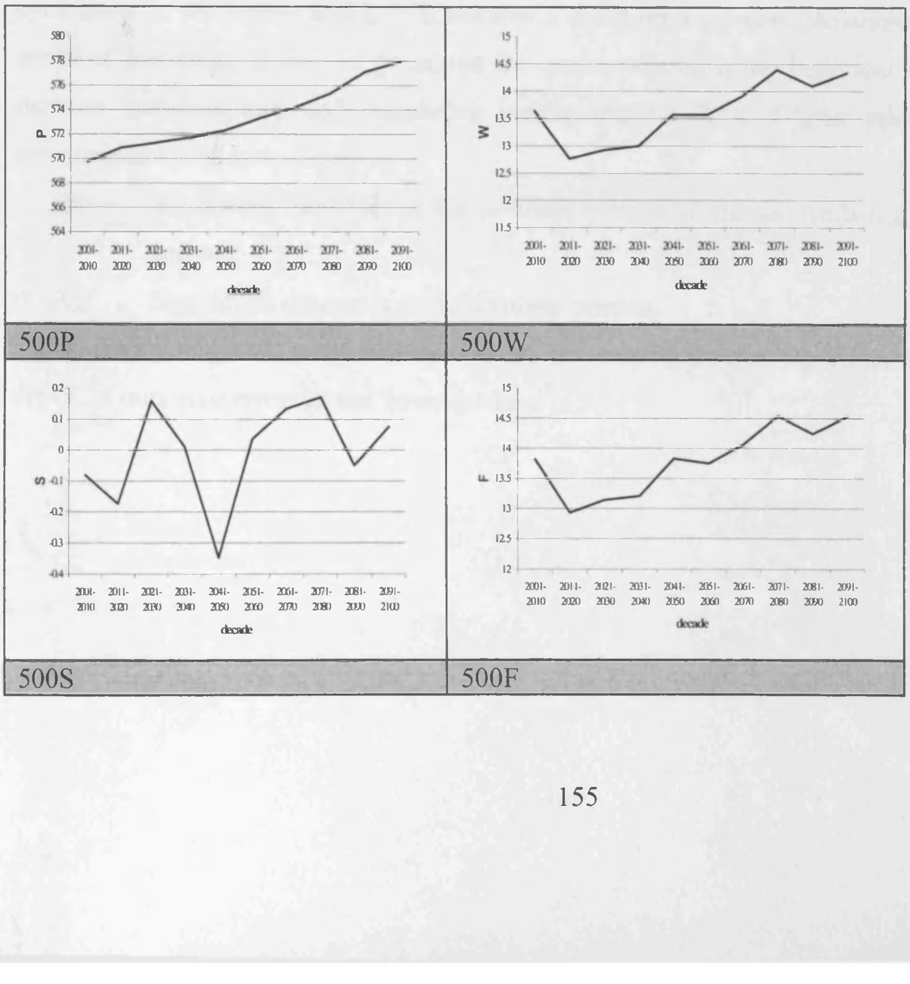

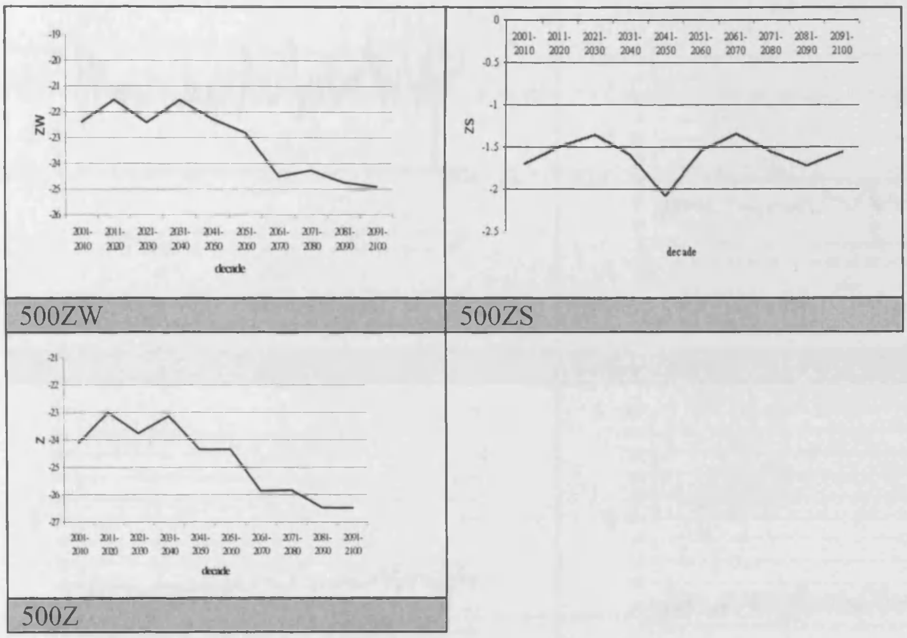

Figure 7.4 *Air flow index decadal means 2001-2100.*

7.5 Modelling rainfall from 500INDFUT
7.5.1 Winter rainfall time series 2001-2100

Although a vigorous zonal circulation (*500F* and *500W*) suggests more active baroclinic disturbances, the large increase in negative vorticity (*500Z*) indicates a strong decrease in cyclonicity in the region and a shift towards a much drier climate. Assuming stationarity, time series of precipitation can be generated for each gridpoint using historical linear relationships between historical data and circulation indices (*figures 7.5*). Winter rainfall trends can be summarized as follows,

(i) Significant increases in the northern section of the peninsula (*i.e.* at gridpoints 1, 2 and 3).

(ii) Significant decreases in the southern section.

Unfortunately negative precipitation amounts are modelled reflecting either the inaccuracies of the GCM output or errors in the linear models.

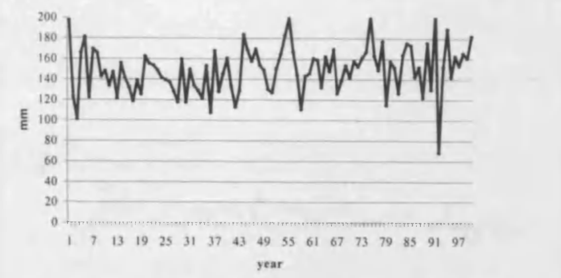

1

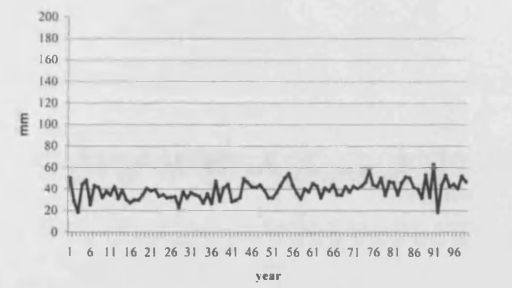

2 $r^2 = 0.196$

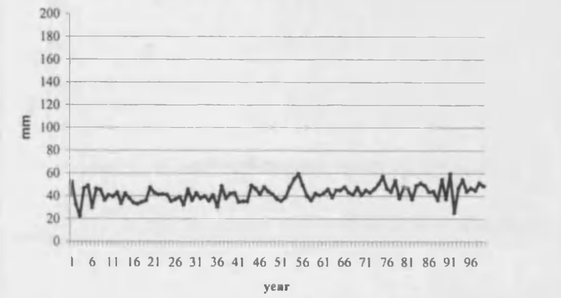

3 $r^2 = 0.187$

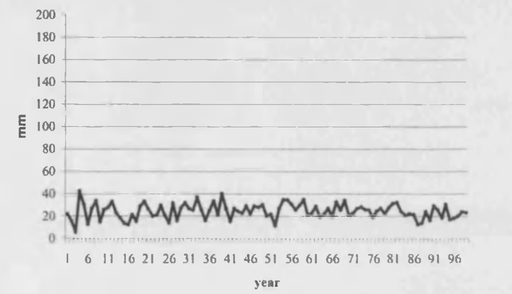

4

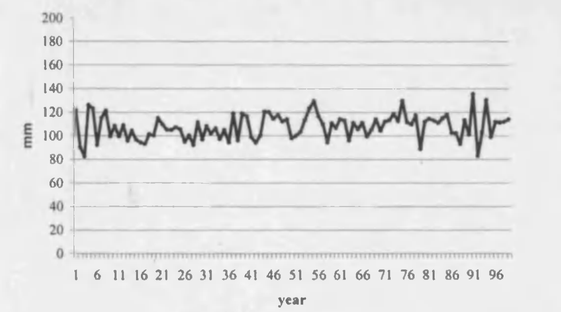

5 $r^2 = 0.056$

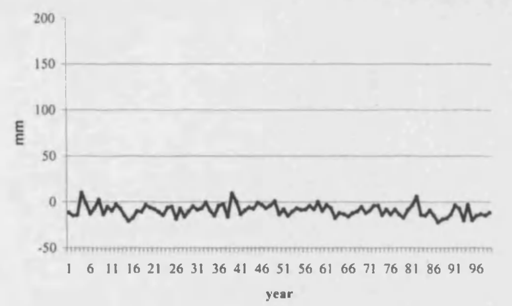

6 $r^2 = 0.058$

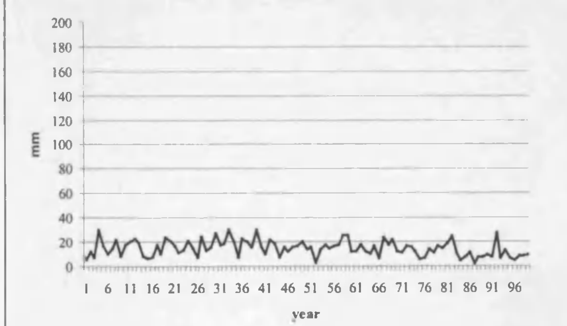

7 $r^2 = 0.084$

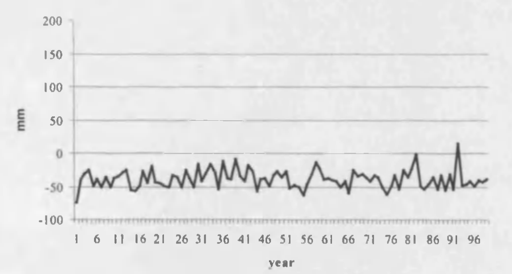

8

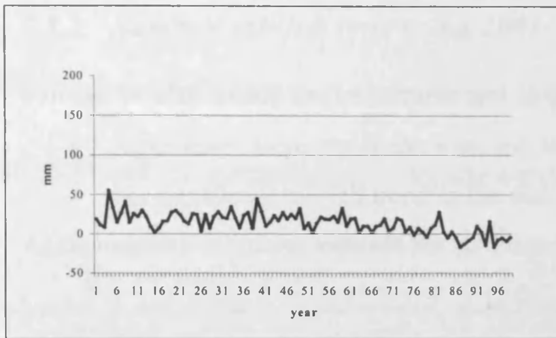

9 $r^2 = 0.301$

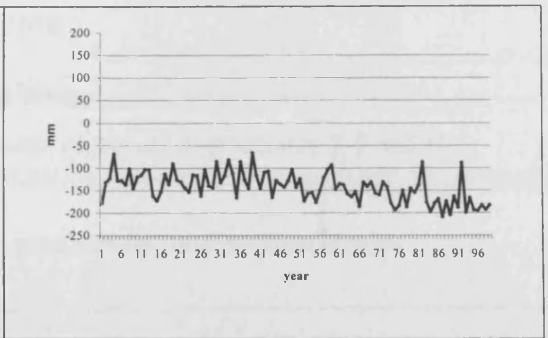

10 $r^2 = 0.417$

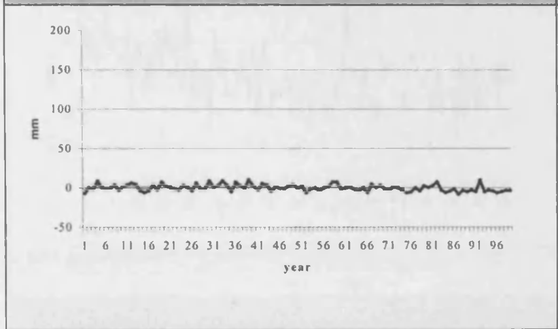

11 $r^2 = 0.101$

Figure 7.5 Winter rainfall estimates 2001-2100 provided by airflow indices.

7.5.2 Summer rainfall time series 2001-2100

Summer rainfall trends can be summarized as follows,

- Significant decreases in the west and south, especially at gridpoints 5, 9 and 10.
- No significant rainfall trend in the east.

Again negative estimates indicate the technique produces far from accurate results.

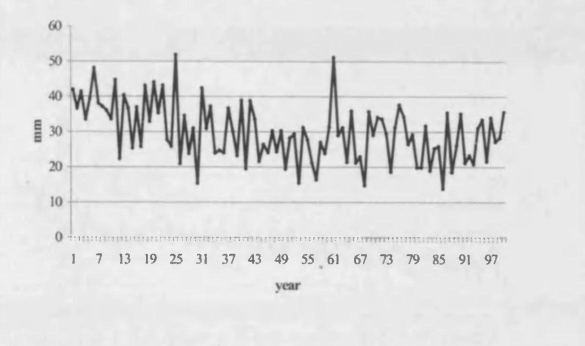

1 r^2 = 0.150

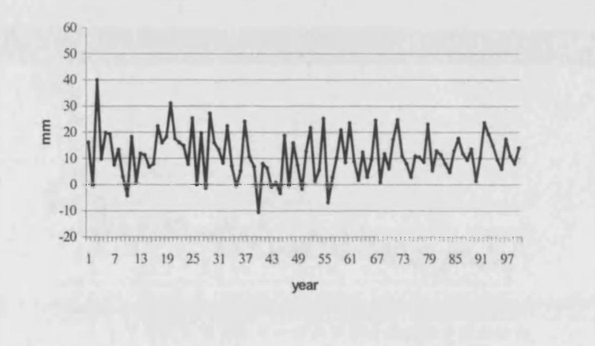

2

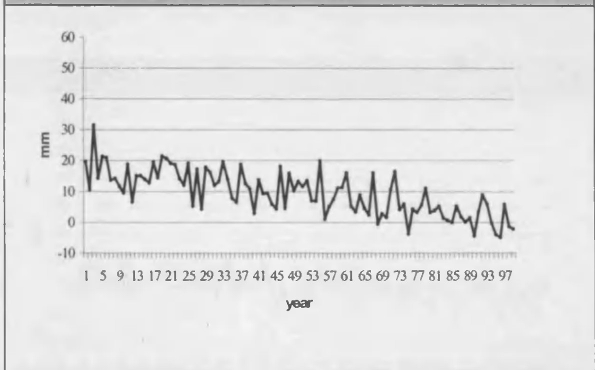

3

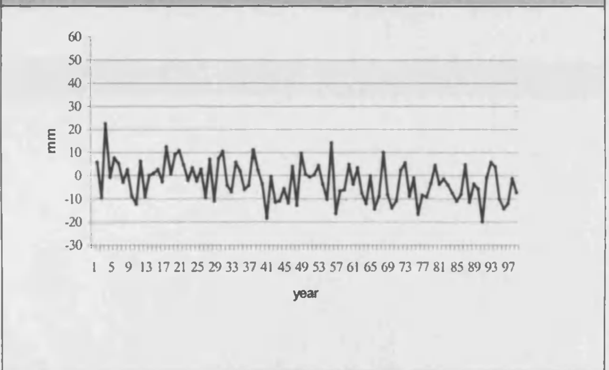

4

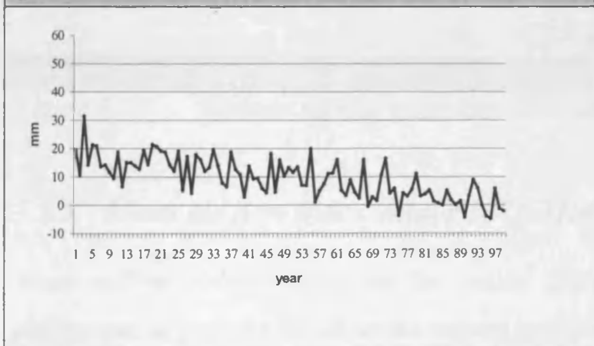

5 r^2 = 0.547

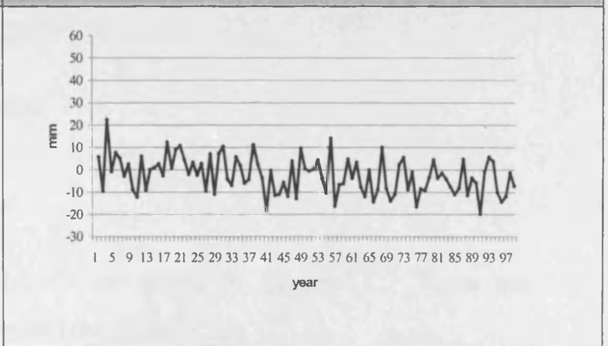

6 r^2 = 0.130

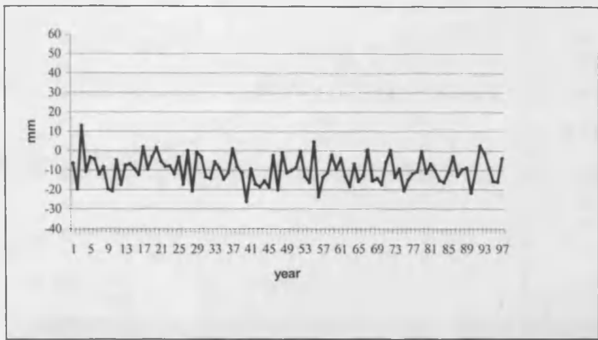

7

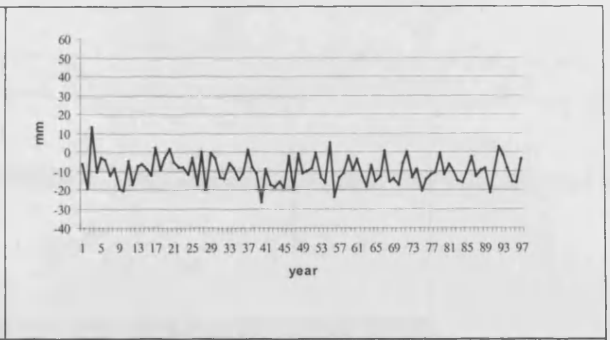

8

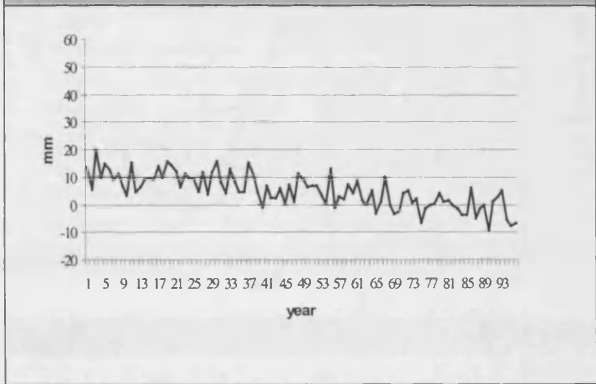

9 $r^2 = 0.577$

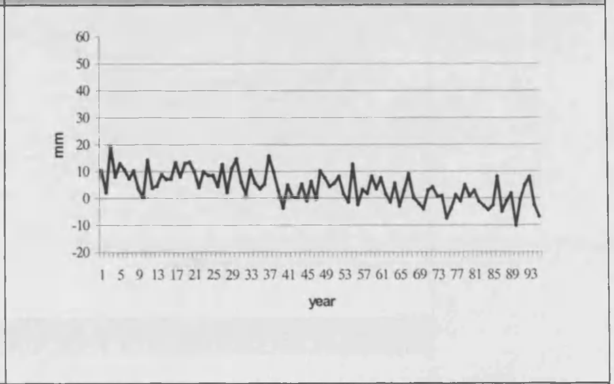

10 $r^2 = 0.437$

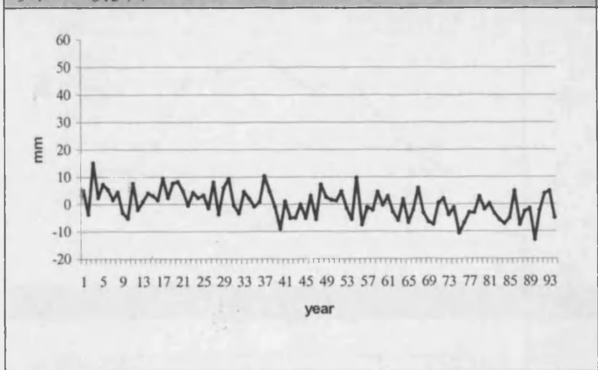

11 $r^2 = 0.263$

Figure 7.6 Summer rainfall estimates 2001-2100.

7.5.3 Mean air flow index values 2071-2100

Mean airflow index values for the period 2071-2100 are given in *figure 7.7*. These are comparable to patterns based on the current time period (see *figure 5.15*).

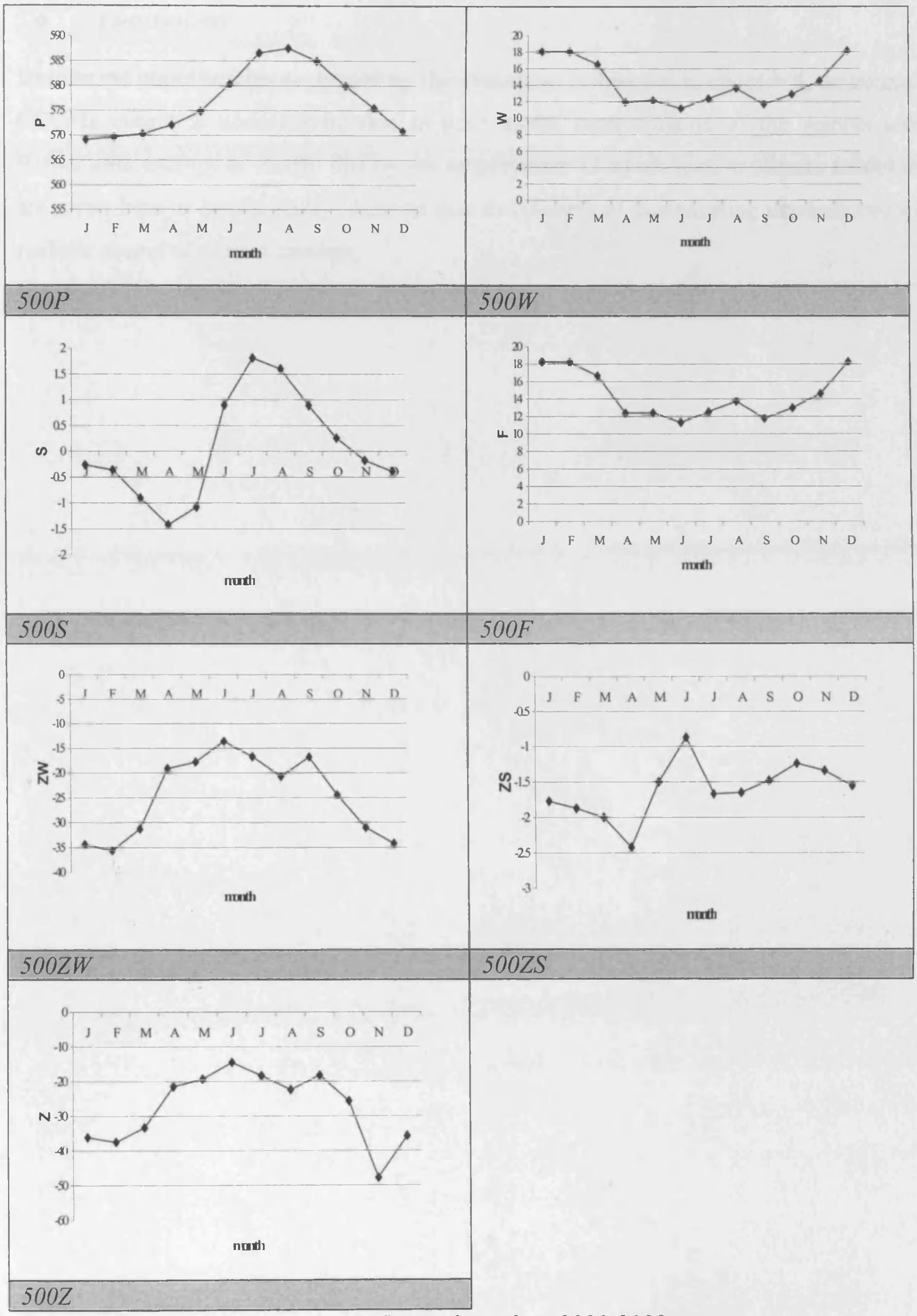

Figure 7.7 Mean monthly air flow index values 2001-2100.

7.6 Conclusions

Despite the opportunities suggested by the evaluative techniques in *chapter 6*, downscaling using CCCMa output is unsuccessful due to poor model representation of the Azores anticyclone. Rather than attempt to rectify this by the employment of an alternative climate model the results are given here to emphatically illustrate that the success of downscaling depends entirely on the realistic output of climate models.

Chapter Eight
Conclusions

8.1 Review of results

This study has examined some of the broad aspects of Spanish temporal and spatial rainfall variability with respect to modes of atmospheric circulation. The following sections identify how the aims of this study have been met.

8.1.1 The regionalization procedure

Regionalization achieves its aim by producing a simple grouping of locations that can be deductively linked to atmospheric processes. It is concluded that,

- Distinct clusters of stations emerge which display strong within-group cohesion and between-group-differences. Regional 'precipitation affinity areas' using all year data mirror traditional climatic divisions. Given the extent of the data network regional boundaries cannot be delineated.
- Precipitation regions are identified as a consequence of (*i*) large-scale topographic features (the *meseta*), (*ii)* more localized features (mountain ranges), (*iii)* the interaction between these and atmospheric circulation and finally (*iv*) proximity to the dynamic source of the rainfall event.
- Affinity between locations is allied to geographical proximity except in a few instances. One striking example (*figure 8.1)* is the link between the north-west quadrant and the highland area in the central *meseta.*
- This study shows that clusters change with season – traditional 'boundaries' move reflecting seasonal differences in the dominant precipitation mechanisms. It is proposed that for some applications seasonal division is important.
- It is also proposed that this method can enable the re-allocation of regions using climate change scenario data and this would be useful to long-term water management. A finer network of stations with sufficiently long records for downscaling purposes would improve this activity.

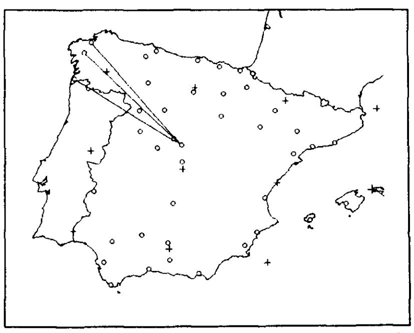

Figure 8.1 Long distance high correlation between rainday numbers (all days).

8.1.2 The circulation classification procedure

It is recognized that climate variability is associated with changes in large-scale atmospheric circulation (Bárdossy and Caspary 1990). Until comparatively recently published research in synoptic climatology was dominated by studies that advocated the use of single synoptic models. Recently several model validation procedures have appeared (*e.g.* Huth 1999) but this present study involves a much more extensive investigation than that of any published work. The project initially set out to compare synoptic catalogues of the Iberian region developed by common statistical techniques (taken from the literature in the 1980s and 1990s) to non-linear alternatives. Nevertheless the non-linear models gave poor rainfall discrimination and the added complexity of developing them (especially ANNs) did not warrant their use. Furthermore this study proposed that a complete evaluation should consider the type of data input (parameter type, atmospheric level, seasonal anomaly, size of data window), as these are highly influential on the output of the method.

8.1.3 The Perfect Prognosis method

A daily model based on the 500hPa contour surface and generated using PCA and CA was the best performer. A 500hPa index-based regression model was the best monthly model. It must be noted that the evaluation statistics give contrasting results, as noted elsewhere by Yarnal (1993), Spellman (1999) and Spellman (2000a).

8.1.4 The Model Output Statistics method - downscaling

In this study the downscaling procedure produced precipitation estimates that were unrealistic. This highlights the fact that any empirical method is only as useful as the modelled GCM output is accurate (Mitchell and Hulme 1999). Nevertheless it was not the objective of this study to compare and contrast climate change scenarios for the Iberian peninsula and therefore only scenarios developed by one (reputable) modelling centre were used.

Errors in the downscaling procedure can be attributed to regional problems with the pressure forecast of CGCM2. There is an underestimation of the strength of the Azores anticyclone both at surface and in the mid-troposphere (based on historical tests) (*table 8.1)*. This reduces NAOI and ZI values and affects modelling based on current climate regression. On the other hand CGCM2 modelled data in the vicinity of the peninsula are slightly less erroneous and although enhancing the magnitude (negative) of certain airflow index values (*Z, ZW, ZS*), reducing the magnitude (positive) of others (*P, F*) and influencing class-based techniques errors, these are perhaps less severe. Downscaling therefore needs to fit models to locations.

	Azores (hPa)	Iceland (hPa)
Historical set	1021.4	1005.8
Modelled Future set	1012.1	1010.4

Table 8.1 Mean monthly values at NAOI 'centres of action' historical past data set and modelled future dataset.

The GCM used in this procedure has performed well in published comparative studies (CCCMA 2003). Empirical downscaling methods assume that a GCM adequately represents the large-scale features of the atmosphere (Yarnal *et al* 2001). GCMs however do show considerable error, even when modelling the largest scale circulation features like subtropical anticyclones (Wilby *et al* 1998, Easterling 1999).

8.2 Review of research issues

Research in synoptic climatology has been periodically reviewed by Barry and Perry (1973), Smithson (1986, 1987, 1988) and Yarnal *et al* (2001). Since this project commenced considerable progress has been made in the field nevertheless some issues common to the application of any synoptic climatological technique as suggested by Yarnal (1993) continue to be relevant,

1. The atmospheric environment is not a critical determinant of the surface environment.
2. The Bergen School conceptual model of the structure and evolution of midlatitude synoptic scale cyclones is not correct.
3. The atmosphere cannot be partitioned into discrete, non-over-lapping intervals.
4. The classification does not identify all important map patterns or synoptic types.
5. The classification methods really do not do what the investigator thinks they are doing.
6. The temporal scales of the observations and the atmospheric-circulation processes do not match.
7. The spatial scales of the gridded data and the circulation do not coincide.
8. Within-group variability is not a problem.

Further issues can be added to this list,

9. The different precipitation response that might occur at the start of the duration of a weather type and at the ends.

10. The spatial locations of grid point data used in the classification may not be optimal.

11. The difficulty in capturing extreme events under a class-based system.

Finally the following issues related to synoptic climatology and empirical downscaling can be addressed,

12. The GCM used to provide gridpoint predictor variables does not adequately represent even large-scale features of the atmospheric circulation.
13. Reliable time series are not of sufficient length to capture the true nature of circulation-environment association.
14. The nature of precipitation data may lead to erroneous modelled output.

Some of theses issues are directly addressed by this project however others will remain as 'cautionary notes' for future work or indeed any study of this nature. In addition, and inevitably some of the issues overlap.

8.2.1 The atmospheric environment is not a critical determinant of the surface environment.

It is a universal truth that mechanisms in the local and regional atmospheric environment exert a control on precipitation amounts (Yoshino 1975, Lamb 1977), but a critical issue is the identification of which aspects of the atmospheric environment are most influential. Wilby and Wigley (2000 p.642) state that *'...there is little consensus ...as to the choice of atmospheric predictor variables...'* for any synoptic model. The objective of this study was to examine the most commonly employed predictors therefore other climatic variables were not examined.

Although Murphy (1999) argues that if downscaling of precipitation is the research goal then it is useful to include a predictor of atmospheric moisture[1], GCMs produce less accurate simulations of these variables than geopotential height or surface pressure (Yarnal *et al* 2001) and may not therefore improve the downscaling process. The integration of other climatic parameters in downscaling models for Spain is the subject of ongoing research.

The choice of atmospheric level must be informed by knowledge of local climatological and meteorological mechanisms. Over Spain classified surface patterns are considerably affected by summer thermal cyclonicity and, although to a lesser extent, by winter thermal

[1] increased lower tropospheric temperature would, *ceteris paribus*, increase the saturation vapour pressure of the air and lead to a rise in precipitable water. This would mean that precipitation events would involve greater volumes of water (IPCC 2001a).

anticyclonicity. This could prompt an overestimation of rainfall incidence in summer and an underestimation in winter, although there is no evidence that this occurs in this study. Furthermore upper air cold pools are frequently unidentifiable on surface charts, particularly in the eastern peninsula region. Results in this study indicate that peninsula-based mid-tropospheric catalogues often outperform surface catalogues, but large-scale surface indices, the ZI and NAOI (which are less influenced by surface features on the peninsula) give comparable results for western regions.

8.2.2 The 'Bergen School' conceptual model of the structure and evolution of midlatitude synoptic scale cyclones is not correct.

Mid-latitude climatological understanding is underpinned by the 'Bergen School' model (Barry and Chorley 1998). One of the main criticisms of most empirical synoptic methods is that no attention is directed towards well-defined theoretical physical mechanisms. In this study, mechanism-specific kinematic information has been incorporated into daily static classification methods in order to reduce within-group variability. This criticism, however, has been aimed at physical modelling as models parameterise poorly understood or difficult-to-model mechanisms that in turn, will affect long- term accuracy (Yarnal *et al* 2001). Yarnal *et al* conclude that to claim one is better is erroneous and that each type of model provides a complimentary perspective on the climate system.

At some sites, particularly in the west, the higher probability of rainfall associated with frontal incidence manifests itself in a better calibrated model. Frontal information must be gained manually from charts and hence even automated methods will be semi-manual if kinematic information is to be included. To complicate matters, Mass (1991) has suggested that there are serious deficiencies between synoptic theory and mapping practice, above all that there is no uniform procedure for defining fronts on synoptic charts and this considerably reduces the data available to the synoptic climatologist. This is part of the objective automated procedure that remains subjective and manual, and unfortunately frontal models will only be useful to downscaling when accurate frontal information is provided by climate models.

8.2.3 The atmosphere cannot be partitioned into discrete, non-over-lapping intervals.

The traditional approach to synoptic climatology is based on 'lumped' patterns in nominal categories (Yarnal *et al* 2001) and this means that classification is cognitively successful. Nevertheless three fundamental problems of nominal catalogues can be isolated which relate to (*i*) classification, (*ii*) scale and (*iii*) stability. The first two issues concern the temporal and spatial restrictions inherent in any daily or monthly classification based on a defined area. For instance, the atmosphere is a multi-dimensional continuum and hence any division will be purely arbitrary.

Daily classification is based on pattern recognition at one temporal instant in a day, in most cases this is 1200Z. Although this avoids the problem of inordinately large datasets it could be that this ‘snapshot’ is not representative of conditions for the majority of that day. Patterns can be transitionary and this, in itself, can be important with respect to some applications. In *chapter 4* a method for obtaining a better understanding of the relationships between weather types and time (*i.e.* conditional probability matrices) is described and such findings need to be built into synoptic models.

Scale problems are related to the classification area and the size of the synoptic systems that affect the area (Perry and Mayes 1998). Different parts of a study region could experience contrary airflow types. The Iberian peninsula, however, being a geographically compact shape (see *appendix 2.2*) of roughly the same dimensions of a travelling Atlantic depression or an upper westerly trough can experience a singular systematic influence (*figure 7.9a and b*).

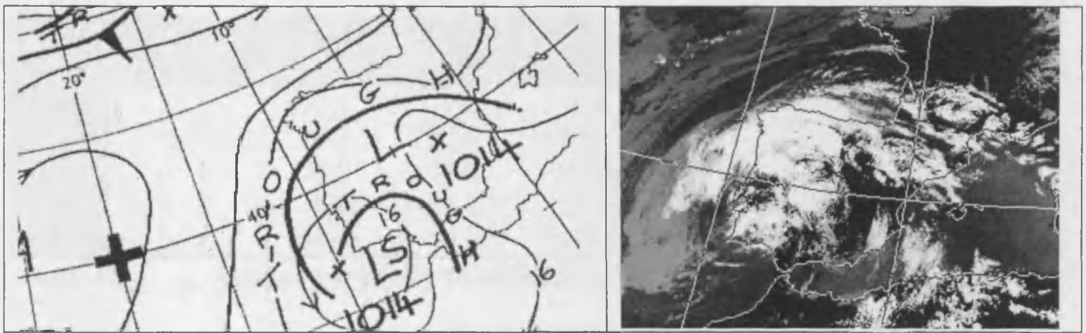

a. 15.07.95 *b. IR-image*

Figure 8.2 System size and the peninsula.

The third factor questions whether any weather pattern and associated meteorological parameters are constant in time. This characteristic is termed ‘stationarity’. With respect to precipitation, occurrences of non-stationarity has been attributed by Wilby (1995) to subtle changes in the dominant precipitation mechanism, for instance, whether stratiform or convective in origin, and further speculation has been directed towards the intensity of circulation or differences in depression trajectories (causing variation in moisture content and thermal characteristics).

In contrast to weather pattern models the continuous models in this study have the advantage of representing the entire continuity of circulation and are able to differentiate among subtle differences in the atmospheric state that can result in distinctly different outcomes at the surface (Yarnal *et al* 2001). Again, however, issues relate to scale and stationarity arise (*see section 8.7.8*).

8.2.4 The classification does not identify all important map patterns or synoptic types

It has already been stated that one of the main drawbacks of the automated approach is that unusual patterns are frequently lost in the classification procedure. This problem is avoided by the use of a manual method coupled with interpreter skill and this is demonstrated by the importance of SEL and SWL patterns in supplying rainfall to locations in their proximity. A greater number of circulation classes captures the uniqueness of less frequent circulation patterns and their precipitation relationships. On the other hand the statistical integrity is affected by small sample sizes given the unavoidable brevity of any catalogue based on available observed data. This is illustrated by the SLPINDC and 500INDC schemes (*table 8.2*). Under both schemes a high degree of variability in rainfall signature occurs under some of the hybrid types.

	% incidence	Murcia	Mahon	Badajoz
A	23.3	10.5	17.5	16.6
W	4.3	26.3	32.1	32.0
CS	0.11	70.8	50.8	103.0
CSE	0.18	36.0	54.7	53.5
CSW	0.25	53.4	60.0	143.2

Table 8.2 Rainfall variability (Coefficient of Variation) under selected SLPINDC.

A small number of classes may reduce resolution and mean that the greatest anomalies (perhaps related to greatest anomalies of rainfall) are subsumed. This study concludes that 500AUT performs well even with 10 classes.

8.2.5 The classification methods really do not do what the investigator thinks they are doing

Significant advances in the analysis of quantitative data in all geographic disciplines have been made in the last decade (Rogerson 2001), predominantly as a response to improvements in computer technology and the computation procedure. Recently synoptic climatologists have been able to increase the range of techniques, and move away from simplistic linear models to more advanced regression models such as multivariate adaptive splines (Corte–

Real *et al* 1995) and non-linear regressions (Cavazos 1999). Similarly eigenvector analysis and applications of ANNs have greatly benefited from increases in computer processing power. In addition all forms of climatic data have become much more readily available in the past decade. Gridpoint data sets have been generated and made freely available to the climatological community by research institutions and this has greatly facilitated work in this field. This study has managed to take advantage of many of these developments.

On the other hand these techniques are often employed by climatologists in a 'black box' fashion. The empirical approach ignores all of the processes operating between the atmospheric scale of the study and the rain gauge. It is also unlikely that all climatologists are experts in any particular statistical technique (Joliffe 1990). Synoptic climatologists need to be aware of the critical effect that subjective decisions can have on stages within a so-called 'objective methodology'.

At an early stage in this analysis neural network approaches (SOM and back propagation) were compared to linear regression methods but it was found that estimates from the former did not improve on the accuracy of the latter. ANNs provide a fine example of a technique that is poorly understood by workers outside the field of computer technology and more accessible user-friendly language and software can only help the application in future years The restrictions of linearity and normality of PCA is a potential major drawback of the technique however it has been shown in this study that these relatively simple linear traditional methods have outperformed much more complex methods of analysis.

8.2.6 The temporal scales of the observations and the atmospheric-circulation processes do not match.

Yarnal *et al* (2001) comment that the time scale of the surface variable is an important consideration. A crucial aspect of this temporal framework is related to the organization of downscaling models. The use of an 'all year' modelling approach in this study minimizes the risk of unanticipated changes in the timing of seasons. Yet such generalized models can mix different seasonally related precipitation processes (*e.g.* mesoscale convective mechanisms and synoptic scale mechanisms) and result in compromised model skill. This is especially the case in a Mediterranean environment and hence in this study a compromise is found by using a high-sun season/low-sun season division. Consequently quite distinct synoptic-environment association is isolated.

Atmospheric circulation and precipitation mechanisms can operate on temporally different modes of variability. Most synoptic analyses have focussed on either daily or monthly data and there are disadvantages and advantages associated with each. From the viewpoint of improved climatological understanding of high frequency processes and the analysis of high intensity events daily records are required but these are incompatible with GCM output. If rainfall intensity is to be examined then a finer temporal resolution is required.

GCM and historical predictions agree that Western Mediterranean rainfall amounts have been decreasing over time however, as has been reported in other geographical areas (Yu and Neil 1993, Mearns *et al* 1997, Hennessey *et al* 1999) these annual changes do not necessarily occur in the same way at different time scales (annual, seasonal, monthly or daily). Each of these temporal scales is linked to various human activities and to ecological or degradation processes (Gonzalez-Hidalgo *et al* 2001) and the seasonal scales used in this study are most important in Spain.

8.2.7 The spatial scales of the gridded data and the circulation do not coincide

This is not a problem if the atmospheric features are larger in size than grid spacing however some small circulation features can get 'lost' between gridpoints. Subjective manual examination of daily weather maps prior to the analysis (on the assumption that these did not miss key features) indicated that the chosen grid used to develop all the objective classifications was sufficiently fine to capture non-convective systems.

8.2.8 Within-group variability is not a problem

The reduction of within-group variability is a central challenge for synoptic climatologists and indeed to any discipline founded on taxonomy. At the centre of traditional weather type approaches is the assumption that precipitation behaviour (such as the mean rainfall amount) of a given circulation pattern (or index value) is constant in time (Wilby *et al* 1995). This homogeneity assumption is necessary to extrapolate future rainfall scenarios from historic relationships. It is fundamental to the success of empirical downscaling yet variability in rainfall signature is seen to occur on decadal and annual time scales. *Table 8.3* shows the variability in mean rainfall amounts associated with selected 500AUT weather types for various sample periods. Model calibration and validation is therefore problematic – any model forecast is entirely dependent on the duration and period used to calibrate the model. For instance a rainfall model used to calibrate 500AUT4 based on the years 1968-1977 would greatly overestimate the long-term amounts associated with this weather type. This is partially overcome by using randomly selected days for the calibration and validation set but the unstable relationship remains.

	1958-1967		1968-1977		1978-1987		1988-1997	
	Mean	COV	mean	COV	mean	COV	mean	COV
4	51.95	99.73	55.30	75.23	46.59	81.09	48.61	70.79
7	36.99	106.11	46.02	86.70	34.67	98.15	39.48	84.22
11	19.24	105.98	25.54	104.66	19.72	122.16	22.79	98.86

Table 8.3 Three 500AUT weather types and mean rainfall characterstics associated with each in four decades.

The methodology used in this study reduces intra-weather type variability by frontal information, however downscaling requires frontal information to be a part of GCM output. Furthermore it could be that large-scale indices or even teleconnections (El Niño) could be used to condition weather type catalogues in the same way as fronts have been used. Finally non-stationarity can occur as a response to changes in the mean trajectory or variations in sea surface temperatures which are considerably harder to objectively quantify.

8.2.9 The different precipitation response that might occur at the start of the duration of a weather type and to that at the end

This point is recognised by Bárdossy and Plate (1991 p44) who comment that '*...further research is needed to estimate rainfall occurrence probabilities for transition days (first and last days of a period with the same circulation pattern).*' It is likely that these probabilities might depend on the actual and preceding (or succeeding) weather type. An identifiable pattern would greatly aid the statistical solution to non-stationarity problems. This study has undertaken a preliminary investigation of duration and transition probabilities of 500AUT weather types. Research is being conducted into this area but as yet no consistent relationship has emerged using samples. At this stage it is speculated that a consistent relationship may be hard to isolate.

8.2.10 The spatial locations of grid point data used in the classification may not optimal

Pressure pattern identification is based on a dense network of grid points (2.5^o by 2.5^o) and it is suggested that an alternative gridpoint selection would make little difference to classifications. On the other hand large-scale indices like the NAOI and the ZI are not centred on the peninsula. Murphy and Washington (2001) comment that the NAOI is not the only Northern Hemisphere, nor even North Atlantic, teleconnection affecting climate variability in Europe. Barnston and Livezey (1987) identify an east Atlantic pattern (centres at approximately 50°N-55°N, 20°W-35°W and over North Africa 25°N, 0°-10°W) and Rodriguez-Puebla *et al* (1998) have found significant association with that and Iberian rainfall. Although this study indicates that the NAOI is strongly related to Spanish rainfall it is questionable whether the NAOI is actually optimal in explaining the precipitation variance in western Europe. Indeed Murphy and Washington (2001) show that a greater proportion of UK and Ireland precipitation variability can be explained by alternative indices based on different centres of action to those of the conventional NAOI.

In addition the examination of large-scale teleconnections on Iberian rainfall continues. Rodo *et al* (1997), Moron and Ward (1998) and more recently Van Oldenburgh *et al* (2000) have found an El Niño teleconnection to spring rainfall in Europe, including Spain. Future work will concentrate on evaluation of large-scale indices using alternative locations

8.2.10 The difficulty in capturing extreme events (or changes in intensity) under a class-based system

Variations in total precipitation can be caused by a change in the frequency of precipitation events, or in the intensity of precipitation per event, or a combination of both. It cannot be assumed that an increase (or decrease) in total rainfall amounts is positively related to a change in the frequency of heavy rainfall events or that event intensity is related to total amounts. The former has been demonstrated by Groisman *et al* (1999), but work by Brunetti *et al* (2000a, 2000b) in Italy suggests that a negative relationship exists. In this study and elsewhere continuous models are found to be more reliable for representing extreme events (see *table 7.4*) (*e.g.* Sailor and Li 1999). This is clearly an area where further work is needed.

	Precipitation in mm under 200 events at tails of vorticity (Z) distribution			
	Highest z	**Highest trimmed mean**	**Lowest Z**	**Lowest Z trimmed mean**
Badajoz	2.0	1.7	0.9	0.4
Burgos	2.8	1.8	1.4	0.7
Murcia	2.2	0.7	0.0	0.0
Salamanca	1.4	1.0	1.0	0.4
Santander	10.8	9.1	6.9	5.3

Table 8.4 Relationship between vorticity distribution and daily precipitation.

8.2.11 The GCM used to predict grid point meteorological variables does not adequately (or worse) represent large-scale features of the atmospheric circulation

Both empirical and dynamical downscaling depends on the accuracy of large-scale information upon which they are driven (Mitchell and Hulme 1997). The results of this downscaling exercise reflect Bengtsson's comments *(section 1.4).* Deficiencies and uncertainties related to GCM output are well-known and have been extensively described elsewhere (Holton, 1979, IPCC 2001). These are related to the need to simplify the workings of the climate system, needed because *'...we neither understand all the physical laws perfectly or can observe the climate completely.'* (Robinson and Henderson-Sellers 1999 p247).

8.2.13 Reliable time series are not of sufficient length to capture the true nature of circulation-environment association

Historical time series (especially monthly datasets) are potentially insufficient to establish a realistic relationship between circulation and rainfall. This is due to limited representation in certain classes especially when the dataset is reduced to calibration and validation sets and then further subdivided on the basis of season (or fronts). Problems can be reduced by stochastic modelling, however such models still require calibration. Furthermore stochastic models poorly represent the expected variance and have problems in replicating autocorrelation of weather types (Richardson 1981). Some of the problem can be overcome by the use of schemes with a reduced number of classes however this could reduce accuracy.

8.2.14 The nature of precipitation data renders modelling highly problematic.

This is perhaps the most insurmountable problem. Precipitation is difficult to model because it is a discrete variable and often highly influenced by local and random factors. Rainfall exhibits a skewed, zero-bound distribution and consequently requires arithmetic transformation to fit normal distributions if parametric methods are employed. Furthermore stochastic methods involve fitting the data to known distributions which could change over time (Zorita and Von Storch 1999).

8.3 Achievements and future directions

The study has been successful in achieving its aims and has indicated some future directions of this research. These directions will be aided by developments in methodology and technique. Yarnal (1993) commented that the future synoptic climatological studies would go in four directions: (*i*) existing (but fine-tuned) empirical-statistical pathways, (*ii*) new empirical-statistical pathways (such as artificial neural networks), (*iii*) simulation models linking regional scale to large–scale and (*iv*) Geographic Information Systems. This study has explored (*i*) and (*ii*) and further work will continue with the addition of the latter approaches.

The achievements of this study can be summarized,

- Regionalization using multivariate techniques generates interpretable rainfall regions which can be seasonally adjusted and quickly re-identified using downscaled climate change data.
- Anomalies in the 500hPa surface provide the best results in the model evaluation procedures.
- Daily standardized data is shown to provide the best input to weather typing.
- Addition of frontal information improves the performance of models at some (western) locations.
- The appropriate daily synoptic models (mean value, weather type, stochastic model, frontal model) should be chosen dependent on sub-region within the study area.
- The use of multi-level and thickness patterns does not significantly improve results obtained by simple surface or 500hPa patterns.
- The use of ANNs does not improve on the use of conventional techniques.
- Stochastic modelling of rainfall in a weather type scheme improves model performance at some sites (mainly those with higher rainfall/raindays).
- Large-scale indices (despite their simplicity) model rainfall well but peninsula-centred index models are most accurate.
- The appropriate monthly synoptic models (NAOI, ZI, IND) should be chosen dependent on sub-region within the study area.
- Preliminary examination of transition probabilities suggests that inter-relationships between weather types could yield valuable synoptic insight especially if different rainfall probability at stages within a 'weather type run' could be captured.
- Transitional probabilities were used to model weather type catalogues (not reported here).

- High rainfall events can be associated with certain weather types and extremes of vorticity distribution.
- GCM output poorly models the climate parameters and this suggests caution must be taken when downscaling in this region.

The future directions of this research can be grouped by priority level. In the immediate future the following should be addressed,

- Stationarity of circulation-precipitation linkage should be examined and, if at all possible, models should be modified to address this problem.
- Appropriate schemes need to be selected to model precipitation in smaller sub-regions on the peninsula.
- The use of other non-circulation parameters (*e.g.* precipitable water) should be tested in future multivariate modelling.
- The use of daily GCM output should be investigated in downscaling approaches.
- Later scenarios from CCCMA (not yet available) should be examined together with output from other modelling centres.

Secondly,

- Improved resolution (spatially and by frontal type) should be attempted without sacrificing the objectives of classification.
- Stochastic techniques should also be employed in regression approaches.
- Improvements in software should aid the application of non-linear techniques.
- Examination of precipitation behaviour related to incidence in weather type sequence could be examined.
- Further work on weather generators using both weather type and index data should continue. Although these have a disadvantage of not being able to capture persistent events they can be used so that changes in variability as well mean changes can be modelled.

Finally,

- In the long term the increased availability of reliable data should eventually improve calibration of these models.
- Other large–scale indices should be evaluated that may have even greater success.
- Further analysis of the synoptic climatology of extreme events is required.

REFERENCES

Abercromby, R., (1883), On certain types of British weather. *Quarterly Journal of the Royal Meteorological Society*, **9**, 1-25.

Abercromby, R., (1887), *Weather: a popular exposition of the nature of weather changes from day to day.* Kegan Paul. London.

Abler, R., Adams, J. and Gould , P. (1971), *Spatial Organization.* Prentice Hall. Englewood Cliffs, New Jersey.

Aizen, E.M., Aizen, V.B., Melack, J.M., Nakamura, T. and Ohta, T., (2001), Precipitation and atmospheric circulation patterns at Mid-latitudes of Asia. *International Journal of Climatology*, **21**, 535-556

Alijani, B. (2002), Variations of 500 hPa flow patterns over Iran and surrounding areas and their relationships with the climate of Iran. *Theoretical and Applied Climatology*, **72**, 41-54.

Allan, R.J., Lindesay, J.A. and Parker, D.E., (1996), *El Nino-Southern Oscillation and climatic variability.* CSIRO Publishing, Collingwood, Victoria.

Almerza, C. and Lopez, J.A., (1996), Variability of the precipitation in Spain and its relation to the North Atlantic Oscillation. *European Conference on Applied Climatology Abstract Volume* **7-10** May Norkopping, Sweden 163-165.

Alpert, P., Neeman, B.U. and Shay-El, Y., (1990), Climatological analysis of Mediterranean cyclones using ECMWF data. *Tellus*, **42A**, 65-77.

Amanatidis, G.T., Paliatsos, A.G., Repasis, C.C. and Bartzis, J.G., (1993), Decreasing precipitation trend in the Marathon area, Greece. *International Journal of Climatology*, **13**, 191-201.

Amanatidis, G.T., Repasis, C.C and Paliatsos, A.G., (1997), Precipitation trends and periodicities in Greece. *Fresenius Environmental Bulletin*, **6**, 314-319.

Andres, M., Tomas, C. and de Pablo, F., (2000), Spatial patterns of the daily non-convective rainfall in Castilla y Leon. *International Journal of Climatology,* **20**, 1207-1224.

Anthes, R.A., Kuo, Y-H., Hsie, E-Y., Low-Nam, S. and Bettge, T.W., (1989) Estimation of skill and uncertainty in regional numerical models. *Quarterly Journal of the Royal Meteorological Society*, **115**, 763-806.

Ayoade, J.O., (1970), The seasonal incidence of rainfall. *Weather,* **25**, 414-418.

Balling, Jnr, R.C. (1984), Classification in Climatology, in *Spatial Statistics and Models* by Gaile, G.L. and Willmott, C.J., (Eds) (1984) D Reidel Publishing Company 81-108.

Bárdossy, A. and Caspary, H-J., (1990), Detection of climate change in Europe by analysing European atmospheric circulation from 1881-1989. *Theoretical and Applied Climatology,* **42**, 155-167.

Bárdossy, A., Duckstein, L. and Bogardi, I., (1995), Fuzzy rule-based classification of atmospheric circulation patterns. *International Journal of Climatology,* **15**, 1087-1097.

Bárdossy, A., Matyasovszky, I. And Bogardi, I., (1994), Knowledge based classification of circulation patterns for stochastic precipitation modelling. In Hipel, K.W., McLeod, A.W.,

Bárdossy, A. and Plate, E.J., (1991), Modelling daily rainfall using a semi-Markov representation of circulation pattern occurrence. *Journal of Hydrology,* **122**, 33-47.

Bárdossy, A., Stehlik, J. and Caspary, H-J., (2002), Automated objective classification of daily circulation patterns for precipitation and temperature downscaling based on optimised fuzzy rules. *Climate Research,* **23,** 11-22.

Barnston, A.G. and Livezey, R.E., (1987), Classification, seasonality and persistence of low-frequency atmospheric circulation patterns. *Monthly Weather Review*, **115**, 1083-1126.

Barry, R.G. and Chorley, R.J., (1998), *Atmosphere, Weather and Climate.* Routledge. London.

Barry, R.G. and Perry, A.H. (1973), *Synoptic Climatology. Methods and Applications.* Methuen. London.

Basist, A., Bell, G.D. and Meentemayer, V., (1994), Statistical relationships between topography and precipitation patterns. *Journal of Climate*, **7**, 1305-1315.

Baur, F. (1931), Die Formen der atmosphärischen Zirkulation in der gemässigten Zone. *Gerlands Beitr Geophys*, **34**, 264-309.

Baur, F., (1936a), Die Bedueutung der Stratosphare fur die Grosswetterlage *Met. Zeit.,* **53**, 237-247.

Baur, F. (1936b), Wetter, Witterung, Grosswetter und Weltwetter. *Z. Angew Met.*, **53,** 377-381.

Baur, F., Hess, P. and Nagel, H. (1944), *Kalendar der Grosswetterlagen Europas 1881-1939* Bad Homburg, Homburg.

Beckmann, B-R., and Buishand, T.A., (2002), Statistical downscaling relationships for precipitation in the Netherlands and North Germany. *International Journal of Climatology*, **22**, 15-32.

Belasco, J.E., (1952), Characteristics of air masses over the British Isles. *Geophysical Memoir*, **11**.

Bell, G.D., (1998), http://nic.fb4.noaa.gov/data/teledoc/telecontents.html

Bellone, E., Hughes, J.P. and Guttorp, P., (2000), A hidden Markov model for downscaling synoptic atmospheric patterns to precipitation amounts. *Climate Research*, **15**, 1-12.

Benestad, R.E., (2001), A comparison between two empirical downscaling strategies. *International Journal of Climatology*, **21**, 1645-1668.

Bengtsson, L., (1995), On the prediction of regional climate change. In *Third International Conference on Modelling of Climate Change and Variability.* Max Planck Institut für Meteorologie. 4-8 Sept.

Bergeron, T., (1928), Über die dreidimensional verknupfende Wetteranalyse, Part 1: Prinzipelle Einführung in das Problem der Luftmassen und Frontenbildung. *Geofys Publik (Oslo)* **5**, 1-111.

Bergeron, T., (1930), Richtlinien einer dynamischen Klimatologie. *Meteoroloschise Zeit*, **47**, 246-262.

Biau, G., Zorita, E., Von Storch, H. and Wackernagel, H., (1999), Estimation of precipitation by kriging in the EOF space of the sea level pressure. *Journal of Climate*, **12**, 1070-1085.

Bonacina, L.C., (1945), Orographic rainfall and its place in the hydrology of the globe. *Quarterly Journal of the Royal Meteorological Society*, **71**, 41-55.

Bonell, M. and Sumner, G., (1992), Autumn and winter daily precipitation areas in Wales. *International Journal of Climatology*, **12**, 77-102.

Brinkmann, W.A.R., (2002), Local versus remote grid points in climate downscaling. *Climate Research,* **21**, 27-42.

Brown, D.P. and Comrie, A.C., (2002), Sub-regional seasonal precipitation linkages to SOI and PDO on the south-west United States. *Atmospheric Science Letters,* **3**, 94-102.

Brunetti, M., Buffoni, L., Maugeri, M. and Nanni, T, (2000b), Precipitation intensity trends in Northern Italy. *International Journal of Climatology*, **20**, 1017-1031.

Brunetti, M., Maugeri, M. and Nanni, T, (2000a), Variations of temperature and precipitation in Italy from 1866 to 1995. *Theory of Applied Climatology*, **65**, 165-174.

Buishand, T.A. and Brandsma, T., (1997), Comparison of circulation classification schemes for predicting temperature and precipitation in the Netherlands. *International Journal of Climatology*, **17**, 875-889.

Burger, H., (1958), Zur Klimatologie der Grosswetterlagen: ein Witterungsklimatologischer Beitrag. *Ber Dtsch Wetterd,* **6**.

Bürger, G., (1996), Expanded downscaling for generating local weather scenarios. *Climate*

Research, **7**, 111-128.

Busuioc, A., Von Storch, H. and Schnur, R., (1999), Verification of GCM-generated regional season precipitation for current climate and of statistical downscaling estimates under changing climate conditions. *Journal of Climate*, **12**, 258-272.

Campins, J., Genoves, A., Jansa, A., Guijarro, J.A. and Ramis, C., (2000), A catalogue and a classification of surface cyclones for the Western Mediterranean. *International Journal of Climatology*, **20**, 969-984.

Canadian Centre for Climate Modelling and Analysis (CCCMA) (2002), http://www.cccma.bc.ec.gc.ca/eng_index.shtml

Carter, T.R., Parry, M.L., Harasawa, H. and Nishioka, S., (1994), IPCC technical guidelines for assessing climate change impacts and adaptations. *IPCC Special Report to Working Group II of IPCC.* London University College London and Tsukaba, Japan. Centre for Global Environmental Research.

Cattell, R.B., (1966), The scree test for the number of factors. *Multivariate Behavioural Research*, **1**, 245.

Cavazos, T., (1997), Downscaling large-scale circulation and local winter rainfall in NE Mexico. *International Journal of Climatology*, **17**, 1069-1082.

Cavazos, T. (1999), Large scale circulation anomalies conducive to extreme precipitation events and the derivation of daily rainfall in north eastern Mexico and south eastern Texas. *Journal of Climate*, **12**, 1506-1523.

Chang, J. (1972) *Atmospheric circulation systems and Climate.* Honolulu. Oriental.

Chen, D., (2000), A monthly circulation climatology for Sweden and its application to a winter temperature case study. *International Journal of Climatology*, **20**, 1067-1076.

Chen, D. and Chen, Y., (2003), Association between winter temperature in China and upper air circulation over east Asia revealed by canonical correlation analysis. *Global and Planetary Change,*

Clark, P.J. and Evans, F.C., (1954), Distance to nearest neighbour as a measure of spatial relationships in populations, *Ecology*, **35**, 445-453.

Cohen, S.T., (1983), Classification of 500mb height anomalies using oblique rotated principal components *Journal of Applied Meteorology*, **22**, 1975-1988.

Compagnucci, R.H., Araneo, D. and Canziani, P.O., (2001), Principal Sequence Pattern Analysis: A new approach to classifying the evolution of atmospheric systems. *International Journal of Climatology,* 21, 197-217.

Comrie, A.C., (1994), A synoptic climatology of rural ozone pollution at three forest sites in Pennysylvania. *Atmospheric Environment,* **28**, 1601-1614.

Comrie, A.C., (1997), Comparing neural networks and regression models for ozone forecasting. *Journal of the Air and Waste Management Association*, **47**, 653-663.

Conway, D., Wilby, R.L. and Jones, P.D., (1996), Precipitation and air flow indices over the British Isles. *Climate Research*, **7**, 169-183.

Corte-Real, J., Xu. H. and Qian, B., (1999), A weather generator for obtaining daily precipitation scenarios based on circulation patterns. *Climate Research*, **13**, 61-75.

Craddock, J.M., (1965), Meteorological application of principal components analysis. *The Statistician,* **15**, 143-156.

Craddock, J.M., (1973), Problems and prospect for eigenvector analysis in meteorology, *The Statistician* **22**, 133-145.

Craddock, J.M. and Flood, C.R., (1969), Eigenvectors for representing the 500 mb geopotential surface over the Northern Hemisphere. *Quarterly Journal of the Royal Meteorological Society,* **95**, 576-593a.

Crane, R.G. and Hewitson, B.C., (1998), Doubled CO_2 precipitation changes for the Susquehanna Basin: downscaling from the GENESIS general circulation model. *International Journal of Climatology*, **18**, 65-76.

CRU (2003), Climatic Research Unit, University of East Anglia. http://www.cru.uea.ac.uk

Danard, M., (1976), A simple model for mesoscale effects of topography on surface winds. *Monthly Weather Review*, **105**, 572-581.

Davis, R.E. and Kalkstein, L.S., (1990), Using a spatial synoptic climatological classification to assess changes in atmospheric pollution concentrations. *Physical Geography*, **11**, 320-342.

Daultrey, S., (1976), *Principal Components Analysis.* Geoabstracts Ltd, Norwich.

Dehn, M., Burger, G., Buma, J. and Gasparetto, P., (2000), Impact of climate change on slope stability using expanded downscaling. *Engineering Geology*, **55**, 193-204.

De Luis, M., Raventos, J., Gonzalez-Hidalgo, J.C., Sanchez, J.R. and Cortina, J., (2000), Spatial analysis of rainfall trends in the region of Valencia (East Spain), *International Journal of Climatology,* **20**, 1451-1470.

DoE (Department of the Environment), (1996), *Review of the Potential of Climate Change in the United Kingdom*. HMSO. London.

Domroes, M., Kaviani, M. and Schaefer, D., (1998), An analysis of regional and intra-annual precipitaion variability over Iran using multivariate statistical methods. *Theoretical and*

Applied Climatology, **61**, 151-159.

Dove, H.W., (1827), Einige meteorologische Unterschungen über den Wind. *Annals of Physics and Chemistry*, **11**, 545-590.

Dytham, C., (1999), *Choosing and Using Statistics: A Biologist's Guide.* Blackwell Science. Oxford.

Easterling, D., (1999), Development of regional climate change scenarios using a downscaling approach. *Climatic Change*, **41**, 615-634.

Ebdon, D. (1985), *Statistics in Geography*, Blackwell, Oxford.

Egger, J. and Hoinka, K.P., (1992), Fronts and orography, *Meteorology and Atmospheric Physics*, **48**, 3-36.

Ekström, M, Jönsson, P. and Bärring, L., (2002), Synoptic pressure patterns associated with major wind erosion events in southern Sweden (1973-1991). *Climate Research,* **23**, 51-66.

El Dessouky, T.M. and Jenkinson, A.F. (1975), An objective daily catalogue of surface pressure, flow and vorticity indices for Egypt and its use in monthly rainfall forecasting. *Synoptic Climatology Branch Memorandum No 46.* Bracknell, Meteorological Office.

El-Kadi, A.K.A. and Smithson, P.A. (1992), Atmospheric classification and synoptic climatology. *Progress in Physical Geography*, **16**, 432-455.

El-Kadi, A.K.A. and Smithson, P.A. (1996), An automated classification of pressure patterns over the British Isles. *Transactions of the Institute of British Geographers,* **21**, 141-156.

El-Kadi, A.K.A.and Smithson, P.A., (2000), Probability assessment of pressure patterns over the British Isles. *International Journal of Climatology*, **20,** 1351-1369.

El Païs, (1992), *Atlas de Espana.* Aguilar. Madrid.

Esteban-Parra, M.J., Rodrigo, F.S. and Castro-Diez, Y., (1998), Spatial and temporal patterns of precipitation in Spain for the period 1880-1992. *International Journal of Climatology*, **18**, 1557-1574.

Estrela, M.J., Peñarrocha, D. and Millán, M., (2000), Multi-annual drought episodes in the Mediterranean (Valencia region) from 1950-1996. A spatio-temporal analysis. *International Journal of Climatology*, **20**, 1599-1618.

Etienne, P. and Godard, A., (1970), *Climatologie.* Armand Colin Collection. University of Paris.

Everitt, B., (1980), *Cluster Analysis.* Heine. London.

Fernandez Mills G., (1995), Principal component analysis of precipitation and rainfall regionalization in Spain. *Theoretical Applied Climatology*, **50,** 169-183.

Flocas, A.A. , (1984), The annual and seasonal distribution of fronts over Central Southern Europe and the Mediterranean. *Journal of Climatology*, **4**, 255-267.

Florit, A. and Jansa, A. (1979), Situaciones de presion en el Mediterraneo Occidental. Repercusiones sobre el tiempo de Menorca y en el resto de Espana. *Trabajos de Geografia.* Departamento de Geografia. Universidad de Palma de Mallorca.

Frakes, B. and Yarnal, B., (1997), A procedure for blending manual and correlation-based synoptic classifications. *International Journal of Climatology,* **17**, 1381-1396.

Gajic-Capka, M., (1993), Fluctuations and trends of annual precipitation in different climatic regions of Croatia, *Theoretical and Applied Climatology*, **47**, 215-221.

Garcia, J.A., Serrano, A., and de la Cruz Gallego, M., (2002), A spectral analysis of Iberian monthly rainfall, *Theoretical and Applied Climatology,* **71**, 77-95.

Garcia, L. and Rieja, A., (1994), *Tiempo y clima en Espana.* Dossat. Madrid.

Genoves, A. and Jansa, A., (1989), *A statistical approach to mesoscale non-alpine west Mediterranean cyclogenesis.* WMO/TP no 298, 77-85.

Gil Olcina, A., (1989), Causas climaticas de las Riadas en aveniadas fluviales e inundaciones en la cuenca Mediterranae. Instituto Universtiatrio de Geografia, Universidad Alicante y caja Ahorros Mediterano, Alicante, 15-30.

Gimeno, L., Ribera, P., Iglesias, R., de la Torre, L., Garcia, R. and Hernandez, E., (2002), Identification of empirical relationships between indices of ENSO and NAO and agricultural yields in Spain. *Climate Research,* **21**, 165-172.

Giorgi, F., (1990), Simulation of regional climate using a limited area model nested in a general circulation model, *Journal of Climate*, **3**, 941-963.

Glasspoole, J., (1922), Relation between annual rainfall over Europe, Oxford and Glenquoich. *British Rainfall,* **65**, 254-269.

Gold, E., (1920), Aids to forecasting: types of pressure distribution, with notes and tables for the fourteen years 1905-1918. *Geophysical Memoir,* **2 (16),** 149-174.

Goldreich, Y., (1994), The spatial distribution of annual rainfall in Israel – a review. *Theoretical and Applied Climatology*, **50**, 45-59.

Gong, X. and Richman, M.B., (1992), An examination on methodological issues in clustering North American precipitation. PP J98- J112 in *Proceeding of the 5th International Meeting on Statistical Climatology*. Atmospheric Environment Service of Canada, Toronto, June 22-26 1992.

Gonzalez-Hidalgo, J.C., De Luis, M., Raventos, J. and Sanchez, J.R., (2001), Spatial distribution of seasonal rainfall trends in a Western Mediterranean area. *International Journal of Climatology*, **21**, 843-860.

Goodess, C.M. and Palutikof, J.P., (1998), Development of daily rainfall scenarios for south-east Spain using a circulation-type approach to downscaling. *International Journal of Climatology*, **10,** 1051-1083.

Goossens, Ch. (1986), Regionalization of the Mediterranean climate. *Theoretical and Applied Climatology*, **37**, 74-83.

Gower, J.C. and Banfield C.F. (1975), Goodness-of-fit criteria for hierarchical classification and their empirical distributions. In *Proceedings of the International Biometric Conference,* pp. 347-362. Raleigh, N.C. Biometric Society.

Gregory, S., (1975), On the delineation of regional patterns of recent climatic fluctuations *Weather,* **30**, 276.

Griffith, D.A. and Amrhein, C.G., (1997), *Multivariate Statistical Analysis for Geographers.* Prentice hall. New Jersey.

Groisman, P.Y., Karl, T.R., Easterling, D.R., Knight, R.W., Jamason, P.F., Hennessy, K.J., Suppiah, R., Page, C.M., Wibig, J., Fortuniak, K., Razuvaev, V.N., Douglas, A., Forland, E. and Zhai, P.M., (1999), Changes in the probability of heavy precipitation: Important indicators of climatic change. *Climatic Change,* **42**, 243-283.

Grotch, S.L. and MacCracken, M.C., (1991), The use of General Circulation Models to predict regional climate change. *Journal of Climate,* **4**, 286-303.

Grundstein, A.J. and Leathers, D.J., (1999), A spatial analysis of snow-surface energy exchanges over the northern Great Plains of the United States in relation to synoptic scale forcing mechanisms. *International Journal of Climatology,* **19**, 489-511.

Hair, J.F., (1995), *Multivariate Data Analysis.* Prentice Hall Englewood Cliffs.

Haltimer, G.J. and Martin, F.L. (1957), *Dynamical and Physical Meteorology* McGraw-Hill. London p 470.

Hanssen-Bauer, I. and Førland, E., (2000), Temperature and precipitation variations in Norway 1900-1994 and their links to atmospheric circulation. *International Journal of Climatology,* **20**, 1693-1708.

Hartigan, J.A. and Wong, M.A., (1979), Algorithm AS 136: a k-means clustering algorithm *Applied Statistics,* **28**, 100-108.

Hartley, S. and Keables, M.J., (1998), Synoptic associations of winter climate and snowfall variability in New England, USA, 1950-1992. International Journal of Climatology, 18, 281-298.

Hay, R.F.M., (1949), The rainfall in eastern Scotland in relation to the synoptic situation. Meteorological Office Professional Notes 98.

Hay, L.E., McCabe, G.J., Wolock, D.M. and Ayers, M.A. (1991), Simulation of precipitation by weather type analysis, *Water Resources Research*, **27**, 493-501.

Hay, L.E., McCabe, G.J., Wolock, D.M. and Ayers, M. A. (1992), Use of weather types to disaggregate general circulation model predictions. *Journal of Climate*, **5** 1002-1011.

Hayhoe, H.N., (2000), Improvements of stochastic weather data generators for diverse climates. *Climate Research*, **14**, 75-87.

Hellström, C., Chen, D. Achberger, C. and Räisänen, J. (2001), Comparison of climate change scenarios for Sweden based on statistical and dynamical downscaling of monthly precipitation. *Climate Research,* **19**, 45-55.

Hewitson, B.C. and Crane, R.G. (1994), Precipitation controls in southern Mexico, in Hewitson, B.C. and Crane, R.G., (Eds) (1994), *Neural Nets: Applications in Geography* Kluwer Academic Publishers.

Hewitson B.C. and Crane, R.G., (1996), Climate downscaling: techniques and application. *Climate Research,* **7**, 85-95.

Hewitson B.C. and Crane, R.G.,(2002), Self organizing maps: application to synoptic climatology *Climate Research, 22*, 13.-26.

Hoard, D.E. and Lee, J.T., (1986), Synoptic classification of a ten year record of 500mb weather maps for the western United States. *Meteorology and Atmospheric Physics*, 35, 96-102.

Holton, J.R., (1979), *Numerical Prediction. An introduction to Dynamic Meteorology,* (2nd Edn). Academic Press. San Diego.

Hughes, J.P. and Guttorp, P., (1994), A class of stochastic models for relating synoptic atmospheric patterns to regional hydrologic phenomena. *Water Resources Research.* **30**, 1535-1546.

Hulme,M., (1992), A 1951-80 global land precipitation climatology for the evaluation of General Circulation Models *Climate Dynamics*, **7**, 57-72

Hulme,M., (1994), Validation of large-scale precipitation fields in General Circulation Models pp.387-406 in, *Global precipitations and climate change* (eds.) Desbois,M. and Desalmand,F., NATO ASI Series, Springer-Verlag, Berlin,466pp.

Hulme, M., (2000), 'gu23wld0098.dat', Version 1.0, March 1999. Constructed and supplied by Dr Mike Hulme at the Climatic Research Unit, University of East Anglia, Norwich, UK. This work has been supported by the UK Department of the Environment, Transport and the Regions (Contract EPG 1/1/85).

Hulme,M., Osborn,T.J. and Johns, T.C., (1998), Precipitation sensitivity to global warming: Comparison of observations with HadCM2 simulations *Geophysical Research Letters*, **25**, 3379-3382.

Hulme, M., Briffa, K.R., Jones, P D. and Senior, C.A., (1994), Validation of GCM control simulation using indices of daily airflow types over the British Isles. *Climate Dynamics*, **9**, 95-105.

Hurrell, J.W., (1995), Decadal trends in the North Atlantic Oscillation: Regional temperatures and precipitation. *Science,* **69**, 676-679.

Hurrell, J.W. and van Loon, H., (1997), Decadal variations in climate associated with the North Atlantic Oscillation. *Climatic Change*, **36**, 301-326.

Huth, R., (1996), An intercomparison of computer-assisted circulation classification methods, *International Journal of Climatology*, **16**, 893-922.

Huth, R., (1999), Statistical downscaling in central Europe: evaluation of methods and potential predictors. *Climate Research,* **13**, 91-101.

Huth, R. and Kysely, J., (2000), Constructing site-specific climate change scenarios on a monthly scale using statistical downscaling. *Theoretical and Applied Climatology*, **66,** 13-27.

Inamdar, S.R. and Singh, S.V., (1993), Relationship between circulation and rainfall over India during the south-west Monsoon season, Part II: 700hPa contour height field and some synoptic indices. *Theorerical and Applied Climatology*, **48**, 1-14.

Instituto de Meteorologia (1988), *Notas para una Climatologia de.....*Publicacion Serie K, INM, Ministerio de Transport, Turismo Y Communicaciones, Madrid.

IPCC (1995), *Intergovernmental Panel on Climate Change Second Assessment – Climate Change 1995.* IPCC, Geneva.

IPCC (2001a*), Intergovernmental Panel on Climate Change Third Assessment Report – Climate Change 2001.* The Scientific Basis. IPCC, Geneva.

IPCC (2001b), *Intergovernmental Panel on Climate Change Third Assessment Report – Climate Change 2001. Synthesis Report.* IPCC, Geneva.

Jenkins, G.S. and Barron, E.J., (1996), *General circulation model and coupled regional climate model simulations over the eastern United States.* GENESIS and RegCM2 simulations. Global Planet Change.

Jenkinson, A.F. and Collison, B.P. (1977), An initial climatology of gales over the North Sea. *Synoptic Climatology Branch Memorandum, No 62,* Meteorological Office. Bracknell.

Joliffe, I.T. (1990), Principal Component Analysis: a beginner's guide. *Weather,* **45**, 375-382.

Jones, G.V. and Davis, R.E., (2000), Using a synoptic climatological approach to understand climate-viticulture relationships. *International Journal of Climatology,* **20**, 813-837.

Joubert, A.M. and Hewitson, B.C., (1997), Simulating present and future climates of southern Africa using general circulation models. *Progress in Physical Geography*, **21**, 51-78.

Kaiser, H.F., (1958), The Varimax criterion for analytical rotation in factor analysis. *Psychometrica*, **23**, 187-200.

Kalkstein, L.S., Tan, G. and Skindlov, J.A. (1987), An evaluation of three clustering procedures for use in synoptic climatological classification. *Journal of Climate and Applied Meteorology*, **26**, 717-730.

Karl, T.R., Knight, R.W. and Plummer, N., (1995), Trends in high-frequency climate variability in the twentieth century. *Nature*, **377**, 217-220.

Karl, T.R. and Riebsame, W.E., (1984), The identification of 10- to 20-year temperature and precipitation fluctuations in the contiguous United States. *Journal of Climate and Applied Meteorology,* **23**, 950-966.

Karl, T.R., Way, W.C, Schlesinger, M.E., Knight, R.W. and Portman, D., (1990), A method of relating GCM simulated climate to the observed local climate. Part I. Seasonal statistics. *Journal of Climate*, **3**, 1053-1079.

Katz, R.W., (1977), Precipitation as a chain-dependent process. *Journal of Applied Meteorology*, **16**, 671-676.

Katz, R.W.and Brown, B.G., (1992), Extreme events in a changing climate. Variability is more important than averages. *Climatic Change*, **21**, 289-302.

Katz, R.W. and Parlange, M.B., (1996), Mixtures of stochastic processes: applications to statistical downscaling. *Climate Research*, **7**, 185-193.

Keevalik, S., Post, P. and Tuulik, J., (1999), European circulation patterns and meteorological situation in Estonia. *Theoretical and Applied Climatology*, **63**, 117-127.

Kent, M., Newnham, R. and Essex, S., (2002), Tourism and sustainable water supply in Mallorca: a geographical analysis. *Applied Geography*, **22**, 351-374.

Kidson, J.W., (1994), An automated procedure for the identification of synoptic types applied to New Zealand. *International Journal of Climatology*, **14**, 711-721.

Kidson, J.W., (1997), The utility of surface and upper air data in synoptic climatological specification of surface climatic variables. *International Journal of Climatology*, **17**, 399-413.

Kidson, J.W., (2000), An analysis of New Zealand synoptic types and their use in defining weather regimes. *International Journal of Climatology,* **20**, 299-316.

Kim, J-W., Chang, J-T., Baker, N.L., Wilks, D.S. and Gates, W.L, (1984), The statistical problem of climate inversion: determination of the relationship between local and large scale climate. *Monthly Weather Review*, **112**, 2069-2077.

Kirchofer, W. (1973), Classification of European 500mb patterns. *Arbeitsbericht der Schweizerischen Meteorologischen Zentralanstalt* Nr 43, Geneva.

Kohonen, T., (1984), *Self-organization and Associative Memory.* Springer Verlag, Berlin. 312p.

Köppen, W., (1874), Über die Abhängigkeit des Klimatischen Charakters der Winde von ihrem Usprunge. *Rep Met* (St Petersburg), **4**, 15.

Kruizinga, S., (1979), Objective classification of daily 500 mb patterns. *Sixth Conference on Probability and Statistics in Atmospheric Sciences.* American Meteorological Society. Boston, Massachusetts, 126-129.

Kulkarni, A. and Kripalani, R.H., (1998), Rainfall patterns over India: Classification with fuzzy c-means method. *Theoretical and Applied Climatology*, **59**, 137-146.

Lamb, H.H., (1950), Types and spells of weather around the year in the British Isles; annual trends, seasonal structure of the year, singularities. *Quarterly Journal of the Royal Meteorological Society*, **76**, 393-429.

Lamb, H.H. (1972), British Isles weather types and a register of the daily sequences of circulation patterns, 1861-1971. *Meteorological Office Geophysical Memoir*, **116**, HMSO. London

Lamb, H.H., (1977), *Climate Present, Past and Future. Climatic History and the Future Volume 2.* Methuen and Co Ltd London.

Lamb, P. and Peppler, R., (1987), North Atlantic Oscillation: Concept and an Application.

Bulletin of the American Meteorological Society. **68**, 1218-1225.

Lana, X. and Burgueño, A., (2000), Some statistical characteristics of monthly and annual pluviometric irregularity for the Spanish Mediterranean coast. *Theoretical and Applied Climatology*, **65**, 79-97.

Lavorel, S., Canadell, J., Ramball, S. and Terradas, J., (1998), Mediterranean terrestrial ecosystems: research priorities on global change effect. *Global Ecology and Biogeography Letters*, **17**, 157-166.

Legates, D.R., (1991), The effect of domain shape on principal component analyses. *International Journal of Climatology*, **11**, 135-146.

Leighly, J.B., (1949), Climatology since 1800. *Transactions of the American Geophysical Union*, **30**, 658-672.

Levick, R.B.M., (1949), Fifty years of English weather. *Weather*, **4**, 206-211.

Levick, R.B.M., (1950), Fifty years of British weather. *Weather*, **5**, 245-247.

Linacre, E., (1992), *Climate Data and Resources. A reference and a guide*. Routledge. London.

Lindersen, M-L., (2001), Objective classification of atmospheric circulation over southern Scandinavia. *International Journal of Climatology*, **21**, 155-169

Littmann, T., (2000), An empirical classification of weather types in the Mediterranean Basin and their interrelation with rainfall. *Theoretical and Applied Climatology*, 66, 161-171.

Llasat, M. (1991), *Gota Fria*, Boixareu Universitaria. Barcelona.

Lolis, C.J., Bartzokas, A. and Katsoulis, B.D., (2002), Spatial and temporal 850 hPa air temperature and sea surface temperature covariances in the Mediterranean region and their connection to atmospheric circulation. *International Journal of Climatology*, **22**, 663-676

Lorenz, E.N., (1956), Empirical orthogonal functions and statistical weather prediction. *Scientific Report*, Statistical Forecasting Project, Department of Meteorology, Massachussetts Institute of Technology, NTIS AD 110268.

Lund, I.A. (1963), Map-pattern classification by statistical methods. *Journal of Meteorology*, **2**, 56-65.

McGregor, G.R., (1999), Winter ischaemic heart disease deaths in Birmingham, United Kingdom: a synoptic climatological analysis. *Climate Research*, **13**, 17-31.

McKendry, I.G., (1994), Synoptic circulation and summertime ozone concentrations at Vancouver, British Columbia. *Journal of Applied Meteorology*, **33**, 627-641.

Maheras, P., (1988), Changes in precipitation conditions in the western Mediterranean over the last century. *Journal of Climatology*, **8**, 179-189.

Maheras, P, Xoplaki, E., Davies, T., Martin-Vide, J. Barriendos, M. and Alcofarado, M.J., (1999), Warm and cold monthly anomalies across the Mediterranean basin and their relationship with circulation 1860-1990. *International Journal of Climatology*, **19**, 1697-1715.

Makrogiannis, T.J., (1984), Local zonal index circulation change in the European area 1873-1972. *Arch Met Geoph. Biocl*, **34B**, 39-48.

Makrogiannis, T.J. and Giles, B.D., (1980), Frequencies, individual and mean tracks of moving anticyclones over south-east Europe. *Journal of Meteorology,* **5.**

Makrogiannis, T.J., Sahsamanoglou, H.S., Flocas, A.A. and Bloutsos, A.A. (1991), Analysis of the monthly Zonal index values and long-term changes of circulation over the North Atlantic and Europe. *International Journal of Climatology*, **11**, 493-503.

Martin, E., Timbal, B. and Brun, E., (1997), Downscaling of general circulation model outputs: simulation of the snow climatology of the French Alps and sensitivity to climate change. *Climate Dynamics*, **13,** 45-56.

Martin Vide, J., (1988), *Espana. El medio y la historia.* Amaya. Madrid.

Mass, C.F., (1991), Synoptic frontal analysis – time for a reassessment. *Bulletin of the American Meteorological Society*, **72**, 348-363.

Mayes, J. (1996), Spatial and temporal fluctuations of monthly rainfall in the British Isles and variations in the mid-latitude westerly circulation. *International Journal of Climatology*, **16**, 585-596.

Mearns. L.O., Giorgi, F., McDaniel, L. and Shields, C., (1995), Analysis of daily variability of precipitation in a nested regional climate comparison with observation and doubled CO2 results. *Global and Planetary Change,* **10**, 55-78.

Mearns, L.O., Rosenweig, C. and Goldberg, R., (1996), The effect of changes in daily and interannual climatic variability on CERES-wheat: a sensitivity study. *Climatic Change*, **32,** 257-292.

Mearns, L.O., Rosenweig, C. and Goldberg, R., (1997), Mean and variance change in climate scenarios: methods, agricultural applications and measures of uncertainty. *Climatic Change,* **35**, 367-396.

Meteorological Office (1962), *Weather in the Mediterranean. Volume 1.* HMSO. London.

Milligan, G.W., (1980), An examination of the effect of six types of error perturbation on fifteen clustering algorithms. *Psychometrika*, **45**, 324-342.

Mitchell, T.D. and Hulme, M., (1999), Predicting regional climate change. Living with uncertainty. *Progress in Physical Geography,* **23**, 57-78.

Mo, K.C. and Livezey, R.E., (1986), Tropical–extratropical geopotential height teleconnections during the Northern Hemisphere winter. *Monthly Weather Review*, **114**, 2488-2515.

Mojeno, R., (1977), Heirarchical grouping methods and stopping rules: an evaluation. *Computer Journal*, **20**, 359-363.

Moron, V. and Ward, M.N., (1998), ENSO teleconnections with climate variability in the European and African sector. *Weather*, **53**, 287-295.

Moses, T., Kiladis, G.M., Diaz, H.F. and Barry, R.G., (1987), Characteristics and frequency of reversals in the mean sea level pressure in the North Atlantic sector and their relationship to long-term temperature trends. *Journal of Climatology,* **7**, 13-30.

Murphy, J., (1999), An evaluation of statistical and dynamical techniques for downscaling local climate. *Journal of Climate* , **12**, 2256-2284.

Murphy, S.J. and Washington, R., (2001), United Kingdom and Ireland precipitation variability and the North Atlantic sea level pressure field. *International Journal of Climatology*, **21,** 939-959

Murray, R. (1973), Monthly mean temperature related to synoptic types over Britain specified by PCSM indices. *Meteorological Magazine,* **101**, 3.5-311.

Murray, R. and Lewis, R.P.W. (1966), Some aspects of the synoptic climatology of the British Isles as measured by simple indices. *Meteorological Magazine,* **95**, 193-203.

Murray, R. and Benwell, P., (1970), PSCM indices in synoptic climatology and long range forecasting. *Meteorological Magazine,* **99,** 232-244.

Musk .L.F. (1988), *Weather Systems. Cambridge University Press.* Cambridge.

O' Hare G.P. and Wilby, R. (1995), A review of ozone pollution in the United Kingdom and Ireland with an analysis using Lamb Weather Types. *The Geographical Journal,* **161**, 1-20

North, G.R., Bell, T., Calahan, R.F.and Moeng, F.J., (1982), Sampling errors in the estimation of empirical orthogonal functions. *Monthly Weather Review*, **110**, 699-706.

Olcina, J. (1994), Metodos de classificacion sinoptica en Espana. Revision y propuesta. *Estudios Geograficos*, **55**, 357-380.

Olsson, J., Uvo, C.B. and Jinno, K., (2001), Statistical atmospheric downscaling of short term extreme rainfall by neural networks *Physics and Chemistry of the Earth part B Hydrology, Oceans and Atmosphere*, **26**, 695-700.

Openshaw, S. and Openshaw, C., (1994), *Artificial Intelligence in Geography.* John Wiley. Chichester.

Paricio, P.L. and Nadal, J.M. (1979), Catalogo de tipos sinopticos para un estudio climatico del Este de la Peninsula Iberica y Baleares. In *Aportacions en homenatge al geograf Salvador Llobet.* pp. 11-27 Dep. de Geografia, Universidad de Barcelona.

Periago, M.C., Lana, X., Serra, C. and Fernandez Mills, G, (1991), Precipitation regionalization: an application using a meteorological network in Catalonia (NE Spain). *International Journal of Climatology*, **11**, 529-543.

Perry, A.H., (1997) The Mediterranean Climate in King, R, Proudfoot, L. and Smith, B. (eds), *The Mediterranean: Environment and Society.* London. Edward Arnold.

Perry, A.H. and Mayes, J.C., (1998), The Lamb weather type catalogue, *Weather*, **53**, 222-228.

Peterson, T. and Easterling, D.R., (1994), Creation of a homogeneous composite climatological reference series. *International Journal of Climatology*, **14**, 671-679.

Pettersson, S., (1956), *Weather Analysis and Forecasting.* Vol 1. MacGraw-Hill. New York

Piervitali, E, Colacino, M. and Conte, M., (1998), Rainfall over the central-western Mediterranean basin in the period 1951-1995 Part 1: precipitation trends. *Nuovo Cimento della Societa Italiana di Fisica C-Geophysics and Space Physics,* **21**, 331-344

Plaut, G. and Simonnet. E., (2001), Large scale circulation classification weather regimes local climate over France, the Alps and Western Europe. *Climate Research*, **17**, 303-324.

Pounds, N.J., (1963), *Political Geography.* New York.

Preisendorfer and Barnet, T.P, (1977), Significance tests for empirical orthogonal functions. *Pre-prints Fifth Conference on probability and Statistics in Atmospheric Science.* Las Vegas Nevada. American Meteorological Society, 169.

Preisendorfer, R.W. (1988), *Principal Component Analysis in Meteorology and Oceanography.* Elsevier. London.

Prezerakos, N.G., (1998), Lower tropospheric structure and synoptic scale circulation patterns during prolonged temperature inversions over Athens, Greece. *Theoretical and Applied Climatology*, **60**, 63-76.

Puigdefabregas, J. and Mendizabal, T., (1998), Perspectives on desertification: Western Mediterranean. *Journal of Arid Environments*, **39**, 209-224.

Quadrelli, R., Lazzeri, M., Cacciamani, C. and Tibaldi, S., (2001), Observed winter Alpine precipitation variability and links with large-scale circulation patterns. *Climate Research*, **17**, 275-284.

Quereda, J., (1983), Enero-Junio de 1983 el semestre mas arido del siglo. *Boletin de la Sociedad Castellonese de Cultura.* **T LIX** 487-497.

Radinovic, D., (1987), Mediterranean cyclones and their influence on the weather and climate. WMO, PSMP Rep Ser num 24.

Ramos, M.C., (2001), Rainfall distribution patterns and their change over time in a Mediterranean area. *Theoretical and Applied Climatology*, **69**, 163-170.

Rasmussen, E.M. and Carpenter, T.H., (1982), Variations in tropical sea surface temperature and surface wind fields associated with the southern oscillation/El Nino. *Monthly Weather Review*, **110**, 354-384.

Rasmussen, E.M. and Wallace, J.M., (1983), Meteorological aspects of the El Nino/southern oscillation. *Science*, **222**, 1195-1202.

Reinel, H., (1952), Die zugbahnen der hochdruckbiete uber Europa alt Kilmatologisches problem. *Mitt. Frank. Geogr. Ges*, **6**, 1-73.

Richardson, C.W., (1981), Stochastic simulation of daily precipitation, temperature and solar radiation. *Water Resources Research*, **17**, 182-190.

Richman, M.B., (1981), Obliquely rotated principal components: an improved meteorological map typing technique. *Journal of Applied Meteorology*, **20**, 1145-1159.

Richman, M.B., (1983), *Specification of complex modes of circulation with T-mode factor analysis.* Reprints Second International Conference on Statistical Climatology. Lisbon, Portugal; National Institute of Meteorology and Geophysics. 5.1.1.

Richman, M.B. (1986), Rotation of principal components. *International Journal of Climatology,* **6**, 293-335.

Rind, D., Goldberg, R. and Ruedy, R., (1992), Change in climate variability in the 21st century. *Climate Change*, **14**, 5-37.

Roberts, C., (2002), Drought management in the Rio Guadalhorce region of Andalucia, Southern Spain. *Land Degradation and Development*, **13**, 151-163.

Robinson, P. and Henderson-Sellers, A., (1997), *Contemporary Climatology.* Longman London.

Rocha, A. (1999), Low frequency variability of seasonal rainfall over the Iberian Peninsula and ENSO. *International Journal of Climatology*, **19**, 889-902.

Rodo, X., Baert, E. and Comin, F., (1997), Variations in seasonal rainfall in southern Europe during the present century , Relationships with the North Atlantic Oscillation and the El Nino Southern Oscillation. *Climate Dynamics*, **13**, 273-284.

Rodrigo, F.S., Esteban-Parra, M.J., Pozo-Vasquez, D. and Castro-Diez, Y., (1999), A 500 year precipitation record in Southern Spain, *International Journal of Climatology*, **19**, 1233-1254.

Rodrigo, F.S., Esteban-Parra, M.J., Pozo-Vasquez, D. and Castro-Diez, Y., (2000), Rainfall variability in southern Spain on decadal to centennial time scales. *International Journal of Climatology*, **20**, 721-732.

Rodriguez-Iturbe, I., Febres de Power, B., Sharifi, M.B, and Georgakakos, K-P., (1989), Chaos in rainfall. *Water Resources Research,* **25**, 1667-1675.

Rodriguez-Puebla, C., Encinas, A.H., Nieto, S. and Garmendia, J. (1998), Spatial and temporal patterns of annual precipitation variability over the Iberian peninsula. *International Journal of Climatology*, **18**, 299-316.

Rogers, J.C., (1976), Sea surface temperature anomalies in the eastern North Pacific and associated wintertime fluctuations over North America 1960-1973. *Monthly Weather Review*, **104**, 985.

Rogerson, P.A., (2001) *Statistical methods for Geography.* Sage. London

Romero, R., Sumner, G., Ramis, C. and Genoves, A., (1999), A classification of the atmospheric circulation patterns producing significant daily rainfall in the Spanish Mediterranean area. *International Journal of Climatology*, **19**, 765-786.

Ronberg, B. and Wang, W.C., (1987), Climate patterns derived from Chinese proxy precipitation records. An evaluation of the station networks and statistical techniques. *Journal, of Climate,* **7**, 391-416.

Rossby, C.G., and collaborators (1939), Relation between variation in the intensity of the zonal circulation of the atmosphere and the displacement of the semi-permanent centers of action. *Journal of Marine Research*, **2**, 38-49.

Roswintiarti, O., Niyogo, D.S. and Raman, S., (1998), Teleconnections between tropical Pacific sea surface temperature anomalies and North Carolina precipitation anomalies during El Nino events. *Geophysical Research Letters,* **25**, 4201-4204.

Rummukainen, M., (1997), *Methods for the statistical downscaling of GCM simulation. SWECLIM Report.* Noorrkopping. Rossby Centre. SMHI.

Sailor, D. and Li, X., (1999) A semi-empirical downscaling approach for predicting regional temperature impacts associated with climate change. *Journal of Climate,* **12**, 103-114.

Sanchez Rodriguez, J., (1993), *Situaciones atmosfericas en Espana.* Ministerio de Obras Publicas, Transportes y Medio Ambiente. Madrid.

Saunders, I.R. and Byrne, J.M., (1998), Using synoptic scale and geopotential height fields generating grid scale precipitation. *International Journal of Climatology*, **19**, 1165-1176.

Schoof, J. and Pryor, S.C., (2001), Downscaling of temperature and precipitation: a comparison of regression-based methods and artificial neural networks: circulation-based downscaling, Mid-Western United States. *International Journal of Climatology*, **21**, 773-790.

Semenov, M.A. and Porter, J.R., (1994), The implications of non-linear responses in modelling of growth and development of wheat in *Predictability and non-linear modelling in natural sciences and economics* by Grasman, J. and Van Straten, G. (eds) Pudoc. Wageningen.

Serra, C., Fernandez Mills, G., Periago, M.C. and Lana, X., (1998), Surface synoptic circulation and daily precipitation in Catalonia. *Theoretical and Applied Climatology* ,**59**, 29-49.

Serrano, A., Garcia, J., Mateos, V., Cancillo, M. and Garrido, J., (1999), Monthly modes of variation of precipitation over the Iberian peninsula. *Journal of Climate*, **12**, 2894-2919

Sharma, S.C., (1996), *Applied Multivariate Techniques.* Wiley. New York.

Skinner, W.R., Flannigan, M.D., Stocks, B.J., Martell, D.L, Wotton, B.M., Todd, J.D., mason, J.AS., Logan, K.A. and Bosch, E.M., (2002), A 500 hPa synoptic wildland fire climatology for large Canadian forest fires, 1959-1996. *Theoretical and Applied Climatology,* **71**, 157-169.

Smith, B. (1997), Water: a critical resource. In King, R, Proudfoot, L. and Smith, B. (eds), *The Mediterranean: Environment and Society.* London. Edward Arnold.

Smithson, P., (1986), Synoptic and Dynamic Climatology, *Progress in Physical Geography,* **10,** 100-110

Smithson, P., (1987), Synoptic and Dynamic Climatology, *Progress in Physical Geography,* **11**, 121-132.

Smithson, P., (1988), Synoptic and Dynamic Climatology, *Progress in Physical Geography,* **12,** 119-129.

Spellman, G. (1996), Synoptic climatology, 'objective' weather typing and tropospheric ozone. *Environment and Society*, **2**, 7-15.

Spellman, G. (1997a), Evaluating indices of mid-latitude circulation. *Journal of Meteorology*, **22**, 237-242.

Spellman, G., (1997b), An air mass based classification of weather in Northampton. *East Midland Geographer*, **20**, 50-62

Spellman, G., (1998a), Analysing air pollution meteorology, *Weather*, **53** 34-42

Spellman, G. (1998b), Investigating the synoptic climatology of precipitation in Mallorca, Spain. *Journal of Meteorology,* **23**, 117-130.

Spellman, G., (1999), An application of artificial neural networks to the prediction of surface ozone concentrations in the United Kingdom. *Applied Geography*, **19**, 123-136

Spellman, G. (2000a), The application of an objective weather-typing system to the Iberian peninsula. *Weather*, **55**, 375-385

Spellman, G. (2000b), The use of an index based regression model for precipitation analysis on the Iberian peninsula. *Theoretical and Applied Climatology* . **66**, 229-240.

Spellman, G., (2000c), Regionalization of rainfall in the Segura River basin, SE Spain. School of Environmental Science Working Paper. http://www.northampton.ac.uk

Spellman, G., (2003), On the universal applicability of seasonal divisions. Unpublished commentary. http://www.northampton.ac.uk/

Stehlik, J. and Bárdossy, A., (2002), Multivariate stochastic downscaling model for generating daily precipitation series based on atmospheric circulation. *Journal of Hydrology,* **256**, 120-141.

Stephenson, D.B., Pavan, V. and Bojaru, R., (2000), Is the North Atlantic Oscillation a random walk? *International Journal of Climatology*, **20b,** 1-18.

Stone, R.C. (1989), Weather types at Brisbane, Queensland: an example of the use of principal component and cluster analysis. *International Journal of Climatology,* **9**, 3-32.

Stooksbury, D.E. and Michaels, P.J., (1991), Cluster Analysis of South-eastern US Climate stations, *Theoretical and Applied Climatology* . **44**, 143-150.

Sumner, G.N., (1983), Seasonal changes in the distribution of rainfall over the Great Dividing Range: general trends. *Australian Meteorological Magazine*, **31**, 121-130.

Sumner, G. (1996) Daily precipitation patterns over Wales: towards a detailed precipitation climatology. *Transactions of the Institute of British Geographers*, **21**, 157-176.

Sumner, G., Guijarro, J.A. and Ramis, C., (1995), The impact of surface circulation on significant daily rainfall over Mallorca, Spain. *International Journal of Climatology,* **15**, 673-696.

Sumner, G., Homar, V. and Ramis, C. (2001), Precipitation seasonality in eastern and southern coastal Spain. *International Journal of Climatology,* **21**, 219-247.

Sumner, G., Ramis, C. and Guijarro, J.A, (1993), The spatial organization of daily rainfall patterns over Mallorca. *International Journal of Climatology,* **13**, 89-109.

Sweeney, J.C. and O' Hare, G.P. (1992), Geographical variations in precipitation yields and circulation types in Britain and Ireland. *Transactions of the Institute of British Geographers,* **17**, 448-463.

Todorovic, P. and Woolhiser, D.A., (1975), A stochastic model of *n*-day precipitation *Journal of Applied Meteorology*, **14**, 17-24.

Tout, D.G and Wheeler, D.A., (1990), The early autumn storms of 1989 in eastern Spain. *Journal of Meteorology,* **15**, 238-248.

Trigo, R.M. and Dacamara, C.C., (1995), Long term variability of circulation weather types affecting Portugal. *Mediterranean desertification and Land Use,* Working Paper Number 55.

Trigo, R.M. and Palutikof, J.P., (1999), Simulation of daily temperatures for climate change scenarios over Portugal: a neural network model approach *Climate Research,* **13,** 45-59.

Van Oldenburgh, G.J., Burgens, G. and Klein Tank, A. (2000), On the El Nino teleconnection and spring precipitation in Europe. *International Journal of Climatology*, **20**, 565-574.

Von Storch, GH., Zorita E. and Cubasch, U. (1993), Downscaling of global climate change estimates to regional scales: an application to Iberian rainfall in wintertime. *Journal of Climate*, **6**, 1161-1171.

Vedecchia, M., Visconti, G., D'Andrea, F. and Tibaldi, S., (1996), A neural network approach for blocking recognition. *Geophysical Research Letters*, **23**, 2081-2084.

Walker, G.T., (1923), Correlation in seasonal variations of weather, VIII: A preliminary study of world weather. *Memorandum of the Indian Meteorological Department* (Poona), **24**, 75-132.

Walker, G.T., (1924), Correlation in seasonal variations of weather, IX: A further study of world weather. *Memorandum of the Indian Meteorological Department* (Poona), **24**, 275-332.

Walker, G.T. and Bliss, E.W., (1930), World Weather, IV: some applications to seasonal foreshadowing. *Memorandum of the Royal Meteorological Society*, **3**, 81-95

Wallace, J.M. and Gutzler, D.S., (1981), Teleconnections in the geopotential height field during the Northern Hemisphere winter. *Monthly Weather Review*, **109,** 784-812.

Walland, D. and Simmonds, I., (1997), North American and Eurasian snow area variability. *Tellus*, **A49**, 503-512.

Walsh, J.E., Richman, M.B. and Allen, D.W., (1982), Spatial coherence of monthly precipitation in the United States, *Monthly Weather Review*, **110**, 272.

Weber, R.O. and Furger, M., (2001), Climatology of near-surface wind patterns over Switzerland. *International Journal of Climatology*, **21**, 809-827.

Weichert, A. and Burger, G., (1998), Linear versus non-linear techniques in downscaling. *Climate Research*, **10**, 83-93.

Wheater, C.P. and Cook, P.A., (2000), *Using statistics in Environmental Science*. Routledge. London.

Wheeler, D. (1990). Majorca's severe storms of September 1989: a reminder of Mediterranean uncertainty. *Weather,* **45,** 21-26.

Wheeler, D., (1996), Spanish Climate. Regions and diversity. *Geography Review,* **11**, 34-40.

White, D., Richman, M. and Yarnal, B., (1991), Climate regionalization and the rotation of principal components. *International Journal of Climatology*, **11**, 1-25.

Whiteman, C.D. and Doran, J.C., (1993), The relationship between overlying synoptic scale flows and winds within a valley. *Journal of Applied Meteorology*, **32**, 1669-1682

Wibig, J. (1999), Precipitation in Europe in relation to circulation patterns at the 500 hpa level. *International Journal of Climatology*, **19**, 253-269.

Wigley, T.M.L., Jones, P.D., Briffa, K.R. and Smith, G., (1990), Obtaining sub-grid-scale information from coarse resolution general circulation model output. *Journal of Geophysical Research*, **95**, 1943-1953.

Wigley, T.M.L. and Jones P.D. (1987), England and Wales precipitation; a discussion of recent changes in variability and an update to 1985. *Journal of Climatology*, **7**, 231-246.

Wilby, R.L., (1994), Stochastic weather type simulation for regional climate change impact assessment. *Water Resources Research*, **30,** 3395-3403

Wilby, R. (1995), Simulation of precipitation by weather pattern and frontal analysis. *Journal of Hydrology*, **173**, 91-109.

Wilby, R.L. (1997), Non-stationarity in daily precipitation series: implications for GCM downscaling using atmospheric circulation indices. *International Journal of Climatology*, **17**, 439-454.

Wilby, R.L., Barnsley, N. and O'Hare, G., (1995), Rainfall variability associated with Lamb Weather Types: the case for incorporating weather fronts. *International Journal of Climatology*, **15**, 1241-1252.

Wilby, R.L. and Wigley, T.M.L., (1997), Downscaling General Circulation Model output: a review of methods and limitations. *Progress in Physical Geography*, **21**, 530–548.

Wilby, R.L., Wigley, T.M.L., Conway, D., Jones, P.D., Hewitson, B.C., Main, J. and Wilks, D.S., (1998), Statistical downscaling of General Circulation Model output: a comparison of methods. *Water Resources Research*, **34**, 2995–3008.

Wilby, R.L. and Wigley, T.M.L., (2000), Precipitation predictors for downscaling: observed and general circulation model relationships. *International Journal of Climatology*, **20**, 641-661.

Wilks, D.S. (1989), Statistical specification of local surface weather elements from large-scale information. *Theoretical and Applied Climatology,* **40,** 119-134.

Wilks, D.S., (1999), Interannual variability and extreme value characteristics of several stochastic daily precipitation models. *Agricultural and Forest Meteorology,* **93**, 153-169.

Williams, J. and van Loon, H., (1976) An examination of the Northern Hemisphere sea-level pressure data set. *Monthly Weather Review* **104**, 1354-1361.

Willmott, C.J. (1978), P-mode principal component analysis, grouping and precipitation regions in California. *Archiv fur Meteorologie Geophysik und Bioklimatologie,* Ser. B, **26**, 277-295.

Wilmott, C.J., (1981), On the validation of models. *Physical Geography*, **2**, 184-194.

Wilmott, C.J., (1987), Synoptic weather map classification: correlation versus sum of square. *Professional Geographer,* **39**, 205-207.

Wilmott, C.J., Acleson, S.G., Davis, R.E., Feddema, J.J., Klink, K.M., Legates, D.R, O'Donnell, R. and Rowe, C.M. (1985), Statistics for the evaluation and comparison of models. *Journal of Geophysical Research*, **90**, 8995-9005.

Winkler, J.A., Palutikof, J.P., Andersen, J.A., Goodess, C., (1997), The simulation of daily temperature time series from GCM output: Part II Sensitivity analysis of an empirical transfer function methodology. *Journal of Climate*, **10**, 2514-2532.

Xoplaki, E., Luterbacher, J., Burkard, R., Patrikas, I. and Maheras, P. (2000), Connection between the large-scale 500 hPa geopotential height fields and precipitation over Greece during wintertime. *Climate Research,* **14**, 129-146.

Xu, C-Y. (1999), From GCMs to river flow: a review of downscaling methods and hydrologic modeling approaches. *Progress in Physical Geography*, **23**, 229-249.

Yamamoto, O., Iwasima, R.T, Sanga, N.K. and Hoshiai, M. (1986), An analysis of climatic jump. *Journal of the Meteorological Society of Japan*, **674**, 273-281.

Yarnal, B. (1993), *Synoptic Climatology in Environmental Analysis. A primer.* Bellhaven Press.

Yarnal, B., Comrie, A.C, Frakes, B. and Brown, D.P., (2001), Developments and prospects in synoptic climatology. *International Journal of Climatology,* **21**, 1923-1950.

Yarnal, B., Comrie, A.C., Frakes, B. and Brown, D.F., (2001), Developments and prospects in synoptic climatology. *International Journal of Climatology*, **21**, 1923-1950.

Yarnal, B. and Draves, J.D., (1993), A synoptic climatology of stream flow and acidity. *Climatic Research,* **2**, 193-202.

Yoshino, M.M., (1975), *Climate in a small area.* University of Tokyo Press, Tokyo.

Yu, B. and Neil, D.T., (1993), Long-term variations in regional rainfall in the south-west of western Australia and the difference between average and high intensity rainfalls. *International Journal of Climatology*, **13**, 77-88

Zhang, X., Wang, X.L. and Corte-Real, J., (1997), On the relationships between daily circulation patterns and precipitation in Portugal. *Journal of Geophysical Research,* **102**, 13495-13507.

Zorita, E. and Von Storch, H, (1999), The analog method as a simple statistical downscaling technique: comparison with more complicated methods. *Journal of Climate,* **12**, 2474-2489.

Zorita, E., Hughes, J. P., Lettenmeier, D.P. and Von Storch, H., (1995), Stochastic characterisation of regional circulation patterns for climate model diagnosis and estimation of local precipitation. *Journal of Climate,* **8**, 1023-1042.

Appendices

Appendix One
CCCMA

a1.1 CGCM2
GHG+A IPCC Scenario 'IS92a' Runs

This ensemble of 3 simulations was performed with the second version of the Canadian Global Coupled Model CGCM2. This model is based on the earlier CGCM1, but with some improvements to address shortcomings identified in the first version. In particular, the ocean mixing parameterization has been changed from horizontal/vertical diffusion scheme to isopycnal/eddy stirring parameterization, and sea-ice dynamics has been included . The model is forced by an effective greenhouse forcing corresponding to that observed from 1900 to 1996 and an increase of CO_2 at a rate of 1% per year thereafter until year 2100 (the IPCC "IS92" scenario). The direct effect of sulphate aerosols is also included by increasing the surface albedo.

All three runs are performed with the same greenhouse gas and aerosol forcing. The only difference is that the runs are initiated from different initial conditions. The reason for doing an ensemble of integrations is to reduce the natural climate variability by taking the ensemble average over all three runs. The differences between the individual integrations are entirely due to natural variability and not due to the differences in the model or forcing.

A total of 201 years of monthly data is available. The first record is for year 1900 month 1 and the last one is for year 2100 month 12. Annual, seasonal and monthly climatologies are also available for four 21-year time windows: 1900-1920, 1975-1995, 2040-2060 (approx. CO_2 doubling relative to the 1975-1995 level) and 2080-2100 (approx. CO_2 tripling).

The data are provided on a 97x48 Gaussian grid (approximately 3.75° lat x 3.75° long).

Decadal means of ocean temperature, salinity, velocity components and sea level rise are available, starting from the year 1901 (20 decades). Only the steric (thermal expansion) component of sea level rise integrated from surface to 1175m depth is calculated. Any contribution due to glacier melt is ignored. Sea-level rise is computed as the difference of the vertically integrated specific volume between corresponding decades of the GHG+A and CONTROL experiments. The data is provided on a 193x96 grid (approximately 1.88° lat x 1.88° long).

The user should be aware that grid box values are not directly comparable to station data. Climate models attempt to represent the full climate system from first principles on large scales. Physical "parameterizations" are used to approximate the effects of unresolved small scale processes because it is not economically feasible to include detailed representations of these processes in present day models. Caution is therefore needed when comparing climate model output with observations or analyses on spatial scales shorter than several grid lengths (approximately 1000 to 1500 km in mid-latitudes), or when using model output to study the impacts of climate variability and change. The user is further cautioned that estimates of climate variability and change obtained from climate model results are subject to sampling variability. This uncertainty arises from the natural variability that is part of the observed climate system and is generally well simulated by the climate models.

Appendix Two

The study area and sources of data

a2.1 Study area shape

This aspect of the study area is not usually considered. To an extent this decision is often based on political boundaries (*e.g.* Sumner *et al* 1995). Nevertheless the nature of the shape of an area is important. All other things being equal compact geographical shapes should demonstrate less spatial variability in environmental variables than more elongated shapes of the same areal extent (*figure a2.1).*

The most commonly measured characteristic of shape is compactness. It is suggested that the more compact the shape the more likely that the entire area would fall under the same circulation regime. Shape of a region can be assessed by how it deviates from the most compact possible shape, a circle. Pounds (1963) suggests the following,

$$S_1 = \frac{P}{A} \quad (Eqn\ a2.1)$$

where P is the length of perimeter and A is the area. A major problem of this shape index is the lack of unit and size independence and the fact that it is highly sensitive to sinuosity of perimeter. S_1 is largely discredited and is not widely used. Other shape indices are listed by Ebdon (1985) and these are listed as S_1 -S_5 in *table a2.1.* In the calculations of these shape index amendment has been made to the true coastline of the peninsula coastal features that have been smoothed out in the determination of perimeter length. The other indices show a only a small departure from the value of 1, but the range is wide from 0.846 to 0.500.

Shape index	Spain
$S_1 = \frac{P}{A}$	0.333
$S_2 = \frac{4A}{\pi L^2}$	0.716
$S_3 = \frac{4A}{\pi D^2}$	0.716
$S_4 = \frac{R_a}{R_c}$	0.846
$S_5 = \frac{R_1}{R_c}$	0.500

A = Area
L = length of longest axis
D = diameter of smallest circumscribing circle
R_c - radius of smallest circumscribing circle
R^i = radius of largest inscribed circle
R_a - Radius of circle with same area as shape

Table a2.1 Shape of the Iberian peninsula as quantified by a variety of shape indices (after Ebdon 1985).

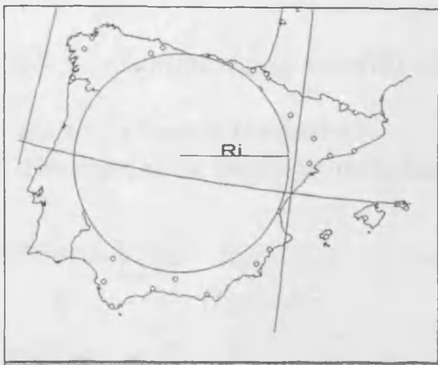

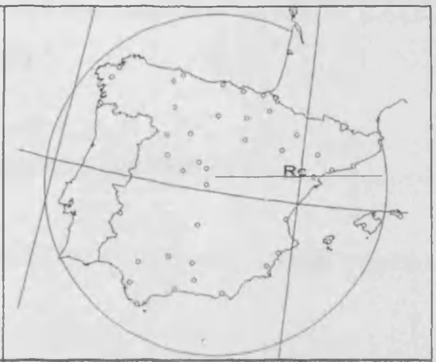

R^i = radius of largest inscribed circle

R_c - radius of smallest circumscribing circle

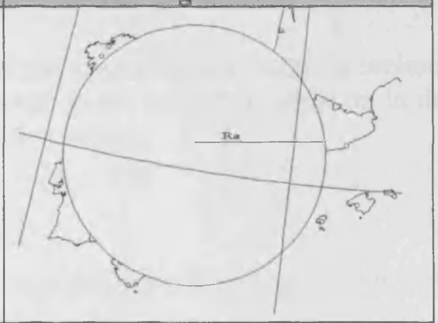

L = length of longest axis

R_a - Radius of circle with same area as shape

Figure a2.1 Calculation of shape indices for the Iberian peninsula.

a2.2 Determining sample window

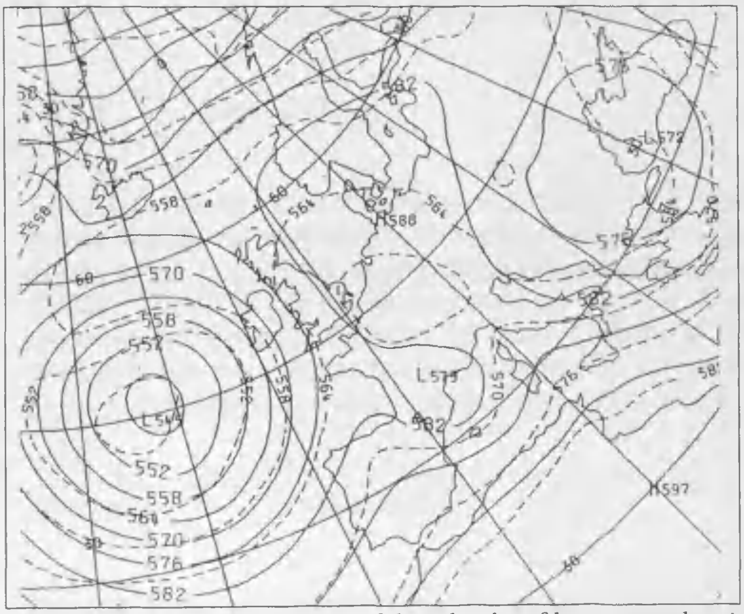

Figure a2.2 Illustration of drawbacks of large sample window

This chart illustrates that a larger sample window (extending to the north and east) would include too much information relating to the extensive low pressure area at the expense of the ridge that is presently controlling conditions over the peninsula.

a2.3 Summarizing rainfall data

a2.3.1 Central tendency

The mean *xi* for the *jth* variable is given by *equation a2.2.*

$$xj = \frac{\sum_{i=1}^{n} xij}{n} \quad (Eqn\ a2.2)$$

where *xij* is the *ith* observation for the *jth* variable and *n* is the number of observations.

a2.3.2 Dispersion of the data

The scatter of observations around the central typical value is commonly measured by the variance which is directly proportional to the amount of variation in the data. The variance for the *jth* variable is given by *equation a2.3.*

$$\frac{s^2{}_j = \sum_{i=1}^{n} x^2{}_{ij}}{n-1} = \frac{SS}{df} \quad (Eqn\ a2.3)$$

where *xij* is the means-corrected data for the *ith* observation and *jth* variable and *n* is the number of observations. The numerator is the sum of squared deviations form the mean and is typically referred to as the sum of squares (*SS*) and the denominator is the degrees of freedom (*df*).

Intercomparison between sites with different distributions is afforded by the Coefficient of Variation (COV) statistic (Linacre 1992) (*equation 2.4*)

$$COV = \left(\frac{SD}{\bar{x}} \right) (Eqn\ a2.4)$$

where *SD* refers to standard deviation and *x* is the mean value.

Seasonality is a defining feature of region. A quantitative measure of the tendency for rainfall to fall in one part of the year is the *seasonal index (SI) (eqn a2.5)* proposed by Ayoade (1970). The SI is derived by summing the absolute deviations of mean rainfall for each month of the year from the expected value if the annual rainfall were uniformly distributed throughout the year. Index scores range between 1, representing an extreme situation when all precipitation falls in a single month, to 0, a total absence of seasonality.

$$SI = \frac{\Sigma \left| R_i - (R_y / 12) \right|}{R_y} \quad (Eqn\ a2.5)$$

where R_i is the mean rainfall (mm) for a month and R_y is the mean annual rainfall (mm) for the station. An example of the calculation of the SI is given in *table a2.2*

Month	J	F	M	A	M	J	J	A	S	O	N	D	total	Mean monthly
Mean mm	74	78	62	56	44	24	4	7	29	48	61	72	559	46.58
													Mean deviation	**SI Index**
Abs deviation mm	27.4	31.4	15.4	9.4	2.6	22.6	42.6	39.6	17.6	1.4	14.4	25.4	249.8	0.45

Table a2.4 *Calculation of Ayoade's Seasonality Index (SI) for rainfall amounts at Jaen, Spain.*

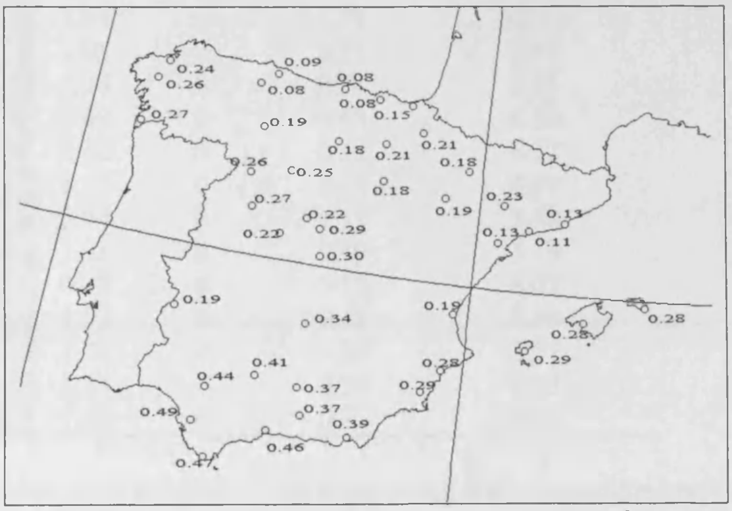

Figure a2.4 *Seasonality Index calculated for mean monthly raindays.*

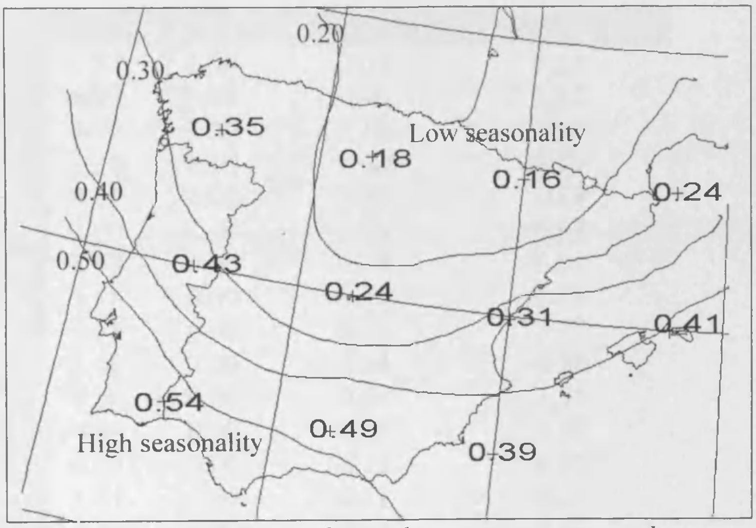

Figure .a2.5 *Seasonality index values for grid point precipitation data.*

Figure a2.4 displays SI values for all rainfall at stations and *figure a2.5* depicts this for the areal grid point datasets. Two areas display low seasonality in *figure a2.4* – a cluster of stations along the north Biscay coast and stations in the north-east Mediterranean. Highest seasonality is found in the south-west quadrant. This pattern is replicated in the areal data.

a2.4 Data Characteristics
a2.4.1 Mean daily rainfall amounts

Location	Mean	Median	TrMean	StDev
Almeria	0.55	0	0.08	2.71
Avila	1.00	0	0.43	3.24
Badajoz	1.38	0	0.56	4.40
Burgos	1.45	0	0.75	3.93
Cuidad Real	1.13	0	0.50	3.39
Gijon	2.62	0	1.57	6.38
Jaen	3.54	0	1.71	10.80
Lerida	1.05	0	0.33	3.99
Madrid	1.24	0	0.54	3.75
Mahon	1.68	0	0.65	5.99
Malaga	1.52	0	0.32	6.82
Palma	1.17	0	0.36	4.59
Pamplona	2.04	0	1.11	5.59
Salamanca	1.06	0	0.49	3.15
San Javier	0.79	0	0.13	4.07
Santander	3.52	0	2.18	8.00
Segovia	1.28	0	0.66	3.57
Seville	1.75	0	0.59	6.33
Soria	1.46	0	0.77	3.93

Table a2.5 Mean daily rainfall characteristics (all units are millimetres) at selected sites (1961-1990). Source INM.

Location	Mean	Median	Tr Mean	SD
Almeria	0.35	0.00	0.02	2.23
Avila	0.99	0.00	0.38	3.52
Badajoz	0.79	0.00	0.18	3.34
Burgos	1.36	0.00	0.62	4.12
Ciudad Real	0.84	0.00	0.30	2.89
Gijon	2.00	0.00	1.01	5.97
Jaen	1.95	0.00	0.70	6.51
Lerida	1.18	0.00	0.33	4.58
Madrid	0.88	0.00	0.28	3.17
Mahon	1.00	0.00	0.24	4.59
Malaga	0.58	0.00	0.04	3.39
Murcia	0.56	0.00	0.06	3.02
Palma	0.87	0.00	0.15	4.33
Pamplona	1.71	0.00	0.81	5.26
Salamanca	0.94	0.00	0.37	3.11
Santander	2.78	0.00	1.48	7.56
Segovia	1.16	0.00	0.52	3.63
Seville	0.86	0.00	0.15	4.04
Soria	1.34	0.00	0.63	3.98

Table a2.6 Mean daily rainfall at each site (Summer months) 1961-1990 Source INM.

Location	Mean	Median	Trmean	SD
Almeria	0.07	0.00	0.02	0.31
Avila	1.02	0.00	0.49	2.94
Badajoz	1.96	0.00	1.03	5.83
Burgos	1.53	0.00	0.89	3.73
Ciudad Real	1.41	0.00	0.73	3.80
Gijon	3.25	0.10	2.19	6.70
Jaen	5.13	0.00	2.94	13.63
Lerida	0.92	0.00	0.33	3.32
Madrid	1.61	0.00	0.85	4.25
Mahon	2.37	0.00	1.18	7.08
Malaga	2.47	0.00	0.83	8.94
Murcia	1.01	0.00	0.22	4.89
Palma	1.51	0.00	0.62	4.85
Pamplona	2.37	0.00	1.42	5.90
Salamanca	1.17	0.00	0.61	3.20
Santander	4.27	0.20	2.93	8.35
Segovia	1.40	0.00	0.81	3.52
Seville	2.53	0.00	1.15	7.71
Soria	1.59	0.00	0.90	3.87

Table a2.7 Mean daily rainfall at each site (winter months) 1961-1990 Source INM

a2.4.2 Time Series Analysis

Although it is outside the scope of this project to investigate in detail the historical changes in precipitation, some simple comments can be made on the nature of temporal variability in the original precipitation datasets.

a2.4.3 Smoothing time series

An underlying trend in rainfall characteristics over any time period can be rendered more apparent by the application of a filtering or 'smoothing' procedure such a running mean. By taking a series of values, for instance, x_1, x_2, x_3, x_4 and x_5, a 5-time unit running mean (or 'moving average') can be obtained from the following procedure

$MA1 = (x_1 + x_2 + x_3 + x_4 + x_5)/5$... $MA2 = ((x_2 + x_3 + x_4 + x_5 + x_6)/5$.....and so on.

The procedure reduces the impact of anomalous values. It is essentially a method used in exploratory examinations of patterns within datasets

Figure a2.6 displays smoothed time series of monthly rainfall at each of the grid point locations. The data have been standardized by monthly mean and standard deviation to counter seasonal effects.

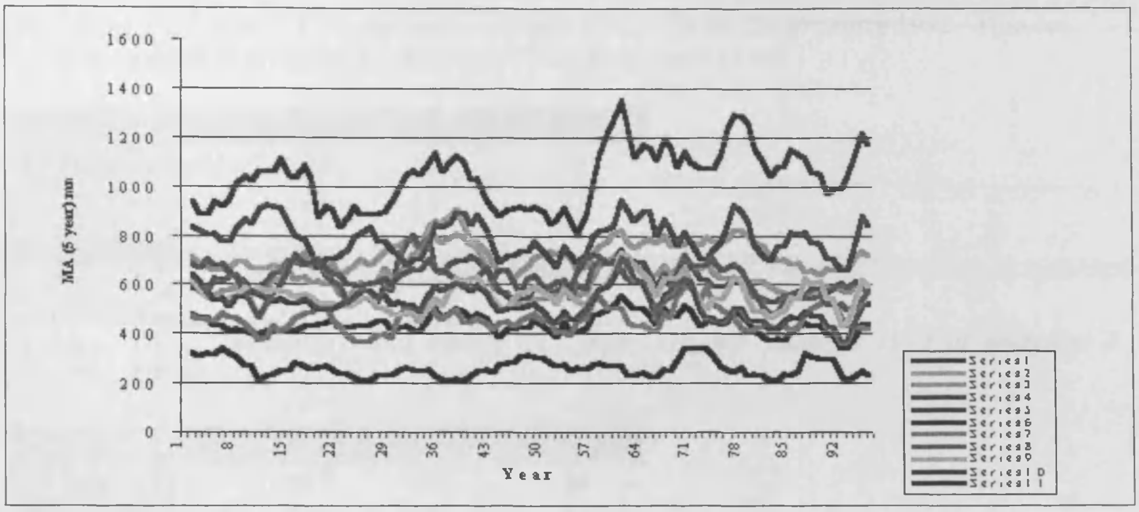

Figure a2.6 Smoothed rainfall time series of annual totals at gridpoint locations.

a2.4.4 Detecting a climatic jump

Suspected switches in the trend of a dataset may be visually apparent (or be made more apparent after smoothing). If the mean of rainfall over a period of a few decades differs with sufficient statistical significance from the mean over the successive period of about the same length a discontinuity in the time series can be assumed. Karl and Riebsame (1984) define this as a '*climatic jump*' and proposed a non-overlapping consecutive epoch analysis to identify 10 to 20-year fluctuations in temperature and rainfall in the USA. Yamamoto *et al* (1986) have developed a technique based on the t-statistic to detect such climatic jumps assuming that observations are independent, normally distributed random variables of equal variance.

If the data employed is either monthly, seasonal or annual rainfall amounts then the parametric student's t-test can be employed. This method was applied to the long-term monthly areal data in *figure a2.6*. The test indicates some following aspects of the time series.

At gridpoint 1 (42.5°N, 7.5°W) a statistically significant climatic jump can be identified occurring at 1961. Gridpoint 2 (42.5°N, 3.75°W) also displays this swing to wetter conditions at about the same point in time (~1960).

Period	n	Mean	SDev	SE Mean
1901-1960	60	964	168	22
1961-2000	40	1150	208	33
		DF	**T-value**	**P-Value**
		71	4.71	0.000

Table a2.8 Student's t test results to identify climatic jump at 1961 at gridpoint 1 (42.5°N, 7.5°W).

Period	n	Mean	SDev	SE Mean
1901-1959	59	707	89	12
1960-2000	41	747	99	16
		DF	**T-value**	**P-Value**
		77	2.09	0.040

Table a2.9 Student's t test results to identify climatic jump at 1960 at gridpoint 2(42.5°N, 3.75°W).

Gridpoint 9 (37.5°N, 7.5°W) indicates a switch towards drier climate since 1972. This can also be detected at gridpoint 8 (40.0°N, 3.75°E) after about 1974.

Period	n	Mean	SDev	SE Mean
1901-1971	71	552	134	16
1972 – 2000	28	468	122	23
		DF	**T-value**	**P-Value**
		53	3.01	0.004

Table a2.10 Student's t test results to identify climatic jump at 1972 at gridpoint 9 (37.5°N, 7.5°W).

Period	n	Mean	SDev	SE Mean
1900-1973	73	635	115	14
1974-2000	26	570	111	22
		DF	**T-value**	**P-Value**
		46	2.53	0.015

Table a2.11 Student's' t' test results to identify climatic jump at 1974 at gridpoint 8 (40.0°N, 3.75°E).

Finally, although not a significant climatic swing in terms of mean values at gridpoint 9 it is noticeable that there is a marked increase in variability of rainfall after 1960 (a standard deviation of 64mm from 1901-1959 and 84mm from 1960-2000.

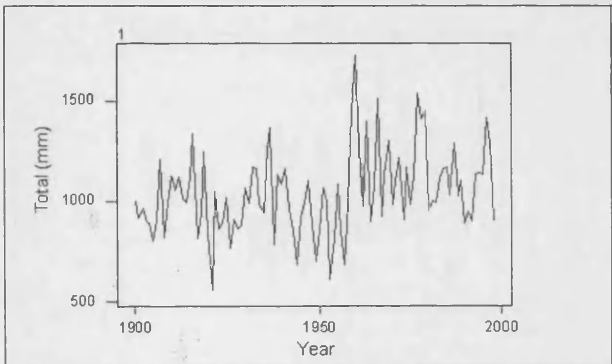

a. Grid point 1 Precipitation time series 1900-2000

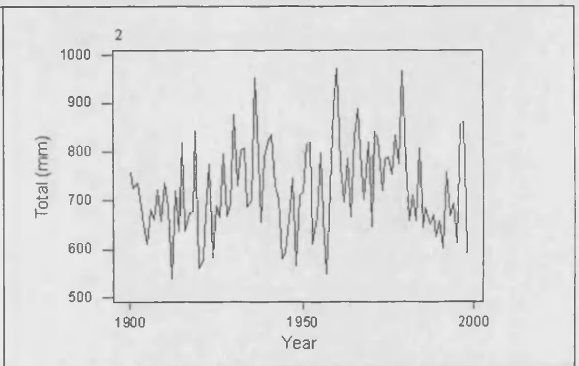

b. Grid point 2 Precipitation time series 1900-2000

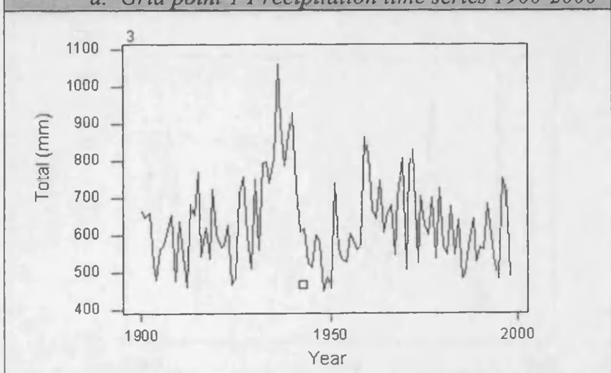

c. Grid point 3 Precipitation time series 1900-200000

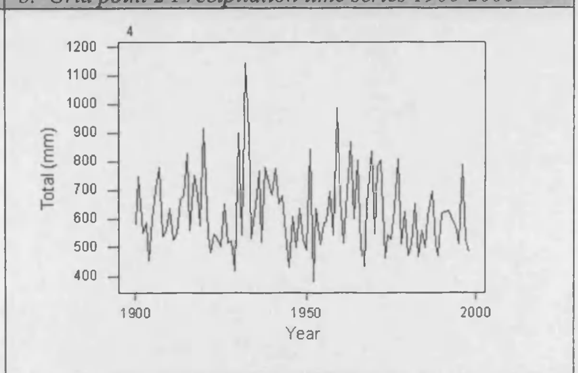

d. Grid point 4 Precipitation time series 1900-2000

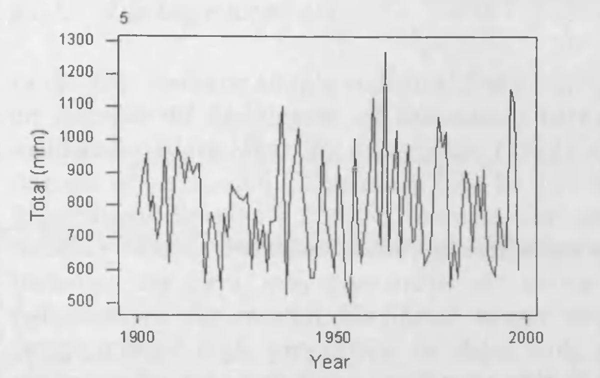

e. Grid point 5 Precipitation time series 1900-2000

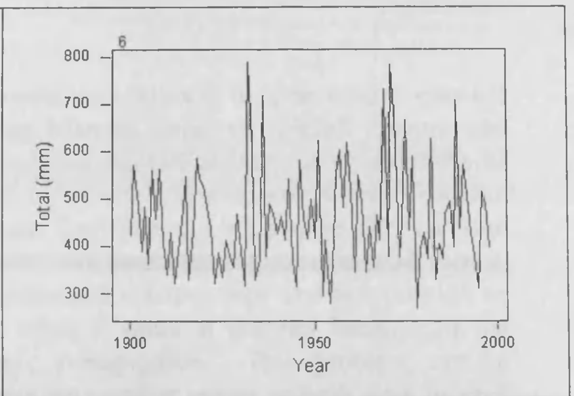

f. Grid point 6 Precipitation time series 1900-2000

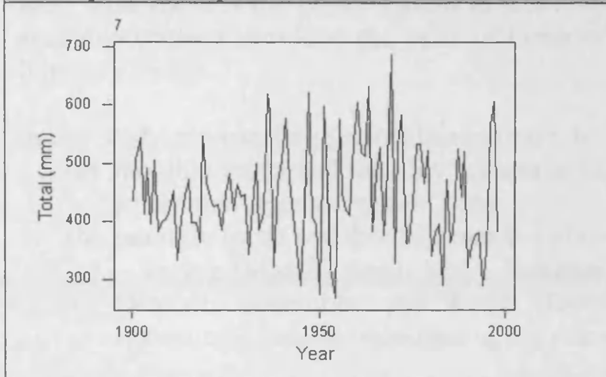

g. Grid point 7 Precipitation time series 1900-2000

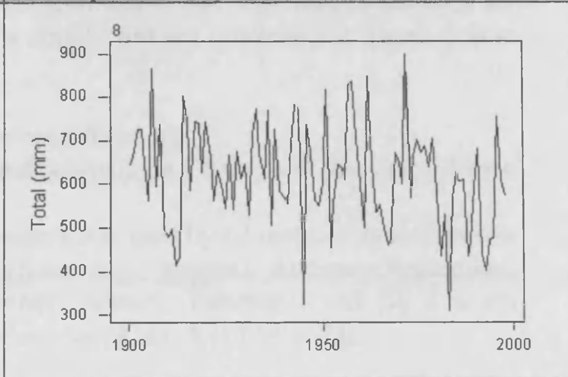

h. Grid point 8 Precipitation time series 1900-2000

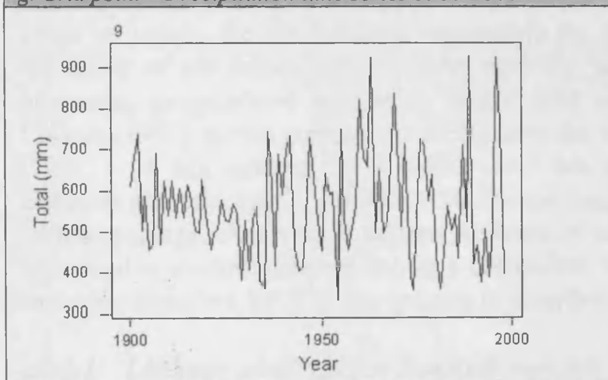

i. Grid point 9 Precipitation time series 1900-2000

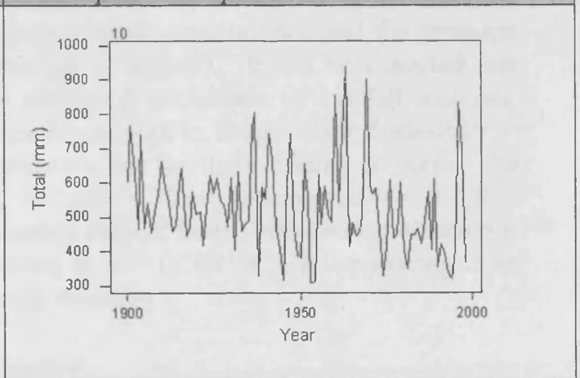

j. Grid point 10 Precipitation time series 1900-2000

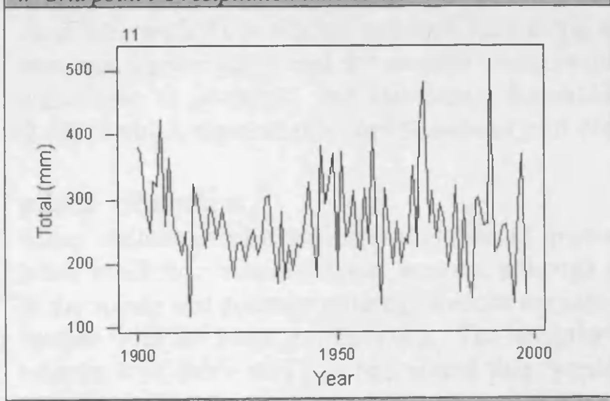

k. Grid point 11 Precipitation time series 1900-2000

Figure a2.7 Annual gridpoint data 1900-2000 (from Hulme 2000).

a2.5. Linkage analysis

In the first instance simple statistical links (*via* correlation methods) may be used to provide an estimate of the degree of association between sites in terms of rainfall amount and incidence. Early work by Glasspoole (1922) identified rainfall affinity using isopleths of degrees of correlation. This could then be mapped for visual interpretation. Given Gaussian distributions Pearson's Product Moment Correlation Coefficients (*'r'*) can be derived from monthly values. However if daily precipitation values are used then the entire rainfall record, including dry days, may give artificially strong statistical relationships and not provide an indication of the rainfall likelihood at one site when it rains at another because of the comparatively high proportion of days with zero precipitation. This problem can be overcome by calculating the coefficient only if rain occurred at either or both sites in each pair. This reduces the positive skew in distributions (Sumner 1988). Correlation between all available stations provided the basis of Gregory's simple linkage analysis for Sierra Leone (Gregory 1965).

In this study comparative regionalizations are developed by using,

(a) monthly totals and monthly number of raindays (using all months of the year – hence an 'annual regionalization') and
(b) monthly totals and monthly number of raindays arranged by *(i)* meteorological season – Spring (March, April, May), Summer (June, July, August), Autumn (September, October, November) and Winter (December, January, February) and *(ii)* a warm season/cold season bissection of the calendar year (AMJJAS/JFMOND).

The correlation of rainfall measured at two locations depends on the distance between them, the kinds of terrain, the mechanisms responsible for the precipitation occurrence and the temporal resolution of the measurement (daily, monthly, seasonal or annual). It can be expected that increasing geographical separation should lead to decreased correlation of rainfall amounts. Linacre (1992) quotes correlation coefficients for monthly rainfall in Otago, New Zealand (*'r = 0.900'* – 16 km spacing, *'r = 0.600'* – 80 km spacing), but for daily rainfall in Jordan the distances are reduced *('r = 0.900'* – 10 km spacing, *'r=0.877'* – 30 km spacing and *'r = 0.400'* – 50 km spacing). Analysis in eastern Australia of monthly rainfall from 1900-1964 at 42 stations compared to a central station shows a correlation falling to *'r = 0.500'* in 430 km spacing in an east-west direction, but 740 km spacing in a north-south direction.

a2.5.1 Linkage analysis for Spanish rainfall stations

Stations in the study area were examined using simple linkage analysis. *Figures 2.26* and *2.27* illustrate rainfall correlation between sites using annual and seasonal values for the number of raindays (*figure a2.8*) and for rainfall totals (mm) (*figure a2.9*). Although the *'r = 0.220'* is significant at $p<0.050$, the (arbitrary) threshold correlation coefficient illustrated is *'r = 0.700'* (which represents a significance of $p<0.0005$).

a2.5.2 Raindays

Many stations exhibit an intercorrelation of greater than *'r = 0.700'* based on annual rainday totals in all four meteorological seasons, although there is considerably less statistical coherence in the spring and summer months. Results are *table 2.8* however this table needs to be viewed in tandem with the maps in *figure* 2.2. The irregular station spacing means that the information in column 2 of *table a2.12* is less sound than would be the case under a more regularly spaced coverage. Stations tend to exhibit greater statistical association in a north-south rather than east-west direction. The greatest amount of significant pairs occurs in autumn (159 pairs – 27% of all possible pairs) where the maximum geographical separation is almost 700 km. Topographic boundaries and the associated 'rainshadowing effects' are evident. Winter is the only season where a linkage across the Cantabrian mountain range can be seen. In all seasons there is the appearance of some co-varying regions and this is most evident in spring, although eastern coastal stations are only associated with other eastern coastal stations. In this season four main regions emerge – (1) the north-west, (2) the north coast, (3) the Balearic Islands and (4) the inland stations (although this is almost segregated into a northern and southern area). In summer the Balearics display a related pattern to some south-eastern Mediterranean coastal stations.

	Number of pairs of stations exhibiting a correlation coefficient $r>0.700$	Percentage of pairs of stations	Maximum geographical separation
Annual rainday totals	152	0.25	580km
Spring rainday totals	86	0.14	520km
Summer rainday totals	69	0.12	340km
Autumn rainday totals	159	0.26	580km
Winter rainday totals	157	0.27	690km

Table a2.12 Characteristics of linkage analysis using rain day totals (it must be noted that the figures in this table are not absolute but determined by the location and the major pluviometric stations) (Based on 1958-1997).

a2.5.3 Rain amounts

Linkage analysis based on rain amounts displays a reduced number of significantly correlated pairs (*table a2.13*). Numbers fall from 100 (17%) in winter to 20 (3%) in summer during which distinct small regions emerge In the wetter seasons there is little connection between stations to the east of the peninsula and those along the sheltered Mediterranean coast. In addition there are no linkages at this threshold between stations to the north and south of the Cantabrian mountain range. In spring five fairly coherent regions develop however there is a reduced number of correlated pairs even between stations that are relatively close. Some relatively long distance correlations (over 500 km) can be seen in a north-south plane but not in an east-west direction. In winter the greatest distance under this threshold is 580 km but only 390 km in an east-west direction. The Balearic Island group emerges in all seasons as unrelated at this threshold to any station on mainland Spain or to each other.

	Number of pairs of stations exhibiting a correlation coefficient $r>0.700$	Percentage	Maximum geographical separation
Annual rainfall amounts	73	0.12	520km
Spring rainfall amounts	46	0.08	220km
Summer rainfall amounts	20	0.03	310km
Autumn rainfall amounts	100	0.17	520km
Winter rainfall amounts	111	0.19	580km

Table a2.13 Characteristics of linkage analysis using rainfall amounts (mm) (it must be noted that the figures in this table are not absolute but determined by the location and the major pluviometric stations) (Based on 1958-1997).

2.5.4 Higher thresholds

As expected the adoption of a higher threshold value for *'r'* leads to a reduction in the number of linked pairs (*Table a2.14*). The mean distance of spacing between stations exhibiting $r = 0.900$ is 70 km (for annual raindays) and 75 km for annual rain amounts.

	Number of pairs of stations exhibiting a correlation coefficient *r>0.900*	Percentage	Maximum geographical separation
Annual rainday totals	5	0.01	120km
Annual rainfall amounts	5	0.01	120km

Table a2.14 Characteristics of linkage analysis using annual rain day numbers and rainfall amounts (mm) (it must be noted that the figures in this table are not absolute but determined by the location and the major pluviometric stations) (Based on 1958-1997).

a2.6 PCA procedure – further comments

a2.6.1 Component loadings

The relationship between the original variables and the principal components is expressed by the component loadings. When squared these are equivalent to the correlation between the component and the original variable *(equation a2.6)*.

$$l_{ij} = \frac{W_{ij}}{\hat{S}_j}\sqrt{\xi_i} \quad \textit{(Eqn a2.6)}$$

where l_{ij} is the loading of the *jth* variable for the *ith PC*
w_{ij} is the weight of the *jth* variable for the *ith PC*
ξ_i is the eigenvalue (the variance) of the *ith PC*
S_j is the standard deviation of the *jth* variable

These can then be used to interpret the components. This is achieved by examining the variables that load highest on each component and subjectively deciding a commonality between them. PCA therefore replaces one set of variables by another. The components are identified in terms of the original variables, the larger the loading the more important is the variable in the interpretation of the component. The components themselves can be sufficient in identifying modes of circulation. Rotation of PCs is a procedure used to improve the interpretability of results (Richman 1981). Various rotations were used in this research but unrotated solutions were found to be satisfactory and further comments on this procedure are not included.

The sum of the squared loadings indicates the total variance accounted for by the component. This value is known as the eigenvalue.

where l_{ij} is the loading of the *jth* variable for the *ith PC*
and ξ_i is the eigenvalue (the variance) of the *ith PC*

The communality is the sum of squared loadings for the variable so that in *eqn a2.7;*

$$h^2{}_{jk} = \sum_{i=1}^{K} L^2{}_{ij} \quad \textit{(Eqn a2.7)}$$

K is the number of components and h^2_{jk} is the communality for variable *j*.

2.7.2 Component scores

The component score for *ith* observation on PC*k* is defined to meet this requirement using *eqn a2.8*

$$S_{ik} = \sum_{j=1}^{N} D_{ij} L_{jk} \quad (Eqn\ a2.8)$$

where d_{ij} is the standardized value for the *ith* observation i on variable *j*
L_{jk} is the loading of the *jth* variable on the *ith PC*
S_{ik} is the score of *ith* observation on the *kth PC*
and summation is over all *n* variables.

Component scores are therefore weighted summed values for the observations over the variables, the weights being the component loadings. The larger the value that an observation has on the variables which have high loadings on a component the larger the score (Johnston 1977). Scores are values for the observations on the new variables and reflect the contribution each new variable (component) makes to the variance of the original variables.

a2.7 PCA component retention

A number of techniques have been employed to determine the number of PCs that should be retained (*table a2.15).*

Method	Advocated by	Used by
Scree Test	Cattel (1966)	Wilmott (1978)
Eigenvalue-greater-than-one		Spellman (1996)
Eigenvalue degeneration	North *et al* (1982)	McGregor (1996)
Rule N	Overland and Preisendorfer (1985)	
Arbitrary threshold	Stone (1989)	Stone (1989)

Table a2.15 Selected means for determining the number of components to retain..

a2.8 Rotation - simple structure

Simple structure is a hypothesis regarding relationships within a dataset and approached by the rotation of factors. The procedure is reviewed extensively by Richman (1981). Rotation is commonly undertaken to maximise the explanatory power of the solution by highlighting groups of variables in the dataset, as sometimes unrotated components exhibit characteristics that hinder the isolation of individual modes of variation (White *et al* 1991). Early applications of rotation were employed by Gregory (1975), Rogers (1976) and Wilmott (1977). Rotation methods can be classified in two ways; inductive or deductive.

Of the inductive methods orthogonal rotation is most frequently used as it retains the constraint that factors should be orthogonal and therefore uncorrelated. This ideal simple structure means that each variable has a loading of either +1.0 or -1.0 or one factor and 0.0 on all others. To get as close as possible to this ideal, the factors are rotated around the origin to the best positions. The most popular rotation is Kaiser's VARIMAX (Kaiser 1958) a rotation that aims to maximise variance. The QUARTIMAX method is less used as it aims for simple structure by maximising a variable's loading onto one component. The solution therefore may include just one component with all major loadings and is difficult to interpret meteorologically.

If the aim of factor rotation is to highlight groups of inter-related variables then orthogonal rotations may not be appropriate as there is an assumption that the factors representing the groups are independent when it is often likely that two or more groups in a set of variables are correlated . For accurate group identification the constraint that axes should be 90° apart is dropped with this rotation the simple structure hypothesis is altered so that every variable has one loading of +1.0 or -1.0 but the other loadings need not be 0.0. This 'oblique' method has been used by Cohen (1983) in the classification of 500 hpa height surface.

The literature does not contain any examples of climatological applications of Deductive rotation methods and these have not applied in this study. The numerous criteria which can be used for any rotation are reviewed by Richman (1986). A simple summary of his recommendations is that whilst rotation is capable of simplifying the interpretation of an *m*-dimensional space, they are not universally recommended. Interestingly

a2.9 Clustering Procedures – further comments

a2.9.1 Clustering techniques

There are a variety of clustering techniques available to the researcher *(table a2.16)*.

Linkage	Description
Single	In this method the distance between two clusters is represented by the minimum distance between all possible pairs.
Complete	This is the opposite to the nearest neighbour method, in as much as the distance between the two clusters is defined as the maximum of the distances between all possible pairs of observations in two clusters.
Centroid	In the centroid method each group is replaced by an average object which is the centroid of that group. The distance between two clusters is the distance between the cluster centroids or means.
Average	In average linkage, the distance between two clusters is the average distance between an observation in one cluster and an observation in the other cluster.
Wards	The Ward's method does not compute distances between clusters instead it forms clusters by maximizing within-cluster homogeneity by using the within-cluster sum of squares as the measure. In other words the Ward's method attempts to minimize within-cluster sum of squares.

Table a2.16 Hierarchical clustering techniques.

a2.9.2 Distance Measures

Distance measures include:

(a) Euclidean distance

$$D_{ab} = \sqrt{\sum_{j=1}^{P}(a_j - b_j)^2} \quad \textit{(Eqn a2.9)}$$

where D_{ij} is the distance between observations *i* and *j* x_{ik} is the value of the *kth* variable for the *ith* subject, x_{jk} is the value of the *kth* variable for the *jth* subject, and *p* is the number of variables

(b) Squared Euclidean distance

$$(D_{ab} = \sqrt{\sum_{j=1}^{P}(a_j - b_j)^2)^2} \quad \textit{(Eqn a2.10)}$$

(c) Mahalanobis Distance

$$MD^2{}_{ik} = \frac{1}{1-r^2}[\frac{(x_i^{\ 2} - x_k^{\ 1})}{s^2{}_i} + \frac{(x_i^{\ 2} - x_k^{\ 2})^2}{s^2{}_2} - \frac{2r(x_i^{\ 1} - x_k^{\ 1})(x_i^{\ 2} - x_k^{\ 2})}{s_1 s_2} \quad \textit{(Eqn a2.11)}$$

Mahalanobis distance is designed to take into account the correlation amongst the variables and is scale invariant. For uncorrelated variables, as in the use of components the Mahalanobis distance reduces to the Euclidean distance for unstandardized data. In the absence of any argument against its use this study uses the most commonly employed Euclidean metric.

a2.10 Regionalization Clustering Procedure

step	clusters	SIM IND
24	20	92.36
25	19	91.14
26	18	90.87
27	17	90.85
28	16	89.67
29	15	89.33
30	14	89.28
31	13	88.62
32	12	88.27
33	11	87.53
34	10	85.19
35	9	85.14
36	8	83.68
37	7	83.34
38	6	82.84
39	5	74.29
40	4	72.58
41	3	68.86
42	2	60.15
43	1	32.06

Table a2.17 Evolution of the similarity index in later stages of the clustering procedure(Annual Raindays).

step	clusters	SIM IND
24	20	94.62
25	19	93.79
26	18	93.63
27	17	92.56
28	16	92.48
29	15	91.94
30	14	91.63
31	13	91.49
32	12	91.43
33	11	89.57
34	10	89.01
35	9	87.46
36	8	85.48
37	7	84.19
38	6	83.10
39	5	80.58

40	4	73.53
41	3	72.03
42	2	60.09
43	1	43.68

Table a2.18 Evolution of the similarity index in later stages of the clustering procedure (Summer Raindays)

step	clusters	SIM IND
24	20	94.29
25	19	94.07
26	18	93.75
27	17	93.20
28	16	93.19
29	15	92.84
30	14	92.55
31	13	92.09
32	12	91.83
33	11	90.02
34	10	88.37
35	9	88.22
36	8	86.83
37	7	86.77
38	6	86.22
39	5	82.99
40	4	77.01
41	3	69.25
42	2	62.99
43	1	37.56

Table a2.19 Evolution of the similarity index in later stages of the clustering procedure (Winter raindays).

step	clusters	SIM IND
24	20	94.09
25	19	93.99
26	18	93.29
27	17	92.80
28	16	92.61
29	15	92.53
30	14	92.22
31	13	91.78
32	12	91.77
33	11	90.37
34	10	89.72
35	9	89.15
36	8	88.28
37	7	85.45
38	6	78.06
39	5	76.61
40	4	71.72
41	3	53.27
42	2	50.64

43	1	17.70

Table a2.20 Evolution of the similarity index in later stages of the clustering procedure (Annual rain amounts).

step	**clusters**	**SIM IND**
24	20	96.48
25	19	96.13
26	18	95.97
27	17	95.82
28	16	95.38
29	15	95.35
30	14	94.16
31	13	94.13
32	12	92.27
33	11	91.39
34	10	91.11
35	9	90.53
36	8	89.08
37	7	87.02
38	6	86.29
39	5	82.02
40	4	80.83
41	3	66.95
42	2	60.39
43	1	16.80

Table a2.21 Evolution of the similarity index in later stages of the clustering procedure (Winter rain amounts).

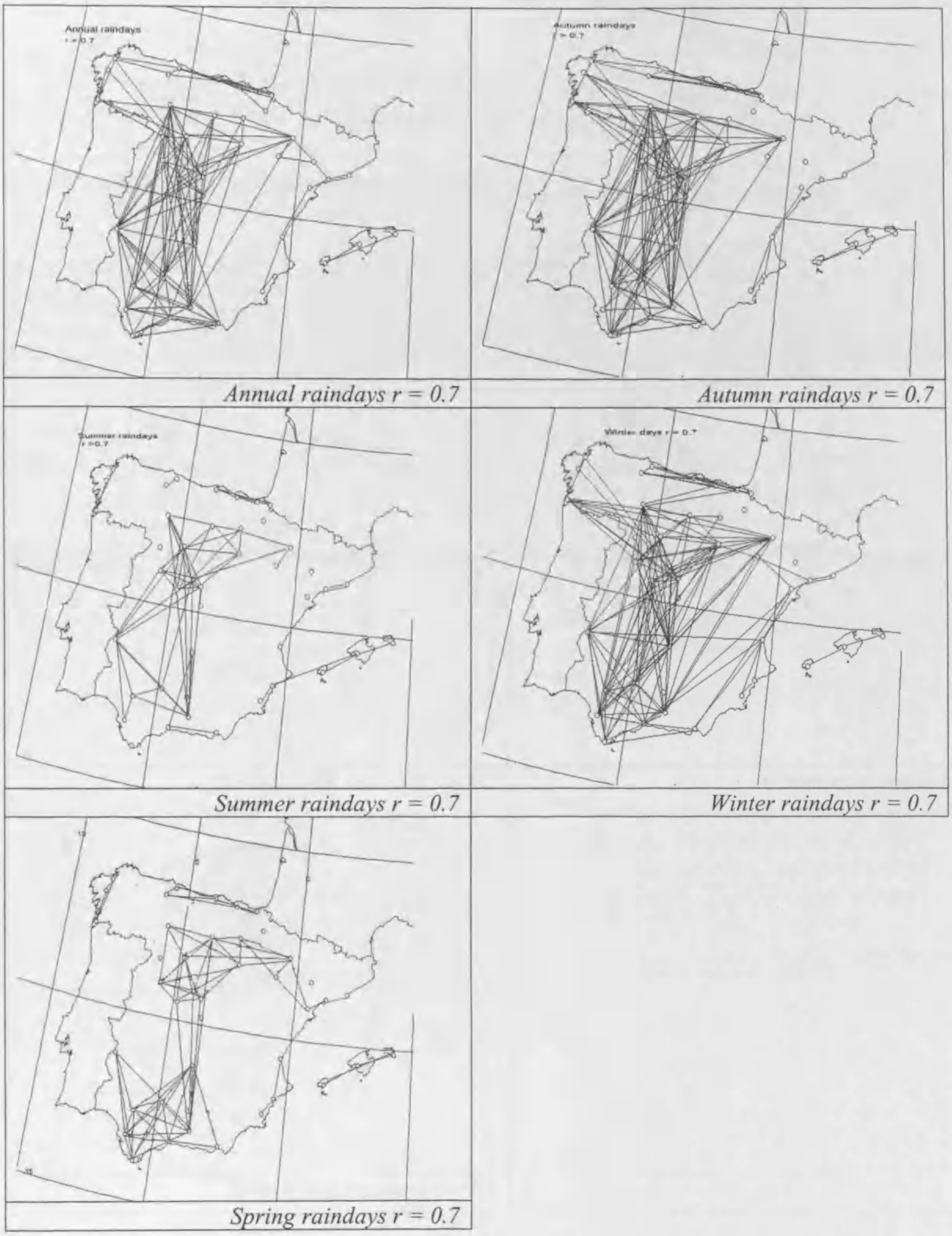

Annual raindays r = 0.7

Autumn raindays r = 0.7

Summer raindays r = 0.7

Winter raindays r = 0.7

Spring raindays r = 0.7

Figure 2.8 Linkage Analysis using rainday data r = 0.7.

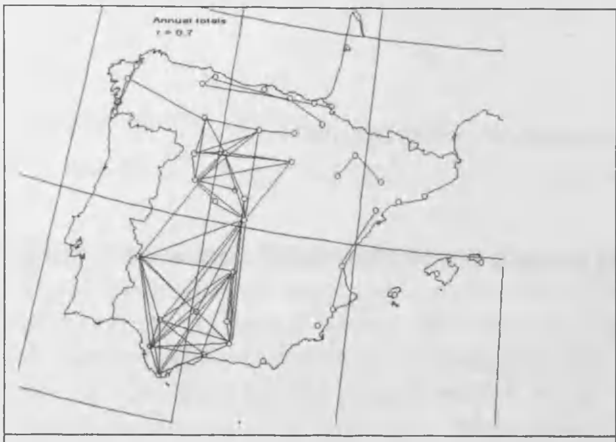

Annual rain amounts r = 0.7

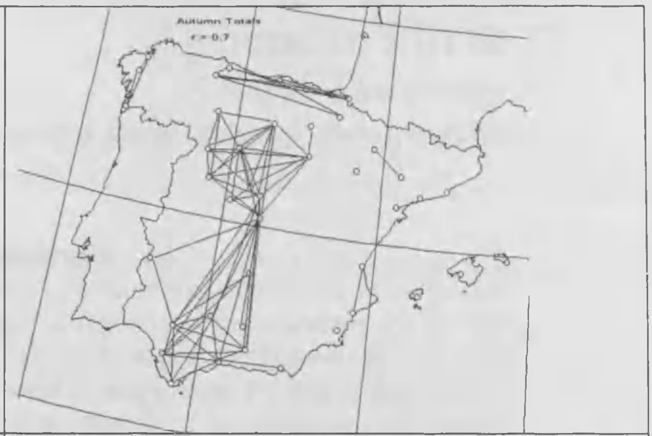

Autumn rain amounts r = 0.7

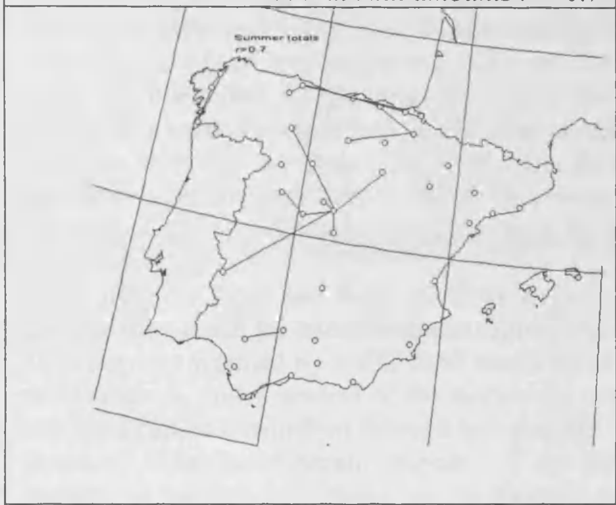

Summer rain amounts r = 0.7

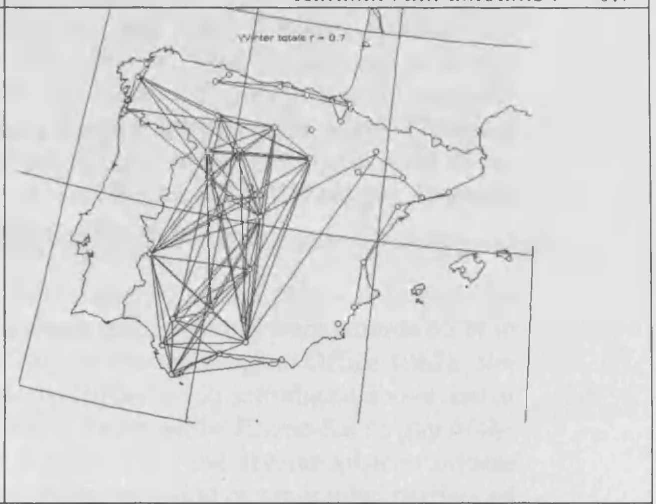

Winter rain amounts r = 0.7

Spring rain amounts r = 0.7

Figure 2.9 Linkage Analysis using rain amounts r = 0.7.

Appendix Three
Synoptic Climatology
Atmospheric circulation and daily manual classification

a3.1 Air mass climatology of the Iberian Peninsula

The classification of atmospheric circulation type is ultimately linked with the identification of prevailing air mass type over the classified region. Mediterranean air masses are familiar to meteorologists working in northern latitudes but arrive in the Mediterranean area after having undergone extensive modification. An air mass typing system for winter and summer months is illustrated in *figure a3.1*. Most writers, when describing Mediterranean air masses, have used an air mass system that is similar to that developed for higher mid latitude areas. The main differences between Mediterranean situations and that of higher latitudes (as originally proposed by Bergeron (1928) and Belasco (1950) is, first, the absence of a true Arctic air mass (the lengthy trajectory from the Arctic circle will greatly modify northern flows), secondly, the replacement of Polar maritime returning with an (effectively) 'Tropical maritime returning' air mass (*TmP*) reflecting the track of air around the northern flank of the Azores anticyclone and, thirdly, the incorporation of two air masses (*TmP/Tmc* and *Tc (mod)* which are highly modified by the presence of the Mediterranean Sea).

Arctic maritime (*Am*) and Polar maritime air (*Pm*) have usually been warmed considerably by the time they reach the Mediterranean region. As a rough guide moving from latitude 55°N to 35°N they are warmed by 6-8°C at all levels up to 500 hPa (Meteorological Office 1962). *Am* and *Pm* arrive under several of the circulation patterns (*figure a3.2*) introduced above and at low level can be channelled through topographic 'funnels' such as the Rhone-Saone gap or the Straits of Gibraltar-Alboran channel. If the air is lifted over the Iberian plateau intense convection and heavy precipitation can develop, however downwind of orographic barriers on the east coast of Spain, dry conditions generally result. Further passage over the comparatively warm sea then causes moisture content to increase and low level temperatures to rise hence renewing instability. Cumulus cloud formation and showers may follow which are most pronounced when the air mass arrives in autumn when the sea is still very warm. Thunderstorms can result which are most violent under Arctic airflow. The Meteorological Office (1962) distinguishes between *Am* and *Ac* (Arctic continental). *Ac* arrives to Spain from the north-east in, primarily, the winter and is generally much less modified than its maritime counterpart.

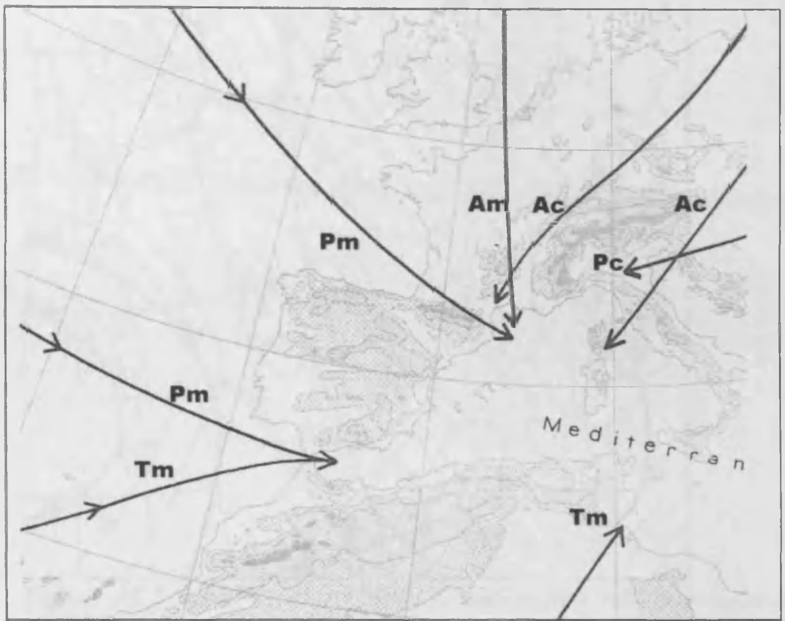

a. UKMO Definition of air masses in the cool season (from the Meteorological Office 1962)

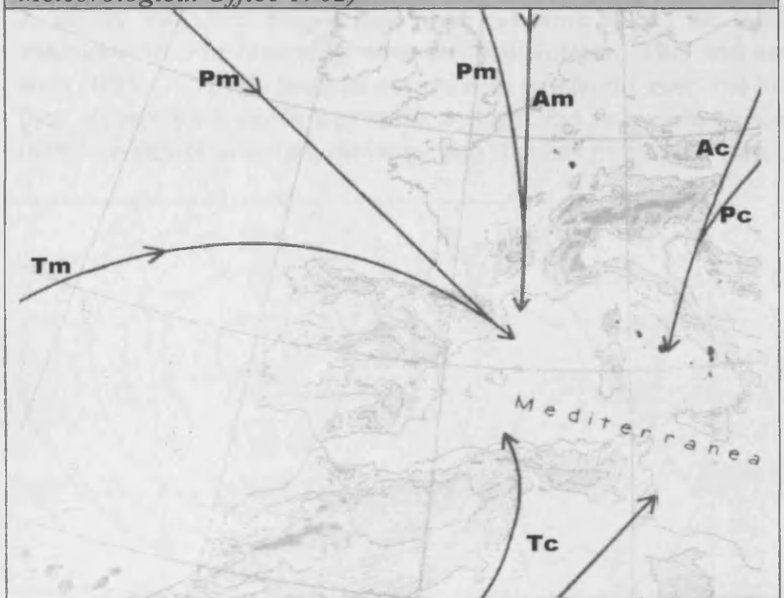

b. UKMO Definition of air masses in the warm season (from the Meteorological Office 1962)

Figure a3.1 Air masses affecting the Iberian peninsula (from the Meteorological Office 1962)

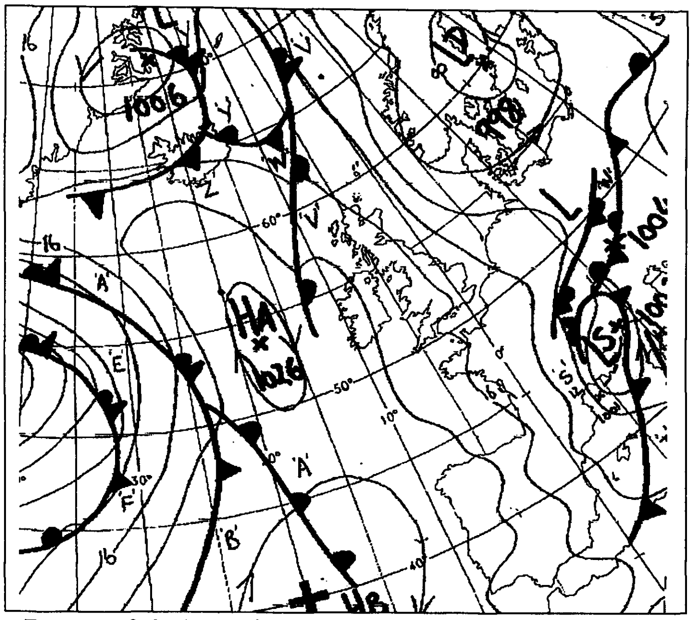

Figure a3.2 A sea level synoptic situation that will introduce the Am air mass to Spain (22 June 1996) (MSLP chart supplied by UKMO).

A highly modified transitional polar maritime (*tPm*) air mass can be identified which is analogous to '*Pm returning*' over the British Isles. This will arrive when a trough lies to the west (*WT*) - it travels from its source near southern Greenland to the vicinity of the Azores but then swings back north-eastwards towards the peninsula (*figure a3.3*). This air stream will therefore exhibit thermal, moisture and stability properties 'transitional' between *Pm* and *Tm*.

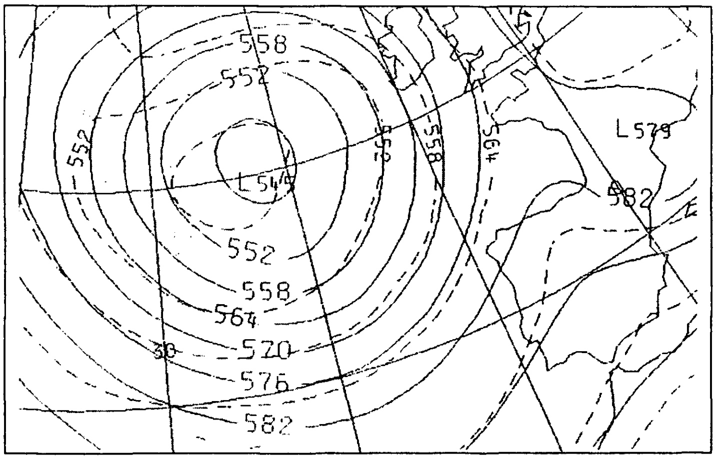

Figure a3.3 An upper air synoptic situation that will introduce the transitional tPm air mass to Spain (11th August 1997) (Upper air chart supplied by UKMO).

Polar continental (*Pc*) air masses enter the Balearic region from the north east and are associated with an anticyclone or ridge of high pressure to the north, commonly extending from Russia (*RCT, RMT*) (*figure a3.4*). This air is often stable above 850 hPa. However like Arctic air it is warmed at lower heights and some moisture is picked up over the sea and therefore can unleash some convective instability in the winter months.

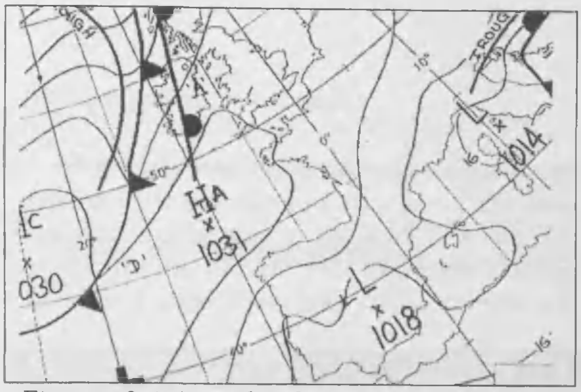

Figure a3.4 A sea level synoptic situation that will introduce Pc air mass to Spain (25th June 1996) (Upper air chart supplied by UKMO).

Tropical maritime (*Tm*) air enters the region on south-westerly zonal air streams (*figure a3.5*). Although moist at all levels this air mass is convectively stable as it is cooled at its base as it heads north. Tropical continental (*Tc*) air, on the other hand is very hot and dry and can become unstable as it moves north across the sea.

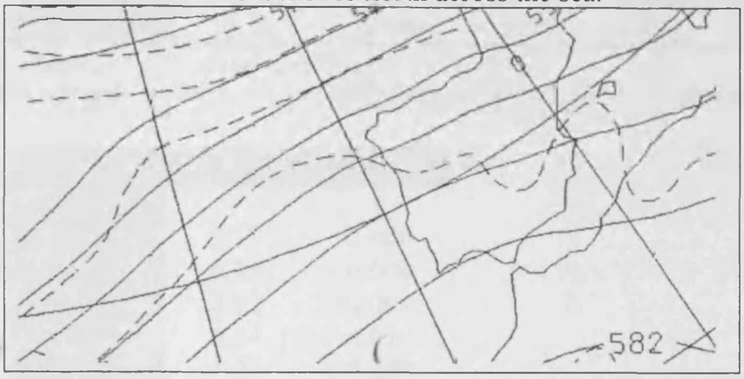

Figure a3.5 An upper air synoptic situation that will introduce the Tm air mass to Spain (24th December 1995) (Upper air chart supplied by UKMO).

Sanchez Rodriguez (1993) has used an alternative air mass classification as described *table 3.1.* This introduces a subdivided continental air mass depending on the distance of its sea trajectory and a 'Mixed' air mass that usually arrives under cyclonic conditions to the south west of in the Balearic area.. Under this classification there is no true Arctic air mass as a consequence of the extensive modification it will have received. Nevertheless in this study the more common Belasco scheme is used.

Air mass	Symbol	Origin	Flow direction
Tropical Continental	Tc	Sahara	S/SE
Tropical African	Tc (mod)	Sahara (but modified by Mediterranean)	E/E-SE
Tropical Maritime	Tm	Atlantic	SW
Tropical-Polar maritime	TmP	As Tm	W or NW
Mixed	TmP Tmc	Gulf of Cadiz or Balearics	E
Polar maritime	Pm	Greenland/Iceland	W
Polar Continental	Pc	Arctic/east of Iceland	N/NE

Table a3.1 Air mass types as described by the Instituto de Meteorologia (Sanchez Rodriguez (1993)

a3.2 Pilot Study – Results

A pilot study was undertaken to assess the relative merits of weather typing schemes. This involved the sampling of charts and the pursuit of all stages of analysis from derivation of circulation catalogue to application of rainfall data and testing via validation statistics. Some of the results of this procedure are displayed in *tables a3.2 and a3.3*. The ANN was developed using Open University *Neuralworks* software.

	500AUT (10)		THICKAUT (12)		SLPANN (15)	
	F	P	F	P	F	P
Badajoz	6.92	0.000	4.11	0.000	0.81	0.600
Burgos	6.76	0.000	4.43	0.000	1.67	0.092
Murcia	4.95	0.000	4.03	0.000	1.26	0.256
Mahon	5.18	0.000	4.46	0.000	0.89	0.533
Malaga	8.14	0.000	5.33	0.000	0.76	0.792
Salamanca	4.98	0.000	3.73	0.000	0.79	0.629
Santander	7.38	0.000	4.78	0.000	0.61	0.792

Table a3.2 Selected ANOVA from pilot study.

	MULTIAUT (16)	
	F	P
Badajoz	3.37	0.000
Burgos	6.76	0.000
Murcia	2.12	0.008
Mahon	0.54	0.920
Malaga	1.22	0.250
Salamanca	1.66	0.053
Santander	2.69	0.000

Table a3.3 Selected ANOVA from pilot study.

a3.3 Existing manual classifications for the Iberian Peninsula

a3.3.1 UKMO classification

The pressure pattern classification of the UKMO (Meteorological Office 1962) covers the entire Mediterranean region (see *table a3.4* and *figure a3.6 a-e*). It is based mainly on the positions, relative to the region, of anticyclonic systems which exert a controlling influence on synoptic conditions in the area and to a smaller extent on the major low pressure areas.

Type	Pressure field	Sub type	Comment
A	An anticyclone or ridge of high pressure lies over the north eastern Atlantic or the British Isles	A1	If the eastern edge is to the west of Ireland this leads to a flow of polar maritime air across the British Isles towards the peninsula
		A2	The eastern edge lies over the British Isles a northerly air stream (modified arctic air mass) is directed south across the North Sea
		A3	A marked eastward extension into northern Europe brings arctic/polar continental air which flows over Scandinavia and France
B	Northern Europe is dominated by an anticyclone. Pressure is low over the Mediterranean.	B1	To the east of the north European anticyclone lies a depression over Russia or Western Siberia
		B2	The north European anticyclone extends into Siberia and there is low pressure south of it from the eastern borders of the Mediterranean eastwards
		B3	The North European anticyclone extends into Siberia eastwards and pressure is high in the eastern Mediterranean

C	A deep depression or sequence of depressions dominates the middle latitudes and westerly prevailing winds cross the peninsula	Over Spain winds are generally between south west and north west bringing polar maritime, polar maritime returning or tropical maritime air
D	An anticyclone dominates central and southern Europe giving easterly winds over most of the Mediterranean	This keeps the region free from depressions and generally easterly winds dominate often from the south east over Spain
E	An anticyclone or ridge (an extension of the Azores semi-permanent anticyclone) covers the greater part of the Mediterranean area	Leads to light winds which are mainly westerly

Table a3.4 The UKMO classification of surface pressure field over the Mediterranean (UKMO 1962).

The UKMO concede that development rapidly into other types, for instance type A develops most frequently into type B and sometimes type C and type D. In addition each sub-type could be developed into further sub-sub types. On the other hand this is a criticism that could be levelled at any form of classification as the main objective is to simplify and generalize.

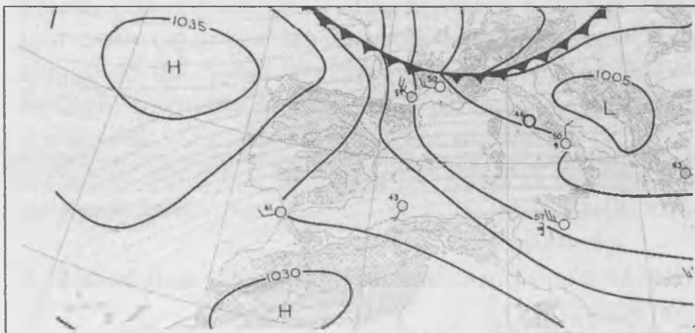

A 19th January 1951

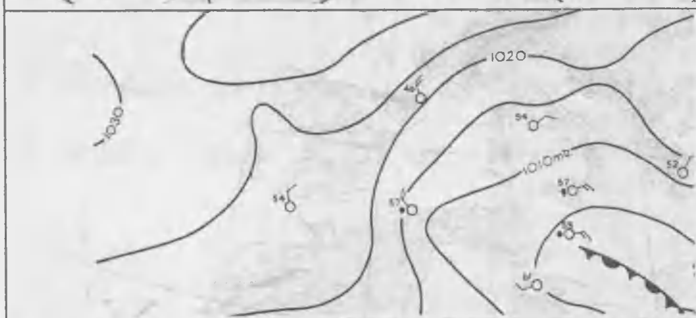

B1 9th April 1954

C 21st February 1947

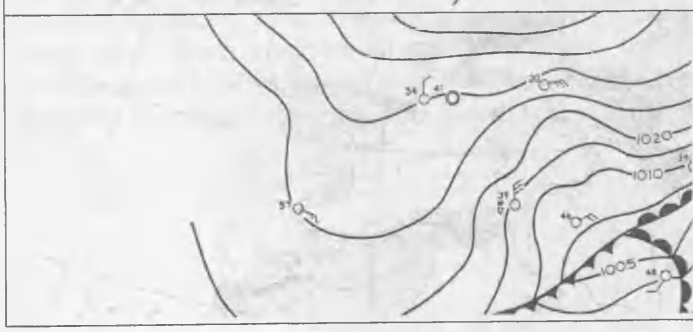

D 3rd February 1949

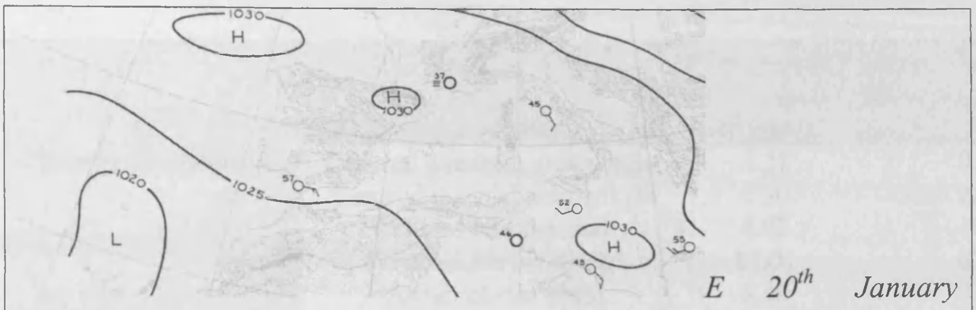

E 20th January 1949

Figure a3.6 a–e Examples of the UKMO classification of surface pressure field over the Mediterranean (Charts reproduced from Meteorological Office (1962)).

a3.3.2 INM (Sanchez Rodriguez) classification

Sanchez Rodriguez (1993) has produced a manual classification of synoptic types based on four main types and several subtypes. The classification is described in *table a3.5*. It is similar to the Lamb Weather Type system for the British Isles and defines a number of cyclonic situations capturing the, perhaps significant, rainfall differences that will occur as a consequence of central location and movement.

MAIN TYPE	SUB TYPE
1. Zonal flow	(a)Westerly
	(b)Easterly
2. Mixed flow (Zonal/Meridional)	(a)South-westerly
	(b)North-westerly
	©North-easterly
	(d)South-easterly
3. Meridional flow	(a)Northerly
	(b)Southerly
4. Weather systems	(a)High pressure
	(b)Low pressure (Atlantic area)
	©Low pressure (Canaries-Madeira-Gulf of Cadiz)
	(d)Peninsula low pressure
	(e)Low pressure over western Mediterranean (Gulf of Lyons - Balearics - Alboran Channel - Algeria)
	(f)Wavy flow
	(g)Trough and troughs

Table a3.5 Manual classification of synoptic types over the Iberian Peninsula (after Sanchez Rodriguez 1993).

a3.3.3 Paricio and Nadal manual classification

Paricio and Nadal (1979) advocated a multi-level manual circulation typing scheme and developed a catalogue for the years 1951-1970 in an analysis of the climate of eastern Spain and the Balearics. The system (*figure a3.7*) has eighteen types and these are described in *table a3.6*. Four types are termed 'convective' and the other fourteen are 'advective' and discriminated by direction of airflow. The use of two levels is an illustration of an attempt to integrate a vertical movement component to the classification.

Main type		Frequency % days per year	Mean rainfall in Valencia (mm)
Convective situations	Centred dynamic anticyclone	4.21	0.01
	Centred thermal anticyclone	0.30	2.97
	Centred low pressure	4.02	10.3
	*Pantano Barometrico**	17.01	0.21
Advective situations	Anticyclonic zonal	8.40	0.04
	Anticyclonic northerly	0.64	0.12
	Cyclonic	4.19	4.22
	Zonal	12.95	0.55
	Hot subzonal	7.38	0.83
	Cold subzonal	10.09	0.29
	Warm subzonal	9.17	0.59
	Northerly	3.69	0.54
	European continental	6.60	0.18
	African continental	1.00	0.51
	East (surface and upper)	2.58	1.31
	East (surface) zonal (upper)	2.01	0.63
	East (surface) low (upper)	4.00	6.45
	Zonal (surface) low (upper)	1.58	2.43

Table a3.6 Types and frequencies of incidences of Paricio and Nadal synoptic types and rainfall in Valencia (see figure 4) for the period 1951-1970 (no significant pattern/no variation in pressure across the region).*

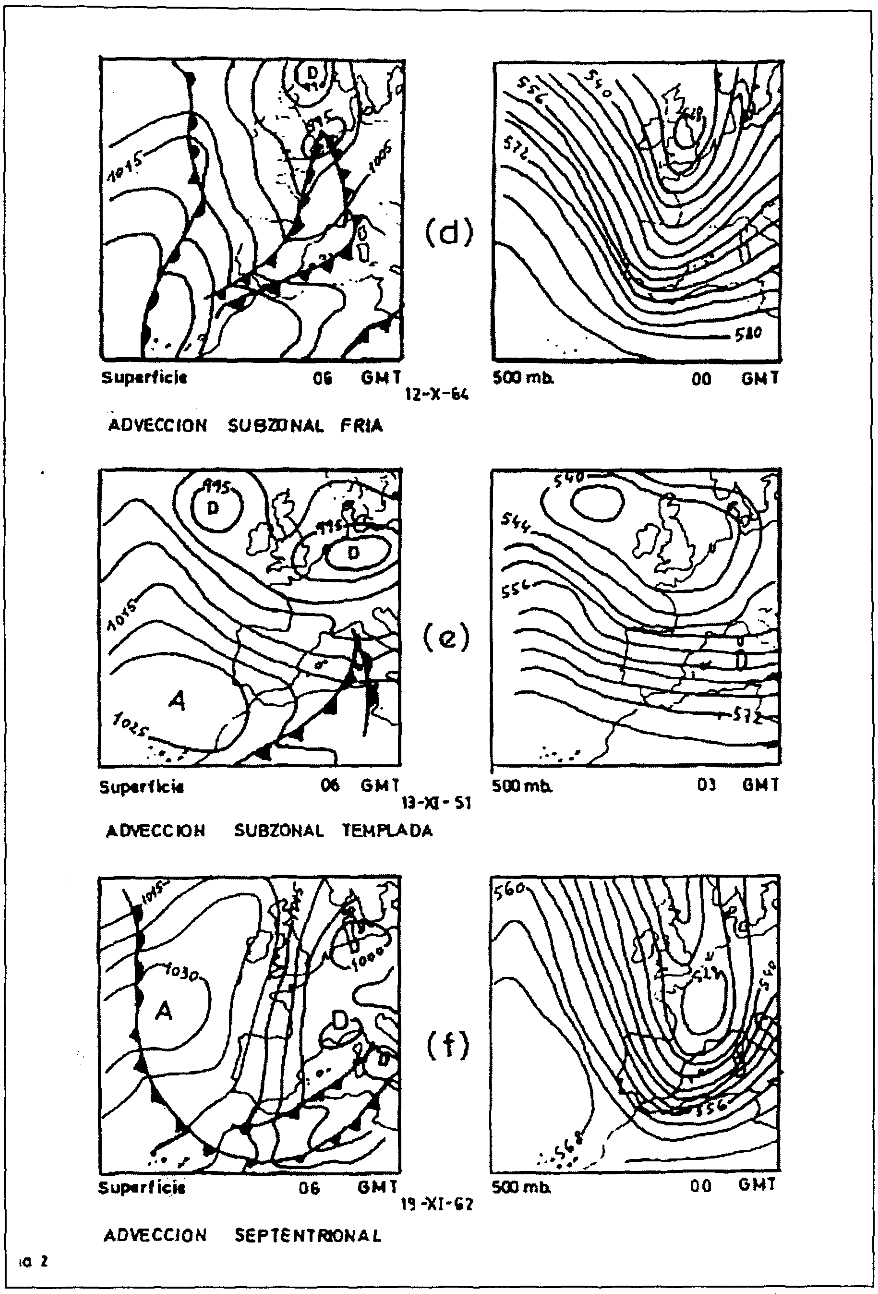

Figure a3.7 Excerpt from Paricio and Nadal (1979) Manual Classification (scanned from the original drawing).

a3.4 Analysis of depression tracks over the Iberian peninsula

Analysis was first undertaken by Van Bebber (1882) who examined the movement of depressions over (northern) Europe for 1876-1880, described five major tracks (*figure a3.8*) and analysed spatial patterns of seasonal weather conditions for each track. Other workers have examined links between depression tracks and precipitation (Hay 1949). One major problem with kinematic analysis is the difficulty in classification of secondary and trough features, both of which may yield significant precipitation events. Furthermore such a classification often ignores important features of pressure systems, such as their intensity (as measured by central pressure or pressure gradient) and the speed of central movement (for instance, from stationary to fast moving). Both of these characteristics may result in considerable variability in rainfall amounts (and contribute to the non-stationarity problem).

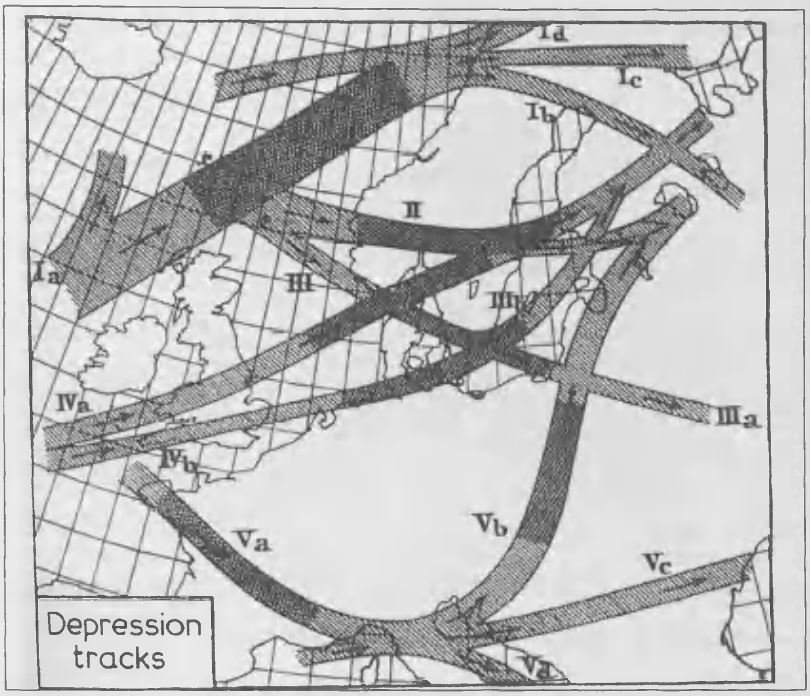

Figure a3.8 Depression tracks over Europe according to Van Bebber (1882) (from Barry and Perry 1973)

Less analysis has been undertaken of anticyclone tracks and the resultant weather due to a difficulty in accurately identifying anticyclone centres. Neverthless Reinel (1960) identified ten anticyclone tracks over Europe (*figure a3.9*) and related these to surface weather. Makrogiannis and Giles (1980) examined the mean tracks and frequencies of moving anticyclones in south-east Europe for the period 1960-1974 and Rohli and Henderson (1997) investigated the trajectory frequency and intensity of winter anticyclones in the Central Gulf Coast of the USA.

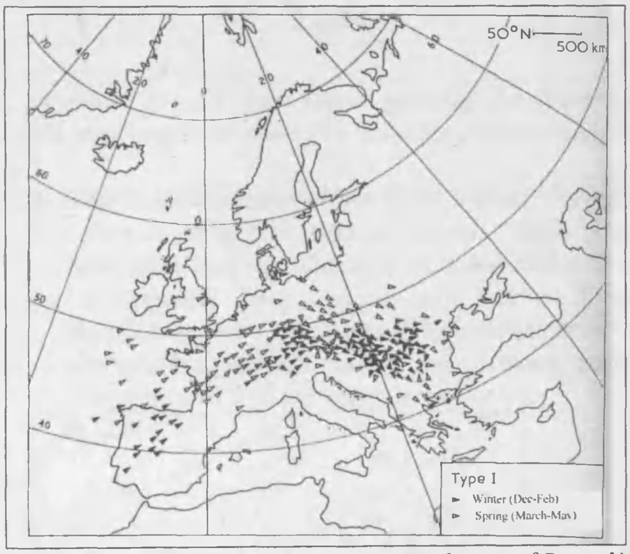

Figure a3.9 Azores-type anticyclones of Reinel's classification (Winters 1947-1957) (from Barry and Perry 1973).

a3.5 Depression tracks relating to the Iberian peninsula

Several writers have developed cyclone and anticyclone climatologies for this geographic region. The UKMO (1962) identify the principal tracks and frequencies of depressions into, and through, the Mediterranean area based on United States Historical Weather Maps from the years 1926-1939 and 1945-1952. Those relevant to the Iberian peninsula are listed in *table 3.12* (the annual frequencies in this time period are given in parenthesis). These are depicted in *figure a3.10.*

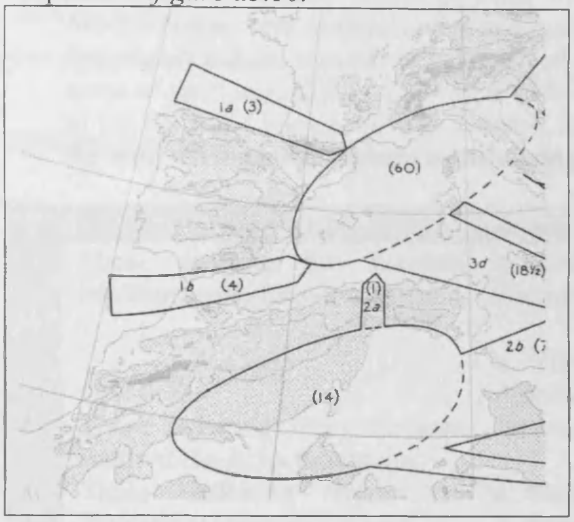

Figure a3.10 Depression tracks in the vicinity of the Iberian peninsula (Meteorological Office 1962).

1) Depressions that enter the Mediterranean basin from outside - entering through the Straits of Gibraltar (*figure a3.12*) or through the Garonne-Carcassonne Gap.

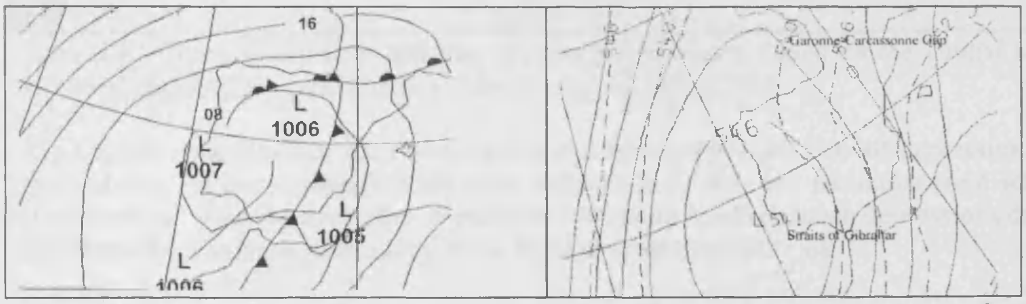

Figure a3.11 A depression entering the Iberian peninsula region via the south west. (a) Sea level pressure chart (b) 500 hPa contour height chart - 20.01.97

2) Thermal depressions that form mainly during the daytime in the summer months as a result of surface heating over land. These occur at times when the broad features of the Mediterranean circulation are settled and will normally remain stationary (*figure a3.12*). Occasionally these systems will produce thunderstorms, however if a new air stream invades the area the thermal depression may become a normal frontal depression. This can also happen if a trailing front crosses the peninsula or if it becomes caught up in the movement of another depression centre.

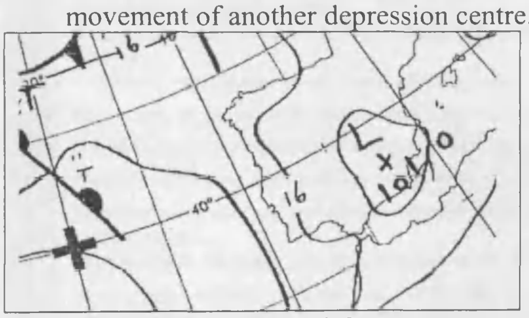

Figure a3.12 A thermal depression over the south east of the peninsula on the 1800Z chart for 10.07.97

3) Lee depressions form on the leeside of a mountain range (*e.g.* the Pyrennees) when deep vigorous currents move towards the range (Campins *et al* 2000). The initiating current almost always carries Arctic or Polar maritime air masses and thus sweeps towards Mediterranean area between west and north-east. Many of the cyclones originating in this region exhibit mesoscale features and weak intensity (Genoves and Jansa 1989) but some of them are strong and cover a wide area (Alpert *et al* 1990). Depressions forming in the Gulf of Lyons contribute towards rendering the Western Mediterranean as one of the most cyclogenetic regions in the world (Pettersson 1956, Radinovic 1987).

	Origin	Track
1	Those entering the Western Mediterranean from the Atlantic	a. Across the Bay of Biscay and through the Garonnne-Carcassonne gap (3) - Van Bebber's *v(a)* b. Through the straits of Gibraltar and through the Alboran Channel (4)
2	Those radiating from the area south of the Atlas mountains	Through the Biskra gap to the Western Mediterranean (1)
3	Those radiating from the Western Mediterranean area	a. Originating in the Gulf of Genoa and heading north eastwards (11) b. Originating in the Gulf of Genoa and heading south eastwards (4.5) c. From the Balearics area to the central Mediterranean (18.5)

Table 3.12 Depression tracks affecting the Iberian Peninsula based on the United Kingdom Meteorological Office classification (Meteorological Office1962).

The UKMO concedes that the classification is quite rigorous and that all depressions do not proceed in a regular manner but are often difficult to fit into any particular rigid scheme of classification. They estimate that as much as 50% of all Mediterranean depressions cannot be satisfactorily classified, particularly those that are short-lived or weak.

As part of this study a catalogue of depression tracks and frequencies was created for the period 1965-1997 using daily surface pressure charts drawn by the UKMO. This catalogue (track types are listed in *table 3.2*) includes tracks that were not explicitly described by the UKMO classification recognizing the fact that depression tracks often pass across the centre of the Iberian peninsula rather than only following topographic depressions or sea channels. *Table a3.13* lists the main track types of the depression catalogue used in this study.

	Description of Depression Track
1	Originating to the south-west passing through the straits of Gibraltar and Alboran Channel then moving east either along the coast or towards the Balearics.
2	Originating to the south-west then crossing the peninsula with the centre passing either across the north coast or towards Catalunya.
3	From north-west to south-east across the peninsula.
4	Originating in the Balearics and generally moving east.
5	Originating in central parts of the peninsula and generally remaining stationary.
6	From the north-east and travelling along the north coast. Travelling to the north of the Pyrenees.
7	From the north-east and travelling across the northern quadrants of the peninsula passing over Catalunya before reaching the Mediterranean.
8	Originating in the south-west and travelling north along the western coast of the peninsula.
9	Moving south-west to north east and crossing the north western quadrant of the peninsula.

Table 3.13 Depression Tracks

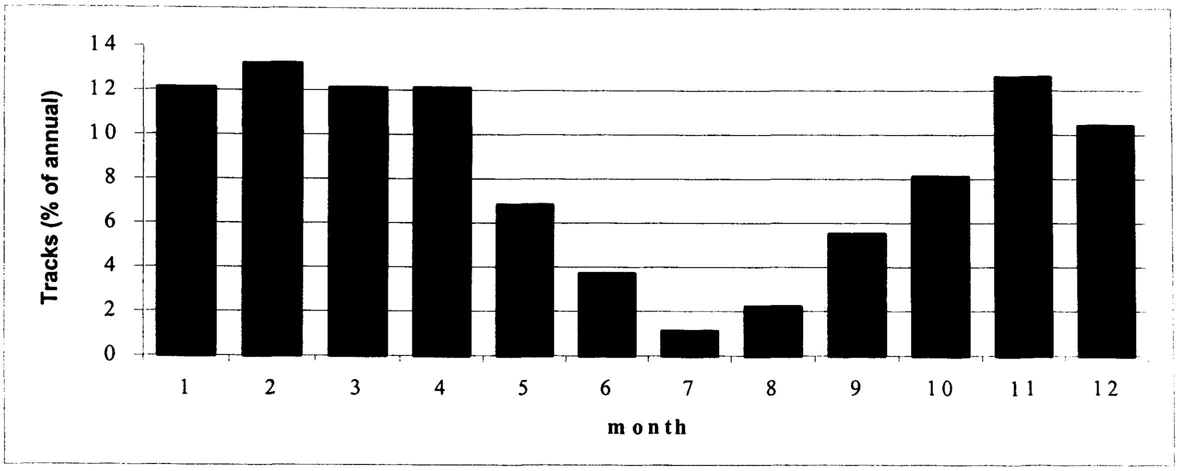

Figure a3.14 Mean monthly percentage of total annual occurrence of depressions in the vicinity of the Iberian Peninsula 1965-1997.

The results are comparable to those of the UKMO (1962) in that depressions behave irregularly and are often difficult to incorporate in any particular scheme. Creation of the catalogue followed a methodology suggested by Radinovic (1978) although an objective method has been attempted by Alpert *et al* (1990). In this case the catalogue was developed using hand drawn surface isobaric charts for the period 1965-1997. This represents a significantly longer period than that of Campins *et al* (2000). The following features were recorded for each depression: the date of occurrence, the exact spatial location of the centre and the direction of movement.

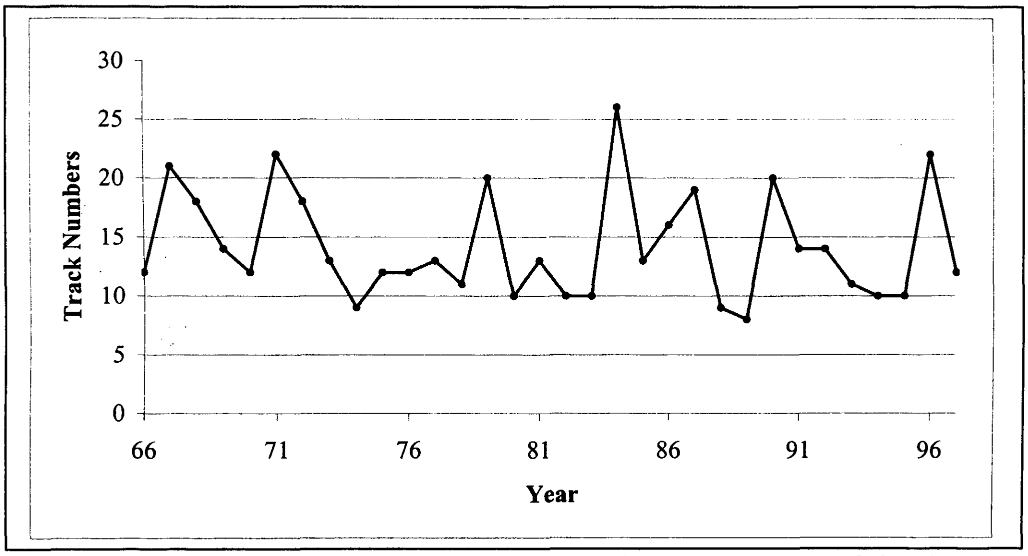

Figure a3.15 Total number of depression tracks in the vicinity of the Iberian peninsula 1965-1997.

It is clear from *figure a3.15* that there is a wide dispersion in numbers of depressions per year that have some influence over the study area

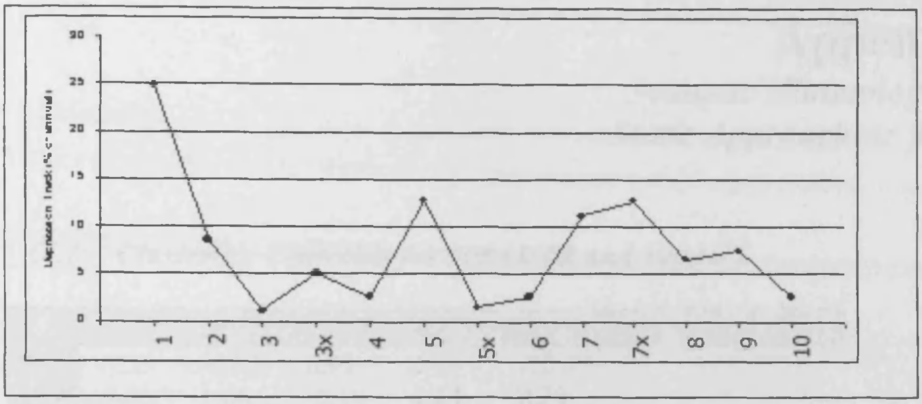

Figure a3.16 Depression types and numbers of appearances in the catalogue 1965-1977.

Table a3.14 demonstrates that at the majority of gridpoints cyclonic systems will have an appreciable impact on resulting precipitation amounts. Nevertheless static synoptic classifications cannot capture this information satisfactorily. A higher frequency of depressions could be associated with particular synoptic types in each under each system and this contention is examined in this thesis. If a significant association can be found between certain types and depression occurrence then this feature could be overlooked for model construction purposes. On the other hand midlatitude cyclonic rainfall events are predominantly associated with the passage of frontal surfaces and fronts have been included in class-based classification schemes by other authors (*e.g.* Wilby 1995).

	1	2	3	4	5	6	7	8	9	10	11
r	0.346	0.372	0.296	0.342	0.430	0.415	0.286	0.373	0.462	0.497	0.260
P	0.000	0.000	0.000	0.000	0.000	0.000	0.000	0.000	0.000	0.000	0.000

Table a3.17 Pearson's Product moment correlation coefficients monthly depression amounts vs monthly gridpoint rainfall amounts (1958-1997).

Appendix Four

Synoptic climatological methods
Static Approaches: Daily Models

A4.1 Clustering Centroids for 500AUTR and 500AUT

	1	2	3	4	5	
P1	-7.25	-6.02	6.99	2.18	-10.09	
P2	-2.02	1.06	-0.19	4.48	0.29	
P3	-0.26	-0.23	-1.91	0.01	0.37	
P4	0.22	0.36	-0.23	-0.79	0.15	
P5	0.09	-0.28	0.24	-0.25	-0.10	
	6	**7**	**8**	**9**	**10**	
P1	-2.25	2.77	9.20	15.42	0.04	
P2	2.57	-4.36	-4.53	-3.05	-0.39	
P3	0.20	-0.07	0.03	0.01	2.08	
P4	-0.40	-0.72	-0.20	0.39	0.23	
P5	0.01	0.09	-0.26	-0.46	0.17	
	11	**12**	**13**	**14**	**15**	**Grand Centroid**
P1	7.48	1.55	-2.97	12.11	5.31	0.00
P2	5.12	0.25	-2.85	1.93	0.26	-0.00
P3	-0.25	-1.83	-0.24	-0.05	2.10	-0.00
P4	-0.29	-0.01	-0.17	1.03	0.42	0.00
P5	0.02	0.13	0.20	0.00	0.02	-0.00

Table a4.1 Results of the clustering procedure (centroid distances) using raw 500 hPa contour heights (500AUTR).

	1	2	3	4	5	6
P1	-9.70	-4.81	1.83	6.54	7.07	0.19
P2	-0.49	2.71	-0.23	4.37	-4.68	-6.01
P3	-0.06	0.03	-2.41	0.06	0.42	-0.28
P4	0.51	-0.12	0.33	0.11	-0.03	-1.07
P5	-0.06	0.01	-0.07	-0.03	0.25	-0.01
	7	**8**	**9**	**10**		**Grand Centroid**
P1	-4.73	12.05	0.66	0.18		0.00
P2	-2.62	0.11	0.11	5.82		-0.00
P3	-0.04	-0.07	2.26	-0.33		0.00
P4	0.25	0.69	0.14	-0.84		-0.00
P5	-0.11	-0.36	-0.05	0.37		-0.00

Table a4.2 Results of the clustering procedure (centroid distances) using standardized 500 hPa contour heights (500AUT).

Appendix Five

Synoptic climatological methods
Static Approaches: Monthly models

a5.1 Pilot Study
a5.1.1 Regression Analysis

	NAOI		ZI		500NAOI		500ZI	
	r	p	r	p	r	p	r	p
1	0.305	S	0.212	S	0.180	S	0.265	S
2	0.329	S	0.234	S	0.197	S	0.180	S
3	0.381	S	0.200	S	0.154	N	0.148	N
4	0.241	S	-0.008	N	-0.013	N	0.041	N
5	0.501	S	0.311	S	0.200	S	0.189	S
6	0.492	S	0.365	S	0.201	S	0.251	S
7	0.161	N	-0.019	N	-0.040	N	0.036	N
8	0.102	N	-0.034	N	-0.021	N	0.018	N
9	0.414	S	0.271	S	0.201	S	0.192	S
10	0.509	S	0.333	S	0.248	S	0.202	S
11	-0.189	S	0.093	N	0.152	N	0.046	N

Table a5.1 PPM correlation coefficients between predicted and modelled (using regression) rainfall amounts (S – significant at p>0.050; N – not significant at p< 0.050).

	SLPIND		500IND	
	r	p	r	p
1	0.758	S	0.701	S
2	0.404	S	0.690	S
3	0.381	S	0.595	S
4	0.351	S	0.411	S
5	0.767	S	0.768	S
6	0.501	S	0.799	S
7	0.299	S	0.412	S
8	0.261	S	0.501	S
9	0.771	S	0.161	N
10	0.602	S	0.512	S
11	0.254	S	0.411	S

Table a5.1 (continued) PPM correlation coefficients between predicted and modelled (using regression) rainfall amounts. (S – significant at p>0.050; N – not significant at p< 0.050).

a5.1.2 Back Propagation Neural Network

	NAOI		ZI		500NAOI		500ZI	
	r	p	r		r	p	r	p
1	0.281	S	0.181	S	0.182	S	0.197	S
2	0.303	S	0.177	S	0.161	N	0.160	N
3	0.354	S	0.193	S	0.173	S	0.100	N
4	0.188	S	0.000	N	0.101	N	0.111	N
5	0.451	S	0.284	S	0.251	S	0.191	S
6	0.362	S	0.329	S	0.200	S	0.203	S
7	0.178	S	0.003	N	0.080	N	0.002	N
8	0.100	N	-0.017	N	0.051	N	0.031	N
9	0.311	S	0.254	S	0.181	S	0.162	N
10	0.488	S	0.288	S	0.197	S	0.217	S
11	-0.157	n	0.141	N	0.142	N	0.170	S

Table a5.2 PPM correlation coefficients between predicted and modelled (using back propagation ANN) rainfall amounts. (S – significant at p>0.050; N – not significant at p< 0.050).

	SLPIND		500IND	
	r	p	r	p
1	0.692	S	0.681	S
2	0.401	S	0.601	S
3	0.372	S	0.562	S
4	0.331	S	0.324	S
5	0.698	S	0.741	S
6	0.477	S	0.782	S
7	0.292	S	0.400	S
8	0.231	S	0.498	S
9	0.752	S	0.182	S
10	0.541	S	0.503	S
11	0.231	S	0.400	S

Table a5.2 (continued) PPM correlation coefficients between predicted and modelled (using back propagation ANN) rainfall amounts. (S – significant at p>0.050; N – not significant at p< 0.050).

a5.2 Clustering procedure results – 500AUTM

	1	2	3	4	5
P1	-0.94	-2.53	4.38	-6.30	9.53
P2	3.80	-2.23	1.26	2.82	4.76
P3	0.58	0.13	0.09	-1.05	-0.06
P4	-0.34	-0.09	0.23	0.76	0.77
P5	-0.02	0.19	0.02	0.00	-0.11
	6	7	8	**Grand Centroid**	
P1	3.57	-11.24	10.83		
P2	-5.06	-1.62	-2.58	0.00	
P3	-0.79	0.40	0.60		
P4	0.11	0.07	-0.41		
P5	-0.09	-0.22	-0.08		

Table a5.3 Results of the clustering procedure (centroid distances) using monthly 500 hPa contour heights (500AUTM scheme).

a5.3 Artificial Neural Networks – Back Propagation method

This is one of the more common structures and is known as a multi-layer perceptron (feed-forward) network. Nodes (or neurons) have uni-directional interconnections between them. These replicate the neurons or nerve cells in the brain and the fibres (axons and dendrites which connect them and carry messages between them). However in comparison the human brain has approximately 10^{11} highly interconnected neurons. Supervised ANN methodology follows a general four-step procedure as described by Openshaw and Openshaw (1994) and summarized here;

First, appropriate data is subdivided into at least two subsets, one for training purposes (the 'training' set) and the other for model validation (the 'test' set). Secondly, the input data is then scaled from 0.0 to 1.0 according to the choice of transfer function (this is often done by the neural network program). The output is eventually transformed back to the full range of *y* values in order to interpret the result.

Thirdly, the architecture (or general layout) of the network is determined - this involves making the following decisions on:

- the number of input variables
- the number of hidden layers
- the number of neurons in each layer
- the type of network to be used.

The basic structure of a multi-layer 'feed-forward' neural network can be described as follows - the neurons (or nodes) in the input layer represent the input variables. the procedure is similar to multiple regression, therefore neurons in this layer represent the independent variables one output, the dependent variable *y*.

Between the input and output layers there are one or more hidden layers, each with a variable number of neurons. According to Openshaw and Openshaw (1997) at least two layers are needed as it is the second layer that increases network power and can permit the modelling of more complex non-linear functions. A third layer is needed when the function is extremely complex, noisy or discontinuous. Unfortunately the determination of the optimal number of layers and the number of neurons is often a process of trial and error. Wang *et al* (1994) suggest that it is the complexity of the dataset that controls input and output neuron numbers, however although several empirical rules have been suggested it is likely that the hidden neuron number is problem-specific.

Each neuron is connected to all neurons in the preceding and following layer by links (represented by the arrows in *figure 4*) which model the synaptic connections of the brain.

Finally the network is trained. In this procedure the weights of neuron inputs are determine. A weight is interpreted as the strength of the connection between a neuron in one layer to the neuron in the next layer and therefore the input into a neuron is a weighted sum of the outputs from all neurons connected to it. Each neuron then takes its input and applies an activation function to it. A number of non-linear functions have been used by researchers however by applying a sigmoidal (s-shaped) transfer function the sum of all weights received by a neuron can be 'squashed on to the range 0.0 to 1.0. The sigmoid function is as follows

$$f(j) = \frac{1}{1 + exp\ (-j)}$$

(the hyperbolic tangent function is also popular in applications).

The output of each neuron is then a smooth non-linear function of the weighted inputs.
As the brain learns by adapting the strength of synaptic connections likewise the synaptic weights in the ANN (like multiple regression coefficients) are adjusted to solve the problem presented to the network.

The process of estimating optimum weights for the links is known as the 'training' or 'learning' process. The algorithm that has been of most use in practical atmospheric applications is the back propagation method (for fuller explanation and mathematics of back propagation see Hewitson and Crane 1994). This is a form of 'supervised learning' because in order to train the network using this method desired outputs must be stated (in the case of function estimation these are the observed values). The ANN output is then compared to the original observations, *y*, and the error is measured (this is often the sum squared error *SSE* or root mean square error *RMSE*).

a5.3.1 Back propagation

The back propagation method can be described as follows; First the weights are set to small random values, the inputs are then propagated forward (passed between the layers) in the ANN until they eventually reach the output layer. Output values can then be compared to the desired output (the observations *y*) using the test dataset and the error measure calculated. This information is then used to correct weights on neurons that contributed most to the error. However as these are not readily identified the errors are back propagated from the output layer back into the whole network (*ie* the feed forward process is reversed). The weights are then adjusted. This procedure is then repeated iteratively until gradually the size of the error and hence the weights stabilize. While training the network a precaution must be exercised to avoid overfitting the network. Overfitting results in the network learning minute details (eg. noise) in the training data at the cost of learning the smooth trend therein. As a result the network fails to generalize and makes erroneous predictions for the new inputs. To ensure that a network is not overfitted training should be stopped as soon as the root mean square error (RMSE) with respect to the test set reaches a minimum.

The training process in summary is therefore;

1. select input variables
2. select network architecture
3. initialize weights
4. apply inputs to network
5. measure error
6. back propagate errors and adjust weights
7. repeat step 4-6 a large number of times until the network converges and training can cease.

Appendix Six

Relating circulation to rainfall - Evaluation of models

a6.1 Analysis of Variance

The rationale of ANOVA is to find out whether there is more variation between the classes than within them. The within-samples estimate is calculated according to *eqn a6.1.*

$$\hat{\sigma}\omega^2 = \frac{\sum^{k}\sum^{n}(x-\bar{x})^2}{N-k} \quad \textit{(Eqn a6.1)}$$

where $\hat{\sigma}\omega^2$ is the within-classes variance estimate , k is the number of classes, N is the number of individuals in each class, N is the total number of individuals in all classes put together and $\bar{x}$ is the mean of each class. The between-samples variance estimate is calculated in *eqn a6.2,*

$$\hat{\sigma}\mathrm{B}^2 = \frac{\sum^{k} n(\bar{x}-\bar{x}_G)^2}{k-1} \quad \textit{(Eqn a6.2)}$$

where is the between classes variance estimate, n is the number of individuals in a class, k is the number of classes, $\bar{x}$ is the mean of a class, and $\bar{x}_G$ is the grand mean of all the data values. The F-statistic *(eqn a6.3)* is calculated to determine how probable it is that the two values are estimates of the same population variance.

$$F = \frac{\hat{\sigma}\mathrm{B}^2}{\hat{\sigma}\omega^2} \quad \textit{(Eqn a6.3)}$$

a6.2 Evaluation statistics - SLPMAN

	F	P
Badajoz	60.05	0.000
Burgos	41.73	0.000
Mahon	9.47	0.000
Malaga	65.43	0.000
Murcia	9.65	0.000
Salamanca	44.05	0.000
Santander	45.12	0.000

Table a6.1 Analysis of Variance of SLPMAN.

a6.3 NAOI and ZI - Calibration regression equations

	a	b	p	rsq
1	57.0	-5.19	0.034	2.7
2	45.8	-1.93	0.111	1.5
3	44.2	-2.10	0.060	2.1
4	32.0	-1.81	0.086	1.8
5	33.4	-2.67	0.174	1.1
6	24.8	-1.85	0.066	2.0
7	19.0	-0.61	0.304	0.6
8	20.9	-1.07	0.411	0.4
9	17.1	-1.75	0.144	1.3
10	15.4	-0.63	0.521	0.2
11	8.90	-0.31	0.570	0.2

Table a6.2 Summer NAOI

	a	b	p	Rsq
1	72.0	-4.53	0.000	26.2
2	51.7	-1.81	0.000	17.0
3	49.5	-1.60	0.000	15.6
4	35.2	-0.984	0.001	6.7
5	45.9	-3.73	0.000	27.7
6	30.2	-1.65	0.000	20.7
7	20.6	-0.50	0.002	5.5
8	23.7	-0.87	0.017	3.4
9	24.1	-2.08	0.000	19.8
10	20.8	-1.58	0.000	20.2
11	10.7	-0.53	0.000	7.2

Table a6.3 Summer ZI

	a	b	p	Rsq
1	142.7	-17.8	0.000	14.0
2	70.5	-6.68	0.000	12.9
3	44.9	-4.45	0.000	15.2
4	40.5	-4.75	0.000	12.5
5	98.9	-18.2	0.000	25.6
6	40.8	-9.10	0.000	36.0
7	19.6	-2.53	0.000	19.4
8	51.0	-4.86	0.005	6.0
9	68.4	-14.8	0.000	34.4
10	59.1	-14.4	0.000	36.0
11	17.3	-2.42	0.001	8.0

Table a6.4 Winter NAOI

	a	b	p	Rsq
1	160.0	-4.01	0.000	13.2
2	74.6	-1.21	0.001	7.8
3	48.4	-0.91	0.000	11.6
4	43.3	-0.84	0.002	7.2
5	112.0	-3.57	0.000	18.3
6	47.0	-1.72	0.000	23.8
7	20.3	-0.35	0.000	19.0
8	49.5	-0.29	0.474	0.4
9	76.6	-2.55	0.000	19.0
10	69.1	-2.75	0.000	24.4
11	18.3	-0.36	0.037	3.3

Table a6.5 Winter ZI

	1	2	3	4	5	6	7	8
1	72.9	89.7	84.4	74.1	81.4	119.7	86.3	83.7
2	49.9	48.7	55.5	57.1	63.3	54.5	47.2	51.9
3	35.9	39.1	46.7	42.9	44.1	43.0	41.1	33.3
4	26.3	28.4	40.7	36.6	33.0	33.7	30.1	33.4
5	43.0	56.0	53.3	45.5	56.6	84.8	54.9	40.2
6	21.0	27.4	27.1	29.1	30.8	36.5	26.4	14.7
7	15.6	15.4	18.6	17.1	18.4	16.2	15.1	12.0
8	34.4	24.4	37.5	35.6	34.8	28.9	27.6	30.4
9	24.4	32.3	34.4	26.4	39.2	53.4	33.1	21.3
10	24.6	24.9	28.3	23.8	32.7	41.1	27.5	20.6
11	13.5	7.8	10.5	14.3	12.4	11.0	9.9	5.5

Table a6.6 Calibration of 500AUTM (means).

Appendix Seven
Downscaling Application and Conclusions

a. 7.1 Empirical downscaling from GCM output

Airflow index decadal means as calculated using GCM output from CCCMA are listed in *tables a7.1-a7.10.*

	Number	Mean	Median	Standard Deviation	Minimum	Maximum
P	120	569.73	568.26	7.54	555.58	583.28
W	120	13.36	13.36	4.12	5.77	26.90
S	120	-0.08	-0.41	2.21	-4.60	-1.05
F	120	13.82	13.76	4.12	5.92	27.04
ZW	120	-22.39	-22.15	10.61	-45.79	-1.05
ZS	120	-1.71	-1.75	2.40	-7.82	7.33
Z	120	-24.09	-23.90	11.18	-50.74	0.30

Table a7.1 Descriptive statistics of monthly index values 2001-2010.

	Number	Mean	Median	Standard Deviation	Minimum	Maximum
P	120	570.88	569.29	7.15	555.74	584.51
W	120	12.76	12.24	4.08	2.78	26.63
S	120	-0.17	-0.47	1.97	-3.77	6.87
F	120	12.93	12.47	4.03	3.52	26.84
ZW	120	-21.52	-21.49	11.41	-48.36	7.70
ZS	120	-1.52	-1.78	2.42	-5.72	6.27
Z	120	-23.04	-23.27	11.97	-49.93	8.85

Table a7.2 Descriptive statistics of monthly index values 2011-2020.

	Number	Mean	Median	Standard Deviation	Minimum	Maximum
P	120	571.28	569.79	7.53	555.74	584.51
W	120	12.92	12.62	4.55	2.79	26.63
S	120	0.16	0.02	2.22	-3.77	6.87
F	120	13.14	12.68	4.46	3.52	26.84
ZW	120	-22.41	-21.81	11.15	-48.36	7.70
ZS	120	-1.36	-1.58	2.21	-5.72	6.27
Z	120	-23.77	-23.88	11.87	-49.93	8.85

Table a7.3 Descriptive statistics of monthly index values 2021-2030.

	Number	Mean	Median	Standard Deviation	Minimum	Maximum
P	120	571.73	570.67	7.57	551.77	585.43
W	120	13.00	13.26	4.13	2.65	23.58
S	120	0.11	-0.02	2.26	-4.49	7.15
F	120	13.21	13.40	4.09	2.90	23.64
ZW	120	-21.54	-22.98	10.07	-41.76	8.18
ZS	120	-1.59	-1.74	2.39	-6.07	5.76
Z	120	-23.13	-23.66	10.85	-45.89	5.68

Table a7.4 Descriptive statistics of monthly index values 2031-2040.

	Number	Mean	Median	Standard Deviation	Minimum	Maximum
P	120	571.28	569.79	7.53	555.74	584.51
W	120	12.92	12.62	4.55	2.79	26.63
S	120	0.16	0.02	2.22	-3.77	6.87
F	120	13.14	12.68	4.46	3.52	26.84
ZW	120	-22.41	-21.81	11.15	-48.36	7.70
ZS	120	-1.36	-1.58	2.21	-5.72	6.27
Z	120	-23.77	-23.88	11.87	-49.93	8.85

Table a7.5 Descriptive statistics of monthly index values 2041-2050.

	Number	Mean	Median	Standard Deviation	Minimum	Maximum
P	120	573.31	573.64	7.32	556.57	586.43
W	120	13.58	13.07	4.34	4.90	25.85
S	120	0.04	-0.18	2.11	-3.56	7.07
F	120	13.75	13.19	4.30	2.92	25.91
ZW	120	-22.79	-21.67	11.45	-48.56	9.47
ZS	120	-1.55	-1.83	2.01	-6.04	4.67
Z	120	-24.34	-23.90	11.78	-50.38	14.14

Table a7.6 Descriptive statistics of monthly index values 2051-2060.

	Number	Mean	Median	Standard Deviation	Minimum	Maximum
P	120	574.22	573.54	7.61	558.06	586.51
W	120	13.91	13.83	4.28	4.90	25.50
S	120	0.13	0.00	2.03	-4.18	7.69
F	120	14.06	13.96	4.27	4.90	25.52
ZW	120	-24.52	-24.70	10.97	-51.40	7.45
ZS	120	-1.34	-1.62	2.03	-6.39	4.43
Z	120	-25.86	-26.58	11.43	-51.93	8.10

Table a7.7 Descriptive statistics of monthly index values 2061-2070.

	Number	Mean	Median	Standard Deviation	Minimum	Maximum
P	120	575.33	574.56	7.31	560.97	588.66
W	120	14.39	13.84	4.16	2.35	26.40
S	120	0.17	0.47	1.98	-7.49	5.36
F	120	14.54	14.19	4.12	3.12	26.42
ZW	120	-24.26	-24.74	10.68	-54.69	1.09
ZS	120	-1.56	-1.61	1.83	-8.42	3.63
Z	120	-25.83	-25.95	10.91	-57.20	-0.36

Table a7.8 Descriptive statistics of monthly index values 2071-2080.

	Number	Mean	Median	Standard Deviation	Minimum	Maximum
P	120	577.11	576.27	7.06	562.66	589.38
W	120	14.09	13.40	5.01	1.38	27.97
S	120	-0.049	-0.049	1.98	-4.91	7.48
F	120	14.24	13.44	4.98	1.50	27.97
ZW	120	-24.74	-25.15	12.56	-52.33	5.01
ZS	120	-1.74	-1.80	1.64	-5.60	3.10
Z	120	-26.47	-26.42	12.67	-54.96	5.00

Table a7.9 Descriptive statistics of monthly index values 2081-2090.

	Number	Mean	Median	Standard Deviation	Minimum	Maximum
P	120	577.33	576.89	6.91	564.88	589.45
W	120	14.35	13.85	4.88	2.35	26.93
S	120	0.08	0.47	2.18	-5.29	4.72
F	120	14.54	13.95	4.76	4.54	27.04
ZW	120	-24.92	-24.32	12.54	-51.64	7.32
ZS	120	-1.57	-6462	1.57	-5.88	6.40
Z	120	-26.48	-25.96	12.80	-53.45	3.18

Table a 7.10 Descriptive statistics of monthly index values 2091-2100.